Division of Infection and Immunity

University College London

PhD Thesis

Metabolic regulation of hepatic immunopathology by myeloid-derived suppressor cells

Author:
Laura Jane Pallett

Supervisor:
Prof. Mala K. Maini

November 7, 2014

Contents

Declaration of Authorship **4**

Acknowledgements **6**

List of Abbreviations **8**

List of Publications and Abstracts **11**

Abstract **12**

List of Figures **16**

List of Tables **17**

1 Introduction **18**
1.1 50 Years of HBV . . . 18
1.2 Overview of Hepatitis B Virus . . . 19
1.2.1 HBV epidemiology, treatment and beyond . . . 19
1.2.2 HBV virology . . . 20
1.3 Natural History of HBV Infection . . . 24
1.3.1 Acute, resolving HBV infection . . . 24
1.3.2 Chronic infection & immune failure maintaining chronicity . . . 27
1.3.3 Cell-mediated immunopathology in CHB . . . 31
1.3.4 Clinical manifestations in CHB . . . 32
1.4 Immunology of the Liver . . . 35
1.4.1 Liver sinusoidal endothelial cells . . . 36
1.4.2 Kupffer cells . . . 38
1.4.3 Hepatocytes . . . 39
1.4.4 Hepatic stellate cells . . . 40
1.4.5 Lymphoid & myeloid cells of the liver . . . 40
1.5 Overview of Myeloid-derived Suppressor Cells (MDSC) . . . 43
1.5.1 Brief history of MDSC . . . 44
1.5.2 MDSC: akin to neutrophils . . . 45
1.6 Immunometabolism: an emerging field . . . 46
1.7 Hypothesis . . . 48
1.8 Thesis Aims . . . 48
1.9 Thesis Overview . . . 49
1.10 Thesis Highlights . . . 49

2 Materials and Methods **50**
2.1 Study Participants . . . 50

2.1.1 Study cohorts . . . 51
2.2 Sample Isolation & Preparation . . . 54
2.2.1 Preparation of peripheral blood mononuclear cells (PBMC) . . . 54
2.2.2 HLA-A2+ screening . . . 54
2.2.3 Freeze/thawing of PBMC . . . 55
2.2.4 Preparation of serum samples . . . 55
2.2.5 Preparation of intrahepatic lymphocytes (IHL) . . . 55
2.3 Multiparametric Flow Cytometry . . . 56
2.3.1 BD TruCount Tubes for gMDSC absolute counts . . . 56
2.3.2 Surface staining of PBMC & IHL for MDSC frequency & phenotype . . . 57
2.3.3 Intracellular staining of PBMC & IHL for MDSC phenotype . . . 58
2.3.4 Staining for T cell/NK cell phenotype & functionality . . . 59
2.3.5 Detection of T cell cytokine production . . . 59
2.3.6 Analysis of regulatory T cells . . . 59
2.3.7 Identification of virus-specific CD8+ T cells . . . 61
2.4 ImageStreamX . . . 62
2.5 Amino Acid Composition Analysis . . . 62
2.5.1 Reagents . . . 62
2.5.2 Sample preparation . . . 62
2.5.3 High-pressure liquid chromatography - tandem mass spectrometry (HPLC-MS) . . . 63
2.5.4 Use of stable isotopes . . . 63
2.6 Serum Arginase I Quantification . . . 64
2.7 Suppression Assays . . . 64
2.7.1 Isolation of gMDSC by magnetic bead isolation . . . 64
2.7.2 Isolation of gMDSC by flow cytometry . . . 65
2.7.3 Staining with Vybrant® CFDA (CFSE) . . . 66
2.7.4 Co-culture: gMDSC with autologous PBMC for suppression of bystander T cell function . . . 66
2.7.5 Co-culture: gMDSC with autologous PBMC for detection of HBV-specific T cell suppression . . . 67
2.8 Co-culture: gMDSC with Primary Hepatic Stellate Cells (pHSC) . . . 67
2.8.1 Isolation of pHSC . . . 67
2.8.2 pHSC staining & co-culture . . . 68
2.9 Statistical Analysis . . . 68
2.10 Reagents . . . 68

3 gMDSC expand in chronic hepatotropic infections 71
3.1 Abstract . . . 71
3.2 Introduction . . . 73
3.2.1 Phenotypic identification of MDSC . . . 73
3.2.2 MDSC: cellular expansion & activation . . . 77
3.2.3 MDSC: in the context of chronic inflammation . . . 79
3.2.4 MDSC: in the context of viral infection . . . 80
3.3 Results . . . 82
3.3.1 Challenges in phenotypic identification of MDSC in CHB . . . 82
3.3.2 gMDSC are preferentially expanded in patients who sustain HBV replication without necroinflammatory liver damage . . . 86
3.3.3 gMDSC are transiently expanded in acute resolving HBV infection and decline at the onset of the hepatic flare . . . 93
3.3.4 gMDSC are also transiently expanded during spontaneous hepatic flares in HBeAg- CHB . . . 96
3.3.5 Absolute counts: gMDSC expand in CHB . . . 98
3.3.6 gMDSC also expand in chronic HCV infection . . . 100
3.3.7 gMDSC accumulate further in the diseased liver . . . 101
3.3.8 Potential factors driving the accumulation of gMDSC in the diseased liver 104
3.3.9 A potential interaction of gMDSC with hepatic stellate cells . . . 106
3.4 Conclusions & Discussion . . . 109

4 MDSC limit hepatic immunopathology in an arginase I-dependent manner 114
4.1 Abstract . . . 114
4.2 Introduction . . . 115
4.2.1 MDSC-mediated immune suppression . . . 115
4.2.2 A role for MDSC in amino acid metabolism . . . 117
4.2.3 Overview of the L-arginine metabolising enzyme arginase I . . . 123
4.3 Results . . . 125
4.3.1 gMDSC express high levels of arginase I . . . 125
4.3.2 The degranulation capacity of gMDSC is enhanced in CHB . . . 127
4.3.3 Serum arginase I levels are increased in CHB . . . 128
4.3.4 Circulating L-arginine levels are depleted in CHB . . . 129
4.3.5 Similarly to CHB, circulating levels of arginase I are increased, and levels of L-arginine are decreased in chronic HCV infection . . . 131
4.3.6 Levels of L-arginine recover on antiviral treatment in CHB . . . 132
4.3.7 MDSC potently suppress T cell responses . . . 134
4.3.8 The effect of gMDSC-mediated suppression *in vivo* during acute, resolving infection and spontaneous flares of HBeAg- CHB . . . 139
4.3.9 gMDSC potently suppress T cell function in an arginase I-dependent manner 141
4.3.10 Regulation of amino acid transporters on T cells affects their metabolic reprogramming in CHB . . . 142
4.4 Conclusions & Discussion . . . 145

5 Discussion and Outlook 149
5.1 Further unanswered questions relating to MDSC . . . 149
5.2 Can gMDSC induce regulatory T cells in CHB? . . . 151
5.3 Can MDSC produce immunosuppressive cytokines? . . . 155
5.4 Can MDSC modulate NK cell function in CHB? . . . 156
5.4.1 A potential role for the NKG2D pathway . . . 157
5.4.2 A potential role for the NKp30 pathway . . . 158
5.5 Can MDSC promote T cell exhaustion in CHB? . . . 159
5.5.1 Is bi-directional signalling via galectin-9 on gMDSC important in CHB? . 160
5.5.2 Can gMDSC promote T cell exhaustion through the PD-L1:PD-1 pathway? 162
5.6 What causes MDSC expansion & contraction? . . . 163
5.6.1 A role for death-ligands in MDSC contraction . . . 163
5.6.2 Differentiation of MDSC affects circulating populations of mature myeloid populations . . . 164
5.7 Further Exploration: gMDSC in animal models . . . 166
5.8 Future Outlook: the therapeutic potential for gMDSC . . . 167
5.9 Overview of potential gMDSC-mediated immune regulation in the context of CHB 168

Bibliography 203

Declaration of Authorship

I, Laura Jane Pallett, confirm that the work presented in this thesis is my own. Where information has been derived from other sources, I confirm that this has been indicated.

Signed: _____

Date: _____

Acknowledgements

The work included within this thesis could not have been done alone. As a result there are a number of people who need to be particularly acknowledged for their contributions, these have been detailed over the page.

But for now I need to make mention of one individual who has supported me throughout, both informally and formally: Mala Maini. Thank you Mala. I may have a ″unique‟ style but you have harnessed this to get the best out of me. You have always been available at the drop of a hat with a fabulous open door policy whilst being an excellent supervisor.

I would also like to take the chance to say a huge thank you to everyone who has been a part of the Maini lab over the four years or so I have been here (in no particular order): Anna, Simran, Dimitra, Uppy, Kasha, Abhi, Nick, Gaia, Antony, Jess, Itziar, Yang, Jia Ying, Ida, Wei-Chen, Jyoti and Kerstin. I would also like to take this opportunity to thank Richard Milne, who I owe a lot to, primarily for believing I would fit-in as part of the Maini lab and sending me to Mala after my two rotations at the Royal Free and for coining the phrase ″The Mainiacs‟ which at times we all most definitely are!

Finally I would like to thank all my fantastic friends, wonderful family and those closest to me everyday, you know who you are. THIS LITERALLY WOULD NOT HAVE HAPPENED WITHOUT YOU!

″Most people say that it is the intellect which makes a great scientist. They are wrong: it is character.‟

Albert Einstein.

Specific Acknowledgements

A special scientific thank you must be extended to a number of different people, for a number of different reasons, just some of those individuals are as follows:

- *Alexander Rodgers*, *Lesley Winter*, *Damilola Otiko*, *Dr.Ingrajit Ghosh*, *Dr. Richard Gilson*, *Prof. William Rosenberg*, *Dr. Patrick Kennedy*, & especially *Prof. Mala Maini* and *Dr. Upkar Gill* for their continued recruitment, monitoring and maintenance of our patient cohorts and their clinical information where necessary. An extended thank you must go to *Dr. Upkar Gill* for the provision of valuable liver tissue, after clinical biopsy, from patients with CHB and chronic HCV infection.
- *Dr. Richard Milne* and *Dr. Eleni Nastouli* and the Clinical Virology Departments at the Royal Free Hospital and University College Hospital for CMV serology and HBsAg quantification.
- *Dr. Pascale Kropf* for her invaluable advice of on the assessment of gMDSC arginase I release and support during the early days of this project.
- *Dr. Niclas Thomas* for sharing his mathematical skill set and invaluable advice on statistical assessment of our complex dataset (extending to multivariant analyses and hierarchical clustering). And for proof-reading and editing of initial drafts, especially for minimising my continued and unnecessary use of ″as such‟ before allowing them to be seen by anyone else!
- *Jia Ying Toh* - a BSc student of mine who spent a large number of hours staining cells for analysis as part of this thesis alongside her own project.
- *Dr. Kasha Singh* - a fellow member of the group - for all her invaluable help and advice with the primary hepatic stellate cell (pHSC) co-culture experiments and for providing data on the capacity of pHSC to produce a range of chemokines and cytokines.
- *Harsimran Singh* - another fellow member of the group - who spent many an hour establishing a protocol for pHSC isolation, and for help isolating/freezing pHSC used during this study.
- *Mr. Guiesppe Fusai* for the provision of liver tissue from surgeries at the Royal Free Hospital used for the isolation of pHSC by Simran and Kasha.
- *Dr. Muzzliffa Haniffa* not only for her ideas and preliminary data that helped in conceiving this project but also for giving us the gMDSC cytospins for use as part of this thesis and

publication.

- *Mr. Francis Roberston and Mr. Brian Davidson* - for the invaluable access to non-diseased liver tissue from transplant surgery, at all times of the day and night.
- And finally a huge thank you to all the patients and healthy control volunteers who have donated blood, often multiple times, throughout the study.

Funding

This work was funded by MRC grant G0801213 to Mala K. Maini, MRC Bench to Bedside studentship to Laua J. Pallett, MRC/AStar grant G0901374 to Mala K. Maini and Antonio Bertoletti, WT Senior Investigator Award to Mala K. Maini, Australian MRC fellowship to Kasha P. Singh.

List of Abbreviations

4E-BP1	eukaryotic translation initiation factor 4E-binding protein 1
AAV-HBV	adeno-associated virus-HBV
ADC	arginine decarboxylase
AdHBV	adenoviral-HBV
ALT	alanine transaminase
AGAT	arginine:glycine amidinotransferase
ARG1	arginase I
APC	antigen presenting cell
APOBEC3*	apolipoprotein B mRNA editing enzyme, catalytic polypeptide-like 3*
ATP	adenosine triphosphate
BCG	Bacillus Calmette-Guerin
Bim	Bcl2-interacting mediator
BFA	brefeldin A
Breg	regulatory B cell
cccDNA	covalently closed circular DNA
CD	cluster of differentiation
CD3ζ	CD3 zeta
CFSE	carboxyfluorescein succinimidyl ester
CMV	cytomegalovirus
CTLA-4	cytotoxic T-lymphocyte-associated protein
CHB	chronic hepatitis B
CXCR*	chemokine receptor *
DC	dendritic cell
DMSO	dimethyl sulfoxide
DNA	deoxyribonucleic acid
EBV	epstein bar virus
EDTA	ethylenediamine tetraacetic acid
eIF2α	eukaryotic translation initiation factor 2 alpha
ELISA	enzyme-linked immunosorbent assay
ER	endoplasmic reticulum
FasL	Fas-ligand
FBS	foetal bovine serum
FcR	FcR blocking reagent
FOXP3	forkhead box P3
Gal9	galectin-9
GCN2	general control nonrepressible 2
GM-CSF	granulocyte macrophage colony-stimulating factor
gMDSC	granulocytic myeloid-derived suppressor cells
HAV	Hepatitis A virus
HBV	Hepatitis B virus
HBeAb	Hepatitis B virus secreted e antigen-specific antibody
HBsAb	Hepatitis B virus surface antigen-specific antibody
HBcAg	Hepatitis B core antigen
HBeAg	Hepatitis B precore-core (secreted e) antigen

HBsAg	Hepatitis B surface antigen
HBx	Hepatitis B regulatory X protein
HCC	hepatocellular carcinoma
HCV	Hepatitis C virus
HDV	Hepatitis delta virus
HEPES	hydroxyethyl piperazineethanesulfonic acid
HEV	Hepatitis E virus
HIV	human immunodeficiency virus
HLA	human leukocyte antigen
HPLC-MS	high pressure liquid chromatography mass spectrometry
HSC	hepatic stellate cell
ICAM1 (CD54)	intercellular adhesion molecule 1
IDO	indoleamine 2,3-dioxygenase
IFNα	interferon alpha
IFNβ	interferon beta
IFNγ	interferon gamma
IHL	intrahepatic lymphocytes
IL-*	interleukin *
iMATE	intrahepatic myeloid cell aggregates for T cell clonal expansion
iNOS	inducible nitric oxide
iTreg	inducible regulatory T cell
JAK	janus kinase
KC	Kupffer cells
L-arg	L-arginine
L-cys	L-cysteine
L-trp	L-tryptophan
L-phe	L-phenylalanine
LCMV	lymphocytic choriomeningitis virus
LSEC	liver sinusoidal epithelial cell
LPS	lipopolysaccaride
mAb	monoclonal antibody
M-CSF	macrophage colony-stimulating factor
MDSC	myeloid-derived suppressor cells
mMDSC	monocytic myeloid-derived suppressor cells
MFI	mean fluorescence intensity
MHC-I	major histocompatibility class I
MHC-II	major histocompatibility class II
MS	mass spectrometry
NK	natural killer cell
NKT	natural killer T cell
NHS	National Health Service
NTCP	sodium taurocholate cotransporting polypeptide
mTOR	mammalian target of rapamycin
nTreg	naturally occurring regulatory T cells
nor-NOHA	hydroxy-nor-l-arginine
NOS*	nitric oxide synthase *
ONOO-	peroxynitrite
ORF	overlapping reading frames
p70 S6	70kDa ribosomal protein S6 kinase
PBS	phosphate buffered sulphate
PBMC	peripheral blood mononuclear cells
PCA	principal component analysis
PCR	polymerase chain reaction
PD-1	programmed death 1
PD-L1	programmed death ligand 1
peg-IFNα	pegylated interferon alpha
PFA	paraformaldehyde
pgRNA	pre-genomic RNA

pHSC	primary hepatic stellate cell
PMA	phorbol 12-myristate 13-acetate
PRR	pattern recognition receptor
rcDNA	relaxed circular DNA
RNA	ribonucleic acid
RNS	reactive nitrogen species
ROS	reactive oxygen species
rpm	revolutions per minute
R.T.	room temperature
S100A*	S100 calcium-binding protein A*
ssDNA	single stranded DNA
STAT*	signal transducer and activator of transcription *
TCA	trichloroacetic acid
TCR	T cell receptor
TDO	tryptophan 2,3-dioxygenase
TGFβ	transforming growth factor β
Tim-3	T cell immunoglobulin- and mucin-domain-containing molecule 3
TLR*	toll-like receptor*
TNFα	tumour necrosis factor α
TRAIL	tumor necrosis factor (TNF)-related apoptosis-inducing ligand
TRAIL R2	TRAIL receptor 2
Treg	regulatory T cell
type-I IFN	type I interferon
UCH	University College hospital
VEGF	vascular endothelial growth factor
WHO	World Health Organisation

List of Publications and Abstracts

PUBLICATIONS

- **Pallett L.J., Gill U.S., Jover-Cobos M., Schurich A., Singh K., Thomas N., Das A., Chen A., Fusai G,, Bertoletti A., Kennedy P.T., Davies N., Haniffa M., Maini M.K.**
  Arginase-dependent metabolic regulation of hepatic immunopathology by myeloid-derived suppressor cells
  submitted, April 2014

- **Heiberg I.L., Pallett L.J., Winther T.N., Hogh B., Maini M.K., Peppa D.**
  Defective natural killer cell antiviral capacity in paediatric HBV infection
  submitted, August 2014

- **Schurich A., Pallett L.J., Lubowiecki M., Singh H.D., Gill U.S., Kennedy P.T., Nastouli E., Tanwar S., Rosenberg W., Maini M.K.** The third signal cytokine IL-12 rescues the anti-viral function of exhausted HBV-specific CD8 T cells
  PLoS Pathogens, (2013), 9(3)

- **Peppa D., Gill U.S., Reynolds G., Easom N.J., Pallett L.J., Schurich A., Micco L., Nebbia G., Singh H.D., Adams D.H., Kennedy P.T., Maini M.K.** Up-regulation of a death receptor renders antiviral T cells susceptible to NK cell-mediated deletion
  Journal of Experimental Medicine, (2013), 210(1) 99-114

ABSTRACTS

- **Pallett L.J., Haniffa M., Schurich A., Gill U.S., Davies N., Jover-Cobos M., Das A., Gilson R., Ghosh I., Kennedy P.T., Bertoletti A., Maini M.K.** Myeloid -derived suppressor cells mediate immunotolerance in chronic hepatitis B (CHB) through arginine deprivation
  Journal of Hepatology, (2014), Supplement No.1(60) S109

Abstract

The liver provides a highly immunotolerant environment, that is exploited by hepatotropic viruses such as Hepatitis B virus (HBV), which establishes persistent infection in more than 350 million people worldwide. In this thesis the potential for myeloid-derived suppressor cells (MDSC) to exert metabolic regulation in this setting has been investigated. We found a mean approximate 9-fold expansion of granulocytic MDSC (gMDSC) in patients with chronic HBV infection (CHB) compared to uninfected, healthy controls ($p<0.001$). The most striking increases were seen in patients replicating HBV in the absence of immunopathology ($p<0.01$). gMDSC expressed high levels of the chemokine receptor, CXCR1, providing the potential for them to be chemoattracted by liver-derived interleukin-8 (IL-8); consistent with this, they were further enriched in the intrahepatic compartment. gMDSC from patients with CHB expressed increased amounts of arginase I, correlating with an increase in serum levels of this enzyme ($p<0.01$). Arginase I metabolises the conditionally essential amino acid L-arginine that is required for proliferating T cells; in line with this was an observed decrease in circulating L-arginine, particularly in those patients without liver inflammation. Liver pathology in CHB is amplified by the recruitment and activation of bystander (non-HBV-specific) T cells; therefore the potential of gMDSC to down-regulate such responses was explored. Purified gMDSC from patients with CHB potently inhibit the expansion of bystander T cells capable of producing pro-inflammatory cytokines or mediating cytotoxicity. This inhibition was blocked using an arginase I-specific inhibitor, N-hydroxy-nor-arginine (nor-NOHA). Taken together, these data demonstrate the capacity for expanded arginase I-expressing gMDSC to regulate liver immunopathology in CHB by depriving T cells of L-arginine.

List of Figures

1.1 Global prevalence of HBV infection 20
1.2 HBV genome 21
1.3 HBV replication cycle 22
1.4 Course of acute HBV disease 25
1.5 Overview of selected mechanisms of the immune response in CHB 29
1.6 T cell exhaustion 30
1.7 Natural course of CHB 33
1.8 Liver micro-architecture 37
1.9 Myeloid cell development & differentiation 44

2.1 Dextramer gating strategy 61
2.2 gMDSC FACSAria purity 65

3.1 Impact of the discovery of MDSC 73
3.2 Identification of MDSC by flow cytometry 83
3.3 MDSC are cryosensitive 84
3.4 MDSC viability is enhanced in heparin 85
3.5 gMDSC expand in CHB 87
3.6 Percentage of myeloid cells remains unchanged in CHB 88
3.7 MDSC expand in immunotolerant patients with no liver inflammation 90
3.8 Hierarchical clustering reveals clear stratification of CHB disease phases 91
3.9 gMDSC frequencies according to clinical parameters 92
3.10 PCA of gMDSC frequencies based on three viral parameters 94
3.11 gMDSC frequencies during acute resolving HBV infection 95
3.12 gMDSC frequencies during acute resolving HBV infection II 96
3.13 gMDSC frequencies during an hepatic flare in CHB 97
3.14 gMDSC frequencies during an hepatic flare in CHB II 98

3.15 Absolute number increase in gMDSC in CHB 99
3.16 Analysis of absolute count of gMDSC by disease phase 99
3.17 gMDSC expand in HCV 101
3.18 gMDSC accumulate 2-fold in the liver in HBV & HCV infection 102
3.19 gMDSC do not accumulate in viral hepatitis and in tumours 103
3.20 Chemokine receptor expression on MDSC subsets 105
3.21 MDSC express CXCR2 106
3.22 pHSC produce IL-6 and IL-8 *ex vivo* 107
3.23 pHSC promote gMDSC survival/accumulation 108

4.1 Mechanism of MDSC function 116
4.2 Metabolism of the amino acid L-arginine 118
4.3 Effect of amino acid starvation on T cell functions 120
4.4 gMDSC express arginase I 126
4.5 Enhanced arginase I expression in intrahepatic gMDSC 127
4.6 gMDSC express CD63 128
4.7 Concentration of arginase I in the serum in CHB 129
4.8 L-arginine depletion in CHB 131
4.9 L-arginine depletion in HCV 132
4.10 L-arginine levels recover on antiviral treatment 133
4.11 gMDSC decline on antiviral therapy 134
4.12 gMDSC are capable of HBV-specific suppression: magnetic-bead enriched gMDSC 135
4.13 gMDSC are capable of bystander suppression: magnetic-bead enriched gMDSC . 137
4.14 gMDSC inhibit T cell proliferation and CD3ζ expression 138
4.15 gMDSC are capable of suppression: FACS sorted gMDSC 139
4.16 Effect of L-arginine on T cells *in vivo* 140
4.17 gMDSC drive L-arginine deprivation *in vivo* 141
4.18 gMDSC suppress T cells in an arginase I-dependent manner 142
4.19 Differential CD98 expression on T cells in CHB 143
4.20 Differential CD98 expression on virus specific T cells in CHB 144

5.1 gMDSC do not induce regulatory T cell subsets 153
5.2 Suppressive cytokine induction by gMDSC 154
5.3 gMDSC produce the immunosuppressive cytokine TGFβ 156
5.4 gMDSC from patients with CHB express MICA/B 158
5.5 NKp30 expression on NK cells in relation to gMDSC 159

5.6 gMDSC express galectin-9 161
5.7 Galectin-9 expression correlates with arginase I production 162
5.8 gMDSC express the PD-1 ligand, PD-L1 163
5.9 Mature myeloid populations are altered in CHB 165
5.10 Overview of potential MDSC-mediated immune regulation 170

List of Tables

2.1 Central London cohort details 53

2.2 East London cohort details 53

2.3 Specific reagent details: surface MDSC mAb 58

2.4 Specific reagent details: intracellular MDSC mAb 59

2.5 Specific reagent details: surface T cell/NK cell antibodies 60

2.6 Specific reagent details: intracellular T/NK cell antibodies 60

2.7 Specific reagent details: dextramer information 61

2.8 Reagent information 68

3.1 Phenotypic marker expression on MDSC subsets 76

Chapter 1

Introduction

1.1 50 Years of HBV

Baruch ″Barry‟ Blumberg (1925-2011), initially discovered the Hepatitis B virus (HBV) in 1965 [1] and subsequently worked on its identification, origin and spread, for which he received the Nobel Prize in Physiology or Medicine on 13 December 1976 [2]. Research started by Blumberg, and continued by others, culminated in the implementation of diagnostic testing and the later development of an effective and fully-approved genetically engineered recombinant vaccination (1986). The discovery of HBV in the mid-1960s led to the virus being initially named ″Australia Antigen‟, because this work took advantage of a reaction between an Australian Aborigine's blood with the serum of an American haemophilia patient. However, in 1967 the ″Australia Antigen‟ was renamed HBsAg after it was reported to be part of the virus. The work of Blumberg and colleagues triggered research leading to the subsequent identification, prevention and treatment of the four other hepatitis viruses: Hepatitis A virus (HAV) in 1973 [3], Hepatitis D virus (HDV) in 1977 [4], Hepatitis E virus (HEV) in 1983 [5], and Hepatitis C virus (HCV) in 1989 [6]. Combined, these five viruses are responsible for the majority of the world's cases of acute and chronic hepatitis [7].

Despite the extensive work of numerous scientists and clinicians over the last 50 years, infection with HBV remains a significant global health problem. The World Heath Organisation (WHO) estimates that two billion people have been infected, with more than 350 million individuals continuing to suffer from ongoing chronic infection. Of the five hepatitis viruses HCV remains the sole virus for which a successful vaccine is unavailable [7]. However great progress has

been made recently in the HCV field, in terms of both treatment and a vaccination [8]. An effective prophylactic vaccine for HBV therefore does exist, although approximately 600,000 people worldwide still die annually from complications attributed to HBV infection. These deaths are the result of ongoing bouts of liver inflammation leading to progressive fibrosis extending to cirrhosis, and ultimately liver failure and hepatocellular carcinoma (HCC) [9]. The existing therapy regimens for HBV rarely achieve full eradication of the virus from the patient and as yet no successful therapeutic vaccine has been developed through to the clinic [10]. Despite all of this, the UK has yet to implement a universal vaccination programme. Ensuring HBV remains a virus that requires clinical attention and continued research.

1.2 Overview of Hepatitis B Virus

1.2.1 HBV epidemiology, treatment and beyond

Transmission of HBV can occur via a number of different routes; parenteral (for example: from illicit drug use, from transfusion products and/or dialysis), sexual and perinatal (from a carrier mother to neonate). Perinatal transmission of HBV typically leads to chronic infection (chronic HBV infection: CHB), whereas in the majority of cases where infection is acquired during adulthood, a successful immune response is elicited resulting in disease resolution and subsequent life-long immunity [11, 12, 13, 14, 15, 16, 17]. Numerically, and more specifically, this equates to HBV persistence in approximately 1.5% of infected adults, 20-30% of those infected as young children and up to 90% of perinatally infected individuals [18].

The frequency and mode of transmission of HBV infection varies geographically (figure 1.1). For example, the carrier rate in western Europe and in the USA is low, between 0.1-2%, increasing in areas of high endemicity (sub-Saharan Africa and parts of Asia), to as high 20% [18]. The most common route of infection also varies between areas; transmission of the virus in areas of high endemicity is largely perinatally or during early childhood. In contrast, infection tends to occur during adulthood in low prevalence areas. Given recent changes in migration patterns into the UK, an area considered to be of low prevalence, the majority of new infections presenting in the clinic tend to be from individuals born in countries with intermediate - high prevalence. Data published by Public Health England detailing a study in London not only confirmed that the main burden of infection with HBV relates to chronicity and its associated clinical events, but also reported that 19 out of every 20 women testing positive for HBV in antenatal clinics were born abroad (data quoted from Public Health England, 2012:

http : *//www.hpa.org.uk/webc/HPAwebFile/HPAweb*$_C$/1317141035027 - 06/09/2014).

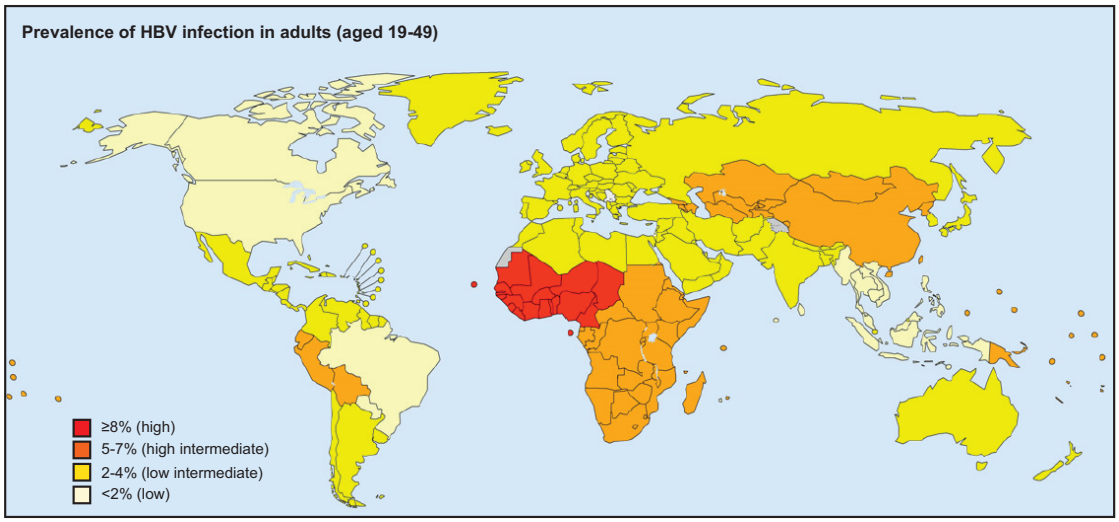

Figure 1.1: Map showing the global prevalence of HBV infection.

Illustration of global endemicity of HBV infection, based on estimated and categorised HBsAg prevalence in adults aged 19-49 for 2005. Adapted from Ott *et al.* [9].

Patients with CHB often require antiviral therapy, which currently tends to be a lifelong commitment. As a result treatment regimens are not only associated with a high economic burden but also viral resistance the possibility of drug toxicity in the patient. The current clinical paradigm for treatment of chronic infection is to reduce the risk of progressive chronic liver disease (progression through to severe cirrhosis and HCC). Current treatment strategies approved by the NHS include a short course of pegylated interferon-alpha (peg-IFNα) and use of antivirals (for example: tenofovir, entecavir, lamivudine) [19]. What is however under current debate in the field, and remains controversial, is the concept of treating earlier in the course of disease to reduce ongoing viral transmission and potentially stimulating immune control to enhance cure rates. This involves looking more closely at the potential to treat younger patients who typically have extremely high levels of viral replication without any clinically overt liver disease (immunotolerant individuals, discussed further on in section 1.3.4). These patients constitute a large infectious reservoir. This question is of particular relevance to the work presented in this thesis.

1.2.2 HBV virology

HBV is a non-cytopathic, hepatotropic virus that is a member of the *Hepadnaviridae* family. This family also includes the following: duck Hepatitis virus, woodchuck Hepatitis virus and

the virus causing ground squirrel hepatitis [20]. HBV is traditionally classified into nine distinct genotypes (A-I) based on divergence in the viral sequence. The prevalence of specific genotypes also varies geographically, and may correlate with clinical outcome and response to treatment.

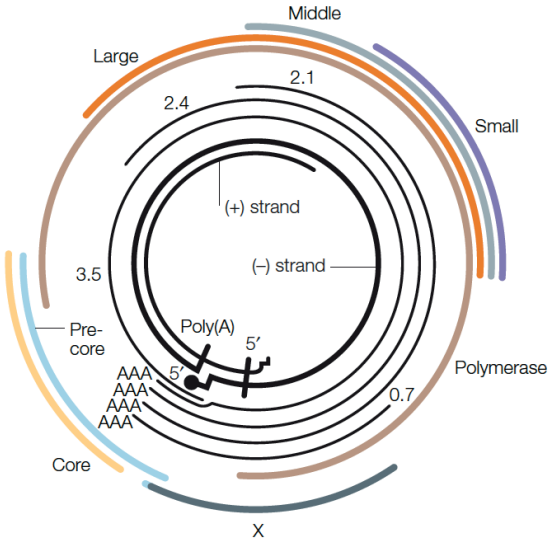

Figure 1.2: Schematic of the HBV genome.

The innermost circles (black) represent the full length minus (−) strand (with the terminal protein attached to its 5' end) and the incomplete plus (+) strand of the HBV genome. The outermost coloured lines represent the translated HBV proteins (described in section 1.2.2): large, middle and small HBV surface proteins, polymerase protein, X protein, and core and pre-core proteins. Adapted from Rehermann & Nascimbeni [17].

HBV has a relatively small genome of approximately 3200 nucleotides encoding four overlapping reading frames (figure 1.2). Until recently, the specific details of HBV entry (infection of hepatocytes) was less well understood; the hepatocyte-specific receptor for HBV had not been correctly identified. It was believed to involve viral attachment to liver cell-associated heparan sulphate proteoglycans [21, 22]. However, a recent study by Yan *et al.* [23] implicated a novel role for an already well described bile acid transmembrane transporter exclusively expressed in the liver (on the basolateral membrane of hepatocytes) in the process of viral entry. This previously elusive HBV hepatocyte receptor is the sodium taurocholate cotransporting polypeptide (NTCP) [23] (figure 1.3). The use of experimental hepatocyte infection models expressing the NTCP protein will no doubt enhance the study of HBV, providing for the first time a semi-physiological *in vitro* system.

After viral entry upon NTCP binding, the process of viral un-coating releases relaxed, partially

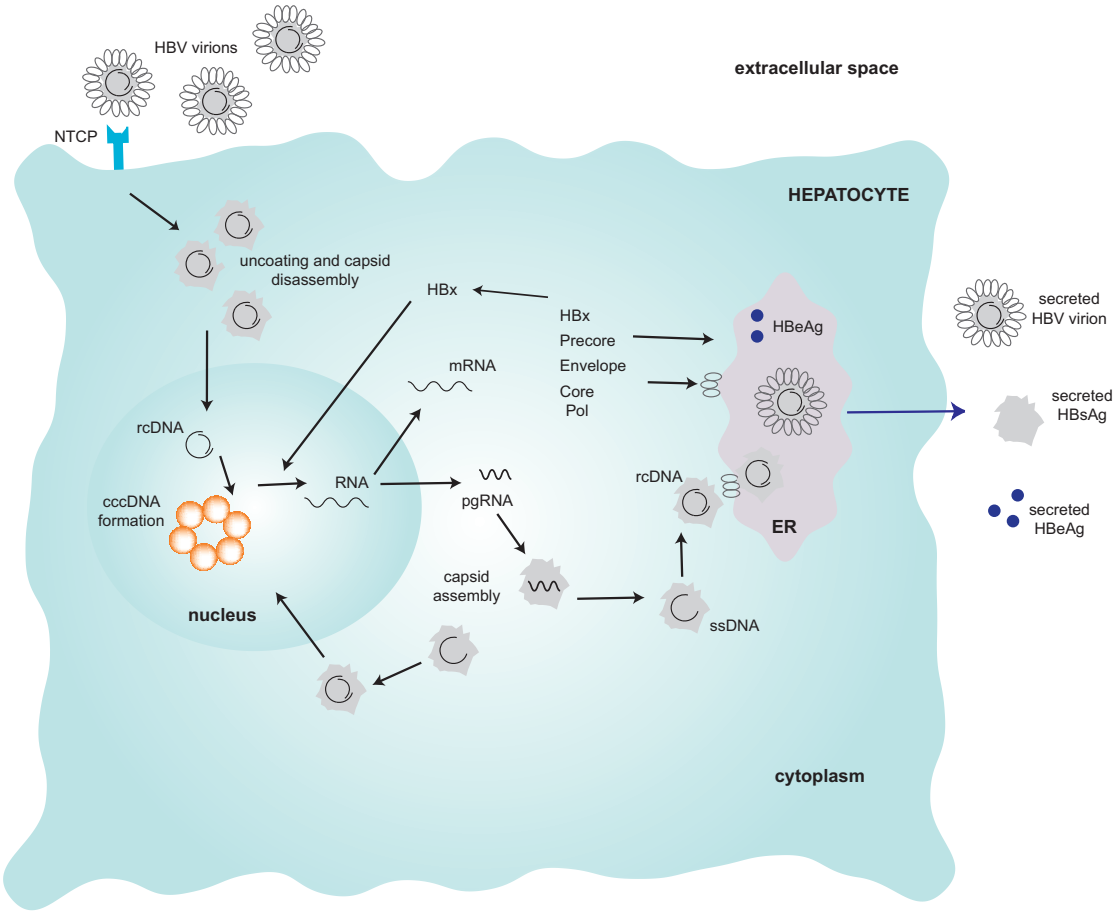

Figure 1.3: Schematic of the HBV replication cycle.

Schematic depicting the life cycle of HBV after entry into the hepatocyte via the bile acid transporter sodium taurocholate cotransporting polypeptide (NTCP). Full details of the HBV replicative life cycle are detailed in the main text in section 1.2.2. Abbreviations used: covalently closed circular DNA (cccDNA), relaxed, partially double stranded DNA (rcDNA), single stranded DNA (ssDNA), endoplasmic reticulum (ER). Adapted from Urban *et al.* [24].

double stranded circular DNA (rcDNA) into the cytoplasm of the hepatocyte (figure 1.3). The HBV genome then translocates to the nucleus, where conversion of the rcDNA into covalently closed circular DNA (cccDNA) minichromosomes occurs. cccDNA act as an ongoing viral template whereby its production establishes a reservoir of self-amplifying virus, which can promote life-long infection [25]. Persistence of cccDNA is one of the main obstacles to overcome in the development of future treatment regimes. Thus, the current goal is a directed therapy that eliminates or restricts the formation of cccDNA, as its presence alone can lead to reactivation of HBV in patients with clinically inactive disease [26]. One recent report by Lucifora *et al.* [27] has suggested new targets with the potential for eradication of such cccDNA reservoirs. The authors demonstrated that by activating lymphotoxin-β receptor, the subsequent up-regulation of apolipoprotein B mRNA editing enzyme, catalytic polypeptide-like 3A (APOBEC3A) and

APOBEC3B cytidine deaminases promotes the deamination and thereby the destabilisation of cccDNA, thus potentially preventing the reactivation of HBV [27].

Following the formation of cccDNA, transcription of the four viral RNAs occurs driven by a host polymerase II enzyme (Pol-II). These newly produced viral RNAs, including the pre-genomic RNA (pgRNA), are subjected to nuclear export for mRNA translation. The four viral mRNAs (shown in figure 1.2) function as follows:

1. the pre-core protein; transported to the endoplasmic reticulum (ER) under direction from a leader sequence, for processing and excretion as the non structural protein - Hepatitis B precore-core (secreted e antigen: HBeAg),
2. HBX protein; which activates HBV promoter activity in the cytoplasm via interaction with transcription factors capable of nuclear entry, making it essential for viral replication,
3. the envelope proteins; of 3 different sizes, small (S), medium (M) and large (L) which transverse the ER membrane as integral membrane proteins, and
4. the core and polymerase proteins which are key to capsid assembly around pgRNA, within which the first single-stranded DNA (ssDNA) is produced.

After translation, the newly formed ssDNA then functions as the template for second-strand synthesis, resulting in nucleocapsid formation containing rcDNA. Mature DNA-containing capsids are then either released from the ER membrane upon interaction with the three, newly formed, envelope proteins, triggering internal budding of secreted infectious virions or returned to the nucleus for cccDNA amplification [17, 28, 24, 29, 30].

Contrary to all other known mammalian DNA viruses, HBV replicates through reverse transcription of an RNA intermediate. The process of reverse transcription is inherently error-prone. Consequently, this step is responsible for the emergence of highly heterogeneous viral populations known as quasispecies. Quasispecies include those containing mutations that affect the production of HBeAg [25]. This can be seen clinically in a subset of patients who re-enter an active phase of disease with increased replication despite the lack of HBeAg, often after decades of inactivity and seroconversion (refer to section 1.3.4).

Another unique feature of HBV is its capacity to secrete large amounts of protein, both circulating HBeAg and Hepatitis B surface antigen (HBsAg), which do not contain the full HBV genome and often outnumber infectious virions by a factor of 10^4 - 10^6 [31]. These two secretable HBV

antigens are believed to be immunomodulatory. They have been proposed to have the capacity to divert the immune response and protect the virus from ongoing immune-mediated deletion.

1.3 Natural History of HBV Infection

HBV is highly replicative in the liver. Reportedly up to 100% of hepatocytes are infected, compared to infection with HCV which infects up to approximately 50% of hepatocytes [32]. However recent work by our group and others suggests this may not be strictly true, indicating HBV infection in the liver may be more localised, even ″patchy‟, compared to previous reports, with some areas remaining uninfected. In either HBV or HCV infection, however, the viruses themselves are generally not directly cytolytic; the ongoing liver injury associated with persistent infection is the result of continued immune mediated attempts to control infection [33, 34, 35]. This concept is discussed in more detail in sections 1.3.1 and 1.3.3. The work included within this thesis focuses on patients with CHB. However, the immune response in acute infection is important to consider as it provides a paradigm of a successful immune response to this virus.

1.3.1 Acute, resolving HBV infection

Much of what we know about HBV infection comes from studies of acute HBV infection in humans, utilisation of HBV infection models in chimpanzees, and the use of transgenic mouse models. During acute infection, HBV DNA increases, and subsequently declines before the peak onset of the clinical symptoms of acute hepatitis (increase in serum alanine transaminase (ALT) levels, an enzyme released by hepatocytes upon damage and the development of jaundice). Similarly the decline in HBV DNA levels occurs prior to the induction of an adaptive T cell-mediated immune response (figure 1.4) [36, 37, 38, 39]. Due to this delayed clinical presentation, obtaining immunological data from the acute phase of HBV infection in humans is challenging. It is also not usually ethically feasible to study early immunological events in the liver.

In addition to the issue of capturing early acute infection in humans, there is a lack of accessible and widely available animal models and/or reliable *in vitro* models for HBV infection that do not rely on the use of transformed hepatocyte cell lines. The animal models currently available for the study of HBV infection are hampered by a number of issues. These include the costs and the ethical concerns relating to their use (particularly the use of chimpanzees), the availability and production of appropriate reagents for analysis (particularly the case with the woodchuck model) and technical difficulties arising from the derivation of often complex transgenic murine

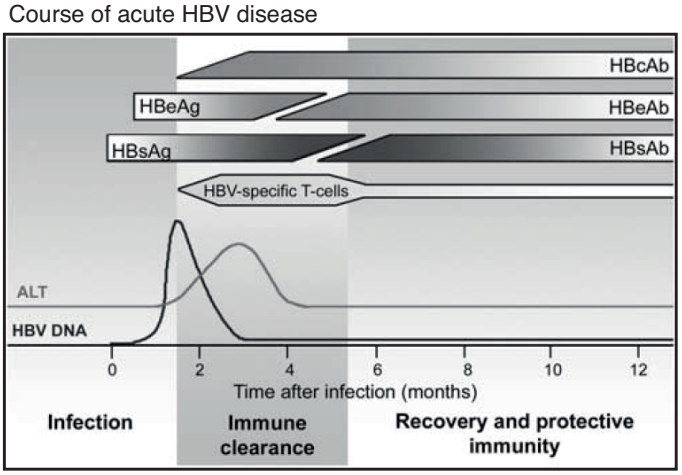

Figure 1.4: Clinical course of acute, resolving HBV infection.

Typical fluctuations observed in clinical parameters over the course of acute viral infection, through to resolution, including viral load (HBV DNA), and degree of liver inflammation (serum ALT). Resolution provides life-long immunity and is characterised by effective immune control rather than complete eradication of the virus. Resolution is typically seen within six months of initial viral infection. Protection is provided by the induction of neutralising HBV surface antigen-specific antibodies (HBsAb) and the activation and expansion of functional HBV-specific T cells. Adapted from Chang & Lewin [38].

models [40] .

Early in the antiviral response innate immune activation is essential; the production of type I interferons (type-I IFN) acts as a first-line mechanism in response to pathogenic detection. An initial up-regulation of a type-I IFN response is observed with viruses such as human immunodeficiency virus (HIV) and HCV. Unusually, evidence suggests that this is not necessarily the case upon infection with HBV, therefore HBV is commonly referred to as a ″stealth‟ virus, largely attributable to the limited activation of an early innate immune response. A pivotal study of experimental HBV infection in chimpanzees carried out by the Chisari group demonstrated a lack of up-regulated type-I IFN-related genes in the liver after entry and the initial expansion phase of infection [41]. These findings were corroborated in human studies where levels of circulating pro-inflammatory cytokines, including type-I IFN, were almost undetectable in patients during early acute HBV infection compared to patients infected with HCV or HIV [39, 42]. These same patients also lacked the common flu-like symptoms. The apparent lack of type-I IFN induction suggests the virus has an inherent ability to evade innate recognition. This may be due to its own replication strategy (previously described in section 1.2.2), using cccDNA that is able to hide in the nucleus from innate sensing mechanisms. More recent data has began to challenge this viewpoint. One line of evidence argues that HBV is in fact successfully recognised by innate

immunity and therefore capable of eliciting a type-I IFN response, but that this response is subsequently rapidly suppressed [39, 33].

Another feature of infection with HBV is the notable delay in viral amplification/replication and therefore spread of the virus during early infection compared to most viruses which immediately enter a phase of logarithmic propagation post infection. In a typical case of acute HBV infection HBV DNA (using a polymerase chain reaction: PCR) is detectable, albeit at very low levels, during early infection, but remains low, not peaking until approximately six weeks post infection. Serum HBV DNA levels dramatically decrease (by approximately 90%) before the detection of liver disease (increased serum ALT). Most HBV DNA is cleared from the liver (and the blood) of experimentally infected chimpanzees prior to the detection of a lymphocytic infiltrate made up of both HBV-specific and non-HBV-specific T cells, and evidence of liver damage [34]. HBV-specific CD4+ and CD8+ T cells are commonly detectable in line with the exponential increase in viral replication [37, 43, 39]. Depletion of the CD8+ T cell compartment following acute infection of chimpanzees results in viral persistence, demonstrating the importance for HBV-specific CD8+ T cell in viral clearance.

The majority of virus is however cleared by non-cytopathic mechanisms, maintained by the production of key cytokines interferon gamma (IFNγ) and tumour necrosis factor alpha (TNFα), secreted by a number of cells, including CD8+ T cells [35, 44]. Recruitment of HBV-specific CD8+ T cells into the liver is driven by chemokines, such as CXCL10 and upon platelet activation [45] to kill infected hepatocytes. Platelets adhere to the sinusoid via CD44, providing aggregates for incoming CD8+ T cells to ″dock‟ to (Matteo Iannacone - personal communication). Evidence also suggests that production of these cytokines can actively down-regulate HBV replication. IFNα, IFNβ or TNFα non-responsive mice fail to control HBV replication [46]. The effects of these cytokines is through multiple mechanisms including the destabilisation of the viral capsid, degradation of viral proteins and the post-transcriptional degradation of viral DNA. This recruitment of HBV-specific T cells into the liver leads to the subsequent recruitment of the non-antigen-specific cellular infiltrate that amplifies liver damage [47].

Following successful control of vireamia, HBsAg is lost from the blood and Hepatitis B surface antigen-specific antibodies (HBsAb) become detectable (figure 1.4), alongside maturation of the HBV-specific CD8+ cells into memory cells that persist long after viral control. Together they mediate protection against subsequent HBV reactivation in the steady-state [48]. The life-long

immunity resulting from HBV resolution is increasingly recognised to be the result of ongoing immune control rather than the complete eradication of the virus, leaving the potential for reactivation under conditions of immunosuppression (for example co-infection with HIV, or following transplantation) [16].

A co-ordinated approach of lymphocytic cytokine production and direct cytolytic function on infected hepatocytes promotes viral control. But what is essential is the balance between immune activation to control the virus and an attempt to maintain low levels of collateral cell-mediated liver damage once immune activation has occurred. The inability to control this balance forms the basis of CHB pathology.

1.3.2 Chronic infection & immune failure maintaining chronicity

The fact that control of HBV infection occurs in more than 95% of those infected as adults [19], provides evidence to support the ability of the immune system to successfully deal with the virus. Although immune control is plausible in all cases, there still remains an issue of chronicity in the remaining $\sim 5\%$ of infected adults or those where infection was acquired early in life. Understanding the inherent ability and co-ordination of both the innate and adaptive immune responses during control of infection, and harnessing such responses forms the basis of targeted strategies in the development of future immunotherapeutics. Given that the goal for HBV immunotherapeutics is still some way off, it is worth considering how the HBV-specific immune response required to drive viral clearance, is markedly diminished in patients with CHB [49, 47]. Mechanisms of immune dysregulation in CHB have yet to be fully elucidated and as a result are not fully understood. What is well known however, is that failure of the immune response to control vireamia is multi-factorial and includes:

- HBV-specific immune suppression,
- the continued production of stable forms of HBV,
- the continued presence of cccDNA (clinically measured as the presence of HBsAg) and,
- viral infection in the liver, a known immunologically privileged site.

A characteristic feature of persistent infections is a dysfunctional, weak and mono-specific T cell response. This is particularly true for patients with CHB who have a profoundly depleted HBV-specific adaptive immune response, characterised by very few detectable HBV-specific CD8+

T cells *ex vivo* [47, 49]. In particular CD8+ T cells directed against the core epitope (region core 18-27) are almost undetectable in HBeAg positive chronic carriers [50]. In individuals with high viral loads and extensive liver damage the circulating HBV-specific CD8+ T cells that are present have a markedly decreased proliferative capacity, compared to those with low level viral replication, in combination with minimal or absent liver disease [47]. The reduction in T cell proliferation and functionality seen in CHB is not unique, and is consistent with responses observed in animal models of other chronic viral infection, specifically in the clone 13 strain of lymphocytic choriomeningitis virus (LCMV) infection model where there is a decrease in TNFα and IFNγ expressing CD8+ T cells [51].

Work over the last few years by our group and others have described multiple mechanisms for immune dysfunction in CHB. These include a study using an unbiased gene expression profiling approach which led to the identification of an up-regulation of the pro-apoptotic Bcl-2 interacting mediator (Bim), which resulted in the description of Bim-mediated attrition of T cells as a key mechanism decreasing HBV-specific T cell numbers [52]. The increased apoptotic propensity and the resultant premature deletion of these cells is thought to be imposed by the tolergenic environment of the liver, and further driven by the nature of liver-specific antigen presentation (described in further detail in section 1.4).

Anti-viral HBV-specific T cells that escape or survive Bim-mediated attrition are often functionally impaired or exhausted. T cell exhaustion is a recognised state of T cell dysfunction, defined by poor effector function, sustained expression of inhibitory receptors and a transcriptional state distinct from functional effector or memory T cells [53]. Exhausted CD8+ T cells were initially described during chronic LCMV infection as virus-specific (tetramer positive) T cells that failed to produce effector cytokines [54]. These cells have subsequently been studied in numerous chronic viral infections in humans, including HIV [55], HCV [56, 57] and HBV. Specifically in CHB the few HBV-specific T cells that are detectable produce less IFNγ, proliferate less and exhibit a phenotypic profile characteristic of exhausted cells [47, 58, 59]. This progressive loss of T cell function and appearance of an exhausted phenotype is influenced by ongoing antigenic stimulation, since strong correlations exist between viral load and extent of exhaustion in LCMV [51]. This is further supported by the fact that in HBV, virus specific T cells are rarely detectable at viral loads exceeding 10^7 copies/ml [50].

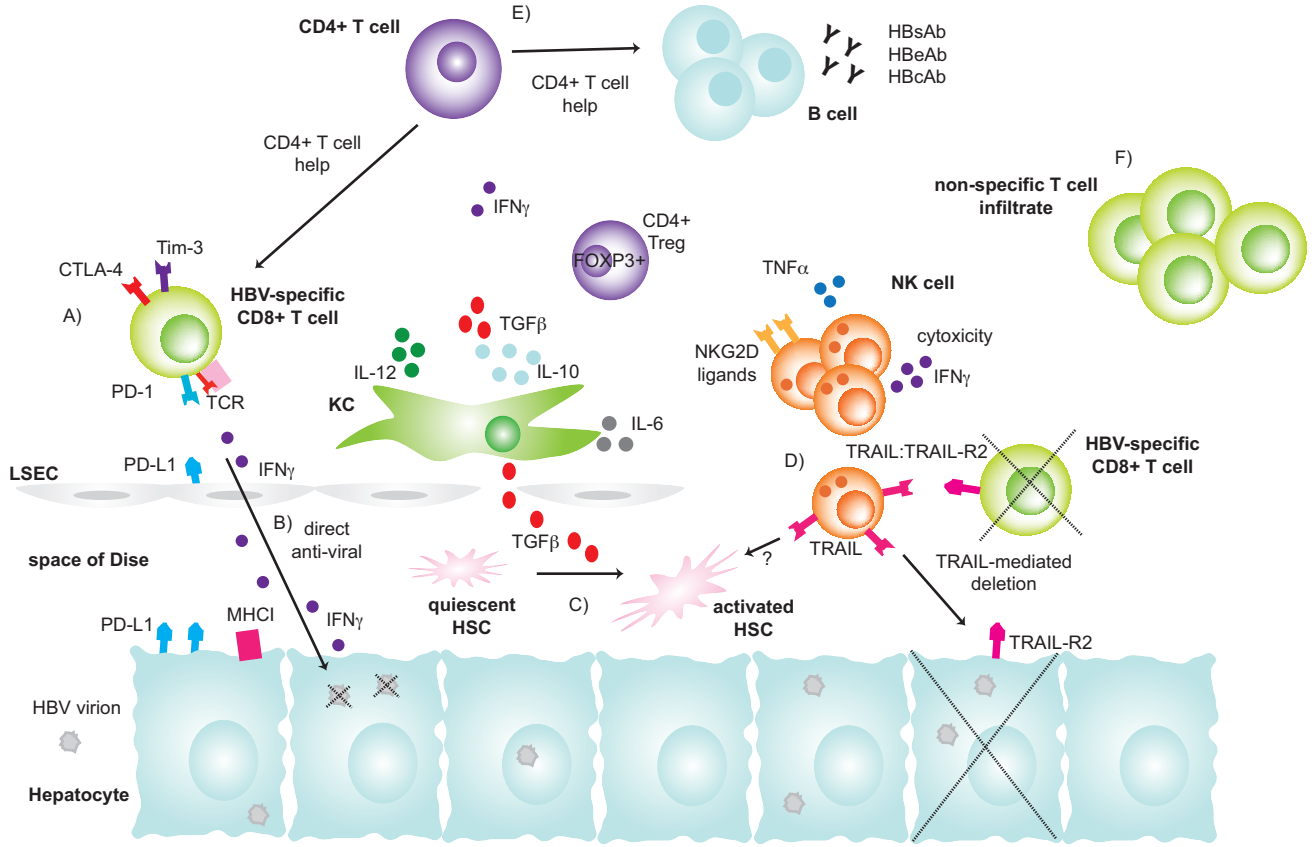

Figure 1.5: Overview of selected mechanisms of the immune response in CHB.

A) Interaction of PD-1 on the surface of HBV-specific T cells with PD-L1 on LSEC and/or hepatocytes driving tolerisation and dampening immune response. B) Direct anti-viral activity of the pro-inflammatory cytokine IFNγ produced by CD8+ T cells, prompting non-cytolytic clearance of HBV. C) TGFβ production by KC, activates quiescent HSC, which can up-regulate TRAIL-receptors marking them for NK cell driven TRAIL-mediated deletion (Singh et al - unpublished). D) TRAIL up-regulation on NK cells results in the induction of apoptosis of HBV-infected hepatocytes, or HBV-specific T cells that up-regulate TRAIL-R2 via TRAIL-mediated deletion. E) CD4+ T cells required for the priming and survival of functional CD8+ T cell responses and B cell activation, enabling the production of antibodies against the virus. F) Recruitment and activation of a non-antigen specific cellular infiltrate. Abbreviations used: liver sinosodial endothelial cell (LSEC), hepatic stellate cell (HSC), Kupffer cell (KC), natural killer cell (NK cell), tumour necrosis factor (TNF)-related apoptosis-inducing ligand (TRAIL), TRAIL-receptor 2 (TRAIL-R2), cytotoxic T-lymphocyte-associated protein (CTLA-4), programmed death 1 (PD-1), programmed death ligand 1 (PD-L1)), T cell immunoglobulin- and mucin-domain-containing molecule 3 (Tim-3).

The state of exhaustion in CHB is accelerated by a number of candidate co-inhibitory signals that are known to be up-regulated on HBV-specific T cells. These include an up-regulation of programmed death 1 (PD-1) [49, 60], T cell immunoglobulin- and mucin-domain-containing molecule (Tim-3) [61] and cytotoxic T-lymphocyte-associated protein 4 (CTLA-4) [59] expression that perpetuate the dysregulated cytokine production in response to peptide stimulation [62]. It is hypothesised that a naive T cell encountering HBV antigen in the context of intrahepatic antigen presenting cells (APC) receives insufficient co-stimulation, outweighed by an excess of co-inhibitory signalling driving exhaustion or a state of T cell tolerance (detailed further in section 1.4 and summarised in figure 1.6).

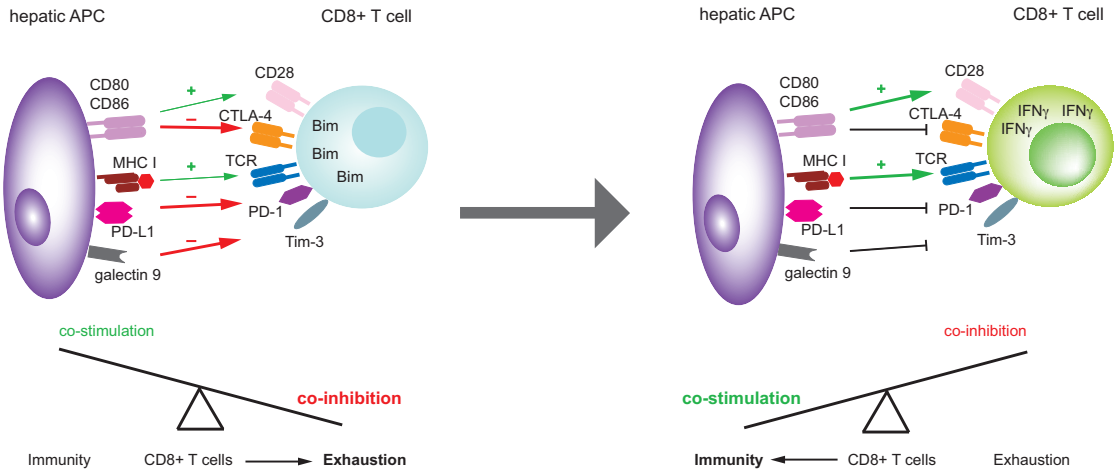

Figure 1.6: Phenotypic balance between co-stimulation and co-inhibition driving T cell exhaustion in CHB.

Schematic depicting the up-regulation and down-regulation of specific receptor-ligand interactions maintaining the balance between stimulation and inhibition of T cells upon interaction with an hepatic antigen presenting cell (APC). Adapted from Schurich and Maini [62].

Another key aspect of the dysregulated immune response in CHB relates to a component of innate immunity, the natural killer cells (NK cells). NK cells orchestrate immune response through the production of effector cytokines and cytotoxicity primarily upon recognition of virally infected cells (and tumour cells). NK cell functionality is determined by a balance between positive and negative signals received through either stimulation of activatory or inhibitory surface receptors. An aberrant up-regulation of the death ligand tumour necrosis factor (TNF)-related apoptosis-inducing ligand (TRAIL) promotes NK-mediated deletion of HBV-specific T cells [63].

In addition to the profound exhaustion of HBV-specific CD8+ T cells, our group has previously noted a global metabolic defect in circulating and intrahepatic T cell proliferation and a specific affect on their ability to produce interleukin-2 (IL-2). These findings were accompanied by an observed down-regulation of CD3ζ, the signalling chain of the CD3 molecule at the surface of global T cells [58].

Down-regulation of CD3ζ is now widely considered a hallmark feature of nutrient deprivation [64, 65, 66, 67], suggesting the potential for metabolic regulation of immune responses in CHB. This defect was associated with preliminary *ex vivo* evidence of a depletion in circulating levels of the conditionally essential amino acid L-arginine in patients with active disease, which was corrected upon L-arginine supplementation *in vitro*. These findings were published by Das *et al.* [58] (Maini group) and raised a number of exciting and interesting research questions that influenced the conception of this project.

1.3.3 Cell-mediated immunopathology in CHB

Before discussing the natural phases of CHB seen in the clinic, it is essential to consider what causes the immunopathology in CHB. Although HBV-specific T cells are essential for control of viraemia [35], they are also considered to play a key role in initiating liver inflammation (and the associated immunopathology).

It was initially thought that the cytotoxic functionality of HBV-specific CD8+ T cells was solely responsible for the destruction of infected hepatocytes during infection. However, this was disputed by early evidence from the murine and chimpanzee models which suggested a direct involvement of an influx of inflammatory granulocytes, induction of chemokine production and a non-antigen-specific mononuclear infiltrate (composed mainly of macrophages, T cells and NK cells) that is recruited into the liver following initial recognition by HBV-specific CD8+ T cells [68, 69]. In the murine system, adoptive transfer of HBV-specific T cells triggered the recruitment of inflammatory neutrophils and mononuclear cells that were demonstrated to amplify liver damage [68]. Subsequent human studies have gone on to support this. An influx of a non-antigen-specific T cells was reported by Maini *et al.* [47] to be most evident in patients with high level, ongoing liver inflammation as measured by raised serum ALT levels, highlighting a role for this infiltrate in potentiating liver disease. Further evidence in support of this is the CD8+ T cell driven recruitment of mononuclear cells, by IFNγ production, which enables the recruitment of NK cells into the liver [70]. Chemokine blockade in the liver has also

been shown to reduce the extent of the non-antigen specific infiltrate, in turn reducing the severity of associated liver disease, whilst maintaining non-cytolytic clearance of the virus [70, 69, 71].

The question of what licenses the HBV-specific T cells to orchestrate this influx of such an inflammatory infiltrate remains to be fully elucidated. It is likely that innate mechanisms are involved in the amplification of liver pathology. Production of the neutrophil chemoattractant IL-8 coincides with peak vireamia, proceeding an hepatic flare and an increase of IFNα with the onset of the flare [72, 73]. Subsequent studies have shown IL-8 to be an essential factor in the recruitment of both neutrophils and NK cells into the intrahepatic environment [74, 69]. Work by our group has also shown that IL-8 can induce hepatocytes to up-regulate TRAIL death-inducing receptors, whilst increased IFNα production induces expression of the reciprocal death-ligand TRAIL on the NK cells promoting NK cell-mediated killing of hepatocytes [72]. A study by Gehring *et al.* [75] described a population of HBV-specific T cells capable of producing IL-8 in the inflamed liver, which were not detected when inflammation subsided during resolution of acute HBV. Although the study did not address directly whether IL-8 producing T cells contribute to or initiate the inflammatory process [75], it remains possible that T cell production of cytokines and/or chemokines may be critical for recruiting the liver-damage causing cellular infiltrate in CHB.

Investigation into other changes in the liver mircoenvironment has suggested a role for the activation of platelets that promote the trafficking of leukocytes, including increases in virus-specific T cells, to the sites of inflammation [76, 45]. It has also been noted that many of the infiltrating T cells in the liver express a distinctive ″liver-homing‟ phenotype. This phenotype is characterised by expression of CD161, chemokine receptors (CXCR6 or CXCR3) and an invariant Vα chain. These cells are capable of producing further pro-inflammatory mediators such as IL-17 in the liver, but their exact role in CHB remains to be elucidated [77].

1.3.4 Clinical manifestations in CHB

Infection with CHB results in markedly contrasting outcomes in the liver, which can be recognised as distinct clinical ″phases‟ of disease. In the categorisation of patients into these phases a combination of virological, serological and biochemical parameters can be used. Therefore the natural course of CHB infection can arbitrarily be divided into four phases. These phases include one where the virus replicates at extremely high levels for many years without any clinically apparent liver disease (known as the immunotolerant phase); or, in contrast, phases characterised

by an active immune-mediated necroinflammatory reaction that attempts to control the virus (active disease) (see figure 1.7 for full details and a temporal scale). What is essential to keep in mind is that categorising patients into such phases, while useful clinically, does not necessarily reflect the true immunology and the ongoing immune-mediated response seen during each phase. The immune mechanisms that distinguish these different phases and the transition between them have yet to be established.

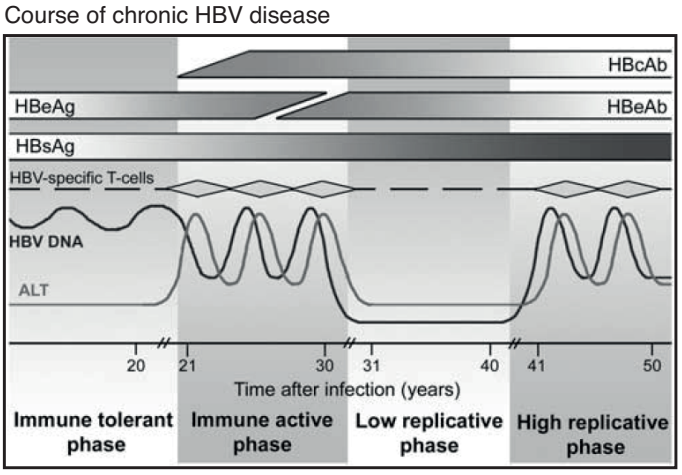

Figure 1.7: Natural course of chronic HBV infection.

Schematic depicting the course of infection a patient with CHB may progress through. The time-line depicts progression of a typical vertical transmission (from mother to neonate) case. These phases are clinically defined by a number of parameters and vary in length. The initial immunotolerant phase is characterised by extreme levels of viral replication and the presence of secreted HBeAg in the absence of any liver disease (as measured by serum ALT, an enzyme released by damaged heptocytes). This phase is then followed by an immune-active phase, where HBV viral loads typically decline at the cost of severe liver disease. In the low replicative phase (inactive phase), viral loads dramatically decrease and serum ALT levels normalise, with liver disease improving. The phase of inactivity can be life-long, but a subset of patients, especially immunosuppressed individuals, can experience high level replication again at the further expense of the liver. The classification and nomenclature associated with each phase, although not perfect, are an important tool for categorising patients in a chronically evolving infection. The clinical cut-offs used in the identification of patients into such phases varies between publications and are discussed in the main text. The exact values used in this thesis are stated in section 3.3.2. Adapted from Chang & Lewin [38].

The immunotolerant phase is more commonly seen in young patients after vertical infection from HBeAg-positive mothers. Immunotolerant individuals are those characterised by serum HBeAg positivity, extremely high viral loads (with a minimum HBV viral load of $\geq 200,000$IU/ml but commonly in excess of 1×10^7IU/ml), and with a normal or a minimally raised ALT, indicative of a lack of liver inflammation. In this phase liver damage and therefore fibrosis progression is commonly limited. This phase is longer in individuals perinatally infected, where it can often

range from 20-30 years (figure 1.7) in stark contrast to those who acquire HBV infection during adulthood in whom this period is short or even absent [78]. Despite the absence of liver inflammation, these individuals have an enhanced risk of HCC because of the HBV polymerase genes reverse transcriptase properties, allowing HBV to integrate randomly into hepatocyte DNA. High level replication over time therefore leads to an accumulation of integration sites [79].

The nomenclature for this particular phase is misleading as there is no clear evidence that these patients experience an HBV-specific immune response that is considered to be any more tolerant than either those with active or inactive disease. For example, it has now been suggested that the T cell response profile of immunotolerant patients may in fact be similar to patients with highly active disease. In some respects, the response is also less compromised than that observed in older, more active patients [80]. What fundamentally maintains patients in this immunotolerant phase remains a key research question.

The mechanisms associated with the loss of immunotolerance and the transition through to active disease phase are mostly still unknown. The ″immune clearance phase‟ (HBeAg+ active disease, see figure 1.7) is associated with a rapidly falling HBV viral load and a shift of hepatocyte expression of Hepatitis B virus-core antigen (HBcAg) from the nucleus to the cytoplasm [81]. This rapid decline in viral load is accompanied by an increase in serum ALT (intermittent periods of raised ALT or flares). In this case the rise in serum ALT is attributable to the immune-mediated response against the virus previously described in section 1.3.3. The immune response attempting to clear the virus comes at the cost of liver damage, consequently causing apoptosis and necrosis of infected hepatocytes. During this phase, again which can last for a number of years, disease activity fluctuates and progressive liver disease often occurs. Individuals who develop CHB that were infected during adulthood advance through to an immune active phase rapidly once infected.

Seroconversion from HBeAg positivity to HBeAg specific antibody (HBeAb) positive is usually followed by a non-replicative or inactive phase, with low-level viral replication (figure 1.7). During this phase, patients have low level viral replication (often barely detectable HBV DNA) and hepatocyte destruction ceases, with a concomitant normalisation in serum ALT values [82]. During this phase a small number of patients successfully clear HBsAg, although this tends to be in only approximately 1% of patients each year [83]. This period of inactive disease can be long-lasting. A subset of patients develop HBV re-activation, even after seroconversion, with

recurrent necroinflammatory liver disease and high-level replication (eAg- active disease, figure 1.7). This occurs in the presence of either the wild type virus (and reversion to HBeAg positivity), or HBV variants that limit re-expression of HBeAg due to mutations in either the pre-core or core promoter region [84].

1.4 Immunology of the Liver

The liver is considered to be the largest internal organ of the body. It functions as the primary site for the metabolism of often harmless gut-derived carbohydrates, proteins and lipids, primarily from ingested food products. Another key function of the liver is to function as a secondary lymphoid organ, central to the process of immune surveillance critical to host immunity and survival. The liver is non-redundant in its role in detecting pathogenic insults and providing host defence. In doing so, the liver is able to screen and protect against pathogenic insult (with the exception of encapsulated bacteria which are detected and removed by the spleen). As such, the liver is widely considered an immunoregulatory organ, whereby it functions to maintain an adequate balance between immune tolerance (immune hyporesponsiveness), and immune surveillance and activity (priming and eliciting robust immune responses where necessary) [85]. For example the introduction of live bacteria or specifically relevant to the work of this thesis, hepatotropic viruses, require a regulated innate and adaptive immune response, that is sufficient for pathogenic elimination or control without disturbing physiological tolerance and function.

The ability of the liver to perform necessary immune surveillance, in other words detecting and responding to pathogenic insult, is a combined effect of both its anatomy (and blood supply) and the diverse network of cellular populations resident therein. The liver receives its blood supply directly from the gastrointestinal tract, meaning it is enriched in both nutrients and numerous bacterial degradation products that gain access from the gut lumen. This results in a large number of antigens passing through every minute. The blood flow into the liver is impressive, it has been reported that 30% of the total blood volume passes through the liver each minute [86]. However, this volume circulates through the liver in a ″sluggish‟ manner primarily due to the extensive sinusoidal network. The sluggish movement through the liver promotes interaction of immune cells with liver resident cells or the infiltrating leukocytes within the hepatic sinusoids [87]. An evolutionary advantage of this slow blood flow may be to ensure pathogens are detected and responded to appropriately [88]. This exposure of the liver to continued harmless antigenic stimulation is a physiological state, so must not lead to overt tissue damage resulting from

activation of immune responses and/or inflammation; thus forming the basis of the concept immune tolerance. A number of mechanisms act to predispose to immune tolerance, including the nature of antigen presentation. This can be specifically harnessed by hepatotropic infections or tumours of the liver to promote their persistence. In evolutionary terms, the liver has been specifically designed to not only efficiently metabolise necessary nutrients and clear toxins but to maximise its immunoregulatory role. Key features which will be discussed in detail in the subsequent sections include, the largest single population of macrophages (resident Kupffer cells (KC)), the greatest density of NK cells and natural killer T cells (NKT cells) and the largest reticuloendothelial network in the body.

1.4.1 Liver sinusoidal endothelial cells

The capacity of liver cells to present antigen and engage with T cells is not limited to classical dendritic cells (DC), specifically, liver sinusoidal endothelial cells (LSEC) are very efficient APC [89, 90]. Often in response to hepatotropic infections, CD8+ T cells display phenotypic features of cells that did not receive sufficient activation (depicted in figure 1.6). Naive T cells do not typically enter non-lymphoid tissues without having been activated previously, to mature and differentiate into effector T cells. The liver, however, represents an exception to this; it has the ability to prime naive T cells, that were previously thought to require professional APC in lymphatic tissue.

The LSEC comprise more than 50% of the non-parenchymal cells in the liver and are critical in pathogen detection, capture, and antigen presentation [91]. Anatomically, LSEC separate heptocytes from the blood flowing through the sinusoidal lumen, with no organised basement membrane (figure 1.8). This feature enables the formation of a gap, the Space of Disse, between the endothelial lining and the underlying hepatocytes [92]. The LSEC do not form tight junctions, preventing total exclusion of heptocytes from the sinusoids. The LSEC are perforated by fenestrations allowing for the extension of membrane protrusions from both heptocytes and infiltrating lymphocytes [93]. The structural nature enables the LSEC to facilitate direct contact with heptocytes and lymphocytes, but also allows for the bi-directional flow of metabolites.

Key to their role in antigen presentation, LSEC inherently express a number of the surface characteristics of classical stimulatory APC, similar to DC. They express numerous pattern recognition receptors (toll-like receptor* (TLR3), TLR4, TLR7 and TLR9), show constitutive expression of both major histocompatibility class I (MHC-I) and class MHC-II, co-stimulatory

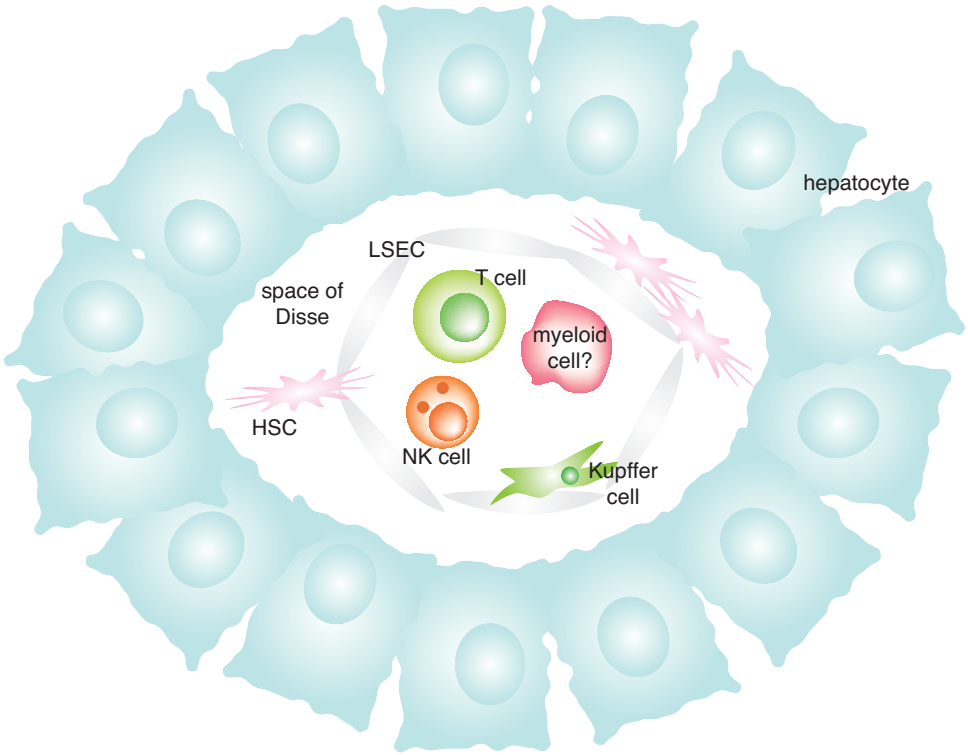

Figure 1.8: Schematic view of the mirco-architecture of the hepatic sinusoid.

Hepatocytes are separated from the blood rich in antigen-specific and non-antigen specific CD8+ T cells, NK cells and myeloid cells, passing through the sinusoids of the liver lined by non-parenchymal LSEC. LSEC have no organised basement membrane, forming the Space of Disse between the endothelial lining and the underlying hepatocytes, perforated by numerous fenestrae. HSC, with an astral phenotype reside in the Space of Disse. Liver resident macrophages, KC, adhere to the LSEC in the hepatic sinusoid. In the context of this schematic, myeloid cells encompasses myeloid-derived suppressor cells; their exact location in the liver is unknown. Abbreviations used: Kupffer cells (KC), hepatic stellate cell (HSC), liver sinusoidal endothelial cells (LSEC) and natural killer cells (NK cells). Adapted from Knolle & Thimme [94].

molecules (CD80 and CD86) and adhesion molecules such as intercellular adhesion molecule 1 (ICAM-1), which together enable LSEC to function potently as liver resident APC [95, 87]. LSEC also express a variety of scavenger, antibody and mannose receptors, enabling the rapid uptake of protein and cellular debris by receptor-mediator endocytosis, but more specifically the internalisation of a wide range of pathogens for presentation. LSEC, through expression of both MHC-I and MHC-II are capable of efficient cross-presentation, resulting in both CD4+ and CD8+ T cell activation.

Antigen presentation by an LSEC results in local maturation of the particular LSEC as an APC and the up-regulation of the co-inhibitory signalling molecule, programmed death ligand 1 (PD-L1). Expression of PD-L1 is crucial to the induction of tolerised T cells that are not fully licensed

with effector function. Initial CD8+ T cell activation by an LSEC results in T cell proliferation and release of cytokine (considered transient CD8+ T cell activation) but over time it is the recognition of antigen in the context of PD-L1 signalling, rather than co-stimulatory molecules, that results in antigen-specific tolerance [89, 96]. Engagement of PD-L1 with its receptor PD-1 on activated T cells results in a phenotypic drive towards T cell exhaustion (as discussed previously in section 1.3.2).

Further exposure of LSEC to other soluble mediators, such as IL-10 and transforming growth factor beta (TGFβ), promotes the induction of T cell tolerance rather than activation via the reduction in surface expression of MHC molecules, and some co-stimulatory molecules, which again limits the capacity of LSEC to elicit immune responses [97]. LSEC also promote tolerogenic T cells by directly limiting the function of liver-resident DC [98].

While a degree of immune tolerance is essential to maintain normal physiology, and antigen presentation by LSEC is a critical mechanism involved in such tolerance, it does lead to problems when attempting to raise an immune response against viral infections or tumours of the liver.

1.4.2 Kupffer cells

KC represent the single largest population of macrophages, making up an estimated 80-90% of all tissue resident macrophages in the body [99]. KC are stationary macrophages, that adhere to LSEC in the hepatic sinusoids. Similarly to LSEC, KC express a range of scavenger receptors, complement receptors, TLR, and antibody receptors that detect, bind and enable internalisation of pathogen. Uptake of such antigens promotes KC activation to produce a number of cytokines and chemokines, which subsequently alert the immune system, including the production of IL-12, IL-6 and TGFβ as depicted in figure 1.5.

As well as being extremely good at the capture and clearance of numerous pathogens, especially bacteria, KC also represent an important APC population in the liver. As with LSEC, KC predispose the liver towards immune tolerance. Although they express MHC-I and MHC-II alongside an array of co-stimulatory molecules, under the steady state KC are poor T cells activators. Continued exposure to lipopolysaccaride (LPS, from the gut) dampens down their ability to prime T cell responses [97]. KC also participate in driving immune tolerance through production of the immune suppressive cytokines IL-10 and TGFβ and expression of molecules

such as Fas-ligand (FasL) and PD-L1 [100]. KC also detect low concentrations of TLR ligands and respond by producing pro-inflammatory cytokines such as IL-6 and type I IFN [101].

1.4.3 Hepatocytes

Hepatocytes are the parenchymal cell population of the liver and are primarily responsible for the metabolic functionality of the liver. They too can act as liver-resident APC, once again crucial to immune regulation via the induction of immune tolerance [102]. Hepatocytes make direct contact with sinusoidal T cells through the fenestrations provided by the structural nature of the LSEC [93] and also constitutively express MHC-I and ICAM-1. Although not constitutively expressed, under inflammatory conditions (for example, IFNγ production), hepatocytes can also express MHC-II [93, 103, 88, 104]. Evidence suggests that hepatocytes present antigen to naive T cells in an ICAM-1-dependent manner [88, 93].

As well as being involved in T cell activation, hepatocytes also play an important role in the regulation of immune surveillance beyond the liver. Such surveillance is achieved via the production of serum constituents, for example, secreted pathogen recognition receptors (PRRs), acute-phase proteins and complement components. These are all important constituents of the innate immune response against pathogenic insult through processes such as the opsonization of pathogens for phagocytosis or activation of the complement cascade [105, 87]). IL-6 produced by KC upon detection of low-level TLR ligands, is able to induce the expression of the acute phase protein, C-reactive protein, by hepatocytes thereby linking functionality of multiple cell types of the liver [106].

Also of note is a novel role for hepatocytes that has been described recently by Benseler *et al.* [107] whereby the liver further induces peripheral tolerance via a mechanism based on the deletion of CD8+ T cells that have been activated locally. The authors demonstrated that recently activated T cells commit ″suicide‟ by actively invading antigen-expressing hepatocytes; a process coined ″suicidal emperipolesis‟. The antigen-specific T cells were shown by microscopy to enter and be contained within the hepatocytes prior to non-apoptotic, lysosomal degradation before the T cell could clonally expand and acquire its cytotoxic effector function [107]. This process, although necessary for the deletion of potentially autoreactive T cells, may be detrimental to the ongoing and necessary immune responses against hepatotropic infections.

1.4.4 Hepatic stellate cells

Hepatic stellate cells (HSC) are perivascular cells located in the Space of Disse that exhibit an astral phenotype. Their anatomical location promotes their interaction with LSEC and hepatocytes whilst separating them from the circulating lymphocytes and myeloid cells in the sinusoid (figure 1.8). Their traditional roles include being the primary site for the storage of vitamin A in cytoplasmic droplets, the regulation of blood flow through the sinusoids due to their contractile nature, and the ability to trans-differentiate from a quiescent state into fibrogenic, proliferative myofibroblasts upon liver injury to promote repair. They achieve this via the production of large amounts of extracellular matrix proteins. They are also a potent source of TGFβ, and so upon continued liver injury HSC are critically involved in the development of fibrosis [108, 109].

In addition, a tolerising role has been more recently described for HSC. HSC can produce a diverse range of chemokines, and are also able to present antigen to T cells [110, 111], although the fate of these T cells once primed is still under debate. However, not only have human HSC been demonstrated to suppress T cell activation (via PD-L1) but they have also been shown to promote the induction of known immunoregulatory cell populations: both regulatory T cells (Treg) and myeloid-derived suppressor cells (MDSC). T cell activation in the context of HSC has been reported to result in the induction of CD4+ Tregs [112, 113]. MDSC will be described in more detail further on in this thesis however human HSC have been shown to promote the differentiation/accumulation of MDSC [114, 115, 116], and in doing so confer tolerance, for example in the context of preventing kidney allograft rejection [114].

1.4.5 Lymphoid & myeloid cells of the liver

The majority of the immunology of the liver covered so far has focused on the non-lymphocytic liver-resident cells and their ability to detect pathogen and/or their role in immune tolerance. Some attention should be given to the populations of lymphocytes both resident and transiting through the liver. Lymphocytes can be found scattered throughout the parenchyma of the liver, as well as in the portal tracts, with the average human liver containing in the order of 10^{10} cells [91]. As already alluded to the composition of the total lymphocyte population of the liver is unusual.

Between 40-60% of the intraheptic pool of lymphocytes are NK cells, which is more than a three-fold enrichment compared to the periphery [117, 118]. NK cells respond to a wide-range

of cell-surface ligands expressed by damaged or infected cells, which ensures self-tolerance is maintained, whilst responding to infected or transformed cells. NK cells kill target cells via the formation of an immune synapse to mediate subsequent lysis by releasing cytotoxic granules (containing perforin and granzyme). However, NK cell functionality is not just restricted to their capacity to ″kill‟ as the name might suggest. NK cells also produce and release the pro-inflammatory cytokines, such as IFNγ and TNFα [119, 120].

Also the ratio of CD4+ to CD8+ T cells is altered in the liver. Under homoeostatic conditions CD4+ T cells outnumber CD8+ T cells in the periphery by approximately two to one. In the liver this ratio is reversed, with CD8+ T cells outnumbering their CD4+ counterparts. These T cells all express the $\alpha\beta$-chain T cell receptor (TCR) and respond to antigen presented in the context of MHC molecules [91]. The liver also contains a large number of $\gamma\delta$ T cells which again have altered frequencies in the intraheptaic environment; in the periphery these cells normally represent approximately 3% of total lymphocytes, but in the liver these cells can represent up to 15% [87]. These cells play a predominant role in the presentation of lipid antigen.

Several lines of evidence suggest that the recruitment of leukocytes into the liver during chronic viral infections is largely mediated by the ability of chemokines to attract leukocytes to specific sites in the liver. The large majority of T cells infiltrating into the chronically inflamed liver express high levels of the following chemokines: CXCR3, CXCR6, CCR1 and CCR5; a tissue-infiltrating phenotype [121, 122, 123, 124]. Induction of the pro-inflammatory cytokines IFNγ and TNFα up-regulates expression of the CXCR3-ligands, CXCL9 and CXCL10. These have specifically been shown to be up-regulated with increased expression of the receptor CXCR3 on both CD4+ and CD8+ T cells in the liver compared to peripheral T cells in chronic hepatitis [121]. Importantly, studies using blockade strategies of CXCL9 and CXCL10 *in vivo* resulted in reductions in the recruitment of mononuclear cells into the liver, particularly those subsets that are known to express CXCR3 [71].

The ligand CXCL16 has also been reported to be up-regulated on hepatocytes [123], and engagement of CXCR6-expressing T cells through this interaction is important for the retention and survival of effector cells in the inflamed liver. More recently a subset of CXCR6+ liver-infiltrating CD8+ T cells which co-express the C-type lectin, CD161, capable of producing IL-17 and IFNγ have been reported in chronic HCV infection. This phenotype characterised by increased CD161+ T cells has also been reported in acute HBV in a limited number of patients.

Notably this phenotype was absent from HIV- cytomegalovirus (CMV)- and influenza-specific T cells [125]. The interaction of CXCR6:CXCL16 has also been shown to be relevant in the process of hepatic homing of NK and NKT cells [126].

Immune regulation in the liver can also be controlled by myeloid-lineage populations beyond that of the resident KC. Recent evidence has demonstrated a role for inflammatory monocyte-derived CD11b+ aggregates, that have been termed ″intrahepatic myeloid cell aggregates for T cell clonal expansion‟ (iMATE). The authors have described these iMATE as structures that provide a ″cocoon-like‟ anatomic framework that enables and promotes the proliferation of CD8+ T cells locally, in the apparent absence of local antigen [127]. The formation of such structures to enhance antigen-specific T cell numbers may be critical in aiding the immune response against hepatotropic infections. While myeloid-cell populations/structures like iMATE could be considered beneficial to an anti-viral or anti-tumour immune response, different populations of immature myeloid cells have also been described in the liver. One such subset is the MDSC. MDSC exhibit a wide-range of immune-suppressive functions, that affect both the innate and adaptive immune systems. Full description and discussion of these cells occurs throughout the thesis and will therefore not be covered in detail here.

Finally the liver microenvironment itself, independent of any single cell subset is involved in driving immune tolerance. In this case the milieu is characterised by a state of nutrient deprivation. This nutrient-poor environment is achieved by the presence of a number of enzymes, central to immune regulation and immunometabolism. Examples of such enzymes include tryptophan 2,3-deoxygenase (TDO, an enzyme involved in the metabolism of L-trytophan to N-formyl-kynurenine), complemented by the action of indoleamine 2,3-dioxygenase (IDO), which when combined give rise to the immunosuppressive molecule kynurenine. The presence of IDO has previously been shown to been a critical mediator in the maintenance of the process of materno-fetal tolerance [128], and in the context of chronic HCV infection, where IDO expression is increased in the liver of patients [129]. KC and liver-resident DC are potential sources of IDO especially under inflammatory conditions. Yan *et al.* [130] specifically demonstrated T cell inhibition (T cell proliferation and induction of T cell apoptosis) upon enhanced levels of kynurenine and reduced tryptophan *in vitro*.

Another key enzyme capable of driving nutrient deprivation is the constitutively expressed arginase I. This enzyme, capable of metabolising the conditionally essential amino acid L-

arginine, is constitutively expressed by hepatocytes. Extracellular arginase I when released from hepatocytes upon damage can deplete L-arginine. Local nutrient deprivation can limit T cell functionality and proliferation [131, 66, 64], thus potentially preventing successful adaptive immunity required upon sensing pathogenic insult. It is also possible that this deprivation could limit immune-mediated damage arising from excessive immune activation in the liver. Interestingly hepatocytes, although potent sources of the enzyme arginase I when damaged, are not the only source. MDSC can also produce and store large amounts of the enzyme [132]. The concept of metabolic regulation by cells such as MDSC in the liver is an exciting area of research.

1.5 Overview of Myeloid-derived Suppressor Cells (MDSC)

Myeloid cells represent the most abundant type of haematopoetic cell in the immune system and have a huge diversity of physiological and pathological function [133]. All cellular components of the blood fall into two distinct lineages, either lymphoid or myeloid and are all generated from haematopoietic stem cells of the bone marrow. Mature lymphoid subsets all differentiate from a common lymphoid progenitor, and similarly all myeloid subsets arise from a common myeloid progenitor [134]. Under physiological conditions, common myeloid progenitors migrate out of the bone marrow into peripheral lymphatic organs having undergone full differentiation and maturation into classical mature myeloid subsets (neutrophil, monocyte, basophil and eosinophil, see the dotted lines in figure 1.9). The full developmental pathway of each individual cell subset and lineage is beyond the scope of this introduction.

What is now widely acknowledged is that under pathological insult or where normal physiological conditions are perturbed, classical myeloid cell development can ″arrest‟, giving rise to an heterogeneous population of cells with an immature phenotype. These cells are the MDSC (see the solid black lines in figure 1.9). The exact origins, differentiation and development of these cells remains to be fully elucidated. However, these cells are of particular interest in hepatotropic infections as they themselves are tolerogenic and immune-suppressive: they could either promote physiological tolerance or be harnessed by pathogens or tumours to prevent a robust immune response.

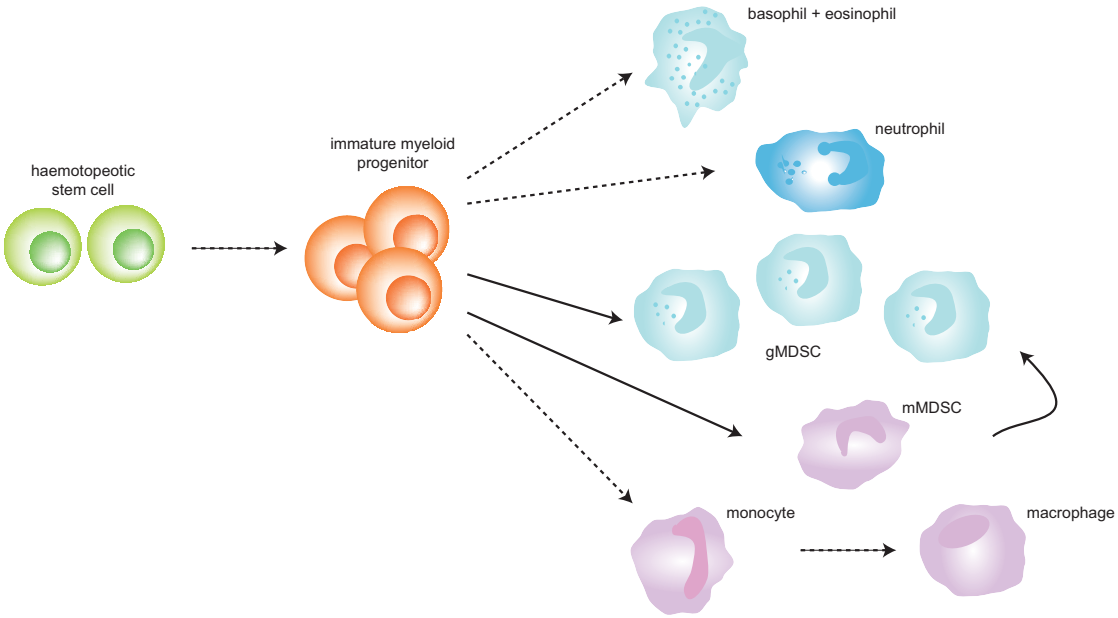

Figure 1.9: Development and differentiation of common myeloid progenitors into myeloid cell subsets.

All myeloid cell subsets arise from a common myeloid progenitor. Soluble mediators, (cytokines, growth factors and chemokines) produced in response to pathological insult, for example, by a tumour, or upon detection of viral infection, promote the aberrant differentiation of common myeloid progenitors, diverting away from full myelopoiesis into mature myeloid cells. The dotted lines represent normal, physiological developmental pathways of immature myeloid precursors into monocytes-macrophages and granulocytes (basophils, eosinophils and neutrophils), and the solid black lines indicate the aberrant pathways of myeloid cell development giving rise to MDSC subsets. Recent evidence suggests a large proportion of gMDSC can arise from further differentiation from the mMDSC confounding the idea of MDSC plasticity [135]. Adapted from Wynn [136].

1.5.1 Brief history of MDSC

Even to date, MDSC remain a relatively newly described cell type that fail to feature in immunological textbooks. Such cells were originally alluded to in the late 1970s, early 1980s (1978-1984) in models of tumour development and systemic Bacillus Calmette-Gurin (BCG) infection. At the time these cells were described as an abnormal population of expanded myeloid cells exhibiting suppressive activity, therefore these cells were termed ″natural suppressor cells‟. With continued research these natural suppressor cells were shown to lack membrane markers for mature lymphocyte populations (B/T/NK cells) and to functionally inhibit lymphocyte proliferation and function [137, 138]. Even at this early stage, while these cells were yet to be formally described, it was noted that they possessed the ability to promote tumour growth through inhibition of anti-tumour responses [138]. The lack of formal description for the cells meant the early study of MDSC was relatively controversial. It was not until the mid 1990s where further study of

these cells went on to describe them more concisely as an heterogeneous population of immature myeloid cells with one key defining feature: the capacity for lymphocyte suppression [139, 140]. From then on the population began to be referred to as myeloid suppressor cells, abbreviated at the time to MSC. This abbreviation created confusion with mesenchymal stem cells, also commonly abbreviated to MSC. However in a letter published in 2007 written by Gabrilovich *et al.* [141] the controversy and inconsistency in naming this cellular phenotype and functionality was highlighted and subsequently the widely accepted nomenclature for these cells as MDSC was coined [141, 142]. MDSC phenotypic identity, the role and their functionality will be discussed in detailed in the subsequent chapters of this thesis.

1.5.2 MDSC: akin to neutrophils

Neutrophils are commonly defined as the effector cells of the innate immune response providing rapid immunity against invading mircoorganisms. Their function involves chemotaxis towards the invading pathogen, enabling engagement to promote the destruction of the infected cell. Neutrophils are increasingly being reported to have multiple phenotypes, thus creating a potential overlap with the granulocytic subset MDSC in the literature, and although their importance in host defence is still widely agreed, only little is known about the basic immunology of the individual neutrophil subsets. It is highly plausible that this lack of knowledge has arisen because of the short-lived nature of these cells. Neutrophils are known to undergo apoptotis in the tissue after engaging pathogens, or as recently reported undergo reverse migration to move out of the tissue of interest shortly after eliciting immune control [143].

The half-life of a neutrophil in peripheral blood was originally postulated to be somewhere between 7-25 hours based on old labelling and tracer experiments using radioactive isotopes [144, 145]. This is now debated; more recent studies have described the half-life of a neutrophil anywhere up to 5.4 days [146, 147]. This discrepancy may be explained by either taking into account the division time of a neutrophil progenitor or allowing for subset differentiation. However taken together with the view that neutrophils may not undergo immediate apoptosis after eliciting effector function (by reverse migration), it is possible that at least a sub-population of neutrophils survive longer than previously thought. Either way the potential for ″neutrophil-like‟ cells to switch phenotypes and exert functionality beyond cytotoxicity against an invading pathogen exists. One such phenotype considered by many is gMDSC (discussed in more detail in the subsequent chapters). Consideration detailing the differences and similarities of gMDSC and classical neutrophils is under ongoing debate and discussion, especially given the large phe-

notypic overlap in marker expression in humans (for example common expression of CD16 and CD66b). This issue with the naming of these cells should not become the focus and distract from the data as long as the functionality of such cells is considered and reported (if authors wish to claim effects seen are MDSC-mediated). Authors will often themselves exclude the study of classical neutrophils by the nature of the common step in PBMC isolations from human samples using density centrifugation with Ficoll.

1.6 Immunometabolism: an emerging field

The emerging field of ″immunometabolism‟ seeks to combine two historically distinct fields; the process of energy metabolism and immunity. A lot is known about the biochemical nature of the pathways involved in cellular metabolism, but surprisingly very little is known about the regulation of these processes in immune cells. Historically metabolic studies have been restricted to adipocytes and/or cancer cells and the specific metabolism of the immune system has been overlooked. It is now emerging that T cell function, survival and differentiation is linked to two key intracellular metabolic pathways: glycolysis and oxidative phosphorylation. The field of immunometabolism specifically focuses on the fact that mounting a successful and effective immune response requires major metabolic changes in immune cells, to enable rapid cellular proliferation and mobilisation.

The metabolism of lymphocytes must be tailored to ensure appropriate functionality. A resting T cell does not require large amounts of synthetic ″building blocks‟ (primarily, amino acids), they simply require energy (primarily in the form of ATP-production) to ensure basal cell processing to maintain the process of immune surveillance. Upon successful TCR engagement with its cognate peptide the resting T cell must undergo a dramatic metabolic reprogramming event to provide the cell with essential biosyntheic components required for nucleotide, lipid and amino acid synthesis. These building blocks are necessary for rapid cell proliferation and functionality: promoting effector cell function. Thus to mediate an adaptive immune response the T cell must significantly increase its amino acid (and glucose) availability. Stimulated lymphocytes therefore need to switch their metabolism from the resting state characterised by a bias towards oxidative phosphorylation to active glycolysis, enhanced glutamine oxidation [148] and more importantly, increased amino acid uptake.

A recent study by Sinclair *et al.* [149] suggested a role for the family of cell surface System

L transporters in immunologically activated T cells. Previous to this publication the relevant amino acid transporters, required to increase uptake, in active T cells were unclear. The authors of this particular study demonstrated the dependence of T cells on such System L transporters when activated by either TCR engagement or pro-inflammatory cytokines, such as IL-2. Experimental triggering of the TCR resulted in enhanced transport of large neutral amino acids (including leucine, and arginine) across the plasma membranes. Specifically, transport of leucine via these System L transporters was shown to be essential for T cell activity via activation of the mammalian target of rapamycin (mTOR) pathway. What is essential to bare in mind is that the ability of the mTOR pathway to sense leucine uptake (and indirectly other amino acids), enables the modulation of cellular responses to nutrient availability and the required switch in metabolic state from resting to active T cells.

Notably the System L transporters are composed of a heterodimer of a heavy chain, CD98 (Slc3a2), and either of the following light chains, Slc7a5, Slc7a8, Slc7a7 or Slc7a6 [150, 151]. In further studies the selective deletion of CD98 confirmed that uptake of leucine (and the indirect increase in other amino acids) through this transport pathway is critical for the proliferative expansion of both T and B cell [152, 153]. As already stated a T cell must undergo a metabolic switch when activated to provide an amino acid (and glucose) rich environment, during this switch the mTOR pathway is one key pathway that is activated. If mTOR activation is prevented, for whatever reason, the cells fails to successfully activate and as a consequence may become tolerised or anergic and instead may favour oxidative phosphorylation rather than increased amino acid uptake and glycoylsis. As is discussed later on section 4.2.2, in conditions of nutrient deprivation, for example in the liver microenvironment in patients with CHB, the mTOR pathway may be inhibited, so T cells become tolerised and display limited functionality [154].

1.7 Hypothesis

It was hypothesised that granulocytic myeloid-derived suppressor cells are capable of limiting immunopathology in the liver associated with CHB infection by depriving infiltrating, non-antigen specific bystander T cells of the amino acid L-arginine.

1.8 Thesis Aims

- Are gMDSC expanded in the context of hepatotropic infections?
- Do gMDSC contribute to the metabolic regulation of immunity in CHB through L-arginine deprivation?
- Are gMDSC capable of suppressing the bystander T cell response implicated in amplifying the liver disease?

1.9 Thesis Overview

In this thesis an expansion of the granulocytic subset of MDSC (gMDSC), expressing increased amounts of arginase I, has been described in patients with chronic hepatotropic infections. These gMDSC accumulate in the liver of such patients (and not in healthy livers), expressing chemokine receptors that may favour egress from the bone marrow and cellular interaction with hepatic-resident stellate cells. This study also provides *ex vivo* evidence of arginase I release into the circulation and a deprivation in the conditionally essential amino acid L-arginine, most significantly in patients with ongoing HBV replication in the absence of overt necroinflammatory liver disease. The data presented indicate that this protective effect may be driven by the capacity of the expanded population of arginase I-expressing gMDSC to potently inhibit T cell responses by depriving them of L-arginine. The contribution of amino acids to T cell function in CHB was further supported by a strong *ex vivo* correlation between their expression of amino acid transporters and the signalling molecule CD3ζ. Overall the study highlights the capacity of gMDSC to moderate tissue damage in a common human infection by constraining key nutrient supplies required by proliferating T cells.

1.10 Thesis Highlights

1. Granulocytic arginase I-positive MDSC accumulate in hepatotropic vial infections
2. gMDSC and arginase I levels segregate with the degree of liver pathology
3. gMDSC can regulate pathogenic T cell responses in CHB by depriving them of L-arginine
4. T cell induction of amino acid transporters implicates metabolic reprogramming in viral infection

Chapter 2

Materials and Methods

2.1 Study Participants

This study made use of human samples obtained from patients attending clinics at four separate sites across London:

1. Mortimer Market Centre (Bloomsbury, London),
2. Royal Free Hospital (Hampstead, London),
3. University College Hospital (UCH, Bloomsbury, London), and
4. Royal London Hospital (Whitechapel, London).

In all cases the study was fully approved by the respective local ethical boards (Camden Primary Care Trust, Royal Free Hospital, UCH or Royal London Hospital). All study participants also gave written informed consent and long-term storage of any samples collected complied with the requirements of the Data Protection Act 1998 and the Human Tissue Act 2004.

A total of 110 patients with CHB, 17 patients with chronic HCV infection and 82 age and sex matched (where possible) healthy, uninfected control volunteers were used within this study. The total number of study participants divides into two cohorts of approximately equal size. Full details of both cohorts of patients and healthy controls are detailed below. Division into either cohort was dependent on the use of different anti-coagulant reagents during sample collection.

All patients with CHB were anti-HCV and anti-HIV antibody negative and were treatment naive unless otherwise stated. Patients with HCV were all HBV and HIV negative and again treatment

naive. A smaller cohort of seven patients with CHB sampled during their course of anti-viral treatment were used, making up a third, separate cohort of study participants. All treatment naive patients with CHB were stratified by a number of disease parameters throughout the study (where appropriate). These were all carried out as a part of their routine disgnostic assessments by the relevant NHS laboratories (virology, biochemistry, histology), and include the following:

1. HBeAg status
2. viral load (determined by real-time polymerase chain reaction PCR)
3. levels of HBsAg (determined by Architect (2step sandwich chemiluminesence mircroparticle immunoassay))
4. biochemical evidence for liver inflammation indicated either by serum ALT levels
5. degree of fibrosis (determined using histological analysis under the ISHAK* scoring system by a trained NHS histopathologist)
6. degree of necroinflammation in the liver (determined using histological analysis by a trained NHS histopathologist)
7. presence of ground glass hepatocytes (determined using histological analysis by a trained NHS histopathologist), and finally
8. CMV seropositivity (determined by measurement of IgG using a commercial assay system (Abbot Architect))

* ISHAK scoring system: a number ascribed to the histological appearance of fibrosis on liver biopsy tissue by a histopathologist - scored from 0-6, with increasing severity [155].

2.1.1 Study cohorts

The two primary cohorts were largely divided for analysis by the different anti-coagulant reagents used during sample collection (ethylenediamine tetraacetic acid (EDTA) or lithium-heparin), which was recorded for all study participants. Samples from the first of these cohorts, which from now on will be referred to as the Central London cohort, were taken in EDTA-containing BD Vacutainers® (obtained from the Mortimer Market centre, the Royal Free Hospital and UCH). These patients and controls are fully summarised in table 2.1. Samples from the second of these cohorts, from now on referred to as the East London cohort, were taken in lithium-heparin containing BD Vacutainers®, (Royal London Hospital), detailed in table 2.2.

Where possible intrahepatic lymphocytes were also obtained (in conjunction with peripheral blood samples) from liver tissue deemed surplus to diagnostic requirement when undergoing routine clinical biopsies from a select group of patients under Dr. Patrick Kennedy and Dr. Upkar Gill at the Royal London Hospital. These ″paired‟ samples are included in the East London cohort.

The third cohort of patients with CHB were those undergoing routine anti-viral treatment. These patients were either treated with Entecavir or Tenofovir for at least one year before inclusion in the study.

It is important to note a fourth cohort of patients were used only to quantify gMDSC. This cohort was made up of a few unique, extremely valuable patients sampled longitudinally throughout the course of acute HBV infection, or over the course of a spontaneous hepatic flare of HBeAg- CHB. The caveat to this distinct cohort of patients was the practice of long-term storage of samples prior to experimentation. Such patients were only used where necessary in specific experiments and their use is noted in the corresponding figure legends.

	Age (years) median (range)	**Sex (%)** male:female	**ALT (IU/L)** median (range)	**Viral load (IU/ml)** median (range)	**HBsAg (IU/ml)** median (range)	**HBeAg (%)** pos:neg
CHB (n=54)	38 (19-72)	61:39	31 (10-586)	9.3×10^4 (blq-7×10^7)	1085 (43-8.3×10^4))	13:87
control (n=55)	34 (24-64)	45:55	na	na	na	na

Table 2.1: Full details of the study participants of the Central London cohort taken in EDTA.
Abbreviations used for both this table, and table 2.2 below: below the level of quantification (blq), serum alanine transaminase (ALT), not applicable (na), Hepatitis B surface antigen titre (HBsAg), Hepatitis B secreted e Ag (HBeAg).

	Age (years) median (range)	**Sex (%)** male:female	**ALT (IU/L)** median (range)	**Viral load (IU/ml)** median (range)	**HBsAg (IU/ml)** median (range)	**HBeAg (%)** pos:neg
CHB (n=64)	37 (17-61)	56:44	35 (10-166)	1.5×10^4 (blq-1.5×10^9)	1.2×10^4 (26-1.6×10^6))	38:62
control (n=37)	34 (24-64)	45:55	na	na	na	na
HCV (n=17)	age	alt	VL	na	na	na

Table 2.2: Full details of the study participants of the East London cohort taken in lithium-heparin.

2.2 Sample Isolation & Preparation

2.2.1 Preparation of peripheral blood mononuclear cells (PBMC)

All venous blood samples were collected in sterile 6 or 9ml BD Vacutainers® containing either EDTA or lithium-heparin and processed immediately. Peripheral blood mononuclear cells (PBMC) were isolated by Ficoll-Plaque Plus™ (GE Healthcare) density gradient centrifugation. 25ml whole blood (diluted where necessary in RPMI 1640 (Invitrogen™)) was layered on 15ml Ficoll-plaque, followed by centrifugation at 2200rpm at 30℃ for 22 minutes with minimum acceleration and brake. PBMC were carefully extracted from the interface using 2ml Pasteur pipettes, then further diluted 1:1 with RPMI 1640 and washed twice by centrifugation at 1600rpm for 15 minutes. Cell counts were determined using a Neubauer counting chamber under light-microscopy; cells were pre-diluted in RPMI 1640, then 1:1 in trypan blue (a cell viability dye that stains nuclei of dead cells). The number of cells was determined using the following formula:

$$N = M \times D \times 10^4$$

N = no. of cells/ml

M = no. of cells counted in central grid, and

D = dilution factor

2.2.2 HLA-A2+ screening

All study participants were screened for expression of human leukocyte antigen-A2 (HLA-A2) by flow cytometry (described below in section 2.3.2). Briefly, during PBMC isolation a small aliquot of isolated PBMC were removed and stained with a directly conjugated monoclonal antibody (mAb) specific for HLA-A2 (Serotech) in phosphate buffered sulphate (PBS: Invitrogen™) for 20 minutes at 4℃ in the dark. Once stained, the cells were washed by centrifugation and fixed using BD Cytofix as per the manufacturers protocol (BD Bioscience) for a further 20 minutes. Once fixed the cells were analysed on a BD LSRII™ or BD Fortessa™ flow cytometer (Beckton Dickinson) for positivity compared to an unstained control. HLA-A2 positive patients were noted and used for specific experiments.

2.2.3 Freeze/thawing of PBMC

Isolated cells not used for direct *ex vivo* experiments were re-suspended at 5×10^6 cells/ml in heat-inactivated foetal bovine serum (FBS) (Invitrogen™) supplemented with 10% dimethylated sulfoxide (DMSO) (freezing media, Sigma-Aldrich®), transferred to cryovials (Corning) and stored in freezing boxes surrounded by isopropanol (MrFrosty, Fisher Scientific) at -80℃ for a minimum of 24 hours. After 24 hours, cryovials (Thermo Scientific) were transferred for long-term storage in gas-phase nitrogen tanks. When required, PBMC were thawed rapidly at 37℃ and washed by centrifugation in 20ml of RPMI 1640. Once washed cells were re-suspended for use in RPMI 1640 supplemented with:

- 10% heat-inactivated FBS (Invitrogen™),
- 100U/ml penicillin /streptomycin (Invitrogen™),
- MEM essential amino acid (Invitrogen™),
- MEM non-essential amino acids (Invitrogen™),
- hydroxyethyl piperazineethanesulfonic acid (HEPES: Invitrogen™),
- β-mercaptoethanol (Sigma-Aldrich®), and
- sodium pyruvate (Invitrogen™).

//NOTE: From this point onwards RPMI 1640 supplemented as above will be referred to as complete RPMI 1640, abbreviated to cRPMI.

2.2.4 Preparation of serum samples

During sample collection, an extra BD Vacutainer® containing no anti-coagulant was filled. The BD Vacutainer ® for serum use was left for a minimum of 30 minutes at room temperature (R.T.) before centrifugation at 1800rpm for 15 minutes. Serum was removed and transferred (500μl per sample) into cryovials and stored at -80℃ for later use.

2.2.5 Preparation of intrahepatic lymphocytes (IHL)

Liver tissue used for extraction of lymphocytes was obtained from liver biopsies once deemed surplus to diagnostic requirement.

Mechanical Disruption

Liver tissue samples were re-suspended in RPMI 1640 and macerated with a plunger taken from a 25ml syringe and a scalpel in small Petri dishes. Following mechanical disruption, the single cell suspension was passed through a 70μm cell strainer (BD Bioscience) followed by multiple washes with RPMI 1640 to prevent clumping minimising cell loss.

GentleMACS™ Dissociation

If liver tissue was not subjected to mechanical disruption the tissue IHL were extracted using a bench-top instrument for the semi-automated dissociation of tissues into single-cell suspensions called a GentleMACS™. In preparation for GentleMACS™ dissociation the tissue was cut-up into small pieces and incubated at 37℃ in 5ml HBSS (with calcium and magnesium) containing DNAseI (0.001%, Roche) and collagenase IV (0.01%, Life Technologies) for 20 minutes in ″C‟ tubes (Miltenyi Biotec). After the incubation the C-tube was transferred to the GentleMACS™ and run on the program identified as ″mouse liver‟ three times. The single cell suspension was then passed through a 70μm cell strainer followed by multiple washes with RPMI 1640 to prevent clumping minimising cell loss as above.

Isolated cells were washed by centrifugation at 1800rpm at 22℃ for 15 minutes. Intrahepatic lymphocytes (IHL) were gently re-suspended, counted (as before for PBMC) and identified from other intrahepatic populations by size, shape and granularity at a high magnification. IHL were always used for direct *ex vivo* experimentation in this study.

2.3 Multiparametric Flow Cytometry

All antibody staining for flow cytometry was performed on a single cell suspension in either 96 well plates (U-bottomed) or in 5ml polypropylene tubes.

2.3.1 BD TruCount Tubes for gMDSC absolute counts

To determine the absolute number of gMDSC, a small number of controls and patients with CHB were used. 50μl of well-mixed anti-coagulated whole blood was added to a BD TruCount™ Tube (BD Bioscience) after the addition of a mixture of mAb (detailed below) for gMDSC identification, with the inclusion of CD45. Surface staining of the cells then followed, in the

presence of a known quantity of beads for 15 minutes at R.T. in the dark. 450μl 1x BD™ FACS Lysing Solution (BD Bioscience) was added to ensure full lysis of red blood cells after staining, prior to flow cytometric acquisition and analysis. Before acquisition on the BD LSRII™, with the threshold of the machine set to expression of CD45. Once analysed using FlowJo v8.8.7 (TreeStar®), absolute counts for gMDSC were calculated manually using the following equation:

$$\frac{\text{number of events in region containing cells of interest}}{\text{number of events in absolute count bead region}} \times \frac{\text{number of beads per test*}}{\text{test volume}} = \text{absolute count}$$

* = value found on each lot of BD TruCount™ Tube packaging.

2.3.2 Surface staining of PBMC & IHL for MDSC frequency & phenotype

To determine MDSC subset frequencies and phenotypes, a minimum of 2×10^6 freshly isolated PBMC were used. Cells were washed in 1x PBS and centrifuged at 1600rpm for 5 minutes. The supernatant was aspirated and cell pellets re-suspended by gentle vortexing. Cells were initially stained to allow detection and removal of dead cells from analysis using an Invitrogen™ Blue Live/Dead® Cell viability assay by staining for 15 minutes at 4℃. Once stained, the Live/Dead® protein dye was washed off using 1x PBS and cells were subjected to a blocking step to prevent unwanted binding of antibody to Fc receptor-expressing cells (FcR blocking reagent: Miltenyi Biotec®) for 15 minutes at 4℃. Surface staining of cells then followed in the presence of the FcR blocking reagent by staining with relevant directly conjugated anti-human mAb for 30 minutes at 4℃ in the dark. Following a washing step with 1x PBS, cells were fixed with 150μl/well or 300μl/tube with 4% paraformaldehyde (PFA). Cells were transferred to 500μl polystyrene tubes for acquisition where necessary. Table 2.3 details the mAb used for the detection of MDSC extracellular antigens. Data were collected on a BD LSRII™ equipped with a UV laser and analysed using FlowJo v8.8.7.

Surface marker	Flurochrome	Clone	Manufacturer	Dilution
CD11b	PE-Cy7	ICRF44	eBioscience	2:100
CD11b	FITC	ICRF44	eBioscience	2:100
CD14	BD Horizon V500™	M5E2	BD Bioscience	2:100
CD14	PerCP	MQp9	BD Bioscience	3:100
CD15	APC	HI98	BD Bioscience	7:100
CD15	FITC	HI98	Biolegend	2:100
CD15	AlexaFluor® 700	SSEA-1	Biolegend	5:100
CD16	APC-eFluor® 780	3G8	eBioscience	1:100
CD16	PE	DJ130c	Miltenyi Biotec	3:100
CD19	PerCP	4G7	BD Bioscience	2:100
CD3	PE-Texas Red® (ECD)	UCHT1	Beckman Coulter	3:100
CD33	AlexaFluor® 700	WM53	BD Bio./eBio.	2:100
CD45	AlexaFluor® 488	HI30	Biolegend	2:100
CD63	PE	HSC6	eBioscience	2:100
CD66b	PerCP-Cy5.5	G10F5	Biolegend	2:100
CD95 (FAS)	PerCP-Cy5.5	X10	eBioscience	1:100
CD178 (FAS-L)	PE	MFL3	Biolegend	1:100
CCR2 (CD192)	PE	K036C2	Biolegend	1:100
CXCR1 (CD181)	FITC	8F1	Biolegend	1:100
CXCR2 (CD182)	PE	5E8	Biolegend	1:100
CXCR4 (CD184)	PE	12G5	Biolegend	1:100
HLA-DR	eFluor® 450	L243	eBioscience	3:100
MICA/B	AlexaFluor® 488	6D4	Biolegend	4:100
PD-L1	PE	M1H1	eBioscience	5:100
Live/dead®	Blue	n/a	Invitrogen™	1:1500

Table 2.3: Directly conjugated anti-human mAb against extracellular antigens used in the identification and phenotyping of MDSC subsets by multiparametric flow cytometry.

2.3.3 Intracellular staining of PBMC & IHL for MDSC phenotype

For detection of MDSC intracellular antigens, cells were blocked and surface stained as described above. Once surface stained, the cells were washed and re-suspended in BD Cytofix/Cytoperm™ for a further 20 minutes at 4℃ in the dark. After fixation and permeabilisation, cells were washed and stained with relevant directly conjugated anti-human mAb in the presence of 0.1% saponin for 30 minutes at 4℃ in the dark. Appropriate isotype controls were used where necessary. After staining the cells were washed and re-suspended in 150μl/well or 300μl/tube and transferred, where necessary, to 500μl polypropylene tubes for acquisition. Table 2.4 details the mAb used for the detection of MDSC intracellular antigens. Data was collected on a BD LSRII™ and analysed using FlowJo v8.8.7.

Intracellular Marker	Flurochrome	Clone	Manufacturer	Dilution
Arginase I	FITC	not available	R&D Systems	5:50
Galectin-9	PE	9MI-3	BD Bioscience	2:100
TGFβ	FITC	TW4-2F8	R&D Systems	3:100
IL-10	PE	JES3-967	Miltenyi Biotec	3:100
CD63	PE	HSC6	eBioscience	2:100
CD66b	PerCP-Cy5.5	G10F5	Biolegend	2:100

Table 2.4: Directly conjugated anti-human mAb against intracellular antigens used for the assessment of MDSC phenotype and functionality by multiparametric flow cytometry.

2.3.4 Staining for T cell/NK cell phenotype & functionality

For the analysis of T cell phenotype and/or functionality either *ex vivo* or after short term co-culture, cells were stained using a similar protocol to that described in section 2.3.2. In the case of T cell/NK cell analysis, cells were stained to allow detection and removal of dead cells from analysis using an Invitrogen™ Blue Live/Dead® Cell viability in conjunction with all other surface mAb. Tables 2.5 and 2.6 detail the mAb used for the detection of extracellular and intracellular antigens for analysis of T cell/NK cell function and phenotype. Data was again collected on a BD LSRII™ and analysed using FlowJo v8.8.7.

2.3.5 Detection of T cell cytokine production

For detection of T cell cytokine production, samples previously frozen down (described in section 2.2.3) were used. PBMC were rapidly thawed, washed and re-suspended in cRPMI for stimulation. 2×10^6 cells were plated per well in 96-well plates (U-bottomed) and incubated in the presence of phorbol 10-myristate 13-acetate (PMA) at 3ng/ml, ionomycin at 100ng/ml, and brefeldin A (BFA) at 1mg/ml, or cRPMI and BFA alone as a negative control for 3 hours. After incubation the cells were washed and stained for cytokine production as a marker of T cell functionality as described in section 2.3.4.

2.3.6 Analysis of regulatory T cells

For the analysis of circulating frequencies of Treg, samples previously frozen down (described in section 2.2.3) were used. All surface staining was done *ex vivo* as described previously. In this case the fixation protocol was slightly amended. Once stained with extracellular markers the cells were fixed and permeabilised according to the manufacturer's protocol with the human FOXP3 buffer kit (BD Bioscience). For the detection of the T cell transcription factor (FOXP3), the staining was then carried out after fixation in the presence of 1x PBS.

Surface marker	Flurochrome	Clone	Manufacturer	Dilution
CD14	BD Horizon V500™	M5E2	BD Bioscience	2:100
CD16	APC-eFluor® 780	3G8	eBioscience	1:100
CD16	PE	DJ130c	Miltenyi Biotec	3:100
CD19	PerCP-Cy5.5	HIB19	BD Bioscience	2:100
CD19	BD Horizon V500™	HIB19	BD Bioscience	1:100
CD127 (IL-7R)	PerCP-Cy5.5	A019D5	Biolegend	1:100
CD3	PE-Cy7	UCHT1	eBioscience	1:100
CD3	PE-CF594	UCHT1	BD Bioscience	1:200
CD4	APC-eFluor® 780	RPA-T4	eBioscience	1:200
CD4	BD Horizon V500™	RPA-T4	BD Bioscience	3:200
CD4	PE	OKT4	Biolegend	2:100
CD56	PE-Texas Red® (ECD)	N901	Beckman Coulter	3:100
CD8a	AlexaFluor® 700	OKT8	eBioscience	1:200
CD98	FITC	MEM-108	Biolegend	2:100
HLA-DR	BD Horizon V500™	G46.6	BD Bioscience	1:100
HLA-DR	eFluor® 450	L243	eBioscience	3:100
NKp30 (CD337)	APC	210845	R&D Systems	1:100
Vybrant® (CSFE)	(FITC)	n/a	Invitrogen™	1μM
Live/dead®	Blue (UV)	n/a	Invitrogen™	1:1500

Table 2.5: Directly conjugated anti-human mAb against extracellular antigens used for the identification of lymphocyte subsets and analysis of phenotype by multiparametric flow cytometry.

Intracellular Marker	Flurochrome	Clone	Manufacturer	Dilution
CD3ζ (CD247)	PE	6B10.2	eBioscience	1:200
FOXP3	Pacific Blue	259D	Biolegend	4:100
GranzymeB	FITC	GB11	eBioscience	1:100
IFNγ	BD Horizon V450™	B27	BD Bioscience	3:100
IL-2	PerCP-Cy5.5	MQ1-17H12	eBioscience	1:50
IL-10	PE	JES3-967	Miltenyi Biotec	3:100
IL-17	APC	BL168	Biolegend	3:100
Ki67	FITC	B56	BD Bioscience	10:100
Ki67	PE	B56	BD Bioscience	10:100
TNFα	FITC	MAb11	BD Bioscience	1:200
TNFα	APC	6401.1111	BD Bioscience	1:100

Table 2.6: Directly conjugated anti-human mAb against intracellular antigens used to assess T/NK cell functionality and phenotype by multiparametric flow cytometry

2.3.7 Identification of virus-specific CD8+ T cells

The phenotype of virus specific cells from HLA-A2 positive individuals were evaluated directly *ex vivo* by HLA-A2-restricted multimer staining using samples previously frozen down (described in section 2.2.3). Total PBMC were thawed from liquid nitrogen storage (as previously described in section 2.2.3) and stained with fluorescently-labelled dextramers against HBV epitopes: core 18-27, envelope 183-191, envelope 335-343, envelope 348-357, and polymerase 508-510 or fluorescently-labelled CMV epitope: CMV pp65 (Immudex), detailed in table 2.7 at 37°Cfor 15 minutes in 1x PBS. The cells were then washed in cRPMI twice and left to rest for one hour. The cells were then stained for other surface markers as previously described in section 2.3.4. A negative control dextramer loaded with an irrelevant peptide was used to aid identification of genuine dextramer positive cells. During analysis CD19+ and CD14+ cells were excluded due to their known capability of binding dextramer non-specifically. The gating strategy for identification of virus specific cells is shown in figure 2.1.

HLA-A2 peptide sequence	Flurochrome	Viral protein	Amino acid region
FLPSDFFPSV	APC	HBV core	18-27
FLLTRILTI	APC	HBV envelope	183-191
WLSLLVPFV	APC	HBV envelope	335-343
GLSPTVWLSV	APC	HBV envelope	348-357
GLSRYVARL	APC	HBV polymerase	455-463
KLHLYSHPI	APC	HBV polymerase	502-510
NLVPMVATV	PE	CMV pp65	495-504
GLCTLVAML	APC	EBV BMLF-1	n/a
GILGFVFTL	APC	Flu	n/a
control	APC	irrelevant protein	n/a

Table 2.7: Full details of the directly conjugated MHC class I-restricted multimers (dextramers) used in this study, supplied by Immudex. Abbreviation used: not applicable (n/a).

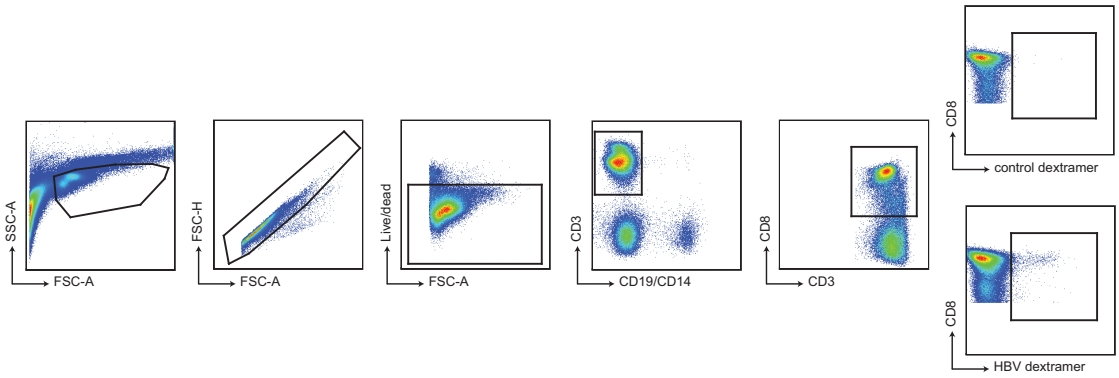

Figure 2.1: Gating strategy for the identification of virus-specific cells. Sequential gating strategy used for the identification of dextramer positive CD8+ T cells. CD3+, live, single lymphocytes were gated on to exclude CD19+/CD14+ cells. Control dextramers were used to determine background antibody staining.

2.4 ImageStreamX

For confirmation of arginase I expression and morphology, novel ImageStream technology was used (combining flow cytometry with the resolution of fluorescence microscopy). PBMC were isolated from fresh blood and stained using the following mAb: CD11b-PE-Cy7, CD15-AlexaFluor700, CD16-PE, HLA-DR-V500, arginase I-FITC. The cells used for imagestream analysis were fixed and permeabilised using BD Cytofix/Cytoperm. The cells was processed on an Amnis ImageStreamX Imaging Flow Cytometer (EMD Millipore Corp.) fitted with a 60x microscope objective. Raw image files were acquired using INSPIRE software (Amnis). After acquisition a compensation matrix was applied to the data to correct for spectral overlap. Data analysis was done using IDEAS software, displaying PBMC using gradient RMS for the brightfield channel to exclude out-of-focus cells and a combined area to aspect ratio dot plot ensured gating on single-cell events. Cells were then gated as: CD11b+CD15+CD16+ for gMDSC identification, excluding cells expressing HLA-DR, for the analysis of arginase I expression.

2.5 Amino Acid Composition Analysis

2.5.1 Reagents

Amino acids: L-arginine, L-citrulline, L-ornithine, L-tryptophan, together with kynurenine were all purchased from Sigma-Aldrich. Stable isotopes were purchased from Cambridge Isotopes Laboratories Inc. Trichloroacetic acid (TCA), methanol and water (all high-pressure liquid chromatography mass spectrometry grade) were purchased from Sigma-Aldrich®.

2.5.2 Sample preparation

For determination of amino acid concentrations by mass spectrometry frozen serum samples were used. Samples were slowly thawed on ice when used. 50μl of serum for each individual was combined with 10μl of the internal standard (mixed stable isotope solution for all proteins for analysis) followed by 100μl of cold 10% TCA solution (5g TCA dissolved in 50μl milliQ water) for deproteinisation, vortexed for three minutes and centrifuged at high speed for 10 minutes at 4°C. 60μl of cold TCA deproteinised serum was transferred to glass tubes for analysis.

2.5.3 High-pressure liquid chromatography - tandem mass spectrometry (HPLC-MS)

Measurements were performed by high performance liquid chromatography followed by mass spectrometry in positive mode (HPLC-MS; Dionex uHPLC system with an Ultimate 3000 RS autosampler and BD Biphenyl-1.9m, 50x2.1mm column switcher with accompanying Thermo Scientific Orbitrap XL system and with electrospray source). 5μl of each standard or sample was injected for analysis. Analytical preparation of the amino acid derivatives was achieved by gradient elution using the following gradient (prepared with 0.1% formic acid - 95% water-0.1% formic acid (FA): 5% acetronitrile-0.1%FA) equilibrated for three minutes, gradient of six minutes up to 10% water-FA: 90% acetonitrile-FA, kept constant for one minute, returned to initial conditions in 0.5 minutes at a flow of 0.4ml/minute at a column temperature of 40℃. The sample was injected directly into the mass spectrometer. The mass spectrometer conditions were as follows: mass spectrometer run time of eight minutes, normal scan, temperature, spray voltage, sheath pressure as stable measurements after calibration. The HPLC system was controlled by Chromoleon Xpress (Thermo Scientific Inc.) and collection of the mass spectrometric data and control of the mass spectrometer was performed by Xcalibur v2.0.7 (Thermo Scientific Inc.).

The reproducibility and recovery of the measurements using the HPLC-MS was determined prior to full protein quantification using a script kindly written and provided by Dr. Niclas Thomas in R v3.0.2, an open-source programming language for statistical computing.

2.5.4 Use of stable isotopes

Many elements in nature have isotopes and some of these are stable. The most abundant of these naturally occurring stable isotopes is C13 (natural abundance of approx. 1.1%). The consequence of elements having several isotopes is that a given molecule will not show up solely as a single peak at the calculated mass when analysed by mass spectrometry, but as a set of peaks, known as the isotopomeric envelope. Consequently, a biological molecule containing five carbons has a 5 x 1.1% chance of incorporating the naturally occurring stable isotope C13. When analysed this feature can be observed as a peak at a mass of +1 (containing one heavy isotope), +2 (containing two heavy isotopes) and so on higher than the expected molecular mass of the molecule; with an abundance of 5.5% compared to the peak at the expected mass. Purchased amino acids with one or two atoms exchanged for (a) stable isotope(s) were used in this study to determine recovery rates. These amino acids/molecules have the same physical properties as

their natural counterparts, but with a mass that can be distinguished, allowing their relative concentration to be quantified.

2.6 Serum Arginase I Quantification

To determine serum concentrations of the enzyme arginase I (liver type arginase - 35kDa) an enzyme-linked immunosorbent assay (ELISA) (Hycult) was carried out as per the manufacturers protocol. Briefly, serum samples stored at -80℃ from controls and a subset of patients with CHB and chronic HCV infection, were thawed out and pre-diluted 1:1 in assay diluent. Concentrations of arginase I were calculated by back calculation to the equation of the line of the standard curves run in duplicate simultaneously in Microsoft® Excel.

2.7 Suppression Assays

2.7.1 Isolation of gMDSC by magnetic bead isolation

Magnetic-labelled beads were used to enrich/deplete gMDSC from freshly isolated PBMC using sequential CD14 negative depletion and CD15 positive isolation (a surrogate isolation protocol for gMDSC). All equipment and reagents used were purchased from Miltenyi Biotec® and used as per manufacturers protocol.

Briefly PBMC were re-suspended in 80μl of ice-cold PBS supplemented with 0.5% FBS and 2mM EDTA (Invitrogen) (refereed to from this point on as MACS buffer) per 10^7 cells. PBMC were incubated with anti-CD14 beads (20μl/10^7 cells) for 15 minutes at 4℃ in the dark. After incubation labelled cells were washed in 2ml of ice-cold MACS buffer and centrifuged for 10 minutes at 300g to remove excess beads. The supernatant was aspirated and discarded and the pellet re-suspended for column isolation. Sterile MS columns were placed in MACS™ magnets and washed through with 500μl of MACS buffer. Up to 10^7 cells were then passed gently through each MS column. Columns were washed through with MACS buffer to elute unlabelled PBMC. The CD14 negative fraction eluted from the columns was kept and re-stained for positive selection under the same protocol with anti-CD15 beads. The second isolation procedure was essentially the same, however after applying the anti-CD15 stained CD14-negative fraction to the column, the labelled cells of interest were eluted from the column by addition of 1ml of MACS buffer by firm application of a plunger to the column. Following the sorting process cells were washed and

re-suspended in cRPMI for use in co-culture experiments. The depleted CD14-CD15- (eluted fraction) was also kept and used in some experiments were stated (referred to as ΔgMDSC).

2.7.2 Isolation of gMDSC by flow cytometry

In order to deplete or isolate cell subsets using flow assisted cell-sorting, 2×10^8 freshly isolated PBMC were obtained from controls. 300μl of 1x PBS supplemented with 10% FBS containing a further 200μl of FcR blocking reagent was added for 20 minutes at 4℃. After FcR blocking, cells were subjected to antibody staining with a combination of the following mAb: CD33 AlexaFluor® 700, CD11b PE-Cy7/CD11b FITC, CD14 PerCP, CD15 APC/CD15 Viogreen™ for 30 minutes, with gentle shaking every 10 minutes at 4℃. Once stained PBMC were washed twice in ice-cold MACS buffer and re-suspended in a volume of cRPMI corresponding to 5×10^7 cells/ml. Before acquisition cells were filtered through a 70μm filter-capped polystyrene tubes (BD Bioscience) to prevent cellular clumps blocking the machine.

Cells were sorted on either a FACSAria™ (Beckton Dickinson) by Jamie Evans or a MoFlow™ XDP (Beckman Coulter) by Thomas Adejumo at low speeds. Cells forming doublets were excluded. Figure 2.2 shows a representative gating strategy used during sorting and the purity achieved. Depleted or sorted cells were collected into polypropylene tubes (BD Bioscience) containing collection media (cRPMI supplemented with 50% FBS). Following the sorting process, cells were washed and re-suspended in cRPMI for use in co-culture experiments.

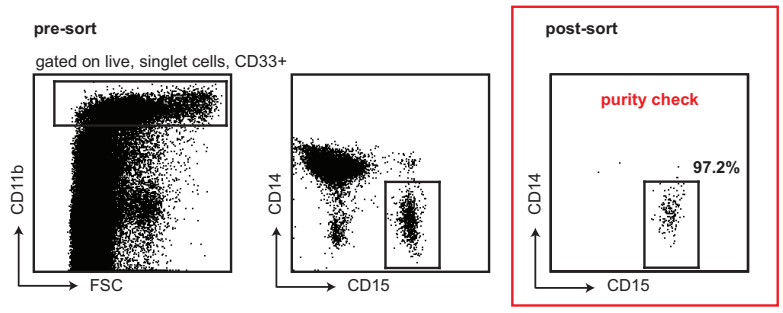

Figure 2.2: Representative gating strategy used for the identification of gMDSC during flow cytometric sorting.

The numerical value in the final plot shows the gMDSC purity after cell sorting, prior to co-culture experimentation.

2.7.3 Staining with Vybrant® CFDA (CFSE)

For co-culture experiments where the proliferative capacity of T cell was assessed, PBMC were stained prior to culture with Vybrant® CFDA (Invitrogen™). 5×10^6 freshly isolated PBMC were re-suspended in 1ml of pre-warmed 37℃ 1x PBS containing 1μM of carboxyfluorescein succinimidyl ester (CFSE). Cells were incubated at 37℃ for 12 minutes and then the reaction stopped by the addition of 1ml of heat inactivated FBS, and washed by centrifugation at 1600rpm for 10 minutes. Cells were then used in co-culture experiments at pre-determined ratios.

2.7.4 Co-culture: gMDSC with autologous PBMC for suppression of bystander T cell function

To assess the potential gMDSC functionality on bystander (non-HBV specific) T cells, 1×10^5 FACS isolated gMDSC or magnetic bead enriched gMDSC PBMC were co-cultured with autologous total PBMC at pre-determined effector:target ratios in 96 well plates (U-bottomed) with various stimuli (listed below). In certain experiments the fraction of cells depleted of gMDSC were also analysed in parallel. Co-culture experiments were all done in the presence of 20IU/ml of recombinant IL-2 (Miltenyi Biotec). The various stimuli used were as follows:

1. 0.5μg/ml plate bound anti-CD3 + 0.5μg/ml anti-CD28 (eBioscience),
2. 0.5μg/ml HLA-A2-restricted NLVPMVATV peptide from CMVpp65 (ProImmune),
3. 0.5μg/ml HLA-A and HLA-B-restricted peptide pool spanning the immune-dominant proteins of CMV, EBV and influenza (CEF) (JPT Peptide Technologies).

All co-culture experiments were incubated for five days at 37℃. On day four cRPMI was changed to cRPMI supplemented with 1μg/ml BFA and cells that had originally been stimulated with peptide were re-stimulated with the same dose of the corresponding peptide. In some experiments autologous total PBMC used for co-culture were previously stained with 1μM Vybrant® CFDA (CFSE labelling, as described in section 2.7.3), to allow detection/monitoring of peptide-specific proliferation. And in other experiments the co-cultures were carried out in the presence of an arginase I specific inhibitor hydroxy-nor-L-arginine (norNOHA, Calbiochem) at 0.5mM for the duration of the assay.

After co-culture, cells were stained for flow cytometric analysis to assess T cell effector functionality as described above.

2.7.5 Co-culture: gMDSC with autologous PBMC for detection of HBV-specific T cell suppression

To assess the potential gMDSC suppression of HBV-specific T cells, a slightly modified version of the protocol described in section 2.7.4 was used. The methodology was the same with the following modification: The stimuli used was either 0.1μg/ml HBV peptide pool (pool of 15mer peptides overlapping by 10 residues spanning the core protein of HBV genotype D) for non HLA-A2+ patients, or a 0.1μg/ml pool of peptides representing HLA-A2 restricted viral epitopes, ″H7‟ containing HBV envelope epitopes: FLLTRILTI, WLSLLVPFV, LLVPFVQWFV and GLSPTVWLSV; HBV core epitope: FLPSDFFPSV; and HBV polymerase epitopes: GLSRYVARL and KLHLYSHPI (ProImmune). On day five the cRPMI was changed to cRPMI supplemented with 1μg/ml BFA and re-stimulated with the corresponding peptide used. If the patient used was HLA-A2+, the cells were stained with the pool of HBV dextramers as described in section 2.3.7 before re-stimulation.

2.8 Co-culture: gMDSC with Primary Hepatic Stellate Cells (pHSC)

2.8.1 Isolation of pHSC

Healthy margins of metastatic liver tissue were obtained in collaboration with Royal Free Hospital surgical staff from consented patients during surgery. All patients signed informed consent, approved by the Royal Free Hospital ethics committee. pHSC were previously isolated by either Dr. Kasha Singh or Harsimran Singh and frozen for long-term storage.

Tissue was digested with DNAseI (0.001%) and collagenase IV (0.01%) before being passed through a tissue press (2mm diameter). The homogenate was then filtered through a 70μm cell strainer and centrifuged at a low speed (500rpm for two minutes) to remove contaminating hepatocytes. The remaining cells were layered for density gradient isolation using Optiprep (Sigma-Aldrich). After isolation, pHSC were suspended in Stellate Cell Medium® (ScienCell Research Laboratories), plated at a density of 5×10^4cells/cm in tissue culture flasks and cultured at 37°C in a humidified atmosphere with 5% CO_2. On day two-four, cell debris and non-adherent cells were removed by washing. When cultures reached confluence, cells were trypsinized and replated; they were passaged twice before freezing as previously described in section 2.2.3.

2.8.2 pHSC staining & co-culture

Pre-isolated pHSC from at least three different donors were thawed and cultured in 25cm^2 tissue culture flasks in Stellate Cell Medium® to approximately 90% confluence. Cells were detached with trypsin, re-plated in 24 well plates in cRPMI and left for 24-48 hours to attach. For staining, 1μg/ml BFA was added for 16 hours prior to cells being detached with MACS buffer and stained for intracellular IL-8 (eBioscience) in the presence of FcR blocking reagent, after fixation and permeablisation with BD Cytofix/Cytoperm. pHSC were acquired on a BD LSRII™ and analysed using FlowJo v8.8.7. IL-8 production was determined after exclusion of dead cells using an Invitrogen™ Blue Live/Dead® Cell viability assay. For co-culture experiments, pHSC were incubated with 2×10^6 freshly isolated PBMC from either controls or patients with CHB in cRPMI for six days. After the culture period the cells were removed by vigorous pipetting and transferred to filtered polypropylene tube prior to staining for gMDSC frequencies as described in section 2.3.2. In certain experiments, where stated, various cytokines/chemokines/growth factors were used at a concentration of 10ng/ml. These included CXCL12, IL-8, IL-6, vascular endothelial growth factor (VEGF), and TNFα.

2.9 Statistical Analysis

Statistical analyses were performed in Prism (GraphPad) using the appropriate tests, with significant differences marked on all figures. For all tests, significance levels were defined as: * = p<0.05, ** = p<0.005, *** = p<0.001. Multivariate analyses were conducted in R 3.0.2, an open-source programming language for statistical computing.

2.10 Reagents

Table 2.8: Full details, including manufacturers and catalogue numbers, of reagents used throughout this study.
* 32 peptides from defined HLA class I-restricted T cell epitopes

Product	**Manufacturer**	**Catalogue No.**
αCD3 purified (functional grade, clone OKT3)	eBioscience	16-0037-85
αCD28 purified (functional grade, clone CD28.2)	eBioscience	16-0289-85
βmercaptoethanol	Life technologies™	31350-010
L-arg free RPMI (+L-glu, −L-arg +phenol red)	PAA	T1090,2500

Continued on next page

Table 2.8 – continued from previous page

Product	Manufacturer	Catalogue No.
Arginase I ELISA kit	Hycult	HK322-02
BD™ CompBeads (anti mouse IgG)	BD Bioscience	51-90-9001229
BSA	Sigma-Aldrich®	A9418-50G
Brefeldin-A	Sigma-Aldrich®	B7651-5MG
CEF extended pool (CMV-EBV-Flu*)	JPT Technologies	PM-CEF-E
CMV peptide (NLV)	ProImmune	n/a
Collagenase IV	Life technologies™	17104-019
Cryovials	Nunc	V7509
BD Cytofix/Cytoperm™	BD Bioscience	554722
DNAse	Roche	11 284 932 001
DMEM (+L-glu, +Pyruvate, +L-glucose)	Life technologies™	41966-029
DMSO	Sigma-Aldrich	D2650
DPBS (−Ca, −Mg)	Life technologies™	14190-169
EDTA	Life technologies™	15575-020
BD™ FACS Lysing Solution	BD Biosciences	349202
FcR blocking reagent	Miltenyi Biotec®	120-000-442
Fetal Bovine Serum (FBS) (heat-inactivated)	Life technologies™	10108-165
Ficoll-Plaque Plus™	GE Healthcare	17-1440-03
BD™ FOXP3 buffer kit	BD Bioscience	560098
Formaldehyde	VWR	20910.328
HEPES buffer solution (1M)	Life technologies™	15630-056
HLA-A2-specific FITC-conjugated mAb	BioRad	MCA2090F
IL-2 (Research Grade)	Miltenyi Biotec®	130-093-901
IL-6 (Research Grade)	Miltenyi Biotec®	130-095-365
IL-8 (Research Grade)	Miltenyi Biotec®	130-093-944
Ionomycin	Molecular Probes (Life tech™)	I24222
L-alanine (13C)	Cambridge Isotope Laboratories	CAS-21764-56-7
L-arginine (guanido-$15N_2$)	Cambridge Isotope Laboratories	NLM-935-PK
L-citrulline (ureido-13C)	Cambridge Isotope Laboratories	CAS-9470-46-2
L- glutamine (amide 15N)	Cambridge Isotope Laboratories	CAS-59681-32-2
L-phenylalanine (ring D5)	Cambridge Isotope Laboratories	CAS-56253-90-8
L-ornithine ($15N_2$)	Cambridge Isotope Laboratories	NLM-3610-025

Continued on next page

Table 2.8 – continued from previous page

Product	**Manufacturer**	**Catalogue No.**
Magnetic CD14 Positive Selection Beads	Miltenyi Biotec	120-000-305
Magnetic CD15 Positive Selection Beads	Miltenyi Biotec	130-046-691
Methyl-L-arginine acetate (L-NMMA)	Calbiochem	53308-83-1
MEM Essential amino acids (50X)	Life technologies™	11130-036
MEM Non-essential amino acids (100X)	Life technologies™	11140-035
Hydroxy-nor-L-arginine (norNOHA: ARGI inhibitor)	Calbiochem	399275
PBS Tablets	Sigma-Aldrich	P4417-100TAB
Penicillin /streptomycin	Life technologies™	15140-122
PMA	Sigma-Aldrich	P8139
Recombinant arginase I	R&D Systems	5868-AR-010
RPMI 1640 (+L-gluatamine)	Life technologies™	21875-054
BD TruCount™ Tubes	BD Bioscience	340334
Saponin	Sigma-Aldrich®	47036-50G-F
Stellate cell media	ScienCell Research Laboratories	5301
Sodium Pyruvate (100mM)	Life technologies™	11360-039
Trichloroacetic acid	Sigma-Aldrich	T9159-500g
TNFα (Research Grade)	Miltenyi Biotec	130-094-014
Trypan Blue	Life technologies™	15250-061
Trypsin-EDTA (1x)	Life technologies™	25300-062
UV (Blue) Live /Dead Stain	Life technologies™	L23105
VEGF (Research Grade)	Miltenyi Biotec	130-094-029

Chapter 3

gMDSC expand in chronic hepatotropic infections

3.1 Abstract

Work presented in this chapter builds on previous work from our group which pointed towards a role for nutrient deprivation in driving a global metabolic T cell defect in CHB. The previous study provided an initial indication that the amino acid L-arginine is depleted and the activity of arginase I, an enzyme involved in its metabolism, is increased in the HBV-infected liver [58]. Therefore it was postulated that an expansion of MDSC, a population known to expand at sites of chronic antigenic stimulation, may contribute to this immunosuppressive milieu in CHB. Using multiparametric flow cytometry this was addressed by analysing the circulating and intrahepatic frequencies of MDSC subsets in two separate cohorts of patients with CHB compared to uninfected, healthy controls. Circulating MDSC with a granulocytic phenotype (gMDSC) were expanded approximately 9-fold in CHB compared to matched controls. MDSC with a monocytic phenotype (mMDSC) were not expanded in the context of CHB. The increase in gMDSC frequencies was most striking in patients replicating HBV in the absence of biochemical or histological evidence of liver damage (the immunotolerant or inactive phase). It also became apparent that gMDSC expansion shows a temporal relationship with viremia in acute HBV infection, and in spontaneous flares of HBeAg- CHB, their decrease coinciding with the onset of liver inflammation. gMDSC only accumulate in the intrahepatic compartment in the diseased liver; they were not found in the healthy liver. Infection with another hepatotropic virus, HCV, also resulted in gMDSC expansion in the circulation that was further amplified in the liver

compartment, whereas CMV serostatus did not affect gMDSC frequencies. Our data therefore show gMDSC accumulation in hepatotropic viral infections that could have the potential to exert immune regulation.

3.2 Introduction

MDSC, as suppressor cells, were first discussed in the introduction in section 1.5.1. The following sections discuss their phenotypic identification, proposed mechanisms involved in their expansion/accumulation, and what is already known about MDSC in relation to chronic inflammation, and more specifically in relation to viral infection.

3.2.1 Phenotypic identification of MDSC

As already stated, MDSC are still a relatively novel cell type, and as a result their discovery and study has become the focus of a rapidly expanding field. Their discovery culminated in them being described as one of the immunological highlights by eminent immunologists writing for Nature Reviews Immunology in 2011 [156] (figure 3.1a). The number of reports being published online citing MDSC has risen dramatically, with an increase in the number of MDSC-related publications returned from a search of ″PubMed‟ from 2 in 1982 to 326 last year (2013) (figure 3.1b).

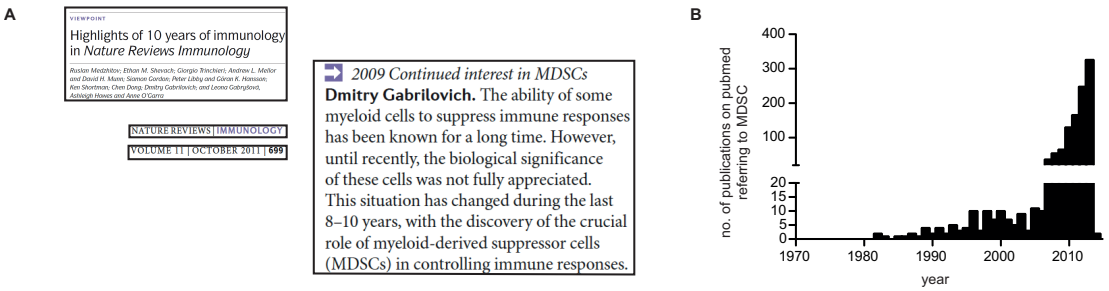

Figure 3.1: Impact of the discovery of MDSC in the literature.

A) Screenshots from an article published in Nature Reviews Immunology in 2011 describing the discovery and study of MDSC to be one of the immunological highlights of the last decade. B) Graphical representation of the number of publications quoting MDSC published online from the 1970s when they were first described to 2013, data obtained from ″PubMed‟.

As well as the initial issue of nomenclature that was discussed in section 1.5.1, the study of human MDSC has been plagued by numerous difficulties. In the past (and even recently) phenotypic identification, and therefore the study of human MDSC, has been challenging and inconsistent. Cellular heterogeneity and a lack of consensus over identification markers has resulted in investigator-dependent phenotypic marker profiles being used when considering a role for MDSC involvement in immune regulation. This issue is now further confounded by the new concept of MDSC plasticity [157, 158]). In contrast to the study of human MDSC, the study of murine MDSC has been relatively clear and more focused. This was largely due to an early literature-led consensus defining a clear set of identification markers.

Since early observations in tumour-bearing mice, murine MDSC have been phenotypically identified by co-expression of the two myeloid-lineage differentiation antigens CD11b and Gr-1. However many researchers would now argue that the minimal markers used for the identification of murine MDSC are insufficient and may require further attention from the field for better phenotypic characterisation. Murine MDSC are more accurately divided into two subsets (monocytic and granulocytic) dependent on expression levels of Ly6C and Ly6G. Monocytic MDSC (mMDSC) have a CD11b+Ly6G-Ly6C^{high} expression profile, with monocytic morphology and preferential expression of inducible nitric oxide (iNOS), whereas granulocytic MDSC (gMDSC) have a CD11b+Ly6G+Ly6C^{low} expression profile, granulocytic-like morphology and expression of arginase I [159]. Clear roles for either subset in the context of pathology has yet to be fully elucidated, however recent analysis by Youn *et al.* [159] in ten different experimental tumour models noted that both subsets of MDSC can expand, but the gMDSC subset predominate. In the same context of experimental tumour models looking to characterise such granulocytic MDSC further, the authors stressed the fact these particular cells share common phenotypic markers with mature classical neutrophils, but these cells are considered to be functionally distinct [160, 161], since neutrophils are not typically immunosuppressive.

Recent progress in the field of murine MDSC is beginning to extend the phenotypic identification panel to include consideration of several other markers. These include a lack of CD11c expression and the presence or absence of IL-4Rα and CD49d. Consequently gMDSC can be better identified as CD11b+Gr-1^{high}Ly-6C^{low}Ly-6G+CD49d- while mMDSC as CD11b+Gr-1$^{int.}$Ly-6C^{high}Ly-6G-CD49d+ [158, 162].

The lack of a human homologue for Gr-1 has been central to the challenge faced by the field of human MDSC. Towards the end of the 1990s, MDSC were beginning to be more extensively described in humans, specifically in patients with granulocyte macrophage colony-stimulating factor (GM-CSF)-secreting tumours of the head and neck [163]. At the time these cells were identified on the basis of lineage negativity (no expression of mature lymphocyte markers) and CD34 expression alongside their capacity to limit T cell proliferation. This work was limited by the fact that CD34 expression encompasses all haematopoetic progenitors. Therefore it was necessary for the field to identify and use further markers to enable the identification of MDSC. This led to the introduction of gating strategies that excluded cells expressing the MHC-II molecule, HLA-DR, and the inclusion of at least one myeloid-lineage marker.

Since then human MDSC have been described by an expression profile containing at least one of (or both of) the myeloid-lineage markers CD11b and CD33, a lack of expression of markers of mature lymphocytes (for example, CD3, CD56, CD19) and a lack of HLA-DR. They are further defined by expression of either the monocytic marker CD14 or the granulocytic marker CD15. Expression profiles of human MDSC from multiple different studies and settings have been reviewed extensively in the literature and are beyond the scope of this thesis, but are discussed in detail in reviews by Gabrilovich & Nagaraj [164], Brandau *et al.* [165], Khaled *et al.* [166], Greten *et al.* [167], and Poschke & Kiessling [168].

MDSC have been predominantly studied in the context of cancer biology, with different phenotypes of MDSC being described in cancers of different origins. Of note it is these different phenotypes seen that form the basis of the idea of MDSC plasticity. MDSC markedly expand systemically when mice are inoculated with transplantable tumour cells and upon development of spontaneous tumours in transgenic murine models with tissue-restricted oncogene expression. In several tumour models, it has been reported that up to 20-40% of all nucleated splenocytes are MDSC, in contrast to the 2-4% seen in wild type mice. As in mice, human gMDSC make up less than $\sim$ 0.5% of isolated PBMC in healthy individuals with reports of up to $\sim$ 10-fold expansion in the circulation of patients with renal cell carcinoma or colorectal cancer [169, 170]. Such phenotypes and functionality of MDSC specifically in cancer have also been extensively reviewed elsewhere [158, 171, 160, 167, 172, 133]. But two key reviews by Gabrilovich in Nature Reviews Immunology have gone a long way to resolving the inconsistencies and confusion in the literature, with the goal of creating a more unified platform for MDSC study in humans [164, 133].

What is evident from the following table, table 3.1 is that human MDSC, either monocytic or granulocytic, express a large number and wide-range of markers. Without routine analysis using the latest technology, CyTOF, that fundamentally increases the number of markers that can be detected simultaneously, considering the expression of all possible markers in one single multi-colour flow cytometry panel would be impossible.

Surface Marker	mMDSC	gMDSC
CCR2	+	-
CXCR4 (CD184)	+	+
CXCR2 (IL-8Rα)	subset	+
CD11b	+	+
CD11c	subset	subset
CD14	+	-
CD15	-	+
CD16	subset; low	+
CD19	-	-
CD3	-	-
CD33	+	+
CD34		
CD39	+	+
CD45	+	+
CD56	-	-
CD62L	low	low
CD66b	-	+
CD80	+	+
IL-4Rα (CD124)	+	+
HLA-DR	- /low	-
M-CSF	+	-
MHC-I	+	+
MHC-II	-	-
VEGFR1	+	+
VEGFR2	+	+

Table 3.1: Phenotypic markers expressed by human monocytic vs. granulocytic MDSC.

+ indicates expression, - indicates lack of expression. Particular phenotypes that remain debated in the field are noted as ″subset‟. Adapted from Talmadge & Gabrilovich [173].

The focus of the following sections is to highlight some of the latest evidence for MDSC in the context of inflammation but more specifically in the context of persistent antigenic stimulation.

3.2.2 MDSC: cellular expansion & activation

The initial concept that chronic inflammation can contribute to tumour initiation and progression was first noted a long time ago. Although at the time this hypothesis was widely overlooked. It is now well established that a link exists between inflammation and cancer [171]. A major immune-mediated mechanism observed during states of chronic inflammation that directly promotes tumour growth is the perturbation of myelopoiesis. Preventing the normal process of mature myeloid cell development can lead to an overwhelming deficiency in functional APC and an increase in immature myeloid cell infiltrates. Such myeloid cell infiltration into cytokine, chemokine and growth factor-rich tumour milieu promotes the development of functional MDSC. Given the very nature of MDSC, their presence in the tumour microenvironment directly and indirectly inhibits both innate and adaptive anti-tumour responses.

A wealth of evidence from both experimental tumour-models and human cancers has provided insight into the induction and/or expansion of MDSC. This has led to the widespread belief that this process is mediated by the combined effect of a number of factors (including cytokines, chemokines, growth factors and pro-inflammatory mediators). Factors reported thus far include: cyclooxygenase-2, prostaglandins, stem-cell factor, macrophage colony-stimulating factor (M-CSF), IL-6, GM-CSF, and VEGF [174, 175, 176, 164, 173, 177]. A number of these factors promote myelopoeisis and/or inhibit myeloid cell maturation.

These factors are considered to be MDSC expansion-promoting factors that can activate internal signalling pathways converging on members of the Janus kinase (JAK) protein family and signal transducer and activator of transcription 3 (STAT3); both of which regulate cell survival, proliferation, differentiation and apoptosis. It is currently widely accepted that STAT3 is the main transcription factor involved in MDSC induction and expansion. Persistent (or aberrant) activation of STAT3 in myeloid progenitors is directly linked to the expansion of MDSC via the inhibition of differentiation into mature myeloid cell populations. Specifically in tumour-bearing mice MDSC expansion is driven by increased expression of phosphorylated STAT3 [178]. In addition MDSC frequencies dramatically decrease upon ablation of STAT3 signalling either by using a conditional knock-out model or the use of selective inhibitors; conversely exposure of haematopeotic stem cells to supernatants from tumour cell cultures activates STAT3 and results

in an *in vitro* expansion of MDSC [178, 179].

More recent evidence suggests activation of STAT3 signalling also promotes MDSC expansion via the induction of S100 calcium-binding protein A8 (S100A8) and S100A9. Both proteins are involved in the inflammatory response and the receptors for which are expressed on the surface of MDSC. Evidence suggests that blocking the action of these two proteins *in vivo* limits the expansion of MDSC observed in tumour-bearing mice [180**?**] (discussed in more detail in section 3.2.3).

The importance of STAT3 signalling in MDSC expansion has since been confirmed in human studies. MDSCs isolated from the tumour site, the draining lymph nodes, and the peripheral blood of patients with squamous cell carcinoma of the head and neck express high levels of phosphorylated STAT3 which correlates directly with their suppressive capacity [181].

Recent emerging lines of evidence also suggest that signalling via STAT3 indirectly regulates the differentiation of MDSC subsets. Signalling via STAT3 has been implicated in the control of acute-phase protein expression. The production of such proteins was demonstrated by Sander *et al.* [182] to enhance MDSC accumulation and survival. In this model of polymicrobial sepsis, IL-6-activated STAT3 signalling in hepatocytes, through interaction with the transmembrane protein, glycoprotein 130 (gp130), resulted in the expression of the acute-phase protein, serum amyloid A and chemokine CXCL1, which cooperate to promote MDSC accumulation in the spleen [182].

The functional activity of MDSC is not only dependent on factors promoting their expansion and survival but also on factors that induce their activation. Candidate MDSC activatory factors include: IFNγ, TGFβ, TLR ligands, IL-4 and IL-13 [164]. These mediators enable downstream activation within the MDSC of further signalling pathways including STAT6, NKκB, or STAT1. It is currently postulated that signalling via STAT1 in the MDSC is the main pathway of activation by the pro-inflammatory cytokine IFNγ. STAT1 is the major transcription factor activated by IFNγ-mediated signalling and blockade of IFNγ production abolished MDSC-mediated T-cell suppression by arginase I [183, 184]. Also MDSC from STAT1 double knock-out mice fail to up-regulate arginase I and iNOS expression preventing them from inhibiting T cell responses *in vivo* [185].

3.2.3 MDSC: in the context of chronic inflammation

In patients with CHB there is continuous, and often high-level antigenic stimulation with repeated episodes of liver inflammation alongside the local tolerisation of specific lymphocytes, mirroring the hallmark features observed in chronic inflammation and cancer biology. Research in both these fields provides insight into a potential role for MDSC in specific immunosuppression in the context of chronic viral infection where MDSC have been relatively under studied. Under conditions of chronic inflammation that result from high bacterial burden, for example, secondary lymphatic organs are often characterised by an immunologically suppressive or altered milieu, including that of CD3ζ down-regulation accompanied by T cell dysfunction [186].

A handful of published studies present evidence for MDSC-mediated chronic inflammation-dependent immunosuppression [187, 188, 189]. While under some circumstances acute inflammation is essential for the clearance of pathogens, excessive or chronic inflammation can become detrimental, potentially preventing the clearance of the initial invading pathogen via the induction of an immunosuppressive environment. In a study by Vaknin *et al.* [188] MDSC were suggested to play a role in the maintenance of such an immunosuppressive environment. The authors specifically proposed a role for TLR signalling-dependent induction of MDSC capable of inhibiting T and NK cell function. The authors discuss the possibility that the immunosuppression arising from TLR-mediated chronic inflammation evolved to limit excessive immunopathology that can arise upon chronic stimulation of the innate immune system, and thus preventing excessive tissue damage [188].

In a more recent study by the same group, Sade-Feldman *et al.* [189] reported that a TNFα-rich milieu resulting from chronic inflammation directly induces an immunosuppressive environment, primarily through the expansion of suppressive MDSC. The authors not only demonstrated MDSC expansion through direct inhibition of the physiological process of myeloid cell maturation, in this case via an up-regulation of the proteins S100A8 and S100A9, but also an increase in the suppressive capacity of the MDSC, with effects on both T and NK cell function. MDSC in this chronic inflammatory setting were reported to up-regulate the activity of two characteristic enzymes, iNOS and arginase I, involved in the metabolism of L-arginine and increased cellular production of reactive oxygen species (ROS). Sade-Feldman *et al.* [189] also demonstrated the ability to overcome MDSC mediated suppression through the use of anti-TNFα therapy. Treatment with etanercept demonstrated the ability to recover expression of the signalling component CD3ζ of both T and NK cells with a concomitant increase in cellular functionality [189].

3.2.4 MDSC: in the context of viral infection

As already stated until very recently MDSC were predominantly studied in cancer, however new evidence is beginning to detail roles for both subsets of MDSC in mediating or promoting the pathogenesis of chronic viral infections. Norris *et al.* [190] have demonstrated a role for MDSC in chronic, but not acute, infection with LCMV infection. Utilising the clone 13 infection strain to confer chronic infection, the authors reported a specific role for MDSC not seen in mice treated with a strain causing acute infection, Armstrong. The authors hypothesised that the two distinct infection patterns induce differing innate immune responses, leading to differential induction of T cell immunity and therefore viral persistence. Within this study the authors reported the innate immune response in LCMV as two temporal phases: an early DC response during the first 72 hours post-infection and a later LCMV-specific expansion of a myeloid cell population. In the latter stages of both strains of LCMV, the expansion of myeloid cells coincided with a peak in the CD8+ T cell response. However in chronic infection the expansion of myeloid cells was sustained and exhibited the phenotypic and functional profile of MDSC. Most importantly MDSC in chronic infection accelerated T cell exhaustion. Elimination of MDSC in this context by antibody depletion directly enhanced T cell functionality and reversed the T cell exhaustion signature.

In other murine models of viral infections, MDSC have also been implicated. Using a model of acute influenza A virus infection, Jeisy-Scott *et al.* [191] demonstrated a role for TLR7 signalling in the induction of MDSC and in the regulation of their ability to suppress T cell function. Specifically in this case infection with influenza, in the absence of functional TLR7 signalling resulted in an accumulation of active MDSC at the site of infection.

MDSC in the context of viral infection have also been studied in a limited number of human infections. Like HBV, HCV is remarkably efficient at persisting in the presence of an ongoing immune response. Infection with HCV during adulthood establishes chronicity in the majority of cases (approximately 80% of individuals). Tacke *et al.* [192] have reported a role for HCV core protein in the induction of an MDSC population; the addition of exogenous HCV core protein to pre-isolated CD33+ resulted in the induction of a population of monocytic MDSC displaying a CD11b+HLA-DR$^{low/neg}$CD14+ phenotype. These cells were capable of suppressing T cell responses, both their IFNγ production upon stimulation and their proliferative capacity, by increasing the production of ROS [192]. This study was supported by the detection of a similar population of cells *in vivo* in the periphery of an extremely small cohort of five patients chroni-

cally infected with HCV [192]. Further evidence has gone on to detail the clinical significance of these MDSC. In this case the authors showed an increase in mMDSC in treatment-naive chronic HCV patients compared to controls in an extended cohort. In this cohort MDSC positively correlated with HCV viral load, extent of liver damage and the activation status of global T cells. In the same study dramatic decline in MDSC numbers was observed upon initiation of anti-viral therapy. However, in contrast to the previous report ([192]), the T cell suppression observed in this study was attributed to arginase I [193]. Notably two further studies have shown increased numbers of MDSC in HCC resulting from chronic HCV infection. In the context of HCC, MDSC functionality has been attributed to their ability to induce CD4+CD25+FOXP3+ Treg [194] and the ability to mediated MDSC-dependent inhibition of NK cell function via the NKp30 receptor-ligand interaction [195].

HCV is not the only chronic viral infection to have been considered. HIV is also a virus capable of subverting the immune system via the potential induction of MDSC. In a recent report, as with HCV core protein, incubation of HIV tat protein with a population of healthy PBMC *in vitro* gives rise to a population of mMDSC (CD33+CD11b+HLA-DR$^{low/neg}$CD14+). This was corroborated by an increase in circulating MDSC in seropositive individuals [196]. Further evidence also suggests a role for the HIV protein, gp120 (but not gp41) in the induction of functionally suppressive MDSC via the production of pro-inflammatory cytokine, IL-6. The authors of this study demonstrated that the neutralisation of IL-6 abrogated expression of phosphoylated STAT3 in the myeloid population and, subsequently reduced MDSC frequencies [197]. Mirroring HCV, treatment with highly active anti-viral therapy results in a significant decline in mMDSC numbers, alongside a steep drop in HIV viral load. While Qin *et al.* [196] failed to see a notable difference in the frequencies of circulating gMDSC in HIV, Vollbrecht *et al.* [198] demonstrate an increase in gMDSC numbers in patients not receiving treatment compared to uninfected controls.

What is apparent is that MDSC have the potential to expand under conditions of chronic viral infection. In this study we utilised multiparametric flow cytometric techniques to analyse valuable patient material. We postulated a subset of MDSC play a vital role in CHB. We also hypothesised that these cells may home to the site of viral replication where they could exhibit suppressive activity, directly functioning to limit T cell mediated liver damage caused by lymphocyte infiltration into the liver.

3.3 Results

3.3.1 Challenges in phenotypic identification of MDSC in CHB

To investigate a role for MDSC and their potential to influence the well-described dysregulated immune response seen in patients with CHB, it was necessary to refine a method for their identification. Historically this has been complicated largely due to the heterogeneous nature of MDSC (as previously discussed in section 3.2.1), and the lack of unique markers for flow cytometric analysis. Very preliminary work from our collaborators in the Bertoletti group looked at a population of MDSC in HBV infection providing us with a clear grounding, enabling our initial work to focus on designing a panel of markers and flourochrome combinations to allow full, reliable and robust identification of both the monocytic and granulocytic MDSC subsets. Figure 3.2a defines and demonstrates the phenotypic markers and gating strategies used.

The granulocytic subset (gMDSC) were defined throughout by expression of CD11b, CD33 and CD15, and a lack of HLA-DR and CD14. Conversely, the monocytic subset (mMDSC), were defined by expression of CD11b, CD33, low levels of HLA-DR and CD14, and a lack of CD15. mMDSC, as their name would suggest, lack expression of CD16 and CD66b, two granulocytic markers that are only evident on the gMDSC population (figure 3.2b). Neither mMDSC nor gMDSC subsets express the classical lymphocytic markers CD3 or CD19 (used for the identification of T- and B cells respectively) (figure 3.2c). The relative number of circulating MDSC for each study participant were determined *ex vivo* from freshly isolated PBMC. The MDSC population was continually presented as a percentage of the total myeloid cell population, identified by high CD11b and CD33 expression (far right hand panel of figure 3.2a).

Prior to full analysis, the gMDSC population in question was confirmed to be granuloyctic in nature using a different technique. gMDSC isolated from two individuals using flow assisted cell sorting using the panel of markers described and depicted in figure 3.2a, underwent morphological analysis using cytospin technology and haematoxylin-eosin staining. These cytospins were done by Muzz Haniffa during her time in Antonio Bertoletti's group. Figure 3.2d demonstrates the existence of multi-lobed nuclei, a feature specific to granulocytic cells, confirming the granulocytic nature of the MDSC population in question in this thesis [165, 132].

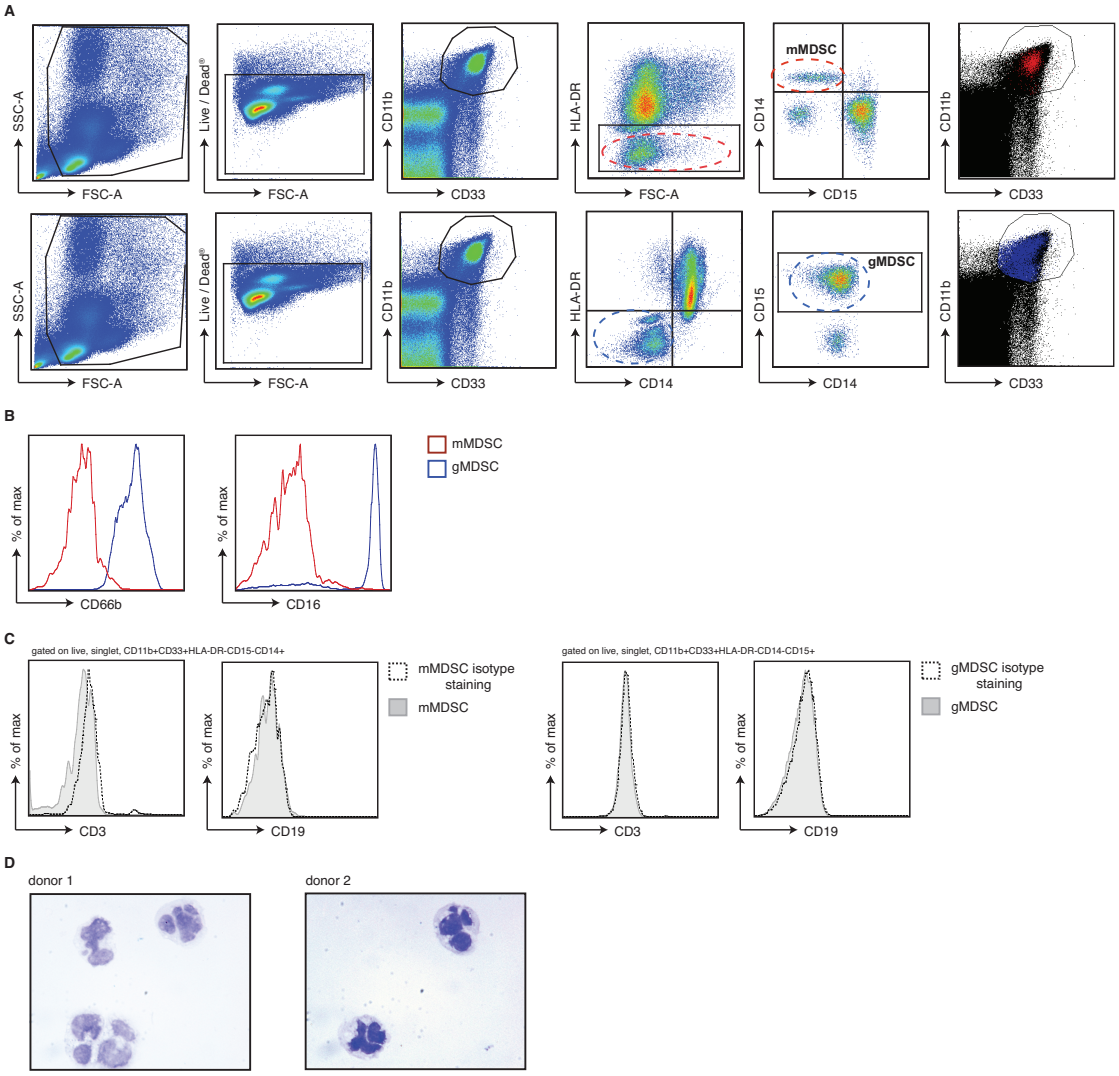

Figure 3.2: Phenotypic identification of monocytic & granulocytic MDSC from freshly isolated PBMC by flow cytometry.

mMDSC phenotypically defined as: CD11b^{high}CD33+HLA-DR^{low}CD15-CD14+, and gMDSC phenotypically defined as: CD11b^{high}CD33+HLA-DR-CD14-CD15+. Analysis was performed by multiparamtric flow cytometry using freshly isolated PBMC. A) Representative FACS plots showing the gating strategy used to identify both MDSC subsets. To represent percentages of circulating MDSC, the MDSC population was calculated as a percentage of total myeloid cells (CD11b^{high}CD33+) by superimposing the gated MDSC population (highlighted on the far right plots) onto the myeloid cell gate during analysis. B) Representative histogram plots showing CD16 and CD66b surface expression on both the mMDSC (red) and gMDSC (blue) subsets. C) Representative histogram plots showing surface expression of CD3 and CD19 on mMDSC, left hand panel, and gMDSC, right hand panel compared to their matched isotype controls. D) Morphological analysis of the gMDSC subset - haematoxylin-eosin staining of flow cytometric isolated gMDSC - Attributed to Muzz Haniffa.

It is important to note that freshly isolated (in other words, never frozen and thawed) PBMC were used for the vast majority of this study as we, and others, have shown that gMDSC are a fragile, cryo-sensitive population [199]. Relative frequencies of gMDSC dramatically declined

when subjected to an overnight freezing protocol (methodology outlined in section 2.2.3) in six study participants (figure 3.3a). The study of MDSC using frozen samples is not impossible, but frequencies are extremely low. This was evident when comparing gMDSC frequencies in a separate cohort of patients with CHB, where a proportionate loss of gMDSC was noted upon freezing (figure 3.3b). Notably mMDSC did not show a reproducible, significant decline in frequencies upon freezing in this extremely small cohort (figure 3.3c).

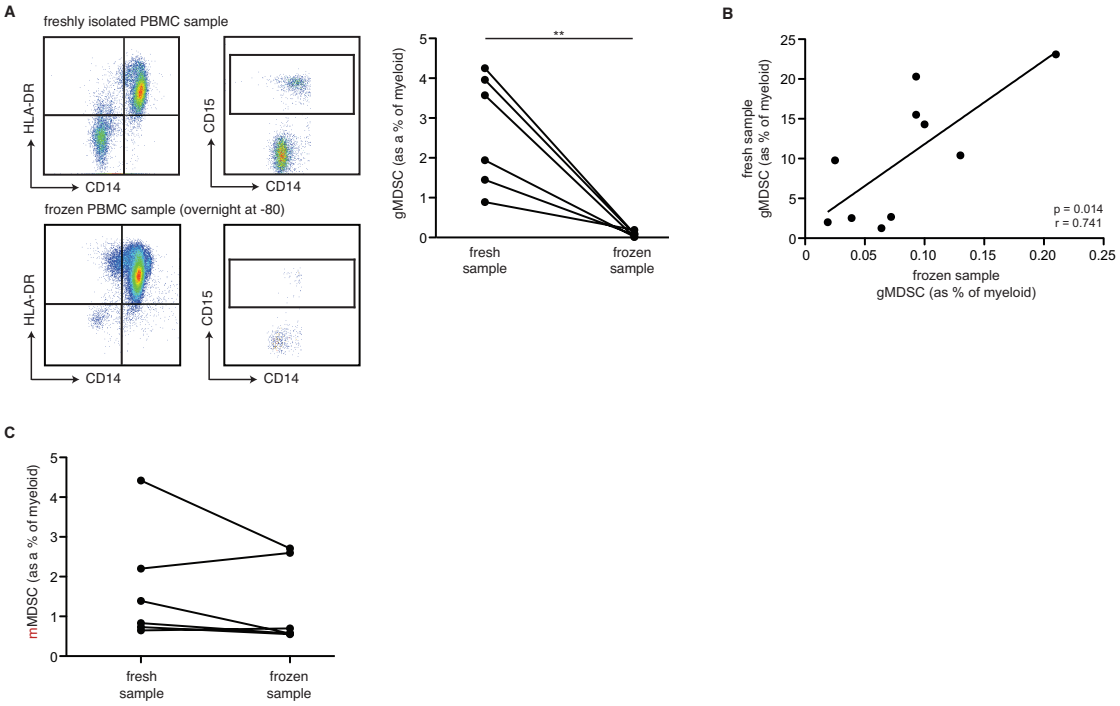

Figure 3.3: MDSC are cryosensitive: identification of MDSC subsets using freshly isolated and frozen and thawed PBMC.

A) PBMC from five patients with CHB and one control were stained for CD33, CD11b, HLA-DR, CD14 and CD15 and analysed for gMDSC frequencies. Representative FACS plots show gMDSC identification in samples stained either when freshly isolated (upper panel) or after a period of 24 hours freezing in FBS supplemented with 10% DMSO at -80°C (lower panel), and cumulative data. B) Correlative analysis of 10 patients with CHB comparing frequencies of circulating gMDSC in fresh versus frozen PBMC samples. C) Cumulative data showing frequencies of circulating mMDSC in the previous six samples (fresh versus frozen). Error bars represent the mean ± SEM. Significance testing was carried out using the paired Students t test, and where significant indicated as: * $p<0.05$; ** $p<0.01$.

Within this study there was the added complication that arose due to the reliance upon multiple NHS centres for continued patient recruitment and sampling. All NHS centres involved in this study used BD Vacutainers® for sample collection containing an anti-coagulant. However, between the centres, the anti-coagulant agents coating the vacutainers varied. gMDSC survival/maintenance in vacutainers coated with lithium-heparin was better than those taken

in EDTA providing further evidence for the fragility of these cells (figure 3.4a). Comparative analysis of isolated PBMC, simultaneously collected into tubes containing either anti-coagulant agent was done in five individuals to confirm this observation (figure 3.4b). From this cumulative data (figure 3.4c) it became apparent that it would be necessary to record the reagent used and to keep data from each patient cohort separate.

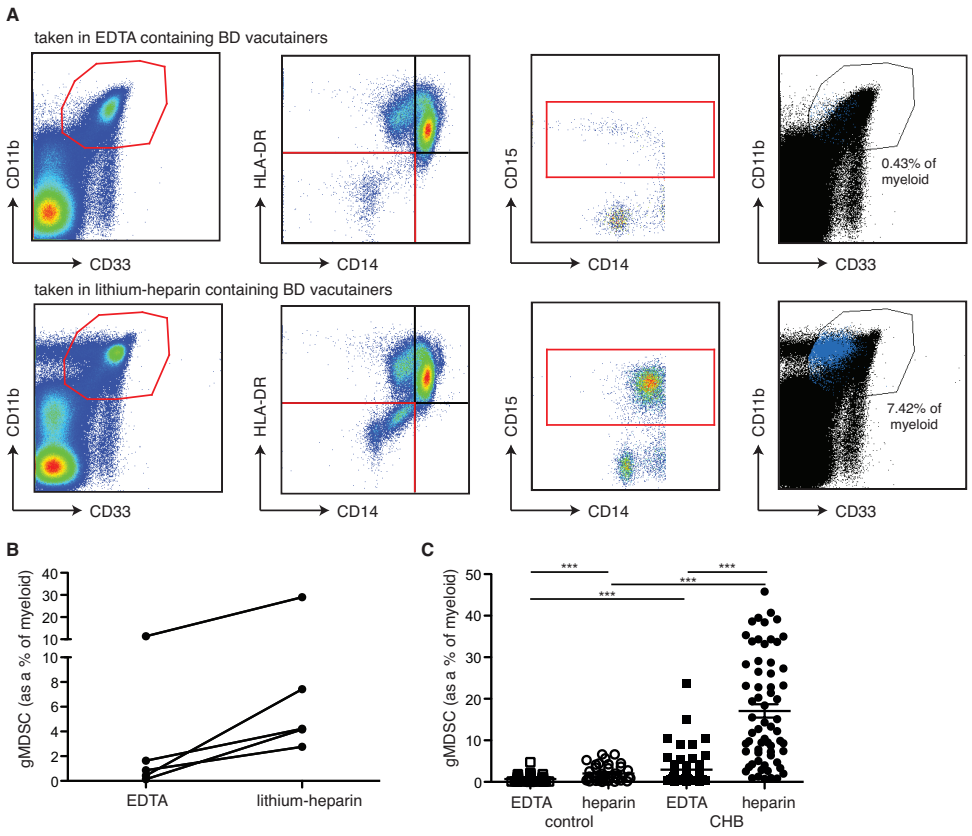

Figure 3.4: MDSC viability is enhanced in lithium-heparin tubes during sample collection.

Identification of gMDSC ($CD11b^{high}$CD33+HLA-DR-CD14-CD15+) using 11-colour flow cytometry from freshly isolated PBMC. A) Representative FACS plots of the gMDSC population from the same study participant using PBMC isolated from blood taken on the same clinic visit in EDTA- or lithium-heparin-containing BD Vacutainers® with the gating strategy used outlined in red. B) Cumulative data for three patients with CHB and two controls where paired samples in both anti-coagulants were obtained. C) Cumulative data for all study participants from both cohorts of patients: 1) Central London cohort - taken in EDTA containing tubes - 56 patients with CHB and 54 controls, and 2) East London cohort - taken in heparin containing tubes - 64 patients with CHB and 37 controls. Error bars represent the mean ± SEM. Significance testing was carried out using either the paired or unpaired Students t test, and where significant indicated as: *** $p<0.001$

In summary to begin studying a role for MDSC in the context of CHB, it was essential to ensure all experiments were done on freshly isolated PBMC (where possible), using the same protocol for isolation to ensure cell viability. Antibody clones and fluorochromes used for all *ex vivo* work

to assess MDSC frequencies remained unchanged throughout, to avoid any potential differences in gating of small cellular populations.

3.3.2 gMDSC are preferentially expanded in patients who sustain HBV replication without necroinflammatory liver damage

To specifically investigate whether MDSC play a role in CHB, their circulating frequencies were examined in carefully characterized patients with CHB. Having established the need to keep the cohorts separate according to the anti-coagulant used during sample collection, it was necessary to classify all study participants into two distinct cohorts: both with age- and sex-matched uninfected controls where possible (details of both cohorts are described in section 2.1 and summarised in tables 2.1 and 2.2).

Circulating gMDSC are highlighted in red in the two representative examples (one control and one patient with CHB) shown in figure 3.5a. The frequency of gMDSC was significantly increased, by a mean of $\sim$ 9-fold, in a cohort of 64 patients with CHB compared to 37 controls from the East London cohort taken in lithium-heparin (cumulative data figure 3.5b). This finding was reproducible in a separately sampled cohort of 56 patients with CHB and 54 controls from the Central London cohort taken in EDTA (figure 3.4c). gMDSC frequencies were proportionately decreased in this second cohort, attributable to a selective loss of gMDSC after collection of blood in EDTA rather than heparin as already described (figure 3.4c). Further gMDSC quantification and extensive study on functionality was typically restricted to samples obtained in lithium-heparin containing BD Vacutainers®. Where relevant, the cohort of patients with CHB taken in EDTA has been included for reference. Also throughout this study due to known reduced granulocyte counts in individuals of African-descent, ethnicity was recorded and were appropriate patients were excluded [200].

The extent of gMDSC expansion was variable within our cohorts of patients with CHB. In some patients circulating frequencies observed were comparable to controls and in others an $\sim$ 22-fold expansion in circulating gMDSC was seen (compared to the mean value for controls) (figure 3.5b). The expanded population of gMDSC accounted for as much as 45% of circulating myeloid cells in some cases. This expansion was a selective expansion in the granulocytic subset of MDSC, frequencies of mMDSC did not significantly differ in patients with CHB compared to controls (figure 3.5c). There was also no clear relationship between frequencies of gMDSC and mMDSC within individuals (figure 3.5d), reinforcing the idea that the two subsets are distinct

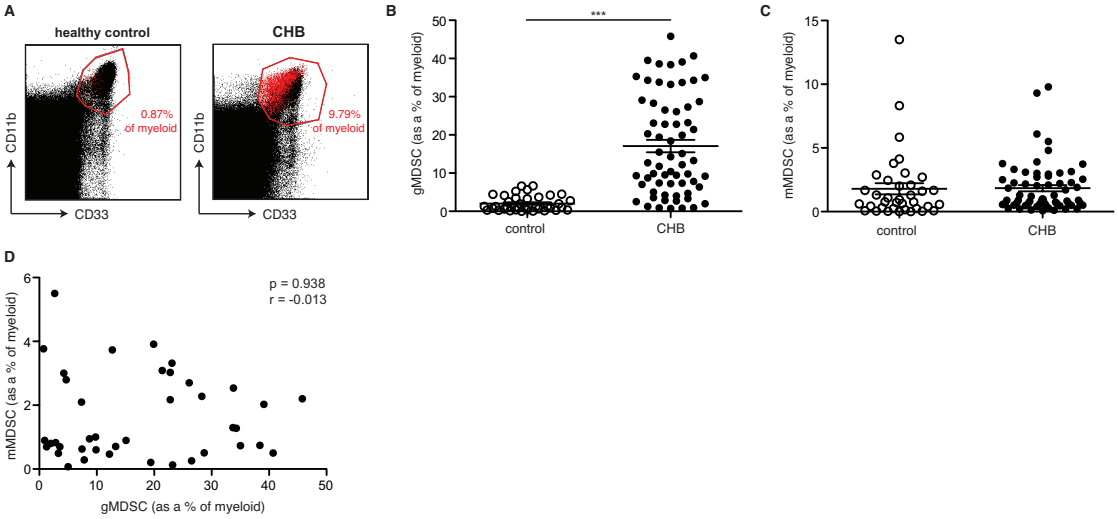

Figure 3.5: Granulocytic, but not monocytic MDSC expand in CHB.

Identification of gMDSC (CD11b^{high}CD33+HLA-DR-CD14-CD15+) using 11-colour flow cytometry from freshly isolated PBMC. A) Representative FACS plots of the gMDSC population, shown in red, from a control and a patient with CHB, respectively. B) Cumulative data showing circulating gMDSC frequencies for our cohort of 37 controls and 64 patients with CHB (East London cohort). C) Cumulative data showing the relative percentages of monocytic MDSC (mMDSC) (CD11b^{high}CD33+HLA-DR^{low}CD15-CD14+) in the same individuals. D) Correlative analysis of circulating frequencies of mMDSC and gMDSC (as a percentage of total myeloid cells) within a cohort of CHB patients. Error bars represent the mean ± SEM. Significance testing was carried out using the either: the Pearson product-moment correlation coefficient or the Students t test, and where significant indicated as: *** $p<0.001$.

and differentially regulated. Given the:

- differences in functionality between gMDSC and mMDSC,
- the lack of HBV-driven expansion in the mMDSC subsets, and
- the predominance of gMDSC within the MDSC compartment,

this study focused on gMDSC and their functionality/role in CHB, with comparisons made to the mMDSC population where appropriate.

Before further evaluation of the data attention turned to consider the total number of circulating myeloid cells in our cohorts since the relative numbers of MDSC were calculated as a proportion of the total myeloid cell population. Total myeloid cells were identified as CD11b^{high}CD33+. No significant difference was seen in the proportion of these cells between controls or patients with CHB (figure 3.6).

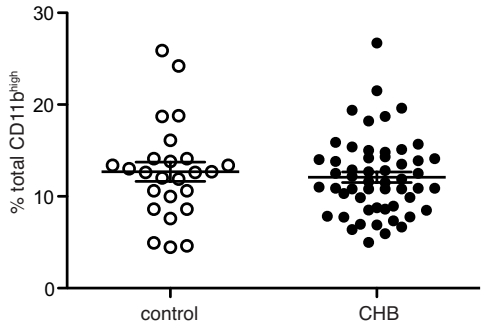

Figure 3.6: The proportion of total myeloid cells in CHB is unchanged.

Cumulative data showing the frequency of myeloid cells, identified as total CD11b^{high}CD33+ cells in the blood of controls and patients with CHB. Error bars represent the mean ± SEM. Significance testing was carried out using the Students t test and was deemed non-significant.

In CHB the degree of liver damage is linked to immune activity rather than viral replication (this concept is discussed in section 1.3.3). To explore the relationship between gMDSC and disease activity, we analysed gMDSC frequencies in a specific subset of the East London cohort who could be clearly classified into a phase of disease as described in section 1.3.4. This was done on the basis of repeated clinical assessments by their hepatologists, Dr. Upkar Gill and Dr. Patrick Kennedy. The clinical and virological parameters considered were; serum alanine transaminase (ALT) levels, ± liver histology to assess liver inflammation, HBeAg status and viral load. These well classified patients were then spilt into the four major phases of infection (as shown in figure 1.7), that patients typically progress through over several decades. Diagnostic cut-off values used to define patients vary significantly across publications and those used in different NHS centres. The European Association for the Study of the Liver (EASL) issue regular guidance however the values used in this study were chosen to be very strict in separating the patients groups to ensure no overlap between the groups and to exclude borderline patients [19].

The phases and their diagnostic limits used in this study were therefore defined as follows:

- immunotolerants: HBeAg+, HBV DNA $>10^7$IU/ml, ALT <40IU/L
- HBeAg+ active disease: HBV DNA $>5 \times 10^5$IU/ml, ALT >60IU/L
- inactive disease: HBeAg-, HBV DNA <2000IU/ml, ALT <40IU/L
- HBeAg- active disease: HBV DNA $>5 \times 10^5$IU/ml, ALT >60IU/L

In doing so it became apparent that patients with ongoing viral replication, and in some cases extremely high levels of active replication, in the absence of liver inflammation (the patients clas-

sified as immunotolerant and those with inactive disease) had significantly more gMDSC than patients with active liver disease (figure 3.7a). Corroborating this, circulating gMDSC were most expanded in patients maintaining low level liver damage as reflected by their serum ALT levels (figure 3.7b). In 42 patients, the availability of liver biopsy tissue allowed histological assessment of the amount of immune-mediated pathology by a histopathologist at the Royal London Hospital. In these patients the percent of gMDSC correlated inversely with hepatic necroinflammatory score (figure 3.7c). The extent of fibrosis was also considered, given the significance in HBV-related liver injury progressing through to cirrhosis and HCC and the well documented expansion of gMDSC in cancer [133]. There was no clear relationship observed between the extent of liver specific fibrosis measured using the ISHAK scoring system upon diagnostic biopsy and gMDSC frequencies (figure 3.7d). These data are however limited by a lack of patients with severe fibrosis or cirrhosis.

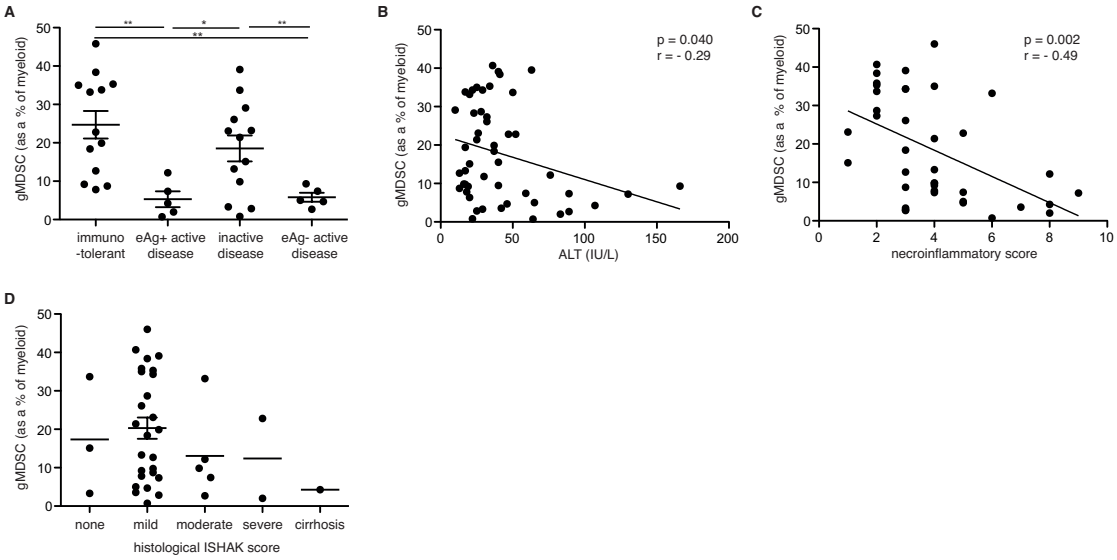

Figure 3.7: gMDSC are preferentially expanded in patients who sustain HBV replication without necroinflammatory liver damage.

Identification of gMDSC ($CD11b^{high}$CD33+HLA-DR-CD14-CD15+) using 11-colour flow cytometry from freshly isolated PBMC. Relative frequencies of circulating gMDSC from the well-characterised East London cohort were classified by: A) disease phase basis of repeated clinical assessments (serum alanine transaminase (ALT) levels, ± liver histology to assess liver inflammation, HBeAg status and viral load). These distinct phases of disease were defined as follows: immunotolerant (HBeAg+, viral load $>10^7$IU/ml, ALT <40IU/L), eAg+ active disease (viral load $>5^5$IU/ml, ALT >60IU/L), inactive disease (HBeAg-, viral load <200IU/ml, ALT <40IU/L), eAg- active disease (viral load $>5^5$IU/ml, ALT >60IU/L); B) by serum ALT (IU/L) alone; and C) by necroinflammatory histological analysis (carried out by an NHS histopathologist) in 42 patients with CHB. D) Extent of liver fibrosis (analysis carried out by an NHS histopathologist after liver biospy using the ISHAK scoring system). Error bars represent the mean ± SEM. Significance testing was carried out using either the: Pearson product-moment correlation coefficient or the Students t-test, and where significant indicated as: ** $p<0.01$; * $p<0.05$.

These findings were then concisely displayed using a method of hierarchical clustering by Euclidean distance. Patients with CHB were clustered in an unsupervised manner based on the similarity of their serum ALT levels, hepatic necroinflammatory score and circulating gMDSC frequencies. The dendrogram represents the similarity of each patient to another, and clearly confirms a high frequency of gMDSC is concordant with low level liver inflammation, as reflected by a low ALT value and a low necroinflammatory score. Furthermore, patients in the immunotolerant phase of disease and with inactive disease robustly cluster together, those with active disease forming a separate, distinct cluster (figure 3.8).

From there consideration turned to the question of whether any viral parameters associated with HBV, or factors relating to the specifics of the cohorts used gave an insight into the driving

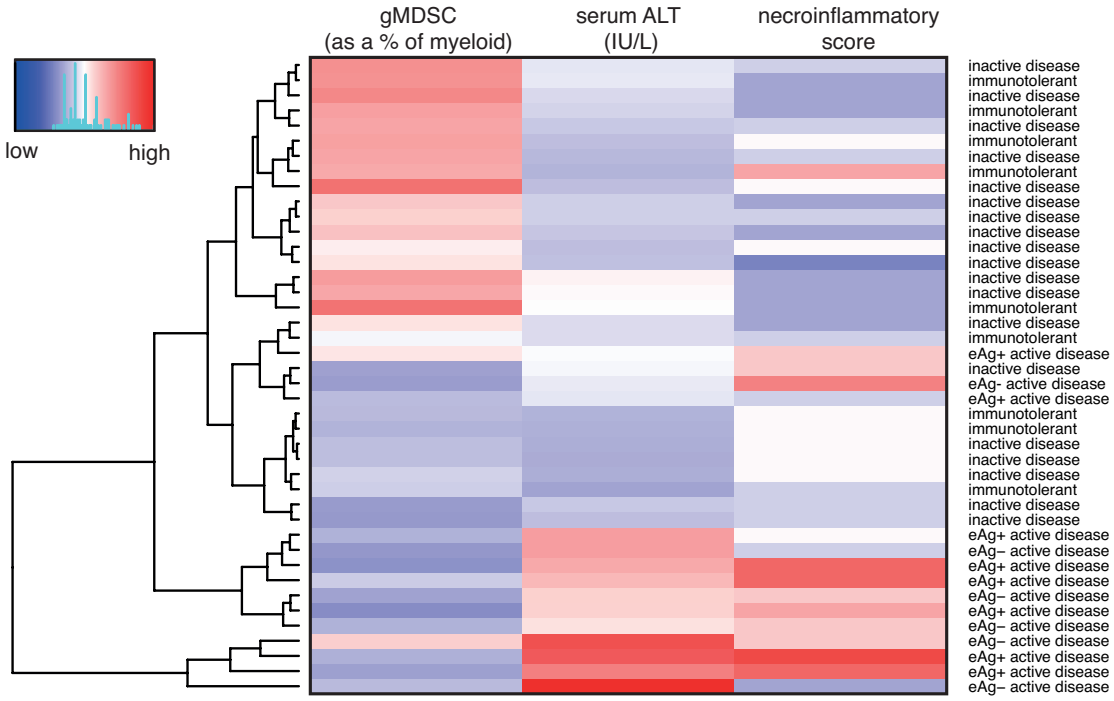

Figure 3.8: Hierarchical clustering reveals clear stratification of CHB disease phases.

Unsupervised clustering based on gMDSC frequencies, serum ALT (IU/L) and necroinflammatory score (as confirmed by an NHS histopathologist). The data analysis performed in the generation of this figure must be attributed to Dr. Niclas Thomas.

factor in the gMDSC expansion observed (previously depicted in figure 3.5a,b).

Co-infection of our cohorts with other viruses was considered first. All patients used in this study were mono-infected for an hepatotropic infection (only infected with HBV). However study participants were often infected with other underlying persistent viral infections, for example, CMV or epstein bar virus (EBV). To assess whether another chronic infection was capable of driving gMDSC expansion (or having a synergistic effect) beyond that of HBV infection analysis into the CMV serostatus was carried out. gMDSC expansion seen in the circulation of patients with CHB was not influenced by persistent infection with CMV. In both controls and patients with CHB, seropositivity for CMV had no influence on the percent of circulating gMDSC (figure 3.9a).

MDSC expansion has previously been reported to occur with the development of immune senescence [201, 202]. Prior to the analysis by strict disease classification the nature of ongoing antigenic stimulation seen in patients with CHB led to the hypothesis that gMDSC may accumulate over the course of disease. The most significant expansion of gMDSC was in the context

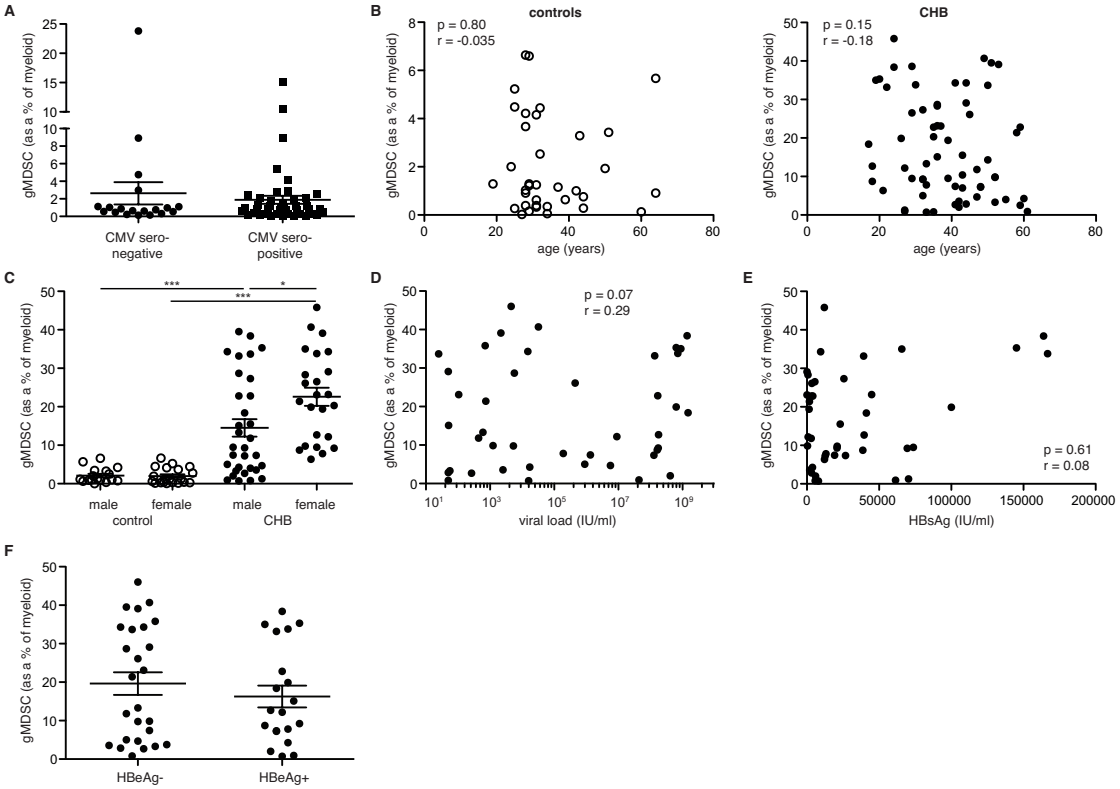

Figure 3.9: gMDSC do not expand in CMV, as a result of aging, or in relation to a number of HBV virological/clinical parameters.

Identification of gMDSC ($CD11b^{high}$CD33+HLA-DR-CD14-CD15+) using 11-colour flow cytometry from freshly isolated PBMC was considerd in relation to a number of clinically relevant parameters to our cohort of East London patients with CHB (compared to controls where necessary). Relative frequencies of circulating gMDSC were classified by: A) CMV serostatus; serology was obtained for a cross-sectional cohort of controls and patients with CHB; B) by age of the participants on the date of sampling (years), controls or patients with CHB respectively; and C) by gender. Patients with CHB were further classified by virological and clinical parameters including: D) HBV viral load (IU/ml); E) quantification of HBsAg (IU/ml); F) the presence of circulating HBeAg. Error bars represent the mean ± SEM. Significance testing was carried out using either: the Pearson product-moment correlation coefficient or the Students t test, and where significant indicated as: *** $p<0.001$; * $p<0.05$.

of immunotolerant disease, a phase normally restricted to the first few decades of life, and those with inactive disease, and therefore minimal antigenic stimulation instantly disputed the original hypothesis. However for the majority of patients, the date of infection was unknown and so impossible to establish accurate durations of infection. For completeness and to ensure there was no role for immune senescence (ageing) in gMDSC expansion, age on the date of sampling was used as a surrogate to address this. Correlating the frequency of circulating gMDSC with age yielded no significant relationship in either the controls or the patients with CHB (figure 3.9b). Thus implying no significant role for immunosenescence (ageing) in gMDSC expansion or continued antigenic stimulation over a number of decades, whether at low levels or not.

As gMDSC expansion could not be attributed to CMV serostatus or was not a prominent feature of ageing in our patients as already shown (figure 3.9a,b), another parameter considered was gender. Gender of patients with CHB is an important factor to consider given that female patients with CHB are reported to develop less severe HBV-related liver disease than their male counterparts [203]. Stratification of both cohorts by gender revealed a significant difference in circulating gMDSC frequencies, but only in the cohort of patients with CHB, not in controls. Female patients with CHB have significantly higher frequencies of gMDSC than males (figure 3.9c). It has recently been shown in a study by Kostlin *et al.* [204], that gMDSC expand during pregnancy and are thought to be involved in the materno-fetal tolerance. The authors of this study do not attribute any particular factor to driving the initial expansion, but it is however possible that increases in female hormones during pregnancy could play a role. It is plausible that gMDSC may respond to hormonal increases, potentially explaining the further increase in gMDSC frequencies seen in female patients with CHB.

Finally specific examination of HBV-specific virological parameters failed to provide any clear insight into what was the driving factor in gMDSC expansion seen in CHB. Frequencies of gMDSC failed to correlate significantly with either: viral load (figure 3.9d), serum HBsAg titre (figure 3.9e) or HBeAg status (figure 3.9f) when considered as independent variables. Additionally, several multivariate techniques were used to investigate whether a more complex, interdependent relationship existed between these variables. No significant relationship was detected using multiple linear regression. Principal component analysis (PCA) also failed to yield a projection of the data which showed any clear clustering by gMDSC frequencies. The majority of patients had similar PC1 and PC2 scores across a large range of both high (red) and low (green) gMDSC frequencies (figure 3.10).

3.3.3 gMDSC are transiently expanded in acute resolving HBV infection and decline at the onset of the hepatic flare

Results from the cross-sectional analysis of gMDSC frequencies with numerous viral parameters in figure 3.9 failed to elucidate a conclusive MDSC-driving factor. In a further attempt to determine the factor involved analysis took advantage of samples stored from extremely valuable patients presenting in clinic in whom the initial pre-clinical HBV replication phase characterising acute infection had unusually, been captured. Three such patients were followed through to resolution of infection. Following the course of acute infection enabled gMDSC frequencies

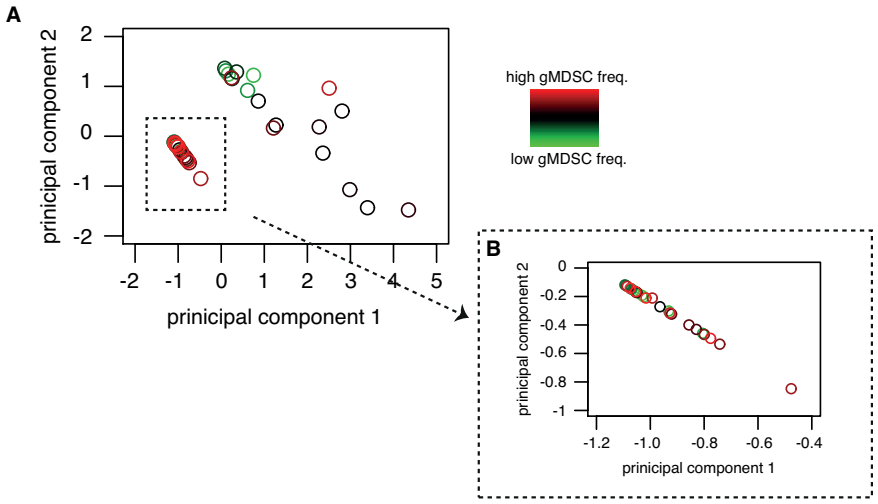

Figure 3.10: Principal component analysis (PCA) revealed no clear separation of gMDSC frequencies based on three viral parameters.

Principal component analysis: using viral load, serum HBsAg titre and HBeAg status as inputs to yield clear stratification of the patients with CHB from the East London cohort by gMDSC frequencies. Patients with low gMDSC frequencies in green and high gMDSC frequencies in red. A) Represents the full dataset with B) showing a zoomed in section (identified by the dotted lines), due to the large number of data-points falling in that region. The data analysis performed in the generation of this figure must be attributed to Dr. Niclas Thomas.

to be monitored longitudinally in relation to the peak and decline in viraemia alongside the subsequent hepatic ALT flare associated with elimination of the virus. One caveat to these data is that the samples had been cryopreserved. It has already been shown in figure 3.3a that gMDSC are a cyrosensitive population indicating that freshly isolated PBMC samples should be used for gMDSC quantification, but to access these particularly dynamic phases of disease in a longitudinal fashion using freshly isolated PBMC within the time constraints of this thesis would not have been possible. Although gMDSC frequencies would be expected to be markedly diminished in these samples, it was previously demonstrated that gMDSC frequencies in freshly isolated and frozen samples correlate (figure 3.3b). This validated interpretation of any trends observed in the datasets for cryopreserved samples from these three acute HBV patients.

Out of the three patients analysed, two individuals were sampled before or coinciding with peak HBV viraemia. In these two individuals, a clear temporal relationship between the induction of gMDSC frequencies and viral load was observed. These two parameters decline in parallel. The third patient (patient A3) did not present in clinic until after peak viraemia, thus making it hard to draw conclusions about the expansion of gMDSC during the viral ″ramp-up‟ phase in this individual. All three patients exhibit the typical delay between peak viraemia and hepatic flare

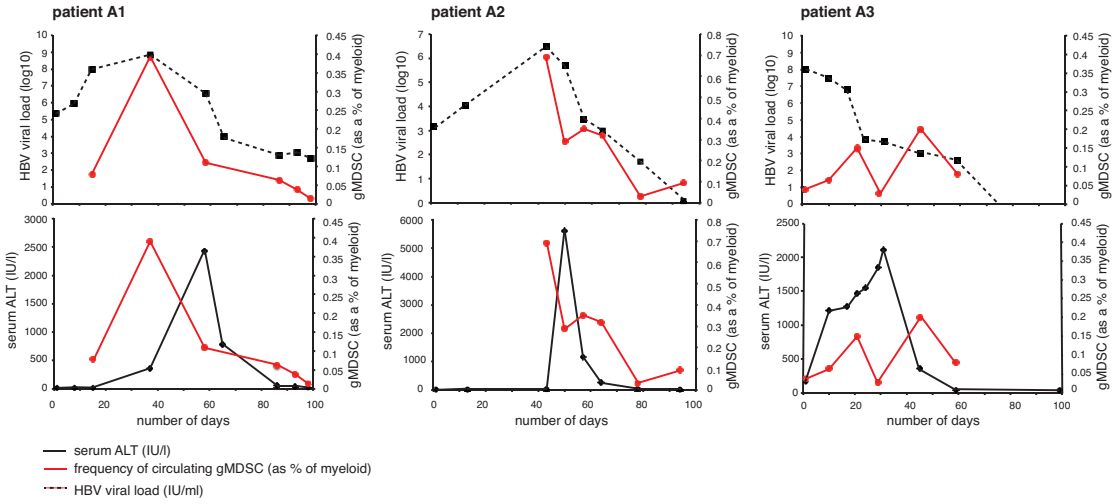

Figure 3.11: gMDSC transiently expand in acute resolving HBV infection and decline at the onset of the hepatic flare.

Identification of gMDSC (CD11b^{high}CD33+HLA-DR-CD14-CD15+) using 11-colour flow cytometry from frozen PBMC samples. gMDSC frequencies were quantified and presented as a proportion of total circulating myeloid cells (CD11b^{high}CD33+) from PBMC cyropreserved from multiple time points where available. The patients were followed from the onset of viraemia and through the subsequent hepatic flare characteristic of acute resolving infection. gMDSC frequencies were plotted for three acute HBV patients sampled against viral load (IU/ml top panel) and serum ALT (IU/l lower panel) over time in days (numerical from initial presentation in clinic) over 100 days.

(as measured by a serum ALT increase above 2000IU/ml) characteristic of acute resolving HBV infection (figure 3.11). The findings presented in figure 3.11 for acute infection mirror the data previously shown cross-sectionally for chronic infection, whereby an inverse relationship between serum ALT and circulating gMDSC frequencies was observed (figure 3.7b). Circulating gMDSC frequencies were highest when high levels of active viral replication are occurring in the absence of any biochemical evidence of liver-specific inflammation. gMDSC numbers rapidly decline at the onset of the hepatic flare. Interestingly these data are in concordance with data reported by Norris *et al.* [190] from the LCMV model. The authors demonstrated a transient increase in MDSC frequencies during acute infection. The authors also showed sustained induction of gMDSC in the chronic setting. The data from these three valuable sample sets provides further *ex vivo* evidence for the induction of gMDSC in the context of viral infection, alongside their ability to suppress liver inflammation.

To ensure the changes in gMDSC frequencies observed over the course of acute disease shown in figure 3.11 were not due to relative changes in the total myeloid populations, gMDSC frequencies were calculated as a percentage of all leukocytes in parallel. Figure 3.12 shows the same three patients with gMDSC frequencies displayed as a proportion of total live cells (identified

using Invitrogen™ Blue Live/Dead®). In all three patients gMDSC frequencies are highest when high levels of active viral replication are ongoing and in two out of three patients the finding that gMDSC decline before the onset of the hepatic flare was corroborated. In the third patient (patient A2), when presented as a proportion of live cells, the decline in gMDSC occurs simultaneously with the hepatic flare (figure 3.12). Without having used BD TruCount tubes to calculate absolute numbers longitudinally it is difficult to comment further.

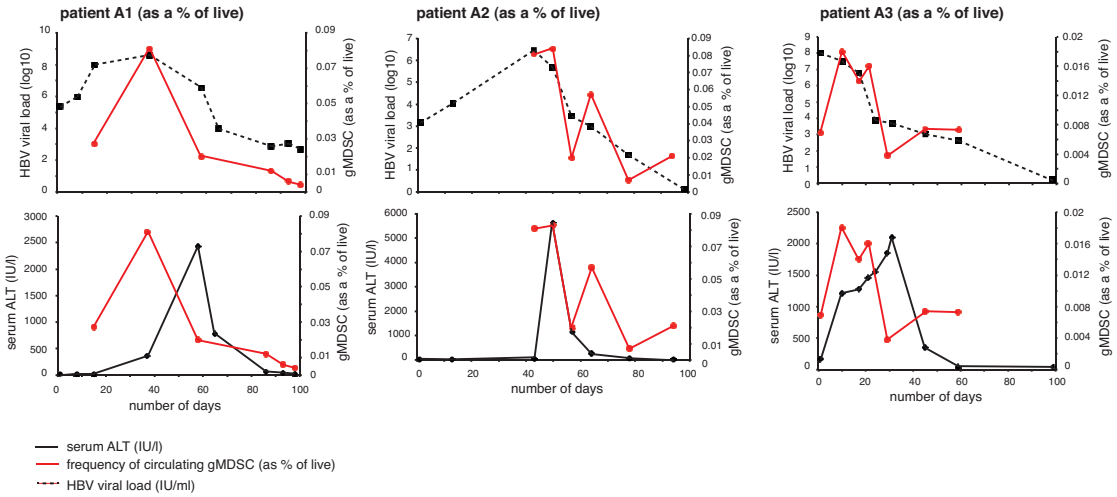

Figure 3.12: gMDSC, when presented as a proportion of total leukocytes, transiently expand in acute, resolving HBV infection and decline at the onset of the hepatic flare.

Identification of gMDSC (CD11b^{high}CD33+HLA-DR-CD14-CD15+) using 11-colour flow cytometry from frozen PBMC samples. gMDSC frequencies were quantified and presented as a proportion of total circulating leukocytes (identified using Invitrogen™ Blue Live/Dead®) from PBMC cyropreserved from multiple time points. The patients were followed from the onset of viraemia and through the subsequent hepatic flare characterising acute resolving HBV infection. gMDSC frequencies plotted for three acute HBV patients sampled against viral load (IU/ml top panel) and serum ALT (IU/l lower panel) over time in days (numerical from initial presentation in clinic) for 100 days.

3.3.4 gMDSC are also transiently expanded during spontaneous hepatic flares in HBeAg- CHB

Having observed relationships between gMDSC frequencies and both viraemia and inflammation in the setting of acute HBV infection, the same approach was taken for two patients with HBeAg- CHB, sampled throughout the course of a spontaneous hepatic flare. The time-course of these longitudinal samples of two patients with CHB is in months compared to the acute HBV patients in days. From the cryopreserved samples obtained from these two patients, the

inverse relationship between serum ALT and circulating gMDSC frequencies was again observed (figure 3.13), mirroring both the cross-sectional data in the context of CHB and the longitudinal analysis of acute HBV infection. The relationship between gMDSC frequencies and vireamia in the setting of CHB is unclear, suggesting the virus may only play a significant role in their primary expansion.

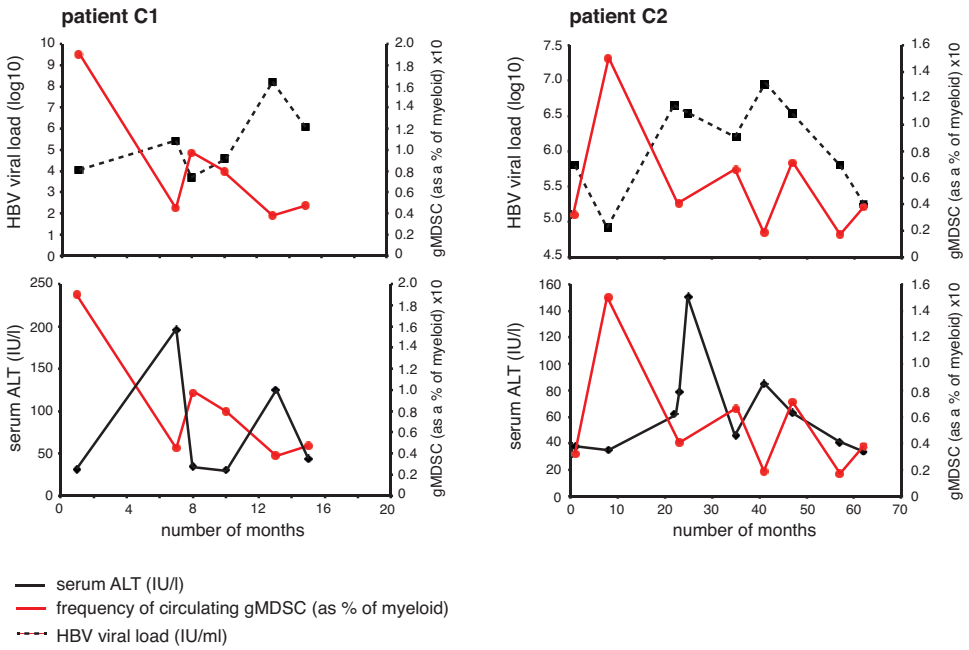

Figure 3.13: gMDSC decline at the onset of the spontaneous hepatic flare in patients with active HBeAg- CHB.

Identification of gMDSC ($CD11b^{high}$CD33+HLA-DR-CD14-CD15+) using 11-colour flow cytometry from frozen PBMC samples. gMDSC frequencies were quantified and presented as a proportion of total circulating leukocytes (identified using Invitrogen™ Blue Live/Dead®) from PBMC cyropreserved from multiple time points. The patients were followed through a phase of highly active CHB. gMDSC frequencies plotted for two patients with HBeAg-CHB against viral load (IU/ml: top panel) and serum ALT (IU/l: lower panel) over time in months.

Similar to the acute resolving HBV patients, gMDSC frequencies over the course of the spontaneous flares in these two patients with CHB were re-plotted as a proportion of total live leukocytes. The findings in the setting of CHB were consistent, regardless of how the gMDSC frequency data was plotted (figure 3.14).

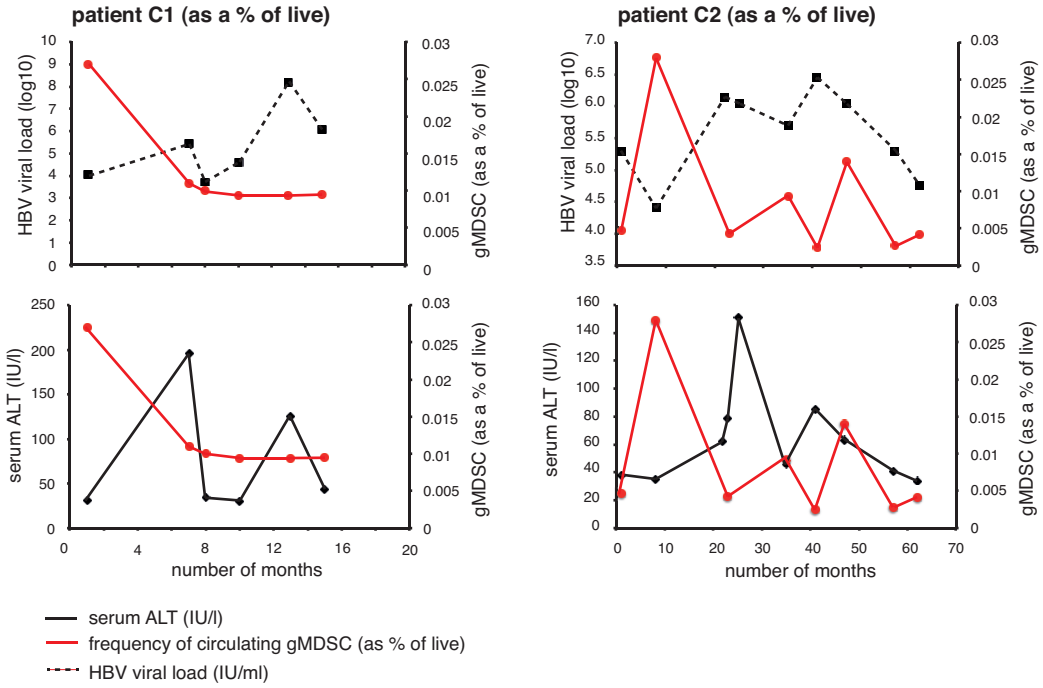

Figure 3.14: gMDSC, when presented as a proportion of total leukocytes, decline at the onset of the spontaneous hepatic flare in patients with active HBeAg- CHB.

Identification of gMDSC ($CD11b^{high}$CD33+HLA-DR-CD14-CD15+) using 11-colour flow cytometry from frozen PBMC samples. gMDSC frequencies were quantified and presented as a proportion of total circulating leukocytes (identified using Invitrogen™ Blue Live/Dead®) from PBMC cyropreserved from multiple time points. The patients were followed through a phase of highly active CHB. gMDSC frequencies plotted for two patients with HBeAg-CHB against viral load (IU/ml: top panel) and serum ALT (IU/l: lower panel) over time in months.

3.3.5 Absolute counts: gMDSC expand in CHB

To confirm the finding that gMDSC frequencies increase in patients with CHB compared to controls (figure 3.5a), further investigation into their absolute numbers was carried out in a limited cohort of study participants. For this the BD TruCount system was utilised. The system makes use of an exact volume of whole blood to compare numbers of gMDSC against a reference bead population. gMDSC were stained and gated in the same way (shown in figure 3.2a), with the inclusion of CD45 to allow the exclusion of contaminating platelets and red blood cells. This protocol makes use of a strong fix-lyse solution, and samples were always analysed on the flow cytometer within a 15 minute time-frame to ensure no bias in gMDSC loss, especially due to their fragile nature. In line with previous findings, the absolute numbers of gMDSC were increased in patients with CHB compared to uninfected controls (figure 3.15).

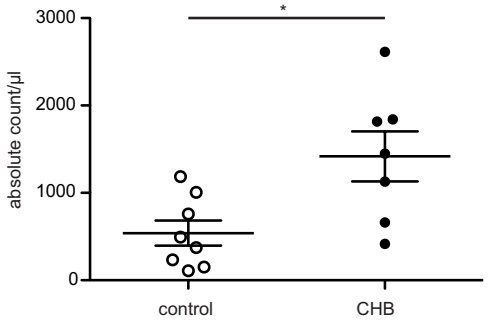

Figure 3.15: gMDSC increase in absolute cell number in CHB.

Identification of gMDSC (CD11b^{high}CD33+HLA-DR-CD14-CD15+) using 11-colour flow cytometry was done using the BD TruCount protocol using whole blood, lysed with BD FACS lyse solution for a maximum of 15 minutes. Error bars represent the mean ± SEM. Significance testing was carried out using the unpaired Students t test, and where significant indicated as: * $p<0.05$.

Data relating to cell counts was also obtained during routine clinical assessment of patients from the East London cohort, enabling consideration of these counts. One caveat to this dataset is the lack of equivalent data detailing numbers of leukocytes for the control cohort. Taking the clinical leukocyte count for each patient and back-calculating with the gMDSC frequencies after FlowJo anlysis of the flow cytometric data, an absolute increase in gMDSC does occur in the absence of liver inflammation (figure 3.16). However these data should be evaluated with caution, given the differences between clinical assessment of leukocyte count using whole blood and the PBMC isolation protocol used in the lab.

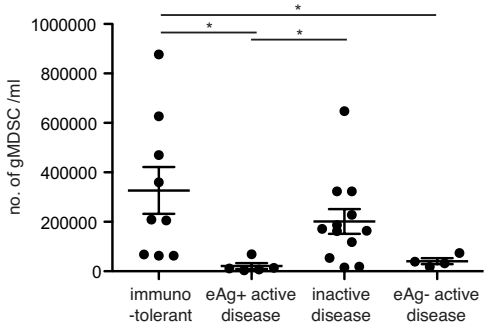

Figure 3.16: Analysis of the absolute count of gMDSC during the different phases of CHB taking into account clinical luekocyte count.

Numbers of gMDSC were calculated by relating the frequency of gMDSC as a percentage of all live cells run through the flow cytometer back to the absolute leukocyte count obtained during routine clinical assessment for the East London cohort. Patients were classified by disease phase, as defined previously. Error bars represent the mean ± SEM. Significance testing was carried out using the unpaired Students t test, and where significant indicated as: * $p<0.05$.

3.3.6 gMDSC also expand in chronic HCV infection

An expansion of MDSC in another chronic hepatotropic infection, HCV infection, has been previously described in a number of published studies. In these studies, the subsets of MDSC analysed were reported to be able to mediate specific lymphocyte suppression [192, 193, 205, 206]. Given the significant expansion of gMDSC in the circulation of patients with CHB, we sought to confirm the presence of gMDSC using the same phenotypic panel in HCV. Similarly to CHB, an expansion in circulating gMDSC was detectable in this cohort of patients with chronic HCV infection (also from the East London cohort, collected in heparin) (figure 3.17a).

In a published study it has been reported that MDSC expansion in chronic HCV infection positively correlates with the degree of liver inflammation, as measured by serum ALT [193]. Since only a small cohort of HCV infected individuals were sampled, it was hard to draw any firm conclusions from our dataset. However the data do suggest circulating frequencies of gMDSC in chronic HCV infection neither associate with serum ALT nor viral load (figure 3.17b,c) in accordance with findings published by Zeng *et al.* [206]. In contrast to CHB, patients with chronic HCV infection do not progress through clearly defined phases of disease. However a striking association was observed between circulating frequencies of gMDSC and age of the patient in the HCV cohort in line with the hypothesis of gMDSC accumulating over time with ongoing antigenic stimulation (figure 3.17d).

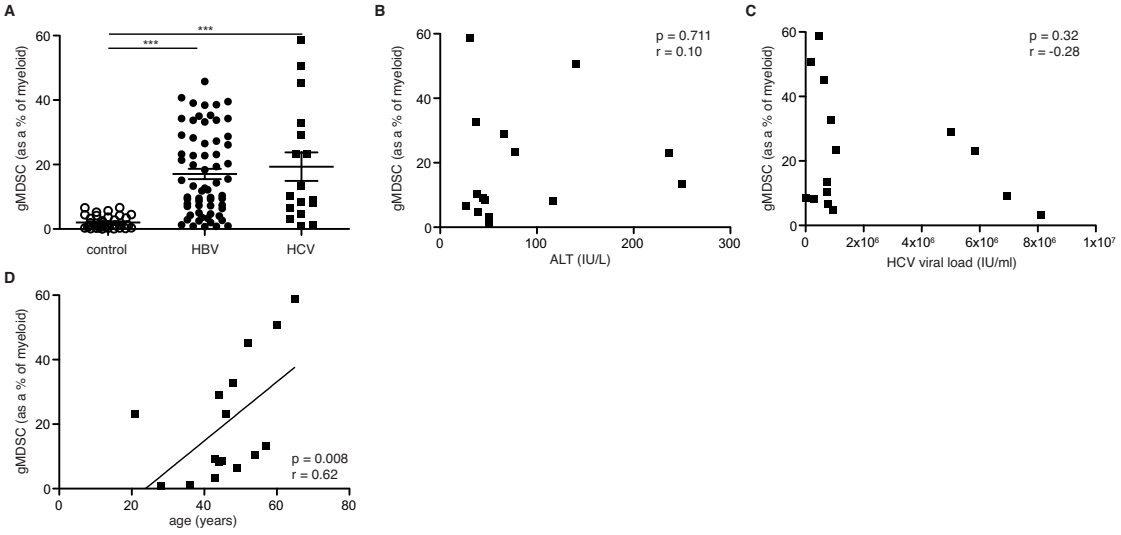

Figure 3.17: gMDSC also expand in HCV and significantly correlate with patient age.

Identification of gMDSC ($CD11b^{high}$CD33+HLA-DR-CD14-CD15+) using 11-colour flow cytometry from freshly isolated PBMC from a cohort of patients with chronic HCV infection. Relative frequencies of circulating gMDSC presented as a proportion of total myeloid cells (as shown in figure 3.2a). A) Cumulative data from the East London cohort (taken in heparin) of the 37 controls and 64 patients with HBV infection already presented in figure 3.5b, and a further 17 patients with chronic HCV infection. The cohort of patients with chronic HCV infection were further classified by: B) serum ALT (IU/L); C) viral load (IU/ml); and D) age of the patient (years) on the date of sampling. Error bars represent the mean ± SEM. Significance testing was carried out using either: the Pearson product-moment correlation coefficient or the Students t-test, and where significant indicated as: *** $p<0.001$; ** $p<0.01$.

3.3.7 gMDSC accumulate further in the diseased liver

HBV and HCV specifically and exclusively infect hepatocytes of the liver, an organ typically manifesting a local milieu of immune tolerance rather than immunity, as discussed in section 1.4 [94, 207, 90]. Analysis therefore turned to consider whether the expanded population of gMDSC circulating in patients with CHB (or chronic HCV infection) could have the potential to accumulate in the liver. Intrahepatic frequencies of gMDSC were determined using valuable paired PBMC and intrahepatic lymphocytes from liver biopsy tissue deemed surplus to diagnostic requirements (figure 3.18a). 16 out of 19 patients with CHB analysed showed an accumulation of gMDSC in the liver, in some cases representing up to a maximum of 56% of the intrahepatic myeloid population (figure 3.18b). Of the three remaining patients with CHB where no liver specific increase in gMDSC frequencies were observed, no apparent clinical differences were noted, providing no evidence for why gMDSC do not accumulate in the liver of some patients.

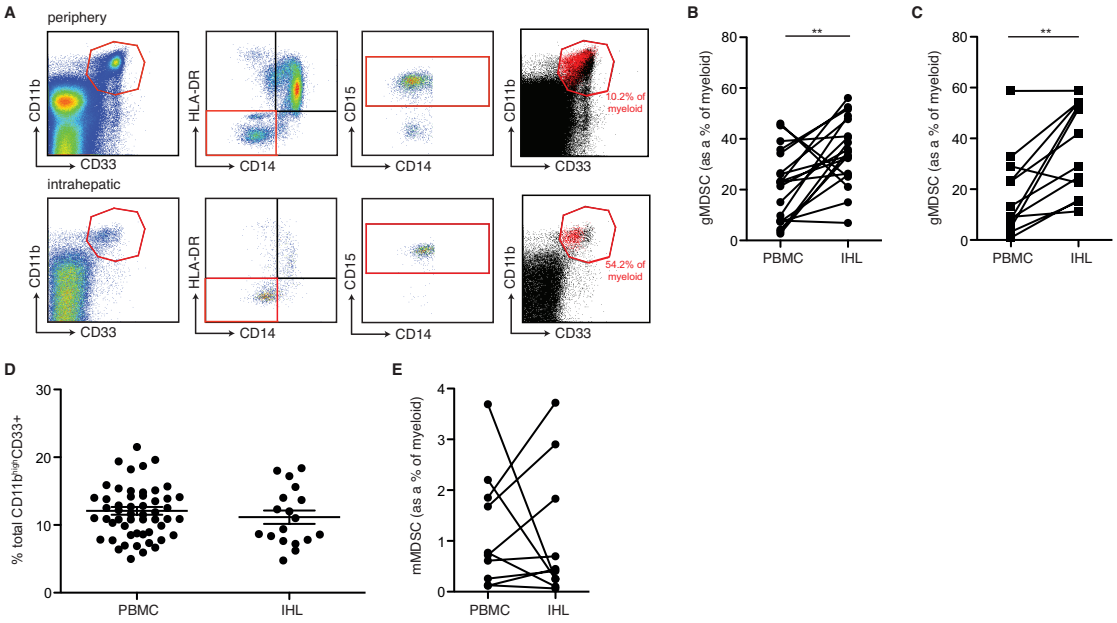

Figure 3.18: gMDSC expand approximately 2-fold in the liver mircoenvrionment in chronic hepatotrophic infections: HBV & HCV.

Identification of gMDSC ($CD11b^{high}$CD33+HLA-DR-CD14-CD15+) using 11-colour flow cytometry from freshly isolated intrahepatic cells. A) Representative sequential FACS plots showing gMDSC identification using a paired (peripheral blood (PBMC) and lymphocytes obtained from a liver biospy (IHL) deemed surplus to diagnostic requirements from the same individual) sample from a patient with CHB. B) Cumulative data showing circulating frequencies of gMDSC compared to intrahepatic frequencies in 19 patients with CHB from the East London cohort. C) Cumulative data showing circulating frequencies of gMDSC compared to intrahepatic frequencies in 12 chronically infected HCV patients. D) Cumulative data from a cross sectional cohort of patients with CHB showing relative frequencies of myeloid cells (identified as $CD11b^{high}$CD33+) between the blood and the liver compartments. E) Cumulative data showing frequencies of circulating mMDSC compared to intrahepatic in a cross section of 10 patients with CHB. Error bars represent the mean ± SEM. Significance testing was carried out using either: the paired or unpaired Students t-test, and where significant indicated as: ** $p<0.01$.

Intrahepatic gMDSC frequencies were also assessed from a cohort of patients chronically infected with HCV. Once again gMDSC were expanded in the liver of patients with HCV, at frequencies comparable to those seen in the CHB cohort (figure 3.18c). The accumulation/expansion of gMDSC in the liver in both disease states was approximately 2-fold. Notably, proportions of myeloid cells between the periphery and the intrahepatic environment remained unchanged (figure 3.18d) and there was no specific, consistent accumulation of the monocytic subset of MDSC in the intrahepatic environment in CHB (figure 3.18e).

This led to the question of whether the accumulation of gMDSC noted in the liver was a general feature of the tolerogenic microenvironment or was only observed in certain pathological

states. In a preliminary attempt to consider this, three intrahepatic samples were obtained from the healthy margins of metastatic liver tissue during surgery. These samples unfortunately had no paired blood available for comparison of circulating frequencies. gMDSC frequencies in these three patients were similar, if not slighlty higher, than those seen in patients with chronic HBV or HCV infection (figure 3.19). One intrahepatic sample was also obtained from a patient with HCC on a HBV background. In this sample approximately 20% of the myeloid cells were gMDSC, in line with the data from patients with CHB (figure 3.19).

In further attempts to assess whether gMDSC accumulation in the liver was a consequence of local infection/tumours or a generalised phenomenon in the liver (whereby MDSC home to the liver under physiological conditions), gMDSC frequencies were assessed in the non-diseased liver. These samples were obtained in collaboration with transplant surgeons, Mr. Francis Robertson and Mr. Brian Davidson, at the Royal Free Hospital. In this case, biopsies of healthy liver tissue (from the donor) and the perfusate (wash-out prior to transplantation) of such tissue were obtained before liver transplantation into the recipient, providing unique access to non-diseased liver tissue. Analysis of gMDSC frequencies in these samples showed that gMDSC do not expand in the healthy liver (figure 3.19), with frequencies analogous to circulating gMDSC in the healthy cohort of study participants (figure 3.5a,b).

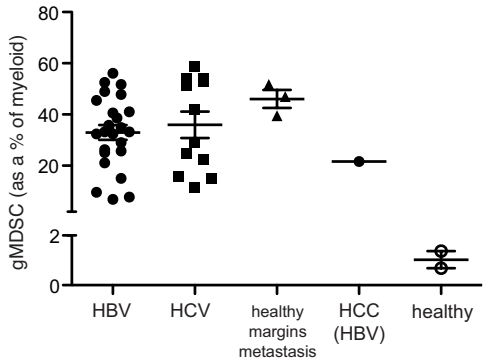

Figure 3.19: gMDSC accumulate in livers with viral hepatitis or tumours, but not in the healthy liver.

Identification of gMDSC (CD11b^{high}CD33+HLA-DR-CD14-CD15+) using 11-colour flow cytometry from freshly isolated intrahepatic cells. Cumulative data from all intrahepatic samples analysed for gMDSC frequencies, including all 19 patients with CHB, 12 patients chronically infected with HCV, three samples isolated from the healthy margins of liver tissue from patients undergoing surgery for metastatic liver disease, one patient with HCC on the background of CHB and two samples from non-diseased liver tissue obtained from a healthy donor prior to transplantation into its recipient.

3.3.8 Potential factors driving the accumulation of gMDSC in the diseased liver

The accumulation of gMDSC in the diseased liver but not the healthy liver led to a question regarding their homing and survival/expansion of gMDSC under these conditions. To address this, circulating gMDSC (using isolated PBMC) were stained with monoclonal antibodies directed initially against a selected panel of three chemokine receptors postulated to be relevant to liver MDSC homing based on recent studies reviewed by Talmadge & Gabrilovich [173].

The first of these chemokine receptor was CCR2, a receptor reported to be critical in the homing of MDSC in LCMV infection [190]. CCR2 has also recently been implicated in allowing the egress of murine inflammatory monocytes from the bone marrow to sites of infection, where they further differentiate into cells with a mMDSC phenotype and the ability to mediated iNOS-dependent suppression [208]. Staining was carried out to assess expression of this chemokine receptor on both subsets of MDSC (figure 3.20a, upper panel), which was found to be expressed at very high levels on the surface of mMDSC compared to the matched isotype control. It is possible then that CCR2 expression on human mMDSC allows for their egress into the circulation. CCR2 was, however, barely detectable on gMDSC from either the uninfected controls or in the cohort of patients with CHB (figure 3.20a, bottom panel).

The second chemokine receptor considered was CXCR4, which was again found to be expressed at lower levels on the gMDSC subset compared to the mMDSC subset. More interestingly however, levels of CXCR4 were lower on the expanded population of gMDSC in patients with CHB compared to controls (figure 3.20b). Full maturation into mature granulocytes under physiological conditions occurs in the bone marrow. An interesting report by Ma *et al.* [209] demonstrated that mature granulocytes are prematurely released into the bloodstream of CXCR4 deficient mice, resulting in an over-abundance of immature granulocytes in the circulation. Down-regulation of CXCR4 on the surface of neutrophils is critical for their mobilisation from the bone marrow in response to GM-CSF, and infection with Listeria monocytogenes [210]. Decreased expression of CXCR4 on gMDSC raises the possibility that a down-regulation of this chemokine receptor enables accelerated egress of these immature myeloid cells from the bone marrow into the circulation of patients with CHB [209].

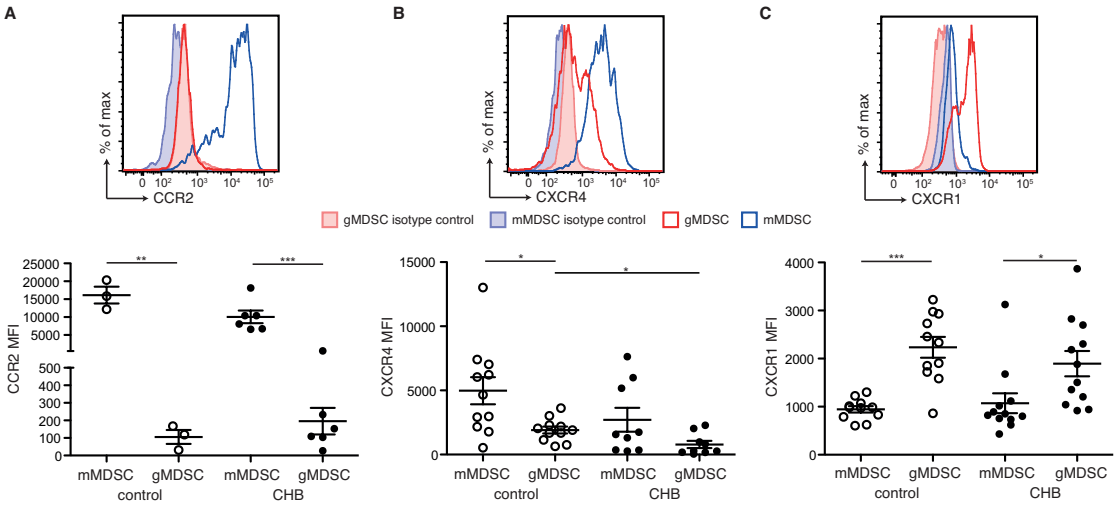

Figure 3.20: Selected chemokine receptor expression on the surface of gMDSC and mMDSC.

Representative histogram plots and cumulative data showing the comparison of chemokine receptor expression on the surface of mMDSC and gMDSC compared to their matched isotype controls between controls and patients with CHB for: A) CCR2; B) CXCR4; and C) CXCR1. Error bars represent the mean ± SEM. Significance testing was carried out using the paired Students t-test, and where significant indicated as: *** $p<0.001$; ** $p<0.01$; * $p<0.05$.

The third chemokine receptor considered was the IL-8 receptor. Although there are two chemokine receptors, CXCR1 and CXCR2, that have similar affinities for IL-8, the process of neutrophil chemotaxis is primarily mediated by CXCR1 [211]. In contrast to the previous two chemokine receptors, CXCR1 expression was significantly higher on gMDSC than mMDSC in both controls and patients with CHB (figure 3.20c). For completeness, expression of the other IL-8 receptor, CXCR2 was briefly considered on both MDSC subsets (figure 3.21a). Expression of CXCR2 mirrored expression of CXCR1, being expressed at significantly higher levels on gMDSC than mMDSC in both controls and patients with CHB (figure 3.21b). However levels of CXCR2 were significantly lower on gMDSC in patients with CHB compared to controls.

Expression of both IL-8 receptors (CXCR1 and CXCR2) on the surface of gMDSC led to the hypothesis that these could contribute to their homing (accumulation) and/or interactions within the liver. IL-8 is a neutrophil chemotactic cytokine that can be produced by several cell types, including hepatocytes, in CHB [72]. Therefore it was postulated that gMDSC expressing the IL-8 receptor could be chemoattracted into the liver by an IL-8 gradient and/or may be able to specifically interact with an IL-8 producing hepatic cell types.

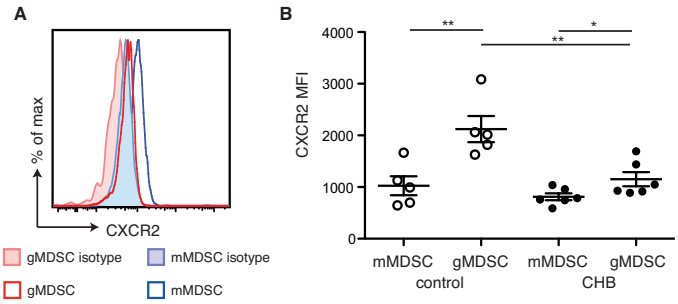

Figure 3.21: gMDSC also express CXCR2, IL-8Rβ.

A) Representative histogram plots and cumulative data showing the comparison of CXCR2 expression on the surface of mMDSC and gMDSC compared to matched isotype controls. B) Cumulative data showing CXCR2 expression levels on mMDSC and gMDSC between controls and patients with CHB. Error bars represent the mean ± SEM. Significance testing was carried out using the paired Students t-test, and where significant indicated as: ** $p<0.01$; * $p<0.05$.

3.3.9 A potential interaction of gMDSC with hepatic stellate cells

A number of recent reports have demonstrated a role for hepatic stellate cells (specialized, liver-resident myofibroblasts, described previously in section 1.4.4) in the induction of MDSC [114, 195]. In these papers the authors describe expansion of MDSC from pre-isolated monocytes upon co-culture with primary stellate cells. Isolated primary hepatic stellate cells (pHSC), from healthy resected liver tissue, were used to test whether they could promote MDSC survival/expansion. Full details on the isolation of pHSC can be found in section 2.8.1, but briefly: liver tissue was obtained from patients undergoing surgery for metastatic liver disease at the Royal Free Hospital (in collaboration with Mr Giuseppe Fusai). The healthy margins of liver tissue from these patients were used to isolate pHSC using a density gradient, excluding all other non-parachymal cells of the liver. Isolated quiescent pHSC were then passaged in culture to ensure full activation of these cells prior to experimentation.

The subsequent experiments were done in conjunction with Dr. Kasha Singh (Maini group). Analysis of these pHSC prior to co-culture experimentation revealed that these cells can produce high levels of the pro-inflammatory cytokine IL-6 *ex vivo*, without the need for any stimulation (figure 3.22a). IL-6 is believed to promote MDSC expansion [177, 212]. It was also observed that these isolated pHSC were capable of producing IL-8 which was previously postulated to be involved in the potential gMDSC accumulation and interaction in the liver (figure 3.22b). It is possible that production of IL-8 by pHSC promotes their interaction with the CXCR1-expressing gMDSC, although this remains to be confirmed.

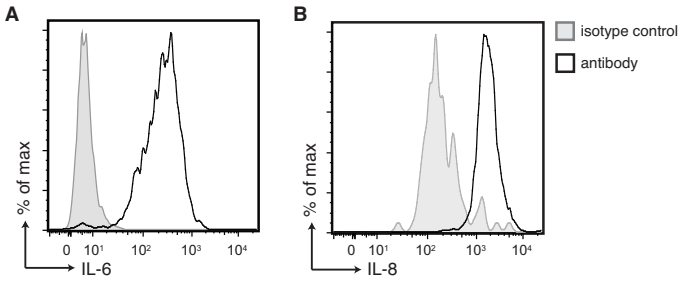

Figure 3.22: pHSC produce two candidate cytokines, IL-6 and IL-8, *ex vivo*.

Primary hepatic stellate cells (pHSC), isolated by density centrifugation and cryopreserved, from margins of metastatic livers. Prior to co-culture experimentation pHSC were stained for production of two candidate cytokines without stimulation. Representative histogram of *ex vivo* intracellular A) IL-6 and B) IL-8 staining. The staining and analysis used in the generation of this figure is attributed to Dr. Kasha Singh.

Upon co-culture, activated pHSC were able to support short-term expansion and/or enhance the survival of gMSDC from PBMC isolated from either controls or patients with CHB, compared to cultures in the absence of pHSC (figure 3.23). What remains to be elucidated is whether the increase in gMDSC frequencies seen upon co-culture with pHSC is the consequence of direct contact between the gMDSC and the pHSC or whether a soluble mediator is released by activated HSC. Also without the use of staining for proliferation, for example CSFE or Ki67 staining, at this stage it is not possible to ascertain whether it is active induction of new gMDSC. The fact that an increase in gMDSC frequencies in the control samples occurs upon co-culture with pHSC may be indicative of MDSC induction from immature precursors or possible transdifferentiation of other subsets, as gMDSC are rarely observed in control individuals.

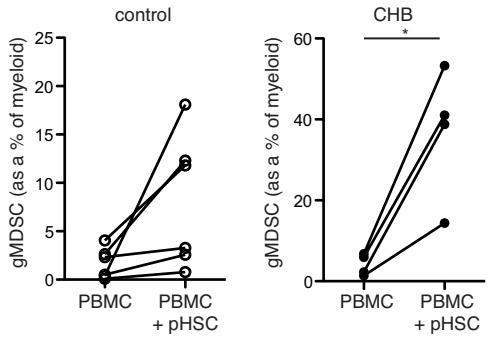

Figure 3.23: pHSC promote gMDSC survival/accumulation *in vitro*.

Primary hepatic stellate cells (pHSC) isolated and cryopreserved from margins of metastatic livers were thawed and passaged to ensure activation before use in co-culture experiments with either PBMC from controls or patients with CHB. PBMC were removed from pHSC six days post co-culture and stained for gMDSC frequencies. gMDSC were identify as $CD11b^{high}$CD33+HLA-DR-CD14-CD15+ using 11-colour flow cytometry. PBMC from six controls and four patients with CHB were co-cultured with or without pHSC. Error bars represent the mean ± SEM. Significance testing was carried out using the paired Students t-test, and where significant indicated as: * $p<0.05$. The data presented in this figure was generated in collaboration with Dr. Kasha Singh.

3.4 Conclusions & Discussion

CHB is a highly prevalent disease worldwide, that is characterised by a failing antiviral immune response which drives a non-antigen specific intrahepatic lymphocytic infiltration. This infiltration results in collateral damage to the tissue of the liver. Previous work by our group suggested that this dysregulated response occurs in association with nutrient deprivation. As a direct result of the differential regulation of this immune-mediated tissue damage in patients with CHB, contrasting outcomes of infection are clearly evident. In the data presented in this chapter it has been shown for the first time that an expansion of a subset of cells with the characteristics of immature neutrophils (the gMDSC), using primary human samples occurs in CHB.

In studying this expanded population it has also been shown that gMDSC have the ability to accumulate at the site of viral replication, which is a highly immunosuppressive and tolerogenic environment. More specifically, by taking advantage of paired samples where is was possible to obtain and isolate cells from both the blood and the liver of a well-characterised cohort of patients during differing clinical phases of disease, it has been demonstrated that MDSC frequencies correlate with the degree of liver immunopathology. gMDSC expansion is most evident in patients with CHB in whom HBV replicates at extremely high levels without any biochemical or histological evidence of liver pathology (the ″immunotolerant‟ phase).

The findings reported in this chapter are strongly supported by a recent flurry of publications demonstrating MDSC functionality in chronic viral infections [190, 189, 198, 196]. Two of these publications focused on a role for MDSC in HIV infection; these groups reported an expansion of MDSC in uncontrolled HIV infection, contributing to the HIV-1-specific and antigen-non-specific impaired T cell responses characteristic of progressive disease. The authors attribute this T cell effect to the enzymatic function of arginase I, in a cell-contact dependent manner. Another key recent report by Norris *et al.* [190] demonstrated an accumulation of MDSC with the ability to suppress T cell function in the murine model of chronic LCMV infection. The authors suggest that MDSC, along with other previously described suppressive mechanisms, counter bystander activation of cellular populations capable of causing immunopathology and inflammation often seen in persistent infections. This likely role for gMDSC mirrors the intricate role for regulatory B cells recently described by our lab in the context of chronic HBV infection [213].

Prior to embarking on this study, no known relationship between gMDSC and HBV infection

had been reported in humans. A publication by Chen *et al.* [214] reported a role for the localisation and function of hepatic MDSC in ″normal‟ and HBV transgenic mice. Frequencies of hepatic MDSC in the context of HBV were approximately twice that of the wild-type mice, but equally as suppressive in either setting [214]. A handful of reports also studied MDSC in the context of HCV in patients and *in vitro*. In the context of HCV, the majority of papers report a role for the monocytic subset of MDSC via arginase I-mediated or ROS-mediated suppressive mechanisms [192, 193, 206, 205]. One very recent paper however failed to show an expansion of either gMDSC or mMDSC in the circulation of patients with HCV compared to controls [215]. This lack of expansion of MDSC is inconsistent with data from this study and previous published studies [192, 193, 205, 206]. The cohort used within this thesis showed a significant ten-fold expansion of gMDSC in the circulation of patients with chronic HCV infection, with no significant expansion of mMDSC compared to controls. The cohort studied here do have variable gMDSC frequencies, so it is possible the patients are markedly different to those included in the study by Nonnenmann *et al.* [215], or the cells were processed differently, given their fragility. It is also possible that the mean age of the cohorts used were significantly different given the relationship between age and gMDSC frequencies.

A key unanswered question, that arises from the work presented in this study, is whether the enhanced accumulation of gMDSC in HBV (and HCV) is driven by a liver-derived or viral factor or both. This has not been fully addressed within the scope of this study. Taken together, the data in this report do raise some potential hints to answer this question. Although no clear cross-sectional correlation between gMDSC frequencies and any viral parameters was noted, a key piece of evidence supporting a role for a viral factor in driving their initial expansion was presented. Data from the acute HBV setting, supports a contribution from the virus in driving initial gMDSC expansion as the peak accumulation of gMDSC coincides with peak viraemia and not the height of liver inflammation. It is possible that a factor induced by the process of ongoing viral replication in the liver drives gMDSC induction, or indeed a viral protein, as reported for the viruses HCV and HIV [192, 197] .

A number of other candidate drivers identified in the setting of tumours, including TNFα, VEGF, and hypoxia-induced HIF-1α [133, 216, 189] would merit future investigation to assess their potential contribution to the differential accumulation of gMDSC seen in the distinct phases of CHB. Of particular note are IL-6 and VEGF [164]. IL-6 is believed to be critical to the early control of HBV infection. It is released by KC and leads to the activation of signalling pathways

that limit HBV replication in hepatocytes shortly after infection (to prevent the death of hepatocytes) [217]. It is possible that this early production of IL-6 is responsible for MDSC expansion as it has previously been implicated in the accumulation of MDSC with suppressive activity in the tumour microenvironment, down-stream of IL-1β-mediated inflammation [177]. IL-6 has also been shown to offer hepatocyte protection from T cell damage in murine Con-A-induced hepatitis by signalling through the gp130 receptor, initiating a STAT3-signalling cascade, inducing production of acute phase proteins [218, 182]. It is possible therefore that IL-6 can either directly interact with infiltrating immature myeloid cells by a similar mechanism to initiate STAT3 signalling, widely accepted as the main transcription factor involved in MDSC induction and expansion [219, 178, 179, 164] or via the indirect induction of acute phase proteins in the HBV infected liver. In addition the combination of IL-6 with GM-CSF has been reported to promote the differentiation of isolated CD33+ (myeloid cells) into a suppressive population with MDSC characteristics *in vitro* [212, 220].

The other particularly relevant mediator is VEGF. The Gabrilovich group has extensively shown a correlation between levels of VEGF and numbers of immature myeloid cells capable of suppressing antigen-specific T cell responses in cancer [169, 221]. More recently circulating MDSC from renal cell carcinoma patients have been shown to express high levels of the VEGF receptor 1 (VEGF-R1) [132]. Although MDSC reportedly express the receptor for VEGF, its role in MDSC expansion is still debated. In patients with renal cell carcinoma, treatment with an anti-VEGF antibody did not alter MDSC frequencies [132], whereas the use of this antibody in mice, caused a decrease in MDSC numbers [222]. If VEGF does promote MDSC expansion in CHB, this may be particularly relevant due to the suggestion that ground-glass hepatocytes in the HBV-infected liver produce VEGF [223]. Expression of this VEGF has been proposed to facilitate HCC progression, but it may also induce suppressive MDSC [224].

It must not be forgotten that HBV exclusively infects the liver. The observation that gMDSC frequencies are increased in hepatotropic infections (HBV and HCV) but not the pleotropic virus, CMV, and are further enriched in frequency in the intrahepatic compartment, implies a potential role for the liver milieu itself. Amongst the specialized resident cell types in the liver, HSC are stromal cells that are best known for their capacity to differentiate into pro-fibrogenic myofibroblasts. Recent studies have illustrated their additional capacity to promote immunosuppression through several mechanisms, including the generation of MDSC [114, 115, 116]. The co-transplantation of pHSC promotes the survival of islet allografts and this effect can be reca-

pitulated by the MDSC that are induced [114]. pHSC isolated from murine and human livers have also been shown to potently expand MDSC *in vitro* [114, 115, 116], analogous to the effects presented in this chapter. The pathways involved, and whether they induce MDSC proliferation and/or enhance their survival, remain to be elucidated. However the ability of pHSC to produce the chemotactic cytokine IL-8 could facilitate interactions between pHSC and gMDSC, which express high levels of the IL-8 receptor (CXCR1) in our patients. IL-8 has also been implicated as one of the acute phase proteins produced by the liver that can mobilise immature myeloid progenitors from the bone marrow [182]. Likewise, loss of CXCR4 signalling is a key step in promoting the egress of immature granulocytes from the bone marrow [210, 209]. This mechanism is implicated by the reduced levels of CXCR4 found on the expanded population of gMDSC circulating in the context of CHB.

To address the impact of the liver in the steady state, independently of the virus, it was essential to know intrahepatic gMDSC frequencies in the healthy state. To address this, gMDSC frequencies were initially assessed using lymphocytes obtained from the healthy margins of liver tissue extracted during the surgical removal of metastases in the liver. gMDSC in this liver tissue are still present, and at high frequencies. Tissue of this type fails to let us rule out the possibility of a distant effect from the tumour itself in gMDSC induction, given the fact it is well documented that gMDSC expand in the context of tumours [158, 166, 171, 133]. In healthy mice gMDSC have been shown to home to the liver and accumulate there [225]. However in the limited tissue we have obtained from healthy livers gMDSC appear to not be expanded. Further tissue from healthy liver must be assessed in the future to confirm this finding.

There is accumulating evidence suggesting a complex immunoregulatory role for gMDSC in multiple pathologies, including, cancer, infectious diseases, trauma and autoimmunity. In the context of chronic bacterial infection, gMDSC have been shown to not only expand but to increase their functional activity, specifically driven by the inflammatory mediator TNF. Increased serum TNF levels directly intensify local immune suppression by arresting myeloid cell maturation, giving rise to an MDSC population and enhancing key suppressive activity [189]. Not only has TNF been described to influence MDSC expansion, but also the combination of IL-6 and GM-CSF has the potential to give rise to cytokine-induced MDSC [212]. Increased expression of TNF [39] and IL-6 occurs during HBV infection, with a key role for KC-produced IL-6 in the control of early infection [217]. It is therefore possible that inflammatory-mediator driven induction of gMDSC accumulation occurs in viral hepatitis, especially in the liver. This local

increase in numbers of gMDSC suggests a role for MDSC in maintaining the mechanisms of tolerance required for the liver's vital metabolic and clearance functions involved in the uptake of nutrients, waste products and pathogens from the blood [207]. Liver specific expansion of gMDSC emulates findings in the murine model showing preferential homing of MDSC to liver and spleen [225]. There is a possibility that gMDSC accumulate in all livers with inflammation/ pathology where HSC are activated. It would be interesting to consider MDSC populations in livers taken from individuals with non-viral hepatitis, for example alcoholic and non-alcoholic steatohepatitis.

Chapter 4

MDSC limit hepatic immunopathology in an arginase I-dependent manner

4.1 Abstract

The data presented in this chapter builds directly on the data presented in the previous chapter and the direct hypothesis that an expansion/accumulation of an MDSC population with a granulocytic phenotype could mediate, or limit, the immune-mediated pathology observed in CHB. One key function of gMDSC is their production of immune suppressive regulators, including the L-arginine metabolising enzyme, arginase I, which depletes the amino acid L-arginine required for T cell effector function. Using combined methodology of flow cytometry and isolation techniques for cell culture, the functionality of the expanded gMDSC was assessed. This revealed that gMDSC express large amounts of arginase I and show an enhanced degranulation capacity in CHB. gMDSC expansion directly correlated with increases in circulating arginase I and a congruent depletion of L-arginine. gMDSC potently inhibited the proliferation of both HBV-specific and functionally active bystander T cells in an arginase I-dependent manner. Finally the differential expression of amino acid transporters on *ex vivo* T cells provided evidence for the metabolic reprogramming of T cells in CHB. Taken together the data in this thesis demonstrate the capacity of expanded arginase I+ gMDSC to regulate liver immunopathology by depriving T cells of L-arginine.

4.2 Introduction

4.2.1 MDSC-mediated immune suppression

MDSC exploit a number of different mechanisms to suppress both arms of the immune system; the innate and the adaptive. Given their heterogeneous phenotype, the suppressive activity of MDSC ultimately serves as the defining characteristic for these cells. Their mechanism of action often depends on the monocytic or granulocytic nature of the cells in question, with researchers tending to focus on either one of the two subsets. Previous research has also tended to focus on just one mechanism at a time. Little is known to date about whether the different candidate mechanisms of suppression can act in parallel, in synergy or only independently.

It is possible to broadly summarise the functions of MDSC that have already been described [164, 133] into four major categories. These are as follows:

1. nutrient deprivation from the local microenvironment,
2. interference with lymphocyte trafficking and cell viability,
3. generation and induction of oxidative stress, and
4. expansion and activation of other regulatory cell populations.

These functions are summarised in figure 4.1 over the page.

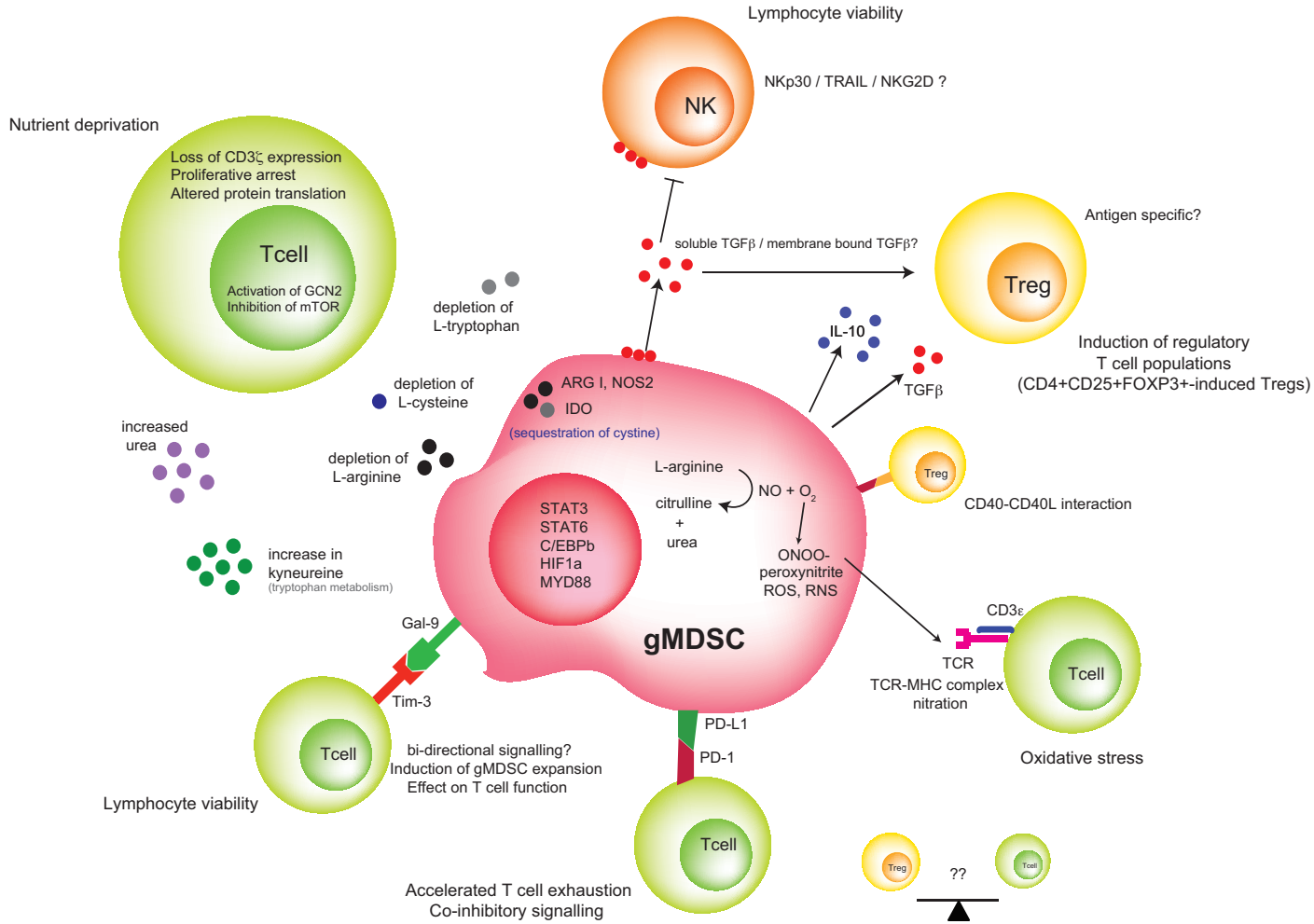

Figure 4.1: Summary of selected mechanisms of MDSC functionality affecting both innate and adaptive immunity.

Abbreviations used: reactive nitrogen species (RNS), reactive oxygen species (ROS), arginase I (ARG), nitric oxide synthase (NOS), indoleamine 2,3-dioxygenase (IDO), tumor necrosis factor (TNF)-related apoptosis-inducing ligand (TRAIL), programmed death ligand 1 (PD-L1), programmed death 1 (PD-1), T cell immunoglobulin- and mucin-domain-containing molecule 3 (Tim-3), galectin-9 (Gal-9), T cell receptor (TCR). Adapted from [133].

The work presented in this chapter concentrates on delineating the first of these mechanism of MDSC suppression in CHB. The potential role for additional mechanisms have been briefly considered or discussed in chapter 5.

4.2.2 A role for MDSC in amino acid metabolism

Historically, the primary suppressive mechanisms of MDSC is their direct role in L-arginine metabolism. MDSC can deprive lymphocytes of a number of vital amino acids essential for cell growth and differentiation. To date MDSC have been reported to play an important, well described role in depriving the immune system of the host of three amino acids; L-arginine, L-tryptophan and L-cysteine. Deprivation of L-phenylalanine has been recently, albeit briefly, described in the murine system, but as yet no translation through to the human system has been reported [226, 227]. It it also worthy of note that MDSC driven amino acid deprivation has only thus far been described for T cells. It is plausible that other lymphocytes require the same amino acids for cellular processes. For example NK cells also express the CD3ζ chain which is the main signalling transduction component of the TCR, down-regulation of which is considered to be a hallmark feature of amino acid deprivation [64].

L-arginine metabolism

The most widely studied of these amino acids subjected to MDSC-mediated metabolic regulation is L-arginine. L-arginine is a conditionally essential amino acid, meaning it must be supplied in the diet during discreet (such as pregnancy) or pathological insult (such as sepsis and trauma), in which the requirement exceeds the body's own production. Under the physiological steady state, L-arginine is however primarily a non-essential amino acid because it is synthesised endogenously via the metabolic pathways of proline, glutamine, or glutamate. Normal serum levels of L-arginine range from 50-150μM [66]. Therefore a significant depletion of L-arginine would be viewed as below 50μM, whereby profound effects on the immune response would be expected. These effects are a down-regulation of CD3ζ and proliferative arrest [66].

It is well described that L-arginine is used in the regulation of multiple biological systems, including the biosynthesis of proteins, creatine and agmatine, as well as the immune response. Key to MDSC function is the role L-arginine metabolism plays in modulating immunity. An association of L-arginine and immune regulation was initially suggested in the 1970s in reports demonstrating that injection of L-arginine in mice undergoing extensive surgery prevented the

phenomenon of post-surgical thymus involution and appeared to increase T cell numbers [228]. L-arginine is mainly metabolised to regulate immune responses by two catabolic enzymes, both of which are expressed at high levels by MDSC. These enzymes both exist as multiple isoforms: nitric oxide synthases (NOS1, NOS2, and NOS3) and the arginases (arginase I and arginase II). Metabolic degradation gives rise to the products nitric oxide (NO) and L-citrulline, and urea and L-ornithine, respectively. L-arginine is also the substrate for two further enzymes: arginine:glycine amidinotransferase (AGAT) and L-arginine decarboxylase (ADC) (figure 4.2). Although limited information about the regulation and immunological roles for AGAT and ADC currently exists.

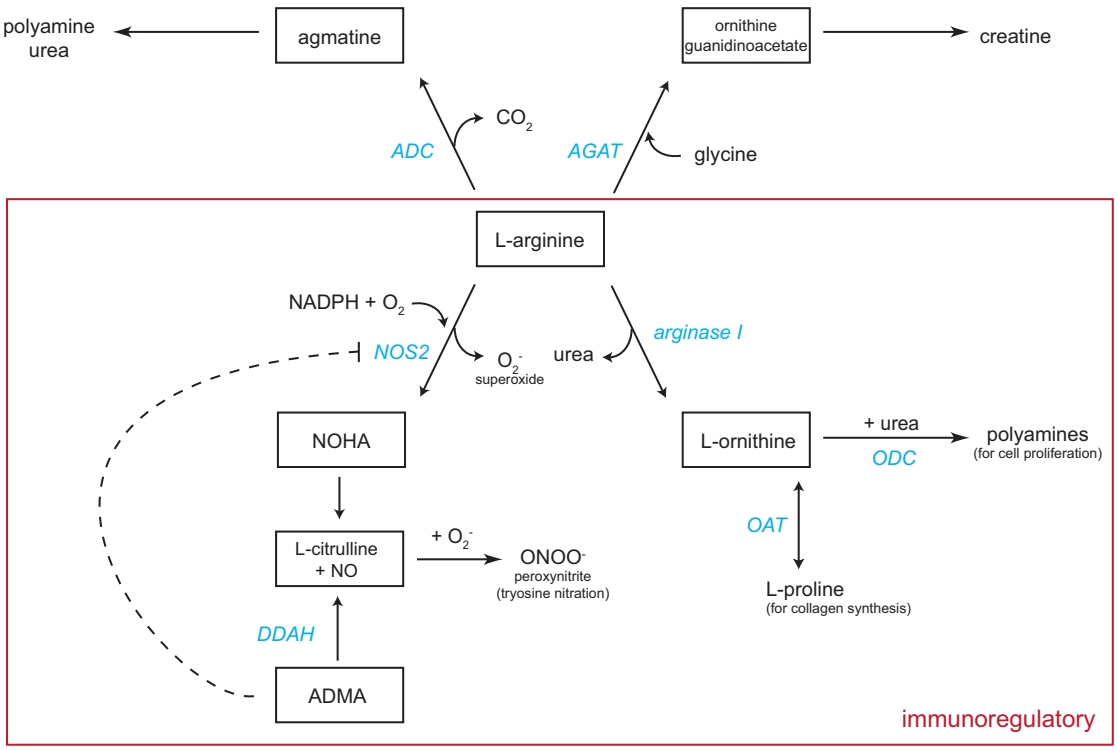

Figure 4.2: Multiple mechanisms involved in the metabolism of L-arginine.

Schematic showing the metabolism of the conditionally essential amino acid L-arginine, via the four major enzymes. Two of these catabolic enzymes, arginase and nitric oxide synthase (NOS), metabolise L-arginine, into components suggested to be involved in immune modulation (highlighted in the red box). The key pathway for the work presented in this thesis is the metabolism by arginase I into L-ornithine and urea. All proteins with enzymatic activity are highlighted in blue text. Abbreviations used: L-arginine decarboxylase (ADC), arginine:glycine amidinotransferase (AGAT), nitric oxide synthases (NOS), asymmetric dimethylarginine (ADMA), nicotinamide adenine dinucleotide phosphate (NADPH), L-ornithine aminotransferase (OAT), L-ornithine decarboxylase (ODC).

Tight control over amino acid levels has emerged as a mechanism for limiting over exuberant

expansion of highly activated proliferating cells. From recent data it is clear there is a close relationship between the availability of L-arginine and the regulation of both CD4+ and CD8+ T cell proliferation and function [64]. Cells deprived of L-arginine arrest in the G0-G1 phase of the cell cycle [229]. Consumption of amino acids from the local environment alters T cell processing through two down-stream signalling pathways; by activation of the internal stress response by general control nonrepressible 2 (GCN2) kinase and through inhibition of mTOR activation [226].

As a direct consequence of an amino acid-poor environment, GCN2 kinase senses and binds uncharged aminoacyl transfer RNA (tRNA), and reacts by phosphorylating serine-51 of the α-subunit of eukaryotic translation initiation factor (eIF2α) [64, 230]. Phosphorylated eIF2α subsequently binds more tightly than usual to eIF2B (and catalyses the exchange of GTP for GDP in the eIF2 complex). Once eIF2B is bound to phosphorylated eIF2α it is unable to exchange GDP for GTP. This lack of exchange inhibits the binding of the eIF2 complex to methionine-bound tRNA, thus inhibiting the process of translation initiation (figure 4.3) [226, 231]. The presence of phosphorylated eIF2α halts translation of newly synthesised mRNA, and manifest as a down-regulation if CDζ [232].

Amino acid availability also regulates the mTOR pathway. Specifically in conditions of low L-arginine, or amplified urea production, mTOR activity within the cell is suppressed [233]. mTOR activation subsequently phosphorylates at least two proteins critical for translation initiation (and therefore protein synthesis); these are phosphorylation of the 70kDa ribosomal protein S6 kinase (p70 S6: figure 4.3) and an inhibitor of translation initiation, the eukaryotic translation initiation factor 4E-binding protein 1 (4E-BP1). Withdrawal of amino acids results in the rapid deactivation, by dephosphorylation, of both the 70kDa S6 kinase and 4E-BP1 ultimately decreasing protein synthesis. The re-addition of amino acids to mammalian cells, previously nutrient deprived, promotes the rapid reversal of this dephosphorylation, therefore, increasing the extent of p70 S6 kinase [234]. Notably inadequate mTOR activation can result in the induction of ″infectious tolerance‟ exemplified by conversion of naive T cells into regulatory T cells [235, 154]. Of note, amino acid deprivation is not the only factor able to modulate the mTOR pathway, changes in the process of glycolysis or increased cell stress also regulate the phosphorylation status of the p70 S6 subunit [233].

Preliminary unpublished work from the Stauss group failed to demonstrate a role for the GCN2 pathway in L-arginine-depletion driven immune suppression. The use of short-hairpin RNA

targeting of the GCN2 pathway failed to recover T cell proliferation and cytokine production after polyclonal activation under conditions of nutrient deprivation, specifically low L-arginine. Instead impairment in the ability to phosphorylate the p70 S6 kinase was observed in both the GCN2 knock-down and wild type cells when deprived of L-arginine. These data, together with reports in the literature [234] implicate inhibition of the mTOR pathway, independently of the GCN2 signalling cascade and its role as a critical nutrient-sensing mediator. Artificial, *ex vivo* activation of the mTOR pathway could render lymphocytes resistant to conditions of L-arginine deprivation (personal communication - Mathias Zech and Hans Stauss).

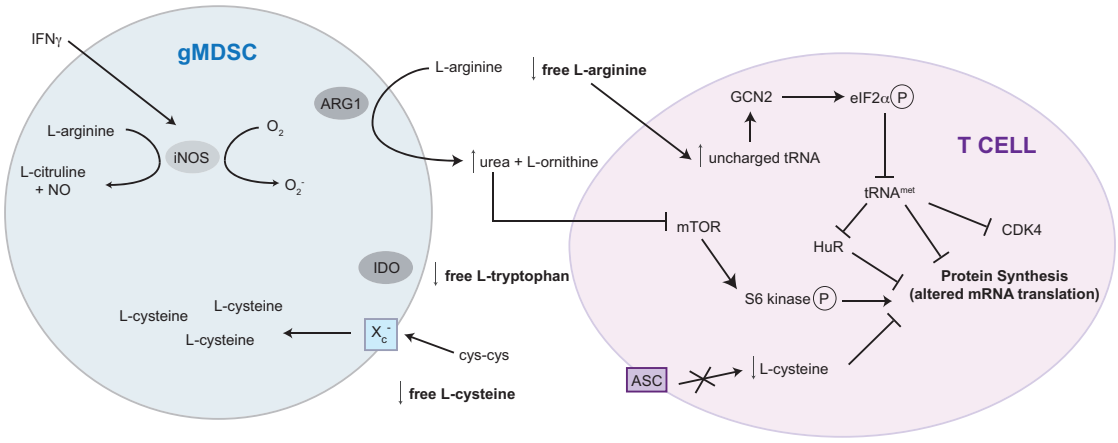

Figure 4.3: Effect of amino acid starvation on T cell functions.

gMDSC have the capacity to deplete essential amino acids (those depicted here: L-arginine, L-tryptophan and L-cysteine) by either ezymatic degration or via the sequestration of synthetic intermediates. Amino acid deprivation has profound effects on the T cell, reducing both functionality, and proliferation. T cells sense amino acid levels via two main pathways: the GCN2 and mTOR pathways. Full details of the pathways and effects of amino acid starvation have been detailed in the main text in relation to L-arginine in section 4.2.2, but also apply to the other amino acids. Abbreviations used: arginase (ARG), indoleamine-2,3-dioxygenase (IDO), mammalian target of rapamycin (mTOR), inducible nitric oxide synthase (iNOS), general control nonderepressible 2 (GCN2), eukaryotic translation initiation factor 2α (eIF2α), nitrix oxide (NO), transfer RNA (tRNA), human antigen R (HuR).

Evidence is also emerging describing a role for L-arginine deprivation in driving other downstream effects beyond defective ribosomal translation of newly synthesised transcripts. The depletion of cytosolic L-arginine by arginase I, also results in the transfer of electrons from the reductase and oxygenase subunits of the often co-expressed enzyme iNOS to surrounding oxygen, generating superoxide species (figure 4.3). This production of superoxide can combine to generate several reactive nitrogen species (RNS). More specifically superoxide can combine with NO, a by-product of L-arginine degradation, to generate peroxynitrite (ONOO-) (figure 4.1). Peroxynitrite is an highly oxidising reagent that subsequently damages numerous biological targets.

Peroxynitrite molecules achieve this by crossing membranes within or between cells functioning as intra- and inter-cellular signalling molecules capable of inducing the post-translational modification of proteins, through tyrosine nitration. A study by Brito *et al.* [236] demonstrated that the extracellular addition of peroxynitrite to human T cells primes them to undergo apoptotic cell death. This pathway was noted to be particularly prevalent amongst activated T cells and was achieved by inhibition (nitration) of necessary signalling proteins, preventing the ongoing phosphorylation of downstream signalling molecules [236]. More recently it has also been reported that production of peroxynitrite, driven by MDSC-mediated metabolism of L-arginine, is capable of direct nitration of the TCR. Such nitration of the TCR prevents successful antigen peptide-MHC interactions and the subsequent loss of cell surface signalling components, dramatically limiting T cell responsiveness to antigenic stimulation when in close cell to cell contact [237].

L-tryptophan metabolism

Metabolism driven by TDO and/or IDO result in local depletion of another key nutrient, in this case the essential amino acid L-tryptophan. Metabolism of L-tryptophan results in the increased production of kynurenine-based metabolites. Similarly to L-arginine, the combined effects of L-tryptophan degradation have been shown to limit T cell proliferation and induce T cell apoptosis via the GCN2 pathway (figure 4.3) [230].

IDO is a rate limiting enzyme in the metabolism of L-tryptophan along the immunomodulatory kynurenine pathway. Consequently IDO is well-established as a predominant endogenous suppressive factor of host immune responses, being implicated in the maintenance of materno-fetal tolerance, transplantation and tumourigenesis. Expression of IDO as an immune regulator by inhibitory DC induces immune tolerance in cancer patients and tumour-bearing animal models [128, 238]. Pro-inflammatory cytokines, such as IFNγ and TNFα have been implicated in the induction of IDO in DC [239, 240].

The specific role for IDO in immune suppression is well accepted. The a role for TDO, however, is less well characterised, but perhaps more relevant to the study of hepatotropic infections, since TDO is predominantly expressed in the liver. A study by Schmidt *et al.* [241] demonstrated the ability of TDO-expressing cells to inhibit T cell proliferation and their production of IFNγ. TDO could therefore also act as a key regulator of immune tolerance essential to the homoeostasis of the liver. Although this particular study only showed the potential role for TDO in immune

tolerance during liver transplantation [241]; the evidence for its role *in vivo* during hepatotropic infections remains unclear.

More recently studies have begun to provide evidence that one mechanism of MDSC-mediated immunosuppression can be attributed to L-tryptophan metabolism via their production and expression of IDO (figure 4.3). Recent work by Yu *et al.* [242] reported that not only was a population of MDSC (with a granulocytic phenotype) increased in breast cancer tissue but that these cells expressed IDO. The up-regulation gMDSC IDO at the tumour site correlated significantly with an infiltration of suppressive Treg. Further use of an experimental IDO-inhibitor (1-MT) partially inhibited the T cell suppression observed. The exact molecular mechanism involved in the up-regulation of IDO expression in MDSC is currently unknown and therefore requires further investigation, but some recent reports from studies looking at the function of plasmacytoid DC in cancer have reported that arginase I and IDO can act simultaneously [243], indicative of the induction of an immunosuppressive ″program‟ by an MDSC to limit the availability of multiple amino acids.

In addition in a relevant study by Larrea *et al.* [129], the authors demonstrated an up-regulation of IDO in the liver of both experimentally infected chimpanzees and patients with chronic HCV infection. The up-regulation of the enzyme was attributed to HCV-induced IFNγ production, and that persistent IDO expression in the liver microenvironment contributed to T cell tolerance. The authors did not however confirm the source of the increase in IDO expression: it is possible MDSC, known to increase in chronic HCV infection [192, 193] are responsible for the IDO increase observed.

L-cysteine metabolism

Another amino acid that has been implicated in MDSC immunomodulation by nutrient deprivation is L-cysteine. As with L-arginine, L-cysteine is a conditionally essential amino acid (therefore needed in the diet when requirement exceeds the synthetic capacity). L-cysteine is therefore also critical for the synthesis of new proteins (protein translation), and so availability of L-cysteine is essential for proliferation and function. L-cysteine, under physiological conditions, is generated by a cell via two different pathways. The first of these pathways requires expression of the plasma membrane cystine transport xc- that enables the import of disulphide-bonded cystine (the metabolic intermediate) from the oxidising extracellular environment. Once in the cell, the reducing intracellular environment reduces the imported cystine to cysteine [244]. The other

of these pathways relies on expression of the enzyme cystathionase. Cystathionase catalyses the conversion of intracellular methionine to cysteine [245].

A major problem for T cells is that they express neither the xCT chain of the xc- transporter nor the enzyme cystathionase [246]. As such, T cells are dependent on other cells to provide them with L-cysteine. Macrophages and DC largely produce this L-cysteine and export it for T cell use through their plasma membrane via an ASC neutral amino acid transporter [247, 248].

Srivastava *et al.* [131] hypothesised and subsequently demonstrated that MDSC modulate T cell function by limiting extracellular concentrations of not only L-arginine and L-tryptophan but also L-cysteine. The authors showed that MDSC can express the xCT chain of the cystine transporter, enabling them to acquire cystine from the extracellular environment, but lack the ASC neutral amino acid transporter needed for export, meaning MDSC are unable to export L-cysteine. As a consequence, MDSC limit the extracellular availability of L-cysteine by sequestering the metabolic intermediate during L-cysteine synthesis. Limited pools of L-cysteine predispose T cells to oxidative stress, again limiting T cell functionality.

L-phenylalanine metabolism

Finally metabolism of L-phenylalanine has also be reported to be involved in the process of immunoregulation by MDSC (reviewed in [227]). Most of the data depicting a role for its metabolism have arisen from *in vitro* studies and are still rather limited. Interleukin-4-induced gene 1 (IL4I1) is a secreted L-phenylalanine oxidase that produces hydrogen peroxide and phenylpyruvate following the oxidative deamination of L-phenylalanine. Human and mouse IL4I1 can be expressed by APC, including studies showing expression in murine MDSC [249, 250]. A study by Boulland *et al.* [249] specifically reported the role for L-phenylalanine mediated metabolism by IL4I1 in the inhibition of T cell proliferation that was associated with a transient decrease in CD3ζ expression akin to studies looking into a role of L-arginine and L-tryptophan. Further investigation is required.

4.2.3 Overview of the L-arginine metabolising enzyme arginase I

As mentioned previously, two genetically distinct isoforms of arginase exists in mammals, that differ in their tissue distribution and sub-cellular location. These two isoforms are: arginase I, also known as the liver-type arginase, is predominantly found in the cytoplasm of hepatocytes,

where it plays a key role in the final step of the urea cycle; and arginase II, the kidney-type, present in numerous tissues (including the brain, kidneys, small intestine, liver and skeletal muscle), where it associates with the mitochondria, but is not essential to the urea cycle. Mice lacking expression of arginase II show elevated L-arginine levels, providing some limited evidence for arginase II playing a physiological role in arginine homoeostasis [251]. Arginase I however is much more widely studied. Arginase I, although highly expressed by hepatocytes has also been shown to be produced by a number of cells of the innate immune system. In rodents macrophages constitute a major but not sole source of arginase I. Arginase I activation has also been put forward as a hallmark of the alternatively activated macrophage. These cells represents the predominant cell among tumour infiltrating macrophages, in numerous human and murine tumours where they have been reported to suppressor anti-tumour immune responses [67].

Arginase I is also constitutively expressed by granulocytes [252]; death (by apoptosis or necrosis) of such cells at sites of inflammation allows for the release of the enzyme, capable of inducing profound suppression in T cell proliferation and cytokine synthesis [253]. Murine granulocytes also deplete L-arginine by uptake through the cationic amino acid transporter 2B (CAT-2B) [254]. In contrast the mechanism by which human granulocytes, including MDSC, deplete L-arginine remain unclear. It has been proposed that viable human granulocytes expressing arginase I, including MDSC subsets expressing high levels of CD66b, actively degranulate, and thus release the metabolically active enzyme arginase I into the extracellular milieu [132].

MDSC are now widely accepted to be a further potent source of arginase I [170, 255, 181] that inhibits lymphocyte function [67, 66]. What is not known is whether the expanded population of gMDSC seen in our patient cohort (seen in chapter 3), express high levels of the enzyme or whether arginase I mediated immune suppression is a key mechanism involved in the immunopathogenesis of CHB, similar to that reported in a number of other settings [256, 166, 164].

4.3 Results

4.3.1 gMDSC express high levels of arginase I

As shown in figure 4.2 arginase I is one of four enzymes central to the metabolism of L-arginine [67]. An increase in its enzymatic activity in CHB was previously reported by our group [58]. As extensive literature describes gMDSC as a potent source of arginase I it was postulated that gMDSC could suppress inflammation in the liver (implicated in figures 3.7 and 3.8) by production of this enzyme. *Ex vivo* flow cytometric analysis of gMDSC was carried out to determine expression of arginase I using a directly conjugated antibody (figure 4.4a). gMDSC showed strong staining for the enzyme, with low-density neutrophils (CD14-CD15+CD16+) the only other circulating cell type expressing analogous levels (figure 4.4b). Notably the monocytic MDSC subset expressed much lower levels of arginase I than gMDSC (figure 4.4b). Using the latest ImageStream technology (which combines flow cytometry with the resolution of fluorescence microscopy), confirmation of the capacity of gMDSC to produce and store large amounts of arginase I was observed (figure 4.4c). The comparison of a large number of study participants revealed that the percentage of gMDSC expressing arginase I in controls and patients was analogous. This was true for both cohorts (the Central and East London); what was striking was the difference in percentage of arginase I positivity in gMDSC of patients in relation to the anticogulant used during sample collection. When taken in lithium-heparin, gMDSC expressed a mean ± SEM of 81.2±3.2% (figure 4.4d, right-hand panel) compared to a mean ± SEM of just 56.2±4.2% when taken in EDTA (figure 4.4d, left-hand panel).

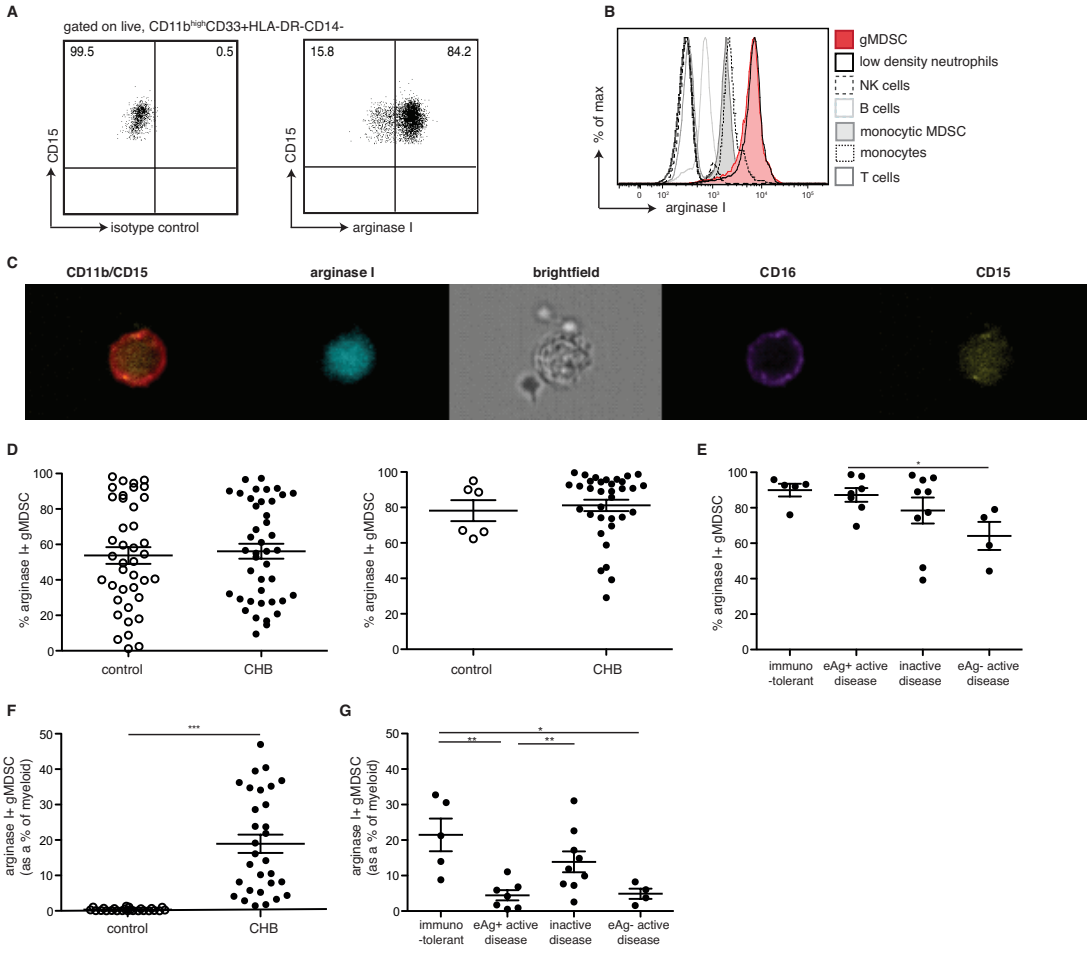

Figure 4.4: Arginase I expressing gMDSC are increased in CHB.

A) Representative FACS plots showing gMDSC arginase I staining compared to a matched isotype control from a patient with CHB. B) Analysis of PBMC subsets for expression level (mean fluorescence intensity, MFI) of intracellular arginase I. Lymphocyte subsets were identified as: CD3-CD19+ B cells, CD14-CD16+CD15+ low density neutrophils, CD3+ T cells, CD3-CD56+ NK cells, and HLA-DR+CD14+ monocytes. C) Representative ImageStream ISX with a 60x objective showing a CD11b/CD15/CD16 co-expressing cell displaying granular arginase I staining. D) Cumulative data showing the percentage of gMDSC expressing arginase I in controls and patients with CHB from the Central London cohort (taken in EDTA) and the East London cohort (taken in lithium-heparin), respectively. E) Arginase I expressing gMDSC from a subset of patients who were well classified on the basis of repeated clinical assessments (East London cohort) (serum alanine transaminase (ALT) levels, ± liver histology to assess liver inflammation, HBeAg status and viral load) into distinct phases of disease as defined in section 3.3.2. F) Cumulative data for arginase I levels in relation to the percentage of arginase I-expressing gMDSC as a proportion of the total myeloid cell compartment ($CD11b^{high}CD33+$). G) Categorisation of arginase I+ gMDSC as a percentage of total myeloid cells by disease phase. Error bars represent the mean ± SEM. Significance testing was carried out using the unpaired Students t-test, and where significant indicated as: *** $p<0.001$; ** $p<0.01$; * $p<0.05$.

Upon further analysis of gMDSC expressing arginase I using a subset of the East London cohort, who were classified into distinct phases of disease, there seemed to be a stepwise trend towards

decreasing arginase I production as CHB disease progresses (figure 4.4e). There was a marked increase in the proportion of arginase I+ gMDSC circulating in patients with CHB compared to controls when analysis took into account the increased frequency of circulating gMDSC present in these patients (figure 4.4f). The percent of arginase I+ gMDSC was significantly higher in the immunotolerant phase of disease and those with inactive disease than those with active disease (figure 4.4g), mirroring the data showing gMDSC frequencies depicted in figure 3.7a.

In an attempt to assess the suppressive capacity of intrahepatic versus circulating gMDSC, the extent of arginase I expression was assessed (using MFI values). Intrahepatic gMDSC express more arginase I than their circulating counterparts (figure 4.5). This suggested that intraheptic gMDSC may have an enhanced potential to mediate immunosuppression through the depletion of local concentrations of L-arginine compared to those in the periphery of patients with CHB.

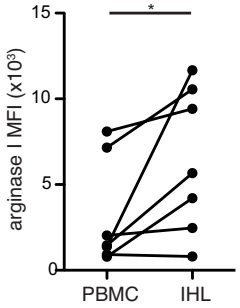

Figure 4.5: Enhanced arginase I expression in intrahepatic compared to peripheral gMDSC.

Freshly isolated PBMC or intrahepatic lymphocytes were stained for CD33, CD11b, HLA-DR, CD14 and CD15 and gated as shown in figure 3.2a to identify gMDSC. Mean fluorescence intensity (MFI) of arginase I expression between circulating (PBMC) and intrahepatic (IHL) gMDSC using seven paired samples from patients with CHB. Error bars represent the mean ± SEM. Significance testing was carried out using the paired Students t-test, significance indicated as: * $p<0.05$.

4.3.2 The degranulation capacity of gMDSC is enhanced in CHB

Arginase I is thought to be stored in azurophilic granules, expressing CD63, in the cytoplasm of gMDSC [252, 257]. Upon activation, it is believed gMDSC can degranulate and therefore release these granules. This capacity to degranulate can be measured by incorporation of CD63 at the cell surface of gMDSC [258], thus allowing for its detection by flow cytometry (figure 4.6a). Patients with CHB express more CD63 on the surface of their gMDSC compared to controls (figure 4.6b), implying an enhanced capacity for degranulation. In an attempt to address this

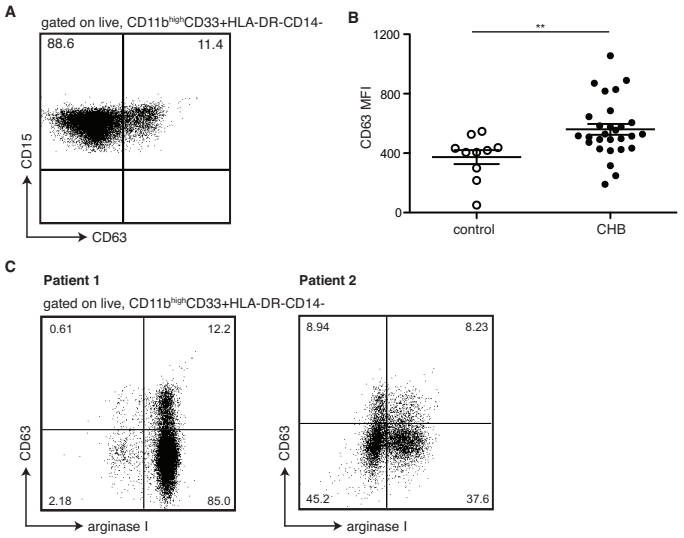

Figure 4.6: gMDSC have an enhanced capacity for degranulation in CHB.

Freshly isolated PBMC were stained for CD33, CD11b, HLA-DR, CD14 and CD15 and gated as shown in figure 3.2a to identify gMDSC. A) Representative FACS plots showing extracellular surface staining for the auzophilic granule marker, CD63 in a patient with CHB. B) Cumulative data of the mean fluorescence intensity (MFI) of CD63 expression on the surface of gMDSC from 10 controls and 30 patients with CHB. C) Co-staining of arginase I expression by an MDSC with CD63 expression on its surface in two representative patients with CHB. Error bars represent the mean ± SEM. Significance testing was carried out using the unpaired Students t-test, and where significant indicated as: ** $p<0.01$.

postulate, arginase I was co-stained with CD63 (figure 4.6c) in a limited number of patients. This showed a clear population of gMDSC that co-stain for surface CD63 and intracellular arginase I, suggesting the potential for the release of arginase I by gMDSC degranulation (figure 4.6c). The percentage of the total arginase I stored in gMDSC found to co-stain with CD63 was however highly variable between patients (figure 4.6c), implying that not all of the arginase I that a gMDSC can produce is stored in CD63-expressing granules. What remains to be elucidated is whether the proportion of arginase I stored in CD63-expressing granule varies between patients with CHB and controls, or between peripheral gMDSC or intrahepatic gMDSC. It is possible that more arginase I is stored in these granules, poised for release in the liver or in immunotolerant patients (and those with inactive disease).

4.3.3 Serum arginase I levels are increased in CHB

Consistent with the expansion of gMDSC with an enhanced degranulation capacity, a significant increase in serum arginase I was detected by ELISA in patients with CHB compared to controls (figure 4.7a). A robust correlation was observed between the concentration of serum arginase

I and circulating gMDSC frequencies (figure 4.7b), supporting the notion that gMDSC can act as a major source of arginase I in CHB. The preferential expansion of arginase I+ gMDSC in patients in the immunotolerant phase was mirrored by the most significant increase in serum arginase I in these patients (figure 4.7c). Taken together these data suggest gMDSC may have the capacity to suppress liver inflammation through an arginase I-dependent mechanism. This was further reinforced by the fact that the concentration of circulating arginase I correlated inversely with serum ALT (figure 4.7d,e).

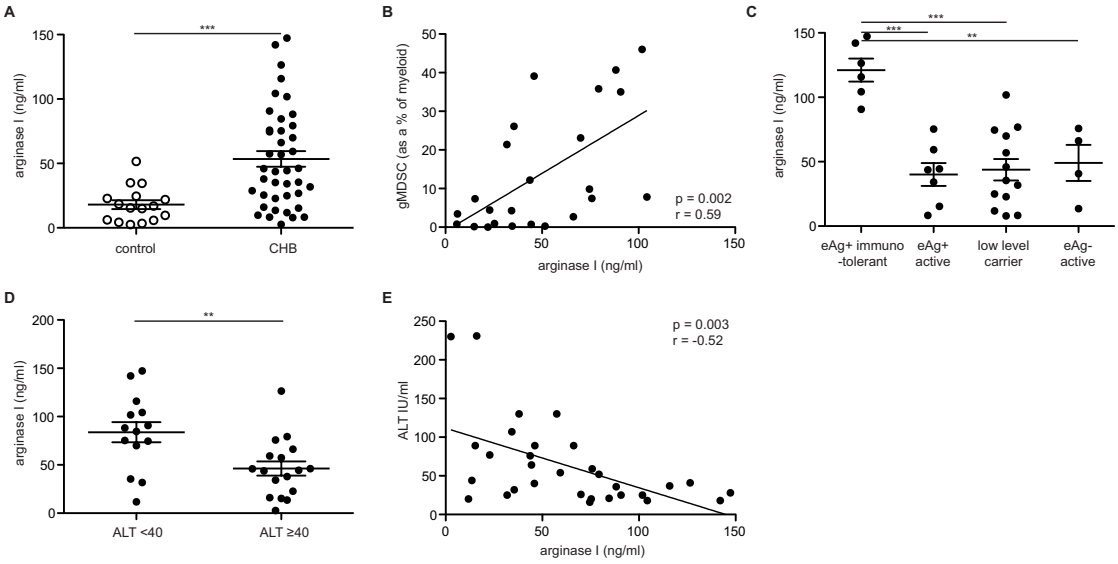

Figure 4.7: Serum levels of arginase I are increased in patients with CHB.

Circulating arginase I levels were determined by ELISA using stored serum samples. A) Serum concentrations of arginase I (ng/ml) from 16 uninfected controls and 41 patients with CHB. B) Correlation of serum arginase I levels with circulating frequencies of gMDSC previously assessed in a cohort of the East London patients with CHB. Further cross-sectional analysis of arginase I levels in the CHB cohort by C) disease phase (as previously defined); D) and E) by degree of liver inflammation, as measured by serum ALT (IU/L). Error bars represent the mean ± SEM. Significance testing was carried out using either: the Pearson product-moment correlation coefficient or the unpaired Students t-test, and where significant indicated as: *** $p<0.001$; ** $p<0.01$.

4.3.4 Circulating L-arginine levels are depleted in CHB

The role arginase I plays in the depletion of the conditionally essential amino acid L-arginine has been well described and reviewed extensively [67]. L-arginine metabolism by arginase I gives rise to the metabolites L-ornithine and urea (see figure 4.2). Previous work from our group reported a depletion of L-arginine in a small group of patients with high levels of HBV-related liver inflammation [58].

To further test the functionality of the increase in arginase I+ gMDSC and serum arginase I already presented, tandem high-pressure liquid chromatography mass spectrometry (tandem HPLC-MS) was employed to measure levels of circulating amino acids and derivatives using stored serum samples. In this current study the cohort size analysed was greatly increased (to include 69 patients with CHB) and the same finding was observed; enhanced L-arginine metabolism occurs in CHB (figure 4.8a). In line with their lower levels of arginase I+ gMDSC and serum arginase I, some patients with raised ALT had higher levels of L-arginine (figure 4.8b). Corroborating arginase I driven metabolism of L-arginine, a non-significant trend towards an increase in circulating levels of the metabolite L-ornithine was observed (figure 4.8c).

The amino acid L-tryptophan, also implicated in immune regulation [259], showed a non-significant trend to decrease in CHB (figure 4.8d). The amino acid L-phenylalanine did not differ between controls and patients with CHB (figure 4.8e); although a study by Boulland *et al.* [249] reported a potential role for L-phenylalanine metabolism in immune regulation by murine MDSC, this did not seem to be evident in human CHB infection.

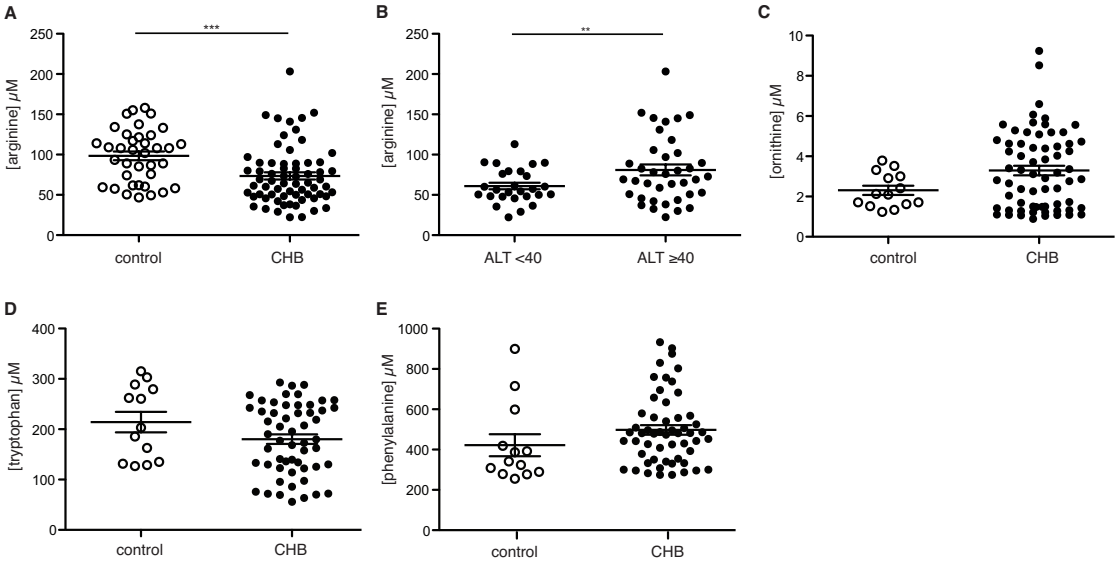

Figure 4.8: Levels of the amino acid, L-arginine, are depleted in CHB.

Tandem high-pressure liquid chromatography mass spectrometry analysis of circulating amino acids. A) Cumulative data showing the circulating L-arginine concentrations (μM) in the serum of 36 controls and 69 patients with CHB. B) Analysis of the CHB patients by serum ALT (IU/L). Cumulative data showing concentrations (μM) of: C) L-ornithine; D) L-tryptophan; and E) L-phenylalanine in sera from controls and patients with CHB. Error bars represent the mean ± SEM. Significance testing was carried out using the unpaired Students t-test, and where significant indicated as: *** $p<0.001$; ** $p<0.01$.

4.3.5 Similarly to CHB, circulating levels of arginase I are increased, and levels of L-arginine are decreased in chronic HCV infection

The notion that gMDSC are capable of suppressing liver inflammation through an increase in numbers and functioning through an arginase I-dependent metabolism of L-arginine in CHB was confirmed in another hepatotropic virus, HCV. In chronic HCV infection, gMDSC expand to analogous frequencies to those seen in patients with CHB (previously shown in figure 3.17a). It was postulated that the same mechanism of immunosuppression could be relevant in HCV. In a small number of patients with chronic HCV an increase in serum arginase I compared to controls was detected by ELISA (figure 4.9a). This increase was similar to that seen in patients with CHB (figure 4.7a) and was corroborated by a significant decrease in the amino acid L-arginine (figure 4.9b).

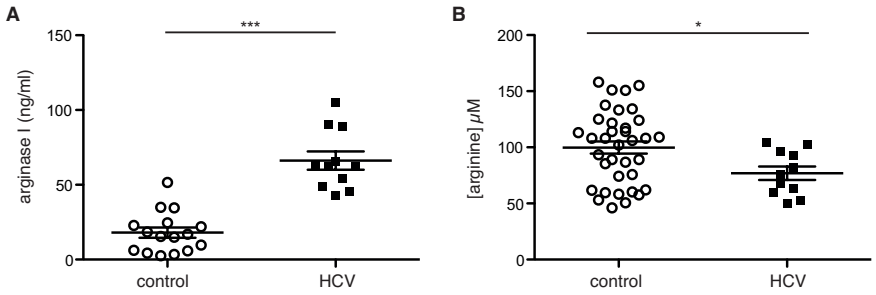

Figure 4.9: Serum arginase I levels are enhanced in HCV, alongside a decrease in circulating L-arginine levels.

A) Serum concentrations of arginase I (ng/ml) determined by ELISA in 16 controls and 11 patients with chronic HCV infection. B) Tandem high-pressure liquid chromatography mass spectrometry analysis of circulating of L-arginine in 37 controls and 11 patients with chronic HCV infection. Error bars represent the mean ± SEM. Significance testing was carried out using the unpaired Students t-test, and where significant indicated as: *** $p<0.001$; * $p<0.05$.

4.3.6 Levels of L-arginine recover on antiviral treatment in CHB

In using cross-sectional studies of patients who have had a highly dynamic disease for many years, it was difficult to distinguish whether the reduction in L-arginine levels (and the associated accumulation of gMDSC) was the cause or result of reduced HBV-related liver inflammation. MDSC have been shown to be induced by chronic inflammation [186, 187], and more recently by TNFα [189]. Once induced, gMDSC could result in suppression of bystander inflammation in the liver, resulting in their association with less active disease. To probe the postulate that initial expansion of arginase I+ gMDSC is driven by HBV-related inflammation, we analysed an additional small cohort of patients with CHB in whom the burden of viral replication and resultant degree of liver inflammation was manipulated by the introduction of antiviral therapy. Using samples obtained from seven patients before and during antiviral therapy, L-arginine levels were noted to be partially restored in five out of seven of these patients once HBV replication was suppressed (figure 4.10a). The degree of L-arginine increase correlated with the extent of disease suppression as measured by a normalisation in their serum ALT (figure 4.10b).

In line with this, in a very limited number of patients on anti-viral treatment, serum arginase I concentrations decreased to values in line with those seen in controls (figure 4.11a), and gMDSC frequencies declined (figure 4.11b). One important caveat to these data is that these patients were sampled at one-off time points whilst on antiviral treatment, and as a result the pre-treatment gMDSC frequencies were unknown. It is important to consider that these patients on antiviral therapy are likely to be patients who had ongoing high level viral replication and

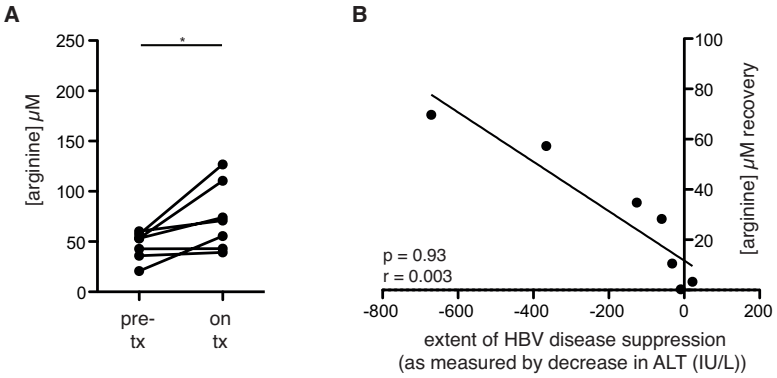

Figure 4.10: Levels of circulating L-arginine recover on antiviral treatment.

Tandem high-pressure liquid chromatography mass spectrometry analysis of circulating amino acids. A) L-arginine concentrations (μM) from seven patients with CHB sera before (pre-tx) and during (on tx) antiviral therapy (* patients had been treated for >1 year) and B) correlation between decrease in ALT and recovery in circulating L-arginine. Error bars represent the mean ± SEM. Significance testing was carried out using either: the Pearson product-moment correlation coefficient or the paired Students t-test, and where significant indicated as: ** $p<0.01$; * $p<0.05$.

liver disease (active disease patients, see figure 3.7a) and therefore unlikely to have had a high frequency of gMDSC prior to commencing therapy. It remains to be elucidated what the effect on gMDSC frequencies would be if patients with either inactive disease or in the immunotolerant phase were treated in clinic; it is these patients in whom gMDSC frequencies would predictably be high to begin with.

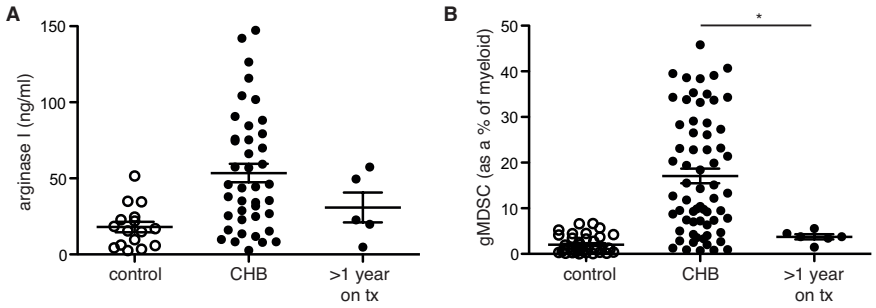

Figure 4.11: Serum arginase I levels and gMDSC frequencies normalise on antiviral therapy.

A) Serum concentrations of arginase I (ng/ml) determined by ELISA in 16 controls, 41 patients with CHB and a small cross-sectional analysis of five patients with CHB during treatment (at least one year of treatment with antivirals). B) Circulating gMDSC frequencies in an extended cohort of patients with CHB to include six individuals during ongoing antiviral therapy (at least one year). Error bars represent the mean ± SEM. The statistical testing for the controls compared to patients with CHB was done in previous figures. For comparison with antiviral therapy significance testing was carried out using the unpaired Students t-test, and where significant indicated as: * $p<0.05$.

4.3.7 MDSC potently suppress T cell responses

Functional evidence was sought to determine whether the expanded population of arginase I+ gMDSC seen in patients with CHB could limit adaptive immunity against the virus, by specifically inhibiting T cell functionality. To address the suppressive capacity of gMDSC in the context of CHB, an assay was established to assess T cell responsiveness *in vitro* after co-culture with autologous gMDSC. To accurately identify gMDSC from PBMC samples multiple markers are required (see gating strategy shown in figure 3.2a), making it difficult to isolate these cells without multiparametric flow-assisted sorting. To bypass the need for a biosafety level three FACS sorter (unavailable during the course of this study), an approach was adopted that utilised magnetic beads. It was not technically possible to isolate gMDSC using the full panel of markers with magnetic beads and so an enrichment for gMDSC was adopted. gMDSC were enriched using a two-step process: CD14 negative selection, to remove contaminating monocytic cells and a subsequent round of CD15 positive selection, ensuring all granulocytic cells were included.

Using a pool of overlapping peptides spanning the HBV core region, PBMC were cultured either in the absence of physiological frequencies of gMDSC (gMDSC depleted: ΔgMDSC) or after the addition of an autologous magnetic bead-enriched population of gMDSC. T cell functionality was assessed by monitoring the production of IFNγ, over and above baseline stimulation in the absence of peptide. As depicted in the representative plots (figure 4.12a), removal of suppressive

gMDSC during peptide stimulation enhanced the response, indicating that the population of gMDSC has sufficient potency to suppress HBV-specific T cell responses at frequencies circulating *in vivo*. Conversely T cell production of IFNγ following HBV-peptide stimulation was almost completely abrogated by the addition of an enriched gMDSC population (figure 4.12a, far right panel). In the four patients with CHB in whom a detectable HBV-specific response was observed to HBV core peptide stimulation, gMDSC-mediated suppression was observed, albeit with variable responses to peptide-stimulation (figure 4.12b). As very few HBV-specific T cells are detectable in the majority of patients [260] HBV-specific suppression assays need to be carried out in more patients to confirm these findings that gMDSC can limit the antiviral T cell response.

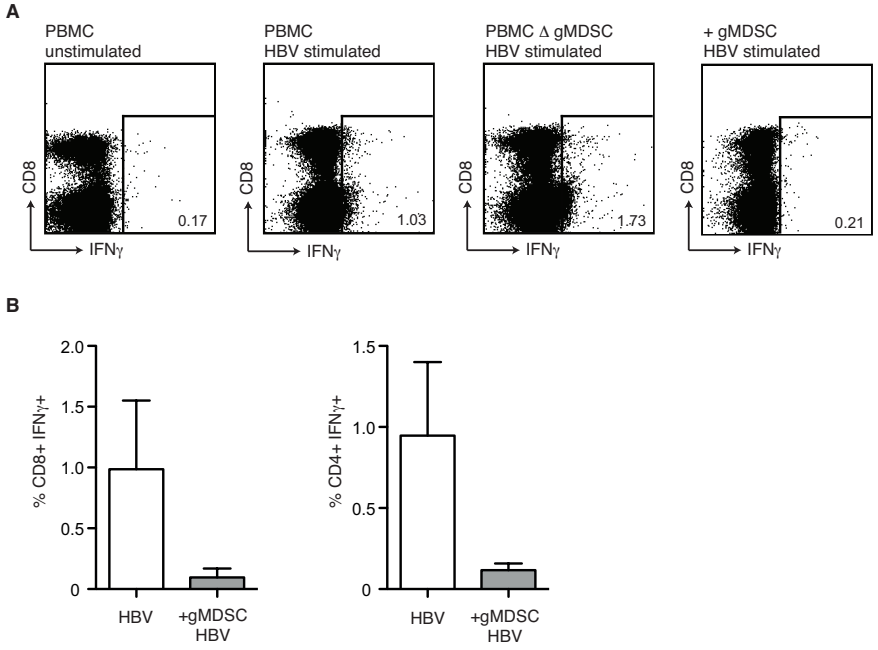

Figure 4.12: gMDSC are capable of suppressing HBV-specific T cells *in vitro*.

gMDSC were enriched or depleted using sequential magnetic bead isolation (CD14-CD15+, Miltenyi) from PBMC obtained from patients with CHB, for co-culture with autologous PBMC. gMDSC-enriched, depleted, or un-depleted PBMC were cultured with 20IU/ml recombinant IL-2 for five days and tested for HBV-specific T cell responsiveness by intracellular cytokine staining following HBV peptide stimulation (using a peptide pool of peptides overlapping the core region). A) Representative FACS plots showing the IFNγ T cell response from a patient with CHB in total PBMC with or without HBV-peptide stimulation, after gMDSC depletion (ΔgMDSC) and the addition of an enriched gMDSC population (+gMDSC) from day zero. B) Cumulative data for CD8+ and CD4+ responses (after subtraction of background response from the unstimulated wells) in PBMC $\pm$ gMDSC (n=4).

As described in the introduction (sections 1.3.1 and 1.3.3), failure of the HBV-specific T cells in the liver to control vireamia results in the recruitment of an inflammatory infiltrate of antigen non-specific or bystander T cells. It is the response of these cells locally that is critical to the

amplification of the HBV-related immunopathology seen in CHB [47, 28]. Bearing this in mind, functional evidence was sought to determine whether the same expanded population of gMDSC could suppress bystander T cell responses in CHB.

To specifically investigate the capacity of gMDSC to limit bystander T cell functionality, T cell responsiveness to influenza, EBV and CMV, viral infections that many of our cohorts have been exposed to, was assessed *in vitro* using a similar assay to that described previously. In this case PBMC from patients with CHB were stimulated with CEF, a pool of peptides representing the immunodominant T cell epitopes from influenza, EBV and CMV, restricted by a range of HLA-A and B alleles. T cell responses were once again assessed, with or without the removal or addition of a magnetic bead-enriched gMDSC population. T functionality was monitored by intracellular cytokine staining.

As illustrated in the representative plots (figure 4.13a), the CEF peptide-specific IFNγ response from T cells was similarly enhanced upon depletion of gMDSC. Confirming the ability of these gMDSC to potently suppress T cell function, production of IFNγ following CEF stimulation was again completely abrogated after the addition of enhanced frequencies of gMDSC (figure 4.13a). All 11 patients with CHB in whom a detectable CD4+ and CD8+ T cell IFNγ response to CEF was seen, showed consistent suppression after the addition of gMDSC (figure 4.13b). Using CEF stimulation, the functional capacity of gMDSC showed a dose-response, confirming their high potency by the ability to maintain some suppression at an effector:target ratio of 1:4 in two independent experiments (a representative example is shown in figure 4.13c).

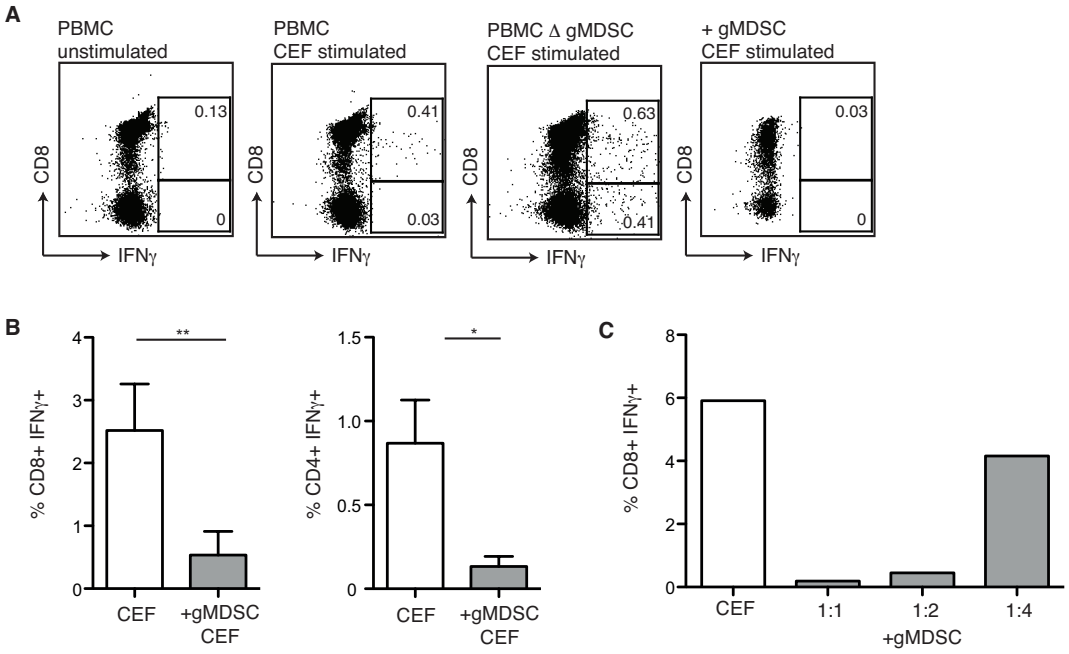

Figure 4.13: gMDSC are capable of suppressing bystander T cell responsiveness *in vitro*.

gMDSC were enriched or depleted using sequential magnetic bead isolation (CD14-CD15+, Miltenyi) from PBMC obtained from patients with CHB, for co-culture with autologous PBMC. gMDSC-enriched, depleted, or un-depleted PBMC were cultured with 20IU/ml recombinant IL-2 for five days and stimulated to test the bystander T cell responses by intracellular cytokine staining following CEF peptide stimulation (an HLA-A and HLA-B-restricted peptide pool spanning the immune-dominant proteins of CMV, EBV and influenza). A) Representative FACS plots showing the IFNγ T cell response from a patient with CHB in total PBMC with or without CEF stimulation, after gMDSC depletion (ΔgMDSC) and after gMDSC enrichment (+gMDSC) from day zero. B) Cumulative data for CD8+ and CD4+ responses (after subtraction of background response in unstimulated wells) in PBMC $\pm$ gMDSC (n=11). Error bars represent the mean $\pm$ SEM. Significance testing was carried out using the paired Students t-test, and where significant indicated as: ** $p<0.01$; * $p<0.05$. C) Representative example: CD8+ T cell IFNγ response to CEF stimulation after co-culture with reducing gMDSC:PBMC ratios in a patient with CHB.

These results were in keeping with their postulated role in suppressing T cell responses capable of mediating non-antigen specific liver damage. The Maini lab [58], and others [261, 65], have previously shown that down-regulation of ζ-chain component of the CD3 signalling complex and a block in proliferation are hallmarks of nutrient deprivation, specifically the deprivation of L-arginine. In line with this, T cells cultured with gMDSC showed a down-regulation in expression of CD3ζ (figure 4.14a) and impaired proliferative capacity, assessed by both CFSE dilution and Ki67 expression (figure 4.14b).

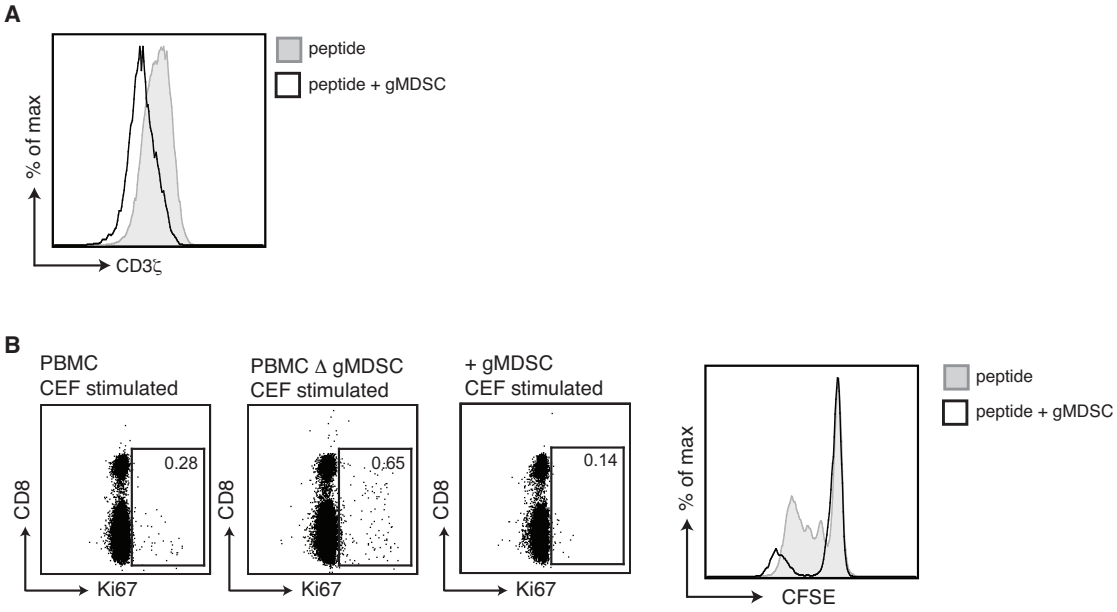

Figure 4.14: gMDSC limit the capacity for T cell proliferation and can down-regulate CD3ζ expression.

gMDSC were enriched using sequential magnetic bead isolation (CD14-CD15+) from PBMC obtained from a patient with CHB for co-culture with autologous PBMC. Enriched or undepleted PBMC were cultured with recombinant IL-2 for five days and stimulated to assess T cell phenotype and functionality in response to either an HLA-A and HLA-B-restricted peptide pool spanning the immune-dominant proteins of CMV, EBV and influenza (CEF) or to an HLA-A2-restricted CMVpp65 peptide (NLV). A) CD3ζ expression in CD3ϵ+ T cells after addition of gMDSC and B) intracellular Ki67 staining of CD3+ T cells upon depletion (ΔgMDSC) or enrichment of gMDSC (+gMDSC), CFSE dilution at day five.

Since we did not have access to a biosafety level three sorter during this study, corroboration of the findings that gMDSC enriched cultures can suppress both antiviral and bystander T cell responses obtained with magnetic bead-enriched MDSC was sought using FACS-sorting of blood from a control without HBV infection. This allowed the isolation and experimentation of a highly purified population of gMDSC (figure 4.15a). These cells similarly suppressed T cell production of IFNγ and TNFα (figure 4.15b) and down-regulated CD3ζ expression (figure 4.15c). All these data combined indicate that gMDSC could impede the functionality and expansion of T cells capable of driving liver pathology by depleting their L-arginine supply.

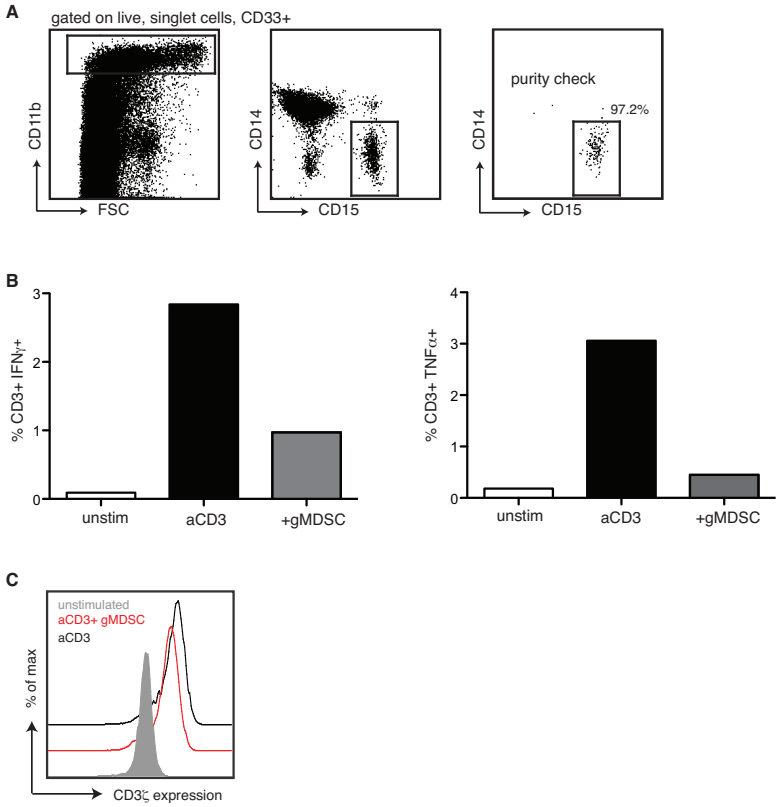

Figure 4.15: T cell effector function is suppressed by the addition of a highly purified gMDSC population.

T cell functionality was assessed in response to stimulation with plate-bound anti-CD3 and soluble anti-CD28 with or without the addition of FACS-purified gMDSC at an effector:target ratio of 1:2 on day five of co-culture. A) Gating strategy used on the BD FACSAria to isolate a 97% pure population of gMDSC. The cells were stained and isolated using the following phenotypic marker criteria: CD33+CD11b+CD14-CD15+ from freshly isolated PBMC for a control study participant. B) T cell production of IFNγ and TNFα and C) CD3ζ expression on the CD3ϵ+ T cell population.

4.3.8 The effect of gMDSC-mediated suppression *in vivo* during acute, resolving infection and spontaneous flares of HBeAg- CHB

Having observed gMDSC-mediated suppression of T cell proliferation, cytokine production and a down-regulation of CD3ζ *in vitro*, evidence was sought to confirm these effects *in vivo*. This was done using the cryopreserved longitudinal sample sets from the three patients with acute HBV and the two spontaneously flaring HBeAg- patients with CHB that were analysed previously to establish the temporal evolution of gMDSC frequencies (figures 3.11 and 3.13). Longitudinal analysis of a patient sampled through the course of acute HBV infection showed a temporal correlation between serum L-arginine and the hallmark feature of nutrient deprivation, T cell CD3ζ down-regulation (figure 4.16).

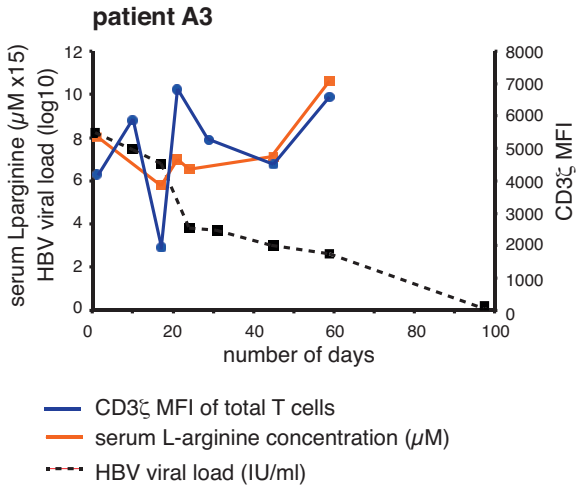

Figure 4.16: Effect of L-arginine deprivation on T cell CD3ζ expression *in vivo* during acute, resolving HBV infection.

Serum concentration of L-arginine (μM), measured using tandem HPLC-MS and T cell expression of CD3ζ on CD3ϵ-expressing cells was plotted over the course of infection in a patient with acute, resolving HBV infection (days numbered from the date of presentation in clinic). The dotted line shows the viral load in the individual throughout the phase of disease captured.

T cell CD3ζ expression showed some temporal correlation with L-arginine concentrations in figure 4.16,. Further analysis was carried out for all the longitudinal patients (3 patients with acute HBV and 2 with CHB) using T cell expression of CD3ζ as a surrogate marker for L-arginine availability *in vivo* where serum L-arginine measurements were not available. In all cases an inverse relationship was observed between the frequency of arginase I-expressing gMDSC and T cell expression of CD3ζ over the course of disease, suggesting potential metabolic nutrient deprivation driven by gMDSC *in vivo* (figure 4.17).

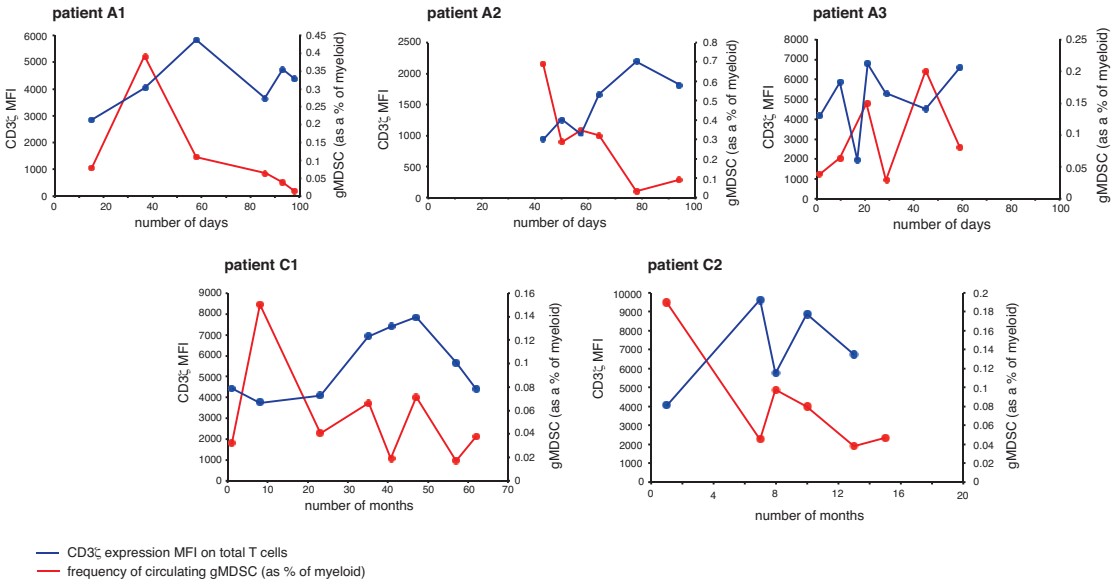

Figure 4.17: Relationship between CD3ζ expression and circulating frequencies of gMDSC through the course of acute, resolving HBV infection and spontaneous flares of HBeAg- CHB disease.

Identification of gMDSC ($CD11b^{high}$CD33+HLA-DR-CD14-CD15+) using 11-colour flow cytometry was done on frozen PBMC samples. gMDSC frequencies were plotted for three patients with acute, resolving HBV infection over time in days from presentation in clinic as already depicted in figure 3.11 (red line), alongside expression of CD3ζ (presented as MFI) on all T cells (blue line) in the upper panel. The lower panel depicts the same analyses for two patients through spontaneous flares of HBeAg- chronically evolving HBV infection (CHB) over time in months.

4.3.9 gMDSC potently suppress T cell function in an arginase I-dependent manner

To further confirm gMDSC-driven suppression of T cells observed *in vitro* and *ex vivo* (figures 4.12 and 4.13) was mediated by their capacity to deplete L-arginine, their suppressive activity in the presence or absence of the specific arginase I inhibitor, N-hydroxy-nor-L-arginine (norNOHA), was assessed. This was done by returning to the *in vitro* suppression assay described in section 4.3.7. In this case, upon addition of the enriched population of gMDSC, norNOHA was also added at the time of CEF-peptide stimulation and left in culture for the duration of the assay. Addition of norNOHA to the culture abrogated the suppressive activity previously seen, enabling the restoration of T cell IFNγ responses (figure 4.18a). gMDSC could likewise suppress CD8+ T cell TNFα and granzyme B activity, two mediators critical in driving cell-mediated pathology in the liver, in an arginase I-dependent manner (figure 4.18b,c).

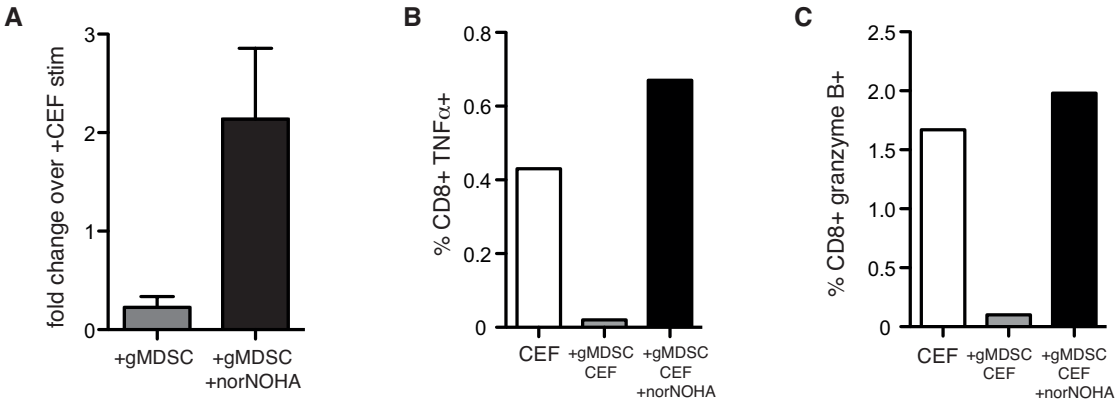

Figure 4.18: gMDSC suppress T cells in an arginase I-dependent manner.

gMDSC were enriched using sequential magnetic bead isolation (CD14-CD15+, Miltenyi) from PBMC obtained from patients with CHB, for co-culture with autologous PBMC. gMDSC-enriched, or undepleted PBMC were cultured with 20IU/ml recombinant IL-2 for five days and stimulated to test bystander T cell responses by intracellular cytokine staining following CEF peptide stimulation (an HLA-A and HLA-B-restricted peptide pool spanning the immune-dominant proteins of CMV, EBV and influenza). A) Cumulative data showing fold change in CD8+ IFNγ response to CEF in gMDSC enriched cultures in the presence or absence of an arginase I specific inhibitor norNOHA (n=3). Representative examples showing B) CD8+ TNFα and C) CD8+ cytotoxicity (granzyme B accumulation) in the presence or absence of gMDSC and norNOHA.

4.3.10 Regulation of amino acid transporters on T cells affects their metabolic reprogramming in CHB

The system L amino acid transporters have recently been shown to play a critical role in the metabolic reprogramming required for a proliferative response to TCR-mediated signalling [149, 262]. The family of System L amino acid transporters (Slc7a5, Slc7a6, Slc7a7, Slc7a8) that form heterodimers with the CD98 heavy chain [149, 151] in peripheral T cells has been shown to be required for arginine uptake; deletion of Slc7a5 in immunologically activated T cells prevented their arginine uptake [149]. T cells from patients with CHB were therefore stained for CD98.

As expected, *ex vivo* levels of CD98 on global T cells were low but the percent of positive cells, and their levels of expression were increased in some patients with CHB compared to controls (figure 4.19a). Although CD98 has been reported to reflect T cell activation [151], the variability of its expression on T cells within the CHB cohort did not correlate with their expression of the activation marker HLA-DR (figure 4.19b). Instead, there was a strong positive correlation between levels of expression of CD98 and expression of CD3ζ in CD3ϵ+ T cells in CHB (figure 4.19b). Suggesting that those T cells with low level CD98 expression had been unable to

compensate for arginine deprivation by enhancing their amino acid uptake. This is in line with the finding that genetic deletion of Slc7a5 prevents increases in L-arginine uptake in antigen-stimulated murine T cells [149].

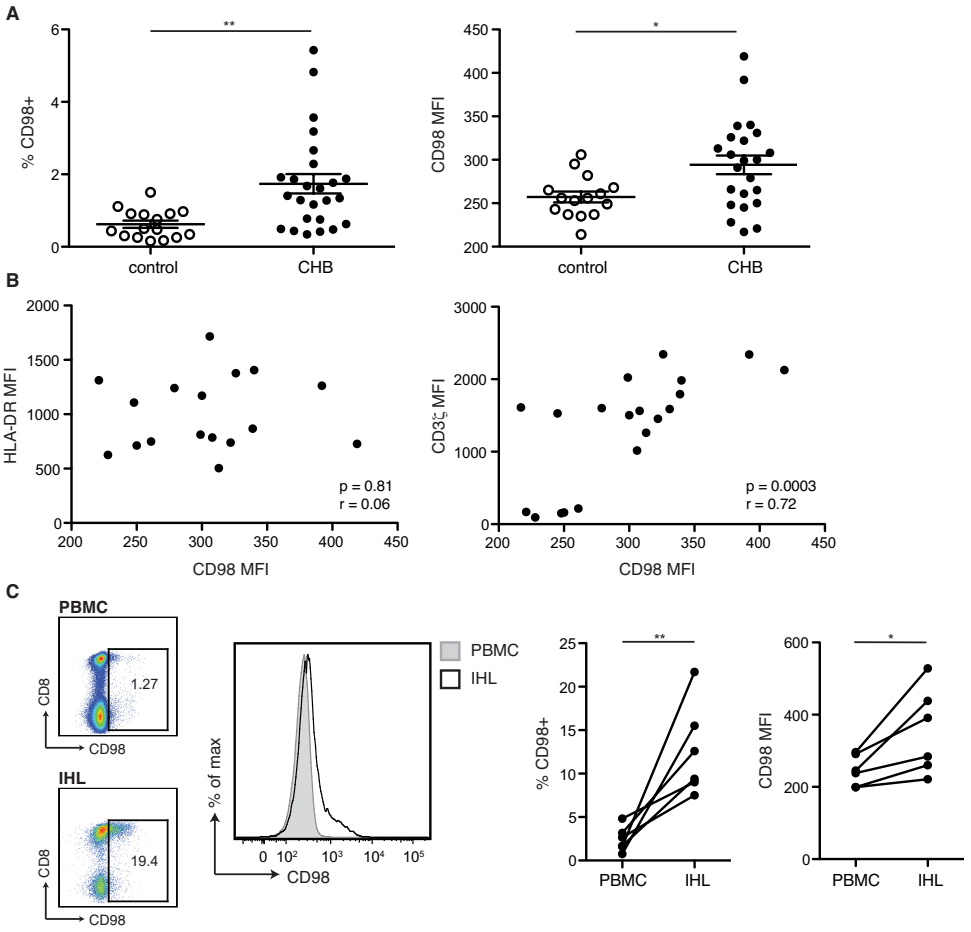

Figure 4.19: Differential CD98 expression on T cells in CHB.

A) Cumulative data showing expression levels (% and MFI) of CD98 on CD3+ T cells from 16 controls and 26 patients with CHB. B) Cumulative data for CD98 MFI in relation to surface HLA-DR and CD3ζ expression on T cells (identified by CD3ϵ expression) from the CHB cohort. C) Representative histogram of CD98 expression levels on peripheral (PBMC) and intrahepatic (IHL) CD3+ from a patient with CHB, and the cumulative data for six patients with paired PBMC and IHL samples. Error bars represent the mean ± SEM. Significance testing was carried out using either the: Pearson product-moment correlation coefficient or the paired or unpaired Students t-test, and where significant indicated as: *** $p<0.001$; ** $p<0.01$; * $p<0.05$.

It has previously been shown that levels of Slc7a5 on rat hepatocytes can increase in response to arginine starvation [263]. It was therefore hypothesized that T cells infiltrating the extensive liver vasculature that may be subjected to prolonged periods of L-arginine deprivation could have a ″compensatory‟ increase in CD98 expression. To investigate this, paired blood samples and surplus liver biopsy tissue from six patients with CHB were used for the comparison of

circulating and intrahepatic T cells. The number of T cells expressing CD98 directly *ex vivo*, and the level of their expression, was increased in the intrahepatic (IHL) compared to circulating (PBMC) compartment in all the patients with CHB examined (figure 4.19c).

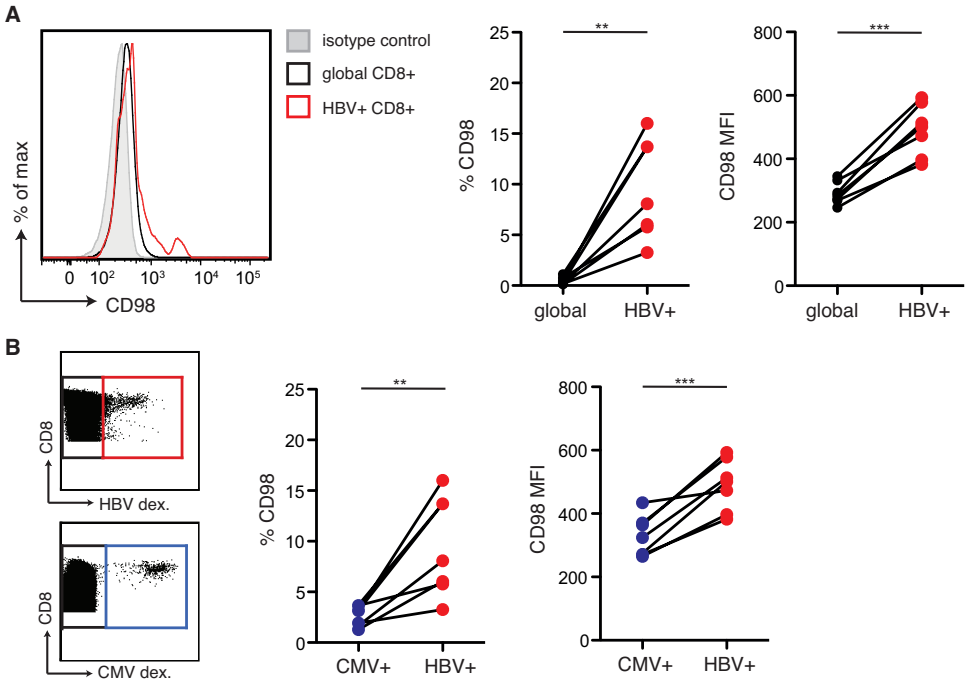

Figure 4.20: Differential CD98 expression on virus-specific T cells in CHB.

A) Representative histogram plot of CD98 expression levels on global (non-HBV specific) CD8+ T cells and HBV-specific (dextramer+) T cells and the cumulative data from six patients with CHB. B) Representative example of identification of paired HBV and CMV-specific CD8+ T cells using the relevant HLA-A2 dextramers and comparison of their CD98 expression in six patients with CHB. Error bars represent the mean ± SEM. Significance testing was carried out using either: the Pearson product-moment correlation coefficient or the paired or unpaired Students t-test, and where significant indicated as: *** $p<0.001$; ** $p<0.01$; * $p<0.05$.

Further investigation determined the expression of CD98 on HBV-specific CD8+ T cells, which are known to have encountered their antigen in the tolergenic liver milieu, identified directly *ex vivo* by HLA/peptide dextramer staining (directed against a panel of HLA-A2-restricted HBV epitopes). HBV-specific CD8+ T cells had significantly higher expression of CD98 compared to global CD8+ T cells in all six patients examined (figure 4.20a). For comparison, CD8+ T cells directed against an HLA-A2 restricted immunodominant epitope from CMV in these same six patients with CHB were examined; HBV-specific CD8+ T cells had consistently higher CD98 than their CMV-specific counterparts (figure 4.20b).

4.4 Conclusions & Discussion

The *ex vivo* data presented in this chapter, including strong intracellular antibody staining, the ELISA data and the *in vitro* suppression assays, all implicate arginase I as a major effector mechanism of the expanded gMDSC population in CHB. In patients with CHB (and controls), a large proportion of gMDSC are capable of expressing this enzyme that has immuno-regulatory potential, whilst the level of arginase I expressed per gMDSC is increased in the liver compared to the circulating fraction. However, it is possible that this expanded population of gMDSC could utilise supplementary suppressive mechanisms, as summarised by Gabrilovich *et al.* [133]. It is possible that other mechanisms of suppression relating to amino acid metabolism, could function in synergy with arginase I. For example, via the production of peryoxnitrites as a result of co-expression of arginase I with another L-arginine metabolising enzyme iNOS. In addition to suppressing T cells that could mediate cytolytic destruction of hepatocytes and produce pro-inflammatory cytokines, it remains to be determined whether MDSC are able to exert other anti-inflammatory effects in the HBV-infected liver, potentially through inhibition of other infiltrating leukocytes [133, 164, 171]. This is particularly relevant as L-arginine-depleting MDSC have the potential to down-regulate pro-inflammatory immune responses mediated by local NK cells or macrophage populations such as KC. Previous work in murine models has revealed that the production of pro-inflammatory cytokines by macrophages can be inhibited by MSDC [182] and more specifically by L-arginine deprivation [264]. This may be especially critical to the dampening down of liver damage during the immunotolerant phase of disease, when viral replication is extremely high in the absence of overt liver disease.

Human MDSC have been shown to be able to release arginase I upon degranulation [132]. This is consistent with the observation of an increase in the degranulation marker CD63, eluding to the storage of arginase I in cytoplasmic granules, and the close correlation between frequencies of gMDSC and serum arginase I concentrations. gMDSC potently suppressed T cell effector function and proliferation, in an arginase I-dependent manner, limiting the proliferative expansion of bystander T cell responses that have previously been implicated in causing the liver damage triggered by ongoing HBV infection [47]. Further work is needed to confirm the direct link between enhanced arginase I production by the expanded gMDSC population and increased L-arginine metabolism observed in CHB? It still remains to be established whether the CD63-expressing granules actively release arginase I into the serum, or whether L-arginine can be taken up by the gMDSC for internal degradation, as described for murine MDSC. Human gMDSC do not express CAT-2B used by murine MDSC to take up L-arginine [254]; whether another mecha-

nism is utilised for L-arginine uptake in humans is unclear. It is also plausible that the relatively short-lived nature of gMDSC (and neutrophil subsets) is critical for their arginase I-dependent immunomodulation; necrotic cell death of gMDSC may be essential for arginase I release [253].

Activation and/or the activity of arginase I may also be dependent on the surrounding conditions; for example, environments low in NO (differential activity of iNOS) can actually promote enhanced arginase I activity, through nitroslytation of internal cysteine residues in the enzyme [265]. Arginase I activity in CHB may also be directly related to the hypoxic liver micronenvironment [266], since MDSC under conditions of hypoxia (via the mediator HIF-1α), up-regulate arginase I [216], with a simultaneous down-regulation in other MDSC functionality (specifically ROS production). The authors of this particular study attribute the ability of MDSC to suppress non-antigen specific responses to this up-regulation of arginase I activity. It is thought MDSC in peripheral lymphoid organs primarily mediate antigen-specific T cell inhibition via the production of ROS (and subsequent peroxynitrite production) and exert their effect only via close cell to cell contact, with little effect driven by arginase I [237, 267]. With this in mind the hypoxic environment of the liver, may directly influence the increase in arginase I expression seen in intraheptic gMDSC via HIF-1α, enabling them to limit the non-antigen-specific bystander T cells, with a less profound inhibitory effect on liver-resident or infiltrating HBV-specific T cells.

Hepatocytes are another notable source of the enzyme arginase I; it was first recognised almost thirty years ago that the previously isolated hepatic soluble lymphocyte inhibitory factor [268] was arginase I, released by damaged hepatocytes [269]. Subsequently, our group, and others, showed that arginase I could be transiently induced in acute [270] and spontaneous flares of HBeAg- chronic [58] HBV infection and postulated that it might derive from damaged hepatocytes. Although hepatocytes constitutively express arginase I, they cannot degranulate, so can only release it when apoptotic or necrotic [271, 272, 273]. In this thesis, evidence presented demonstrates enhanced arginase I release in the immunotolerant and inactive phases of CHB, where there is minimal hepatocyte damage. This implies that the increases in serum arginase I seen in these phases are likely to predominantly derive from increases in arginase I+ gMDSC. It is likely that the depletion of L-arginine noted in the circulation is further accentuated in the liver milieu, since in the liver gMDSC express more arginase I and are likely to be brought into prolonged, close contact with infiltrating T cells in the narrow-lumen sinusoidal vasculature. Activation of locally infiltrating MDSC to express more arginase I, allowing enhanced suppression of neighbouring bystander T cell responses, has similarly been reported in a murine tumour

model [216].

As mentioned in the introduction in section 1.6, the emerging field of immunometabolism is a novel and exciting area of research. More specifically, the metabolic regulation of T cells is key to their function and differentiation, yet has been relatively understudied. The robust correlations observed between circulating gMDSC frequencies, arginase I, and the degree of liver pathology, point towards the relevance of metabolic immunoregulation *in vivo* in CHB. This is further reinforced by novel data presented in this chapter showing differential expression of amino acid transporters on global T cells, and more importantly on intrahepatic and HBV-specific T cells. Depriving T cells of adequate supplies of L-arginine *in vitro* has been shown to inhibit their proliferative potential by causing T cell arrest in the G0/G1 phase of the cell cycle [64]. It was previously reported by our group that this was reflected in the hallmark down-regulation of CD3ζ on the global T cells in our patients, and was associated with defects in the expansion of functional responses in CHB [58]. The evidence in this chapter suggests that virus-specific T cells can differentially regulate their expression of key amino acid transporters *in vivo*, providing an additional rheostat to modulate the intracellular availability of amino acids to T cells in persistent viral infections. This is supported by recent work demonstrating that a light chain of the system L transporter, Slc7a5, functions as a critical checkpoint in controlling the metabolic response of T cells to antigen [149]. It is possible that a compensatory up-regulation of amino acid transporters in response to extracellular availability of amino acids [263] facilitates the reprogramming of metabolically stressed cells more generally, for example by enhancing T cell access to the amino acid leucine that, that like arginine, regulates effector function through the mTOR pathway [149, 234].

It is worth bearing in mind that it is likely that CD98 is not the transporter required for the direct uptake of extracellular L-arginine. It is thought that an up-regulation of CD98 indirectly increases intracellular levels by allowing for the direct uptake of other neutral amino acids, for example, leucine, that is required for the synthesis of other cellular transporters critical for L-arginine uptake (personal communication - Doreen Cantrell). However the up-regulation of surface CD98 seen particularly on intrahepatic T cells in CHB does imply an indirect increase in arginine uptake, along with a bystander effect of increasing uptake of other key amino acids, indicative of the requirement for T cell metabolic reprogramming in CHB. To take this novel finding further it would be essential to assess other components sensitive to altered amino acid transport and metabolism in the T cells from our patients with CHB. One important down-

stream mediator to consider would be c-Myc, which is particularly sensitive to changes in the metabolism of glutamine and glucose. It is also well-characterised that amino acid deprivation of T cells results in the rapid inactivation of the mTOR complex, mTORC1. This can be experimentally assessed as the loss of p70 S6 of the mTORC1 complex. Particular attention should be given to the mTOR pathway to further the work presented in this thesis. The postulate that T cells in CHB undergo metabolic reprogramming, may well be supported by considering the intracellular levels of p70 S6, since amino acid deprivation inactivates the mTORC1 complex by decreasing the levels of p70 S6, across all patients, but specific analysis into the different phases of disease. Preliminary unpublished data from our group suggests that HBV-specific T cells express higher levels of p70 S6 when compared to global T cells, or their CMV-specific counterparts (Schurich et al - unpublished).

Leucine uptake via the System L transporters (components of CD98) was demonstrated to be critical for sustaining mTORC1 activity in activated T cells, suggesting the ability of mTORC1 to sense leucine uptake allows this kinase pathway to modulate cellular responses to nutrient availability. Therefore up-regulation of CD98, and a subsequent up-regulation in leucine uptake, may be critical to T cells function in CHB when attempting to overcome gMDSC-mediated L-arginine depletion. Assessment of the levels of leucine in the context of CHB (or more locally in the liver during infection) would be an interesting future development.

Chapter 5

Discussion and Outlook

This study has shown that a subset of cells with the characteristics of immature neutrophils (gMDSC) expands in the circulation and liver, particularly in those patients in whom virus replicates at high levels without triggering liver disease. The focus of this thesis was on one of the mechanisms gMDSC can harness to mediate immunomodulation in the context of chronic hepatotropic infections. In this final chapter preliminary data is presented and discussed that attempts to address a number of further questions raised by this study, including consideration of other potential MDSC-mediated mechanisms of immune modulation.

5.1 Further unanswered questions relating to MDSC

The evidence presented in this thesis, showing an expansion in circulating and intrahepatic gMDSC, an increase in serum arginase I, a depletion of L-arginine, functional suppression by these cells and increased amino acid transporter expression on T cells, all favour the postulate that gMDSC drive a state of altered immunometabolism in CHB. It is plausible that this then promotes fine tuning and essentially the ″toning down‟ of the global T cell response in chronic hepatotropic infections. Therefore it is reasonable to extrapolate that this effect on bystander T cells, particularly as these effects are seen in the circulation and not just at the site of infection, is able to confer a state of generalised immune suppression in our patients. This however is not observed clinically; patients with either chronic HBV or HCV infection do not show overt signs of generalised immune suppression. This is in contrast to patients with persistent HIV infection where patients do show clinical signs of viral-mediated immune suppression. The answer to this conundrum is beyond the scope of the work. For example, it is possible that the levels of arginase I (or L-arginine depletion) in the circulation is not able to mediate significant immunosuppres-

sion. It is likely that this effect may require close contact between gMDSC and T cells in the liver microenvironment, where these effects may be more pronounced and able to essentially limit T cells primed and functioning within the liver sinusoids. Whether the same level of L-arginine depletion (or enhanced arginase I expression/activity) also occurs in the lymph nodes, the sites of antigen priming to new infections [274] is unknown.

To consider this question further, focused epidemiological studies analysing large cohorts of patients in relation to specific defects in immune responses and whether subtle, underlying, generalised immune suppression does exist would need to be done. At the time of finishing this thesis it was unknown whether patients with CHB have higher titres of other commonly acquired viral infections, such as CMV or EBV, compared to their non-HBV infected counterparts of similar ages/genders. Patients with CHB may have subtle defects in immune responses raised against other non-cytopathic infections that rely on CD8+ T cell function. Nor is it known whether the global T cell defects reported in CHB promote the reactivation of previously controlled viral infections. It may be possible that in CHB, compensatory mechanisms are employed to maintain adequate immunity to other infections; these could include (but are not limited to) the observation that a state of enhanced global T cell activation occurs in CHB (Schurich et al - unpublished), or as a result of metabolic reprogramming eluded to in this study resulting in enhanced both glucose and amino acid transport (Schurich et al - unpublished).

The field of study relating to MDSC is still in its infancy. It is likely, as with the field of T cell biology, that over time the complexity of MDSC, and their potential subsets with different phenotypes and functions will be more comprehensively defined. The concept of further MDSC subsets being identified has already been initiated by a recent study that evaluated all reported myeloid subsets in humans during a clinical trial. This proposed six human MDSC phenotypes, using one single multiparametric staining panel: MDSC1 (CD14+IL-4Rα+), MDSC2 (CD15+IL-4Rα+), MDSC3 (lineage-HLA-DR-CD33+), MDSC4 (CD14+HLA-DR^{low}), MDSC5 (CD11b+CD14-CD15+), and MDSC6 (CD15+FSC^{low}SSC^{high}) [275]. It is possible therefore that in this study, MDSC have been studied in a crude way and further subset characterisation of the expanded gMDSC populations may provide better understanding of their role in the pathogenesis of CHB. The study of MDSC would be greatly enhanced if better ″tools‟ were available, for example, if reliable *in vitro* techniques existed for their expansion or a standardised isolation protocol. Current methodology makes use of exogenous cytokines (such as GM-CSF and IL-6) or the use of tumour cell-lines to derive MDSC-like cells [220, 212], although it is quite

likely that such cells would change their phenotype over time *in vitro*.

The study of MDSC would also be greatly enhanced by the identification of a unique set of markers, or approaches to enable gMDSC separation from the overlapping fraction of low-density neutrophils which may also have the ability for immunosuppression. Emerging techniques may rely on the identification of candidate peptide molecules that exclusively bind MDSC; the novel peptide-Fc fusion proteins (peptibodies) described by Qin *et al.* [276] may pave the way for future MDSC identification. The use of these newly described peptibodies as treatment, identified MDSC specifically, as their use as a depletion strategy did not affect other immature myeloid cells [276].

5.2 Can gMDSC induce regulatory T cells in CHB?

The established link between gMDSC and the induction of Treg has primarily come from evidence provided by the study of the tumour microenvironment. In addition to infiltrating myeloid cells, tumours attract large numbers of immunosuppressive Treg. This infiltrating population often includes both thymus-derived natural Treg (nTreg) and locally induced Treg (iTreg), both of which utilise contact-dependent and contact-independent mechanisms of immune suppression. The different mechanisms will not be discussed, but include the production of the immunosuppressive cytokines IL-10 and TGFβ and altered adenosine triphosphate (ATP) metabolism via expression of the ectonucleotidase CD39, capable of producing the immunosuppressive and antiproliferative nucleoside, adenosine [277].

CD4+ T cells can be converted to iTreg as a consequence of exposure to antigen in the presence of an immunosuppressive milieu, for example environments rich in TGFβ and/or IL-10. The particular role MDSC play in the induction of either Treg subset remains an area of increasing interest. By virtue of their suppressive capacity, and the fact MDSC expand at sites of chronic inflammation [187, 188, 189], their role in relation to Treg expansion was considered in patients with CHB.

MDSC have previously been shown to promote the induction of Treg *in vivo*. One of the initial studies to show this by Huang *et al.* [278] demonstrated that murine mMDSC (Gr-1+CD115+F4/80+) were capable of inducing a population of Treg, expressing FOXP3 and CD25, *in vitro*. Additionally, adoptive transfer of mMDSC induced IL-10 and IFNγ-dependent

FOXP3+CD25+ Treg *in vivo* that were capable of suppressing anti-tumour responses. Another study by the same group went on to demonstrate that expression of CD40 on the surface of MDSC was necessary for the induction of Treg [279]. Further support for the requirement of MDSC-mediated cell contact in Treg induction was provided by studies in ovarian tumour models where the authors reported the induction of Treg required an up-regulation of CD80 [280]. There is also recent evidence that supports an interaction of MDSC and Treg in humans. Hoechst *et al.* [194] reported a role for CD14+HLA-DR− MDSC from patients with HCC in the induction of functional CD4+CD25+FOXP3+ Treg when co-cultured with autologous T cells. Again the authors attributed this to a cell contact-dependent mechanism; the effect was completely abrogated when MDSC and T cells were separated experimentally [194]. It seems plausible that MDSC may be involved in Treg differentiation in the context of CHB, although conflicting reports on the impact of Treg in CHB pathogenesis exist: circulating Treg numbers have previously been reported to be increased in CHB in some studies [281, 282, 283, 284], but not in others [285, 286].

The hypothesis that the expanded population of gMDSC are capable of inducing Treg, and as such altering the balance between regulatory and inflammatory CD4+ T cell subsets was briefly addressed. This involved analysis to assess whether there was any correlation between the frequencies of CD4+ Treg and gMDSC frequencies *ex vivo*. These data utilised frozen PBMC samples from the cohort of well characterised East London patients with CHB from the same time point as those used to assess circulating gMDSC frequencies previously (figure 3.5a). The following data were obtained and analysed by a BSc student, Jia Ying Toh, under my supervision. Analysis of 27 patients with CHB failed to show a correlation between circulating frequencies of gMDSC and Treg (identified as: CD4+CD127+FOXP3+, figure 5.1a). Neither was a correlation observed with the potently suppressive subset of Treg, those expressing the cell surface ectonucleotidase CD39+ (therefore identified as: CD4+CD127+FOXP3+CD39+, figure 5.1b) [287].

The lack of a direct *ex vivo* relationship between gMDSC and Treg frequencies prompted the hypothesis that gMDSC may instead promote a T cell cytokine profile considered more ″regulatory‟ than ″inflammatory‟. Using cryopreserved PBMC samples from patients in whom the gMDSC frequencies were already known, stimulation for a short time period with PMA/ionomycin was carried out to monitor the cytokine production of both CD4+ and CD8+ T cells from uninfected controls and patients with CHB. The cytokines included were IL-10, IL-2, IFNγ, and TNFα (figure 5.2a), but of specific interest were the percentage of T cells producing either the

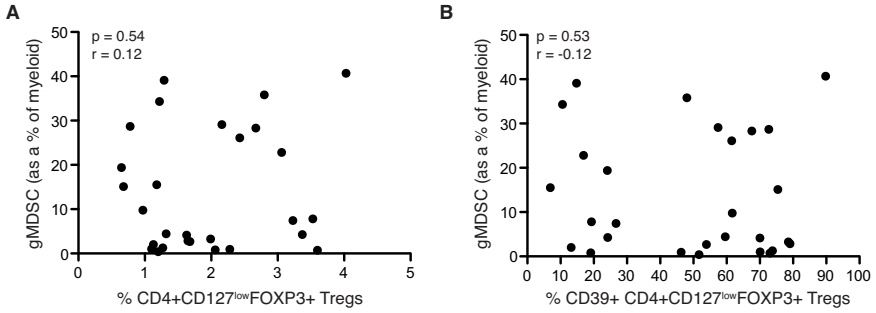

Figure 5.1: gMDSC do not induce regulatory CD4+ T cell subsets in CHB.

Cyropreserved PBMC samples were stained for regulatory CD4+ T cell subsets *ex vivo* and anlysed by flow cytometry. Correlative analysis of frequencies of gMDSC in patients with CHB with: A) the percentage of CD4+CD127+FOXP3+ cells and B) the percentage of CD4+CD127+FOXP3+CD39+. Significance testing was carried out using the Pearson product-moment correlation coefficient and was deemed non-significant. Staining and data analysis performed in the generation of this figure is attributed to Jia Ying Toh.

pro-inflammatory cytokine, IFNγ or the regulatory cytokine, IL-10. No significant differences were observed in the capacity of either T cell subset to produce IFNγ from controls or patients with CHB (figure 5.2b). CD4+ T cells from patients with CHB produced more IL-10 than their control counterparts (figure 5.2c), this increased production of IL-10 failed to correlate with gMDSC frequencies (figure 5.2d).

Taken together, these data imply no direct induction/alteration in the frequencies or functionality of regulatory CD4+ T cell subsets by gMDSC in CHB. What was more striking was the notable trend towards increased production of IL-10 from the CD8+ T cell compartment in the context of CHB (figure 5.2e) and the robust correlation of circulating frequencies of gMDSC with IL-10 production by CD8+ T cells (figure 5.2f). Although gMDSC appear to be unable to promote regulatory CD4+ T cell function in CHB, it remains possible that gMDSC mediated the suppressive (or immune regulatory) capacity of CD8+ T cells. This could be further explored by testing the capacity of gMDSC to induce CD8+ T cells capable of producing IL-10 in co-culture experiments.

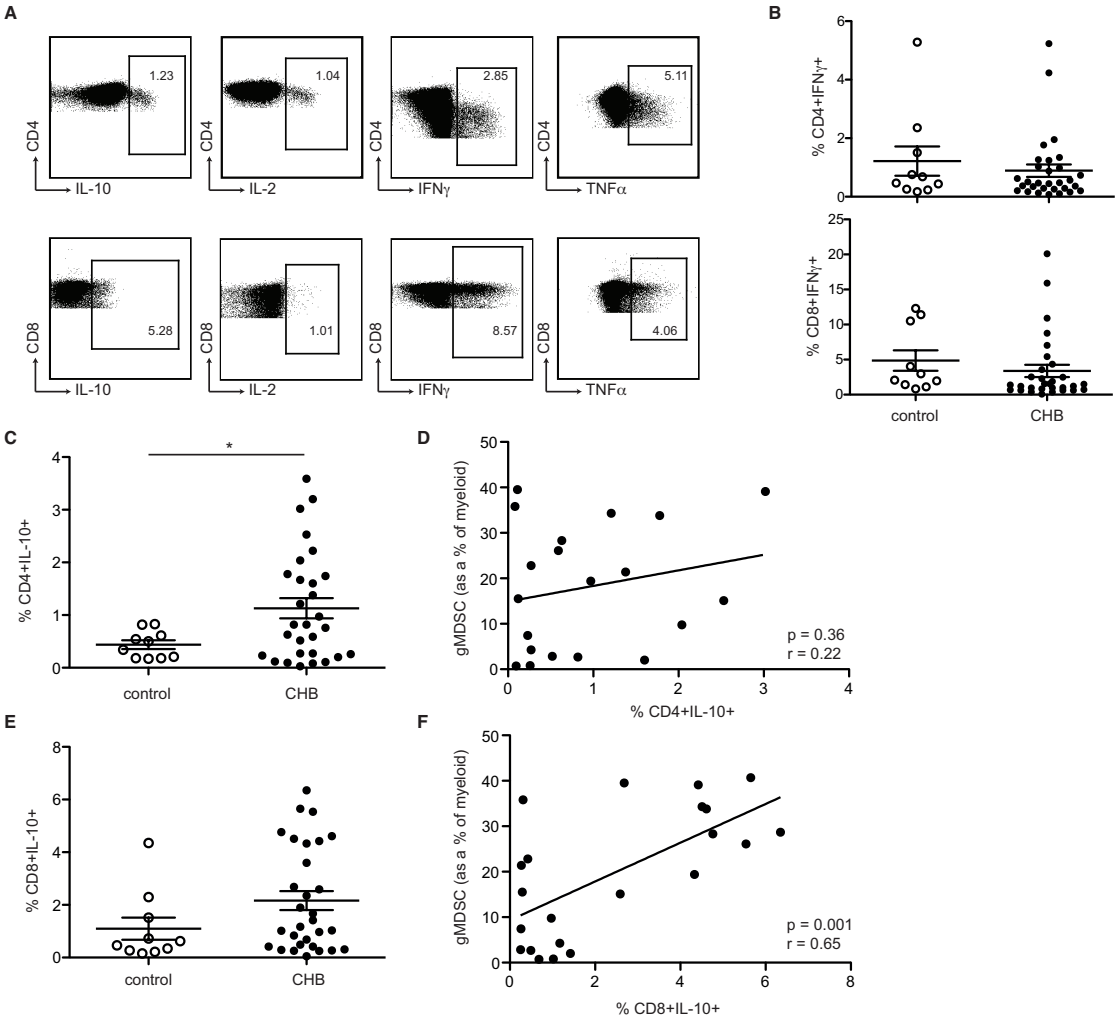

Figure 5.2: gMDSC frequencies correlate with the production of IL-10 from CD8+ T cells but not CD4+ T cells.

Cyropreserved PBMC samples from patients with CHB (East London cohort) were stimulated with PMA/ionomycin in the presence of BFA. CD4+ and CD8+ T cell function was assessed by intracellular cytokine staining. CD3+ cells were identified after exclusion of dead and doublet cells, then analysed for expression of CD8/CD4. A) Representative examples of CD4+ (upper panel) and CD8+ (lower panel) production of IL-10, IL-2, IFNγ, and TNFα respectively. B) IFNγ production from 10 controls and 27 patients with CHB by CD4+ and CD8+ T cells. C) IL-10 production from CD4+ T cells. D) Correlative analysis of gMDSC frequencies with IL-10-producing CD4+ T cells. E) IL-10 production from CD8+ T cells. D) Correlative analysis of gMDSC frequencies with IL-10-producing CD8+ T cells. Error bars represent the mean ± SEM. Significance testing was carried out using either: the Pearson product-moment correlation coefficient or the unpaired Students t-test, and where significant indicated as: *** $p<0.001$; * $p<0.05$. The staining of cells used in the generation of this figure is attributed to Jia Ying Toh, although the gating and analysis was done by myself.

5.3 Can MDSC produce immunosuppressive cytokines?

During extensive phenotypic analysis of the expanded gMDSC population, another known function of MDSC was considered: their production of immunosuppressive cytokines. The postulate that MDSC are a potent source of the well described immune regulator TGFβ [278] was briefly addressed. TGFβ production by gMDSC is thought to drive the induction of regulatory T cell subsets [288], and has more specifically been reported to play a role in chronic viral infection [198]. TGFβ is also a key modulator in the process of liver fibrogensis. As a pro-fibrogenic molecule, TGFβ is directly involved in the activation of HSC [108, 109]. Given the expansion/accumulation of gMDSC in the liver, MDSC production of TGFβ could be particularly relevant in HBV, where fibrosis/cirrhosis related to the virus kills approximately 300,000 people a year [9].

Circulating and intrahepatic gMDSC were assessed for their capacity to produce TGFβ. This was done using a directly conjugated monoclonal antibody without *in vitro* stimulation or Golgi blockade (figure 5.3a). gMDSC have the capacity to produce relatively large amounts of TGFβ *ex vivo*. However, no significant difference was seen in either the percentage of circulating gMDSC expressing TGFβ or their expression level on a per cell basis (using MFI values) in a cohort of 24 uninfected controls and 50 patients with CHB (figure 5.3b). Stratification of the patients by the extent of liver inflammation, as measured by serum ALT or the presence of HBeAg failed to show a difference in gMDSC production of TGFβ. Further stratification by viral load revealed a significant increase in gMDSC TGFβ production. gMDSC from patients with less ongoing viral replication produce more TGFβ (figure 5.3c). Clearly apparent was the marked increase in the proportion of TGFβ+gMDSC circulating in patients with CHB compared to controls when analysis took into account the increased frequency of gMDSC (figure 5.3d), and interestingly the proportion of gMDSC able to produce TGFβ was significantly enhanced in the liver compared to the periphery (figure 5.3e). The functional effect of gMDSC producing TGFβ was not considered experimentally. An important future experiment would be to co-culture gMDSC and T cells in suppression assays (similar to those described in section 4.3.7) in the presence of TGFβ blockade.

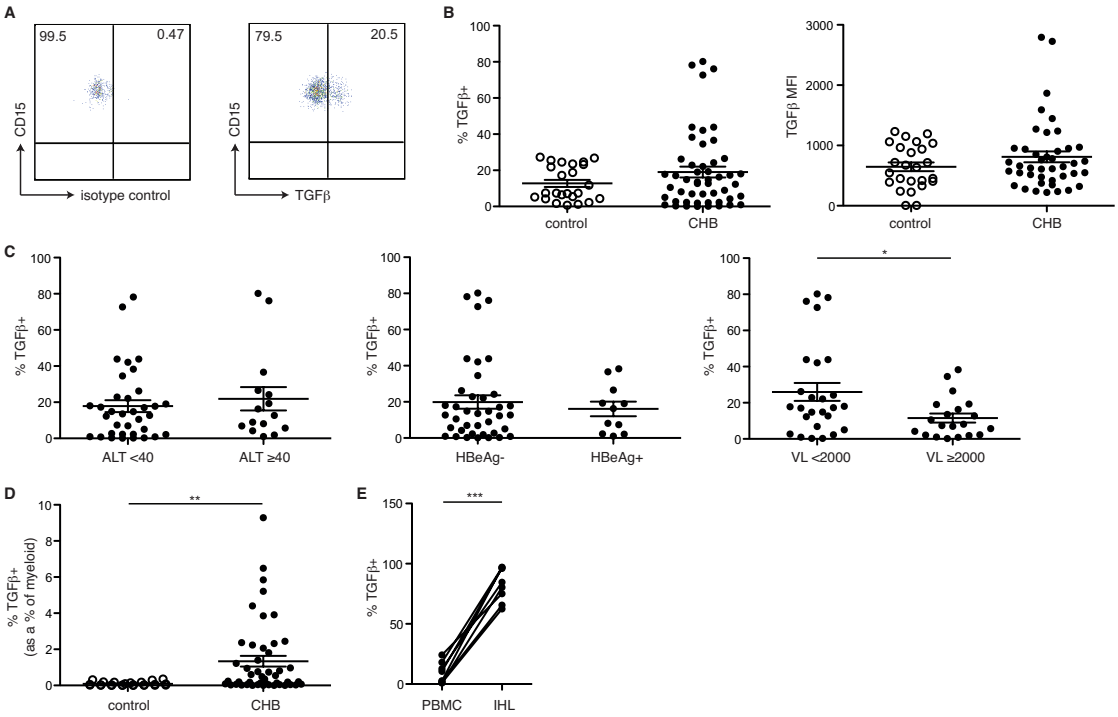

Figure 5.3: *Ex vivo* staining of gMDSC for TGFβ.

Freshly isolated PBMC were stained for CD33, CD11b, HLA-DR, CD14 and CD15 and gated as shown in figure 3.2a to identify gMDSC. A) Representative FACS plots showing gMDSC TGFβ staining *ex vivo* compared to its matched isotype control from a patient with CHB. B) Cumulative data showing: percentage and mean fluorescence intensity (MFI), respectively, of gMDSC expressing TGFβ in 24 controls and 50 patients with CHB. C) Percentage of gMDSC expressing TGFβ from the cohort of patients with CHB was further classified by serum ALT (IU/L), the presence of HBeAg, or viral load (IU/ml) using EASL guidelines [19]. D) Cumulative data for TGFβ levels in relation to the percentage of TGFβ-expressing gMDSC as a proportion of the total myeloid cell compartment ($CD11b^{high}CD33+$). E) Percentage of TGFβ+ gMDSC in the peripheral (PBMC) and liver gMDSC (IHL). Error bars represent the mean $\pm$ SEM. Significance testing was carried out using either the: paired or unpaired Students t test, and where significant indicated as: *** $p<0.001$; ** $p<0.01$; * $p<0.05$.

5.4 Can MDSC modulate NK cell function in CHB?

Recent work within our group has led to a number of publications demonstrating a role for NK cells in CHB; work has shown both diminished antiviral function in the context of CHB [289] and killing of both hepatocytes and T cells, via the TRAIL pathway [72, 63]. It was therefore important to investigate whether gMDSC can regulate not only T cell, but also NK cell function in CHB. To date very limited data exists considering MDSC and NK cells. There is some existing evidence that suggests gMDSC can suppress NK cell function, although these data are rather limited.

5.4.1 A potential role for the NKG2D pathway

A study by Li *et al.* [290] have demonstrated that a state of heptic NK cell anergy seen in tumour-bearing mice could be attributed to membrane-bound TGFβ on the surface of MDSC. The authors showed that upon co-culturing MDSC with NK cells, the MDSC were able to limit NK cell cytotoxicity and IFNγ production and cause a significant down-regulation in expression of NK cell activatory receptor, NKG2D. Blockade of TGFβ signalling or the experimental separation of MDSC and NK cell during co-culture restored NK cell function. A similar effect was demonstrated by Mauti *et al.* [291], where the authors described an increased permissiveness for metastasis during pregnancy in mice and attributed this to decreased NK cell cytotoxicity and proliferation/viability in the presence of increased numbers of gMDSC [291]. The outcome of MDSC-mediated regulation of NK cell function remains controversial. Further reports have observed that MDSC can activate NK cells, and therefore enhance NK cell function. Nausch *et al.* [292] demonstrated expression of NKG2D ligands on murine MDSC which potently activated NK cells to produce increased amounts of IFNγ whilst maintaining the well-described MDSC-mediated suppression of T cells [292]. It therefore appears a bi-directional cross-talk may occur between NK cells and MDSC.

MDSC in CHB but not from controls express low, but potentially functionally significant, levels of MICA/B, one of the known ligands for the activatory receptor NKG2D (figure 5.4). Recent unpublished work by our group has demonstrated a role for this particular pathway in interactions between NK cells and T cells; up-regulation of T cell expression of NKG2D-ligands drives NK cell activation and cytotoxicty (Huang et al - unpublished). It is therefore possible that gMDSC act the same way as T cells and thereby promote NK cell activation. It is also possible that MICA/B may be expressed at higher levels on intrahepatic than peripheral gMDSC, perhaps contributing to the increased NK cell activation seen in the liver [72]. What remains unknown is whether gMDSC are capable of expressing other NKG2D-ligands, such as ULBP1-6 [293], and the exact function of this interaction.

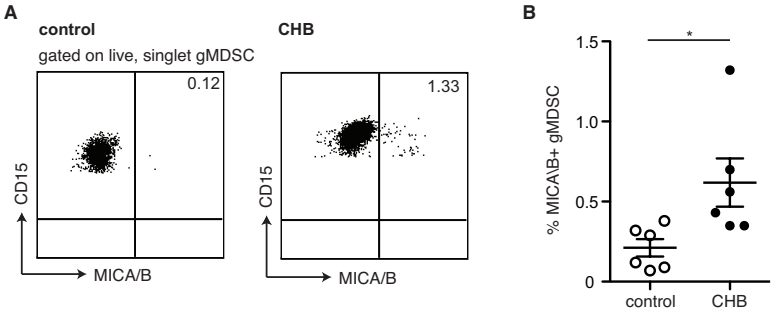

Figure 5.4: gMDSC from patients with CHB express increased levels of the NKG2D ligands, MICA/B.

Freshly isolated PBMC were stained for CD33, CD11b, HLA-DR, CD14 and CD15 and gated as shown in figure 3.2a to identify gMDSC. A) Representative examples of NKG2D-ligands MICA/B expression on the surface of gMDSC from one uninfected control and one patient with CHB. B) Summary data of six uninfected controls and six patients with CHB. Error bars represent the mean ± SEM. Significance testing was carried out using the unpaired Students t test, with significance indicated as: * $p<0.05$.

5.4.2 A potential role for the NKp30 pathway

It also appears that MDSC have the capacity to interfere with multiple signalling pathways that can either activate or inhibit an NK cell. Another NK cell pathway that has previously been implicated in relation to MDSC through another NK cell activatory pathway, the NKp30 pathway. A previous study by Hoechst *et al.* [195] demonstrated a link between MDSC and NK cell function whereby they showed a counter-intuitive inhibition of NK cell function by an expanded populations of MDSC that was primarily mediated through NKp30. The authors discuss how the level of inhibition or activation of the NK cell by a MDSC through NKp30 may be dependent on the density of the corresponding ligand(s) on the MDSC surface.

Using cryopreserved PBMC samples from patients with CHB in whom gMDSC frequencies had previously been assessed, NK cell expression of NKp30 was ascertained (figure 5.5a). The cumulative data for receptor expression showed no significant difference in expression between controls and patients with CHB in this small cohort. The data pointed towards the notion that NKp30 expression on the NK cells in CHB is, however, variable (figure 5.5b). Notably, a positive correlation was observed between the extent of NKp30 expression and circulating frequencies of gMDSC (figure 5.5c). Given the relationship observed, it is plausible that a significant relationship exists between NK cells and gMDSC via this pathway, but what is still unknown is the functional outcome of such an interaction. gMDSC may further drive NK cell activation through this pathway or it is may also be possible that gMDSC express varying densities of

NKp30 ligand(s) that regulate a balance between inhibition and activation of the NK cell, in line with data published by Hoechst *et al.* [195].

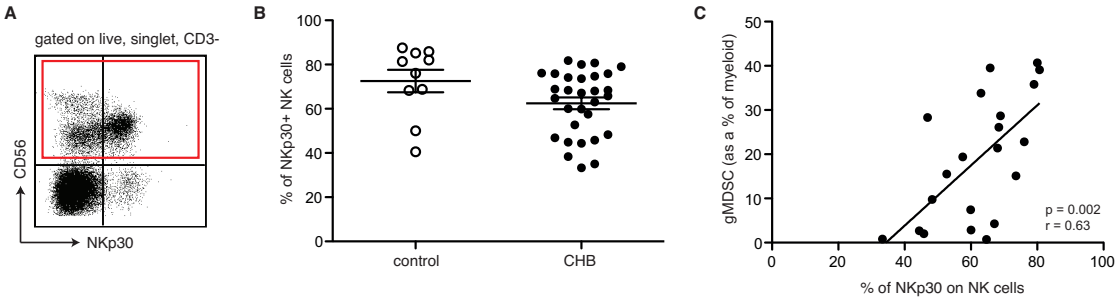

Figure 5.5: NKp30 expression on NK cells positively correlates with circulating gMDSC frequencies in CHB.

Cryopreserved PBMC samples from patients with CHB were used in whom gMDSC frequencies were previously assessed. NK cells were subsequently identified as: live, singlet, CD3−CD56+. A) Representative NKp30 staining on NK cells (highlighted in red) from a patient with CHB and B) summary data for all controls and patients with CHB where NKp30 expression on total NK cells was determined. To establish gMDSC frequencies, freshly isolated PBMC had previously been stained with CD33, CD11b, HLA-DR, CD14 and CD15 and gated as shown in figure 3.2a. C) Correlative analysis between circulating frequencies of NKp30 and percentage expression of NKp30 on total NK cells. Error bars represent the mean ± SEM. Significance testing was carried out using either the: unpaired Students t test or the Pearson product-moment correlation coefficient, and where significant indicated as: ** $p<0.01$.

5.5 Can MDSC promote T cell exhaustion in CHB?

As described in section 1.3.2, CHB is characterised by a dysregulated T cell response which impacts on the antiviral response. Our group and others have extensively considered a role for phenotypic and functional exhaustion in perpetuating this dysregulation. HBV-specific T cells express high levels of a number of characteristic exhaustion markers, including PD-1, Tim3 and CTLA-4 [59, 61, 49, 60]. In this study gMDSC suppression of both HBV-specific and bystander T cell functionality was reported. The main focus of this thesis was concerned with the role gMDSC play in limiting bystander T cell damage in the liver through metabolic regulation. However, gMDSC may additionally limit the already dysfunctional specific antiviral T cells in CHB through other mechanisms.

Alongside the gMDSC-mediated HBV-specific suppression data discussed in chapter 4, the following preliminary evidence supports the notion that gMDSC promote T cell exhaustion, furthering T cell dysfunction through known receptor:ligand interactions.

5.5.1 Is bi-directional signalling via galectin-9 on gMDSC important in CHB?

The S-type lectin galectin-9 binds to the negative regulatory molecule Tim-3 on T cells and induces their apoptotic deletion or functional inactivation. Although galectin-9 is widely accepted to be the ligand for Tim-3, this role has been questioned recently in a single publication [294]. A role for galectin-9/Tim-3 interaction in the deletion and exhaustion of the antiviral response in HBV has recently been proposed. An up-regulation of Tim-3 on CD4+ and CD8+ T cells from patients with CHB compared to controls results in their functional inhibition or deletion upon engaging with the ligand galectin-9. A further up-regulation of the receptor on HBV-specific cells was also reported by our group and others [61, 295, 296]. The study by our group also detected secreted galectin-9 at increased concentrations in the sera of patients with active CHB-related inflammation [61]. Tim-3 mediated inhibition of T cells may not just be solely attributable to the triggering of cell death of IFNγ producing cells. Emerging lines of evidence suggests T cells expressing Tim-3 may also indirectly be involved in the induction of gMDSC [297]. Putting aside the controversy surrounding the potential for galectin-9 and Tim-3 not being a physiological receptor:ligand interaction, gMDSC expression of galectin-9 could exacerbate T cell exhaustion and/or MDSC induction. With this in mind it has also been proposed that the molecule galectin-9 has the capacity for bi-directional signalling, affecting both the expressing and interacting cell [297, 298].

Consideration therefore turned to whether gMDSC could express galectin-9 in CHB. Initial confirmation of gMDSC expression of galectin-9 was achieved using intracellular staining with an antibody against the receptor (figure 5.6a) compared to a matched isotype control. As with expression of the enzyme arginase I, percentage expression and expression levels (as quantified by MFI) of gMDSC galectin-9 were variable and often extremely high on gMDSC from both controls and patients with CHB (figure 5.6b). Despite the variability, particularly in patients with CHB, stratification of the CHB cohort revealed nothing of note; galectin-9 expression appeared to be analogous regardless of the extent of liver inflammation (serum ALT levels), the presence of HBeAg, or viral load (figure 5.6c). However, when taking into account the expanded proportion of gMDSC in the context of CHB, the contribution galectin-9 expression could make to immune suppression is more pronounced in CHB (figure 5.6d). Expression of galectin-9 on gMDSC is significantly enhanced on intrahepatic gMDSC compared to circulating gMDSC (figure 5.6e), making this potential mechanism of immune suppression particularly relevant in the context of hepatotropic infections.

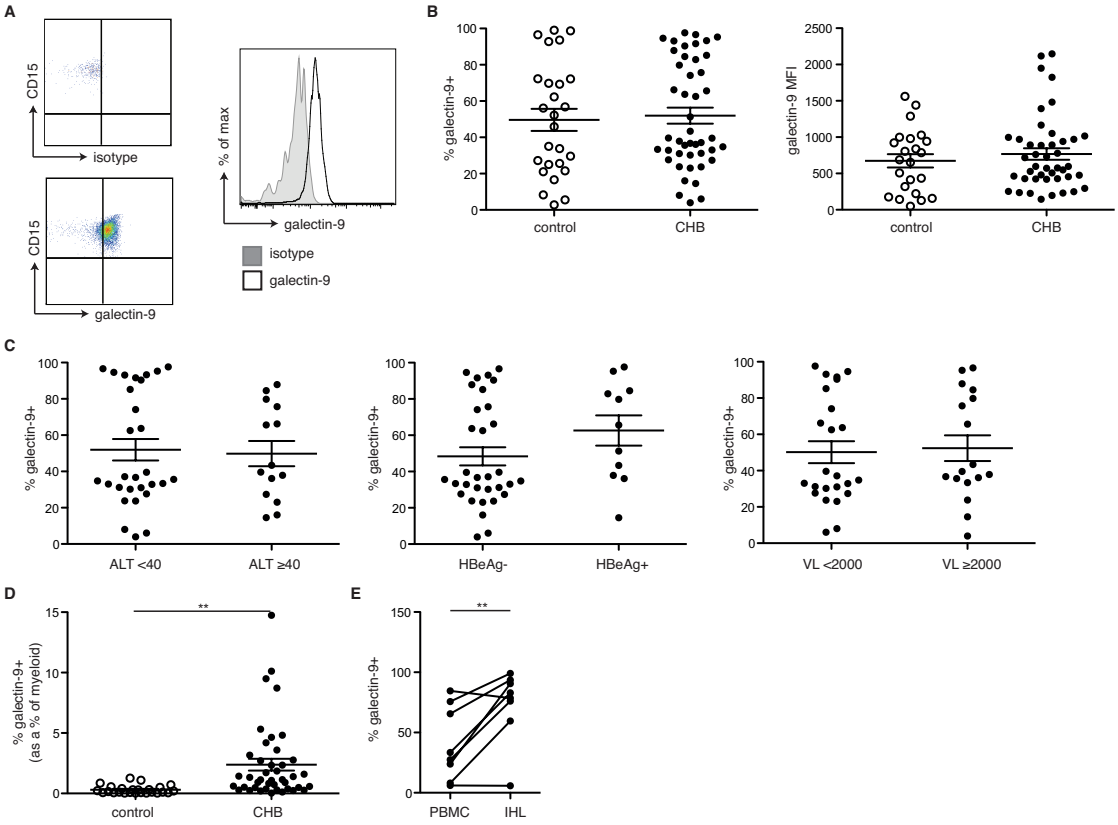

Figure 5.6: gMDSC express galectin-9 *ex vivo*.

A) Representative FACS plots showing galectin-9 staining *ex vivo* compared to its matched isotype control in gMDSC from a patient with CHB. B) Percentage and mean fluorescence intensity (MFI), respectively, of gMDSC expressing galectin-9 in controls and patients with CHB. C) Percentage of gMDSC expressing galectin-9 from the cohort of patients with CHB were further classified by serum ALT (IU/L), the presence of HBeAg, or viral load (IU/ml). D) Cumulative data for galectin-9 levels in relation to the percentage of galectin-9-expressing gMDSC as a proportion of the total myeloid cell compartment ($CD11b^{high}CD33+$). E) Percentage of galectin-9 positive gMDSC in circulating gMDSC (PBMC) and intrahepatic gMDSC (IHL). Error bars represent the mean ± SEM. Significance testing was carried out using either the: paired or unpaired Students t test, and where significant indicated as: *** $p<0.001$; ** $p<0.01$.

Most interesting was the striking association observed between the percentage of gMDSC expressing galectin-9 and their capacity to produce arginase I (figure 5.7). This raises the possibility of two different scenarios: either back-signalling through galectin-9 on the gMDSC drives arginase I expression, or co-expression of these two potentially suppressive mechanisms suggests a state of gMDSC ″activation‟ and readiness for immune regulation. Both scenarios require investigation and pose important future questions, especially since a definitive marker for MDSC activation does not yet exist.

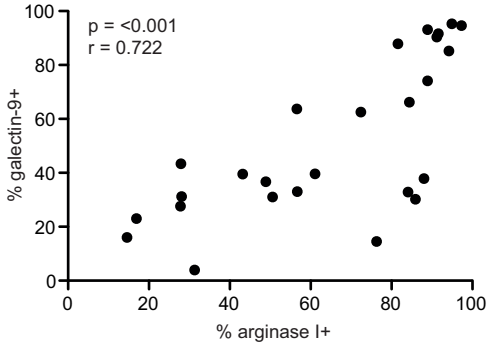

Figure 5.7: gMDSC galectin-9 expression correlates with arginase I production in CHB.

Correlative analysis showing the percentage of gMDSC expressing galectin-9 staining *ex vivo* against the proportion of those gMDSC producing arginase I. Significance testing was carried out using the Pearson product-moment correlation coefficient.

5.5.2 Can gMDSC promote T cell exhaustion through the PD-L1:PD-1 pathway?

It is widely acknowledged that interaction through the PD-1:PD-L1 pathway results in the delivery of a co-inhibitory signal, and therefore promotes T-cell apoptosis, anergy and functional exhaustion [53, 299]. The concept of MDSC interacting with T cells via this pathway is relatively new. Preliminary *ex vivo* showed that gMDSC are capable of expressing the ligand, PD-L1 (figure 5.8a). From this limited analysis expression of PD-L1 detectable on the surface of gMDSC appears analogous between controls and patients with CHB (figure 5.8). The extent of PD-L1 on intrahepatic gMDSC has yet to be analysed and so it remains possible that an up-regulation of PD-L1 could further promote the induction of T cell tolerance in the liver microenvironment.

This is in line with recent evidence for the PD-1:PD-L1 interaction of neutrophils and T cell function. de Kleijn *et al.* [300] recently demonstrated that IFNγ-stimulated neutrophils suppressed T cell proliferation via an up-regulation of PD-L1 [300]. This study was rapidly followed up by a study in HIV infection. The authors of this particularly study demonstrated that neutrophils from patients with HIV-infection up-regulated PD-L1 expression, driven by both inactivated HIV virions and TLR-7/8 ligand. Interestingly, the extent of PD-L1 on the CD15+ neutrophils significantly correlated with plasma levels of arginase I [301], suggesting an interaction via this pathway may also be involved in neutrophil (or MDSC) activation and release of suppressive mediators *in vivo*.

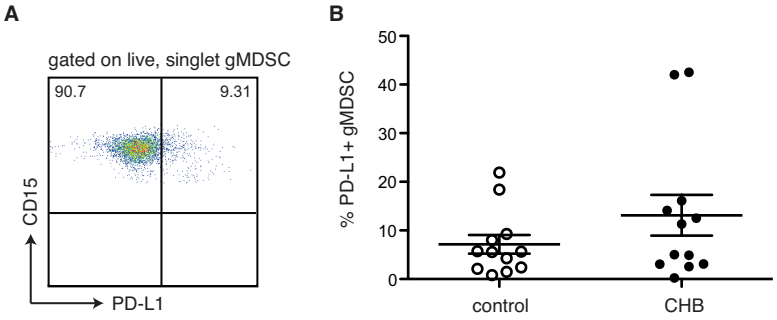

Figure 5.8: gMDSC express PD-L1, a ligand capable of promoting T cell exhaustion through interaction with PD-1.

Freshly isolated PBMC were stained for CD33, CD11b, HLA-DR, CD14 and CD15 and gated as shown in figure 3.2a to identify gMDSC. A) Representative example of PD-L1 expression on the surface of gMDSC from an uninfected control. B) Summary data of 12 uninfected controls and 12 patients with CHB. Error bars represent the mean ± SEM. Significance testing was carried out using the unpaired Students t test and was deemed non-significant.

5.6 What causes MDSC expansion & contraction?

5.6.1 A role for death-ligands in MDSC contraction

Despite being a short-lived population, a number of studies have demonstrated roles for death-ligands in the contraction of gMDSC. It is possible that in the different phases of disease, or by interventions such as antiviral therapy or peg-IFNα treatment, that these ligands may be differentially regulated, promoting MDSC apoptosis.

One such pathway to consider is the Fas (CD95):Fas-ligand (FasL) pathway. Emerging lines of evidence suggest a role for this death receptor pathway in the regulation of MDSC expansion and contraction; a regulatory mechanism controlling the number of circulating MDSC. Apoptosis of murine Fas+ MDSC was demonstrated in response to activated FasL expressing T cells *in vivo*. The authors also showed that FasL deficient mice have increased circulating MDSC frequencies compared to their FasL competent counterparts [302]. Whether this is an important pathway in CHB is a question of interest since gMDSC identified from three independent patients with CHB showed high levels of Fas expression *ex vivo* (data not shown). The particular disease state of these three patients were unknown. It is possible that this pathway may be important during active CHB disease (much like in HCV infection), where an up-regulation of FasL on infiltrating lymphocytes [303, 304] may provide a direct mechanism for the deletion of gMDSC, which have the potential to suppress immunopathology.

Another death-ligand pathway implicated in the contraction of MDSC frequencies is the TRAIL pathway. Interaction via this pathway could lead to TRAIL-mediated deletion, similar to that occurring with hepatocytes and T cells [72, 63]. Condamine *et al.* [305] have recently shown that MDSC apoptosis is increased as a result of enhanced expression of TRAIL receptors, specifically TRAIL-receptor 2, in both a murine model and on gMDSC identified from patients with non-small cell lung cancer [305] . It remains unknown whether gMDSC in the context of CHB can express TRAIL-receptors. This is of particular interest because previous work by our group showed that circulating NK cells up-regulate TRAIL when liver damage is ongoing, with further increases in expression on intraheptaic NK cells [72]. It is therefore plausible that in patients with active CHB disease, an interaction of gMDSC expressing TRAIL-receptors infiltrating into the liver with TRAIL-expressing NK cells leads to their deletion. If TRAIL-expressing NK cells can directly eliminate gMDSC, this may be one mechanism pertaining to a lack of gMDSC in active CHB.

5.6.2 Differentiation of MDSC affects circulating populations of mature myeloid populations

Finally, another question this study raises is in relation to the process of MDSC differentiation and its potential impact on mature myeloid cell differentiation. As discussed in section 1.5 the accumulation of MDSC often occurs upon pathological insult and is believed to be the result of a disruption of the physiological process of myleopoeisis. More specifically, MDSC accumulation can arise from a halt in differentiation and maturation of immature myeloid progenitors into mature myeloid subsets (as depicted in figure 1.9). Perturbation of the physiological process is thought to be driven by a number of growth factors, cytokines and chemokines. It is conceivable that when MDSC populations increase/accumulate in the circulation of patients with CHB there may be a concomitant decrease in the frequencies of mature myeloid subsets. Using the markers already included in the original antibody panel for quantification of gMDSC frequencies, it was possible to address this in a limited manner based on different gating strategies [306]. Figure 5.9a demonstrates alternative gating strategies used to assess circulating frequencies of non-classical monocytes (CD11b+CD33+CD14+CD16+) and classical monocytes (CD11b+CD33+CD14+CD16-) respectively. Populations of classical granulocytes could not be assessed due to the use of density centrifugation over Ficoll, which excludes these cells.

Using this approach to look at mature myeloid cell populations a decrease was observed in the population of classical monocytes in patients with CHB compared to uninfected controls. This

raises an interesting question: if MDSC with a granulocytic phenotype are the subset expanding in CHB, why is a decrease in monocytes observed? Three potential scenarios arise: 1) an expansion of gMDSC limits the pool of immature myeloid progenitors able to differentiate into mature monocytes, 2) the mature monocyte population provides a population of cells from which suppressive MDSC can expand, either by a process of de-differentiation of mature populations, or 3) by further differentiation of an mMDSC into gMDSC [115, 135].

An increase in non-classical (inflammatory) monocytes was also noted, which may be related to the suppressive nature of these cells (figure 5.9b). It is of note however that the gating strategy used for gMDSC identification does not necessarily exclude low density neutrophils, which can be identified as CD14-CD15+CD16+ (personal communication - Pascale Kropf), and may therefore overlap phenotypically with gMDSC.

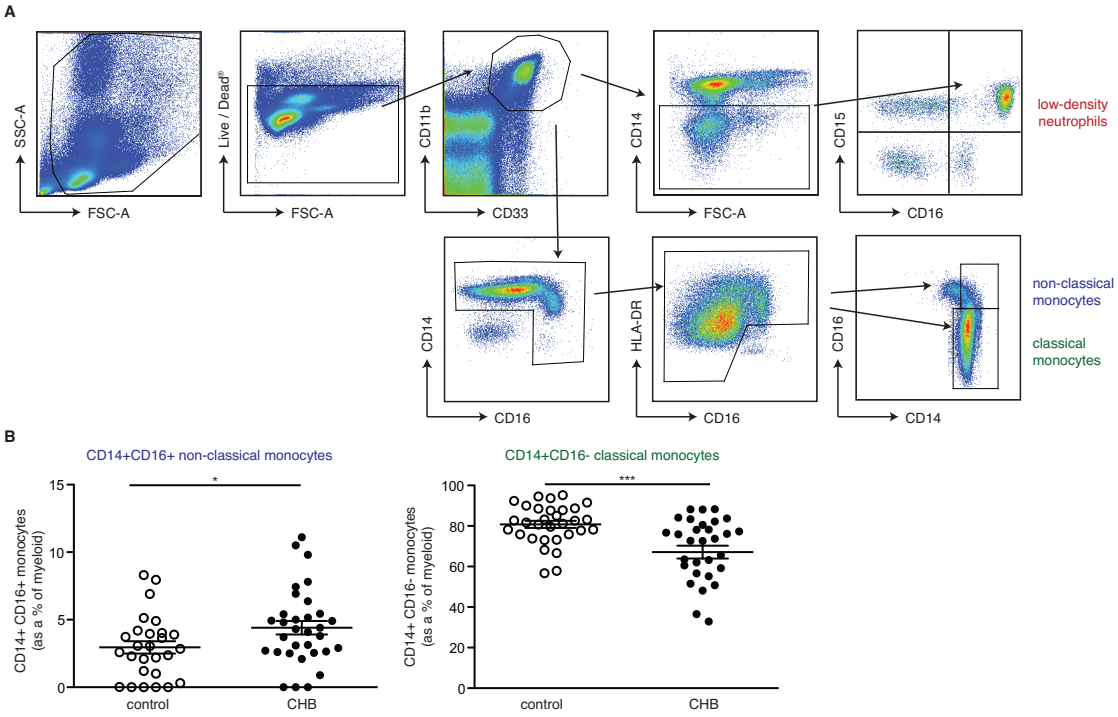

Figure 5.9: Populations of mature myeloid cells are also altered in patients with CHB.

A) Representative gating strategy used to identity CD14+CD16+ non-classical monocytes and CD14+CD16- classical monocytes in freshly isolated PBMC by flow cytometry. B) Relative frequencies of circulating subsets of monocytes respectively represented as a percentage of myeloid cells. Error bars represent the mean ± SEM. Significance testing was carried out using either the unpaired Students t test, and where significant indicated as: *** $p<0.001$; * $p<0.05$.

5.7 Further Exploration: gMDSC in animal models

Although mice hepatocytes lack the NTCP receptor and restriction factors necessary for natural HBV infection, two mouse models have been described that utilise adenoviral (AdHBV) or adeno-associated virus (AAV-HBV) vectors to shuttle the HBV genome into murine hepatocytes [307, 308, 309]. Particularly interesting future work to build on the data presented in this thesis would entail looking at gMDSC function and development in either of these two models. These two models are currently being implemented within the Maini group.

The first of these, the AdHBV model provides an opportunity to tailor the outcome of HBV infection, by using varying doses of AdHBV. By using a high or low viral dose of the AdHBV it is possible to elicit either acute or chronic HBV infection, respectively. More specifically a high viral dose leads to a transient increase in ALT levels, reflecting immune-mediated hepatocyte damage [307]. In using this particular model the comparison of the induction and maintenance of MDSC in acute resolving or during chronic HBV infection could be assessed. It would also be interesting to consider, in more detail, their *in vivo* effect on disease outcome by depleting them, or by simply blocking one mechanism of action at a time. Most pertinent would be to consider arginase I-dependent suppression, using the inhibitor nor-NOHA (plus or minus the re-addition of exogenous L-arginine). Infection of mice with the AAV-HBV construct mimics the state of immunotolerance. The viral load in these mice is extremely high, HBeAg is produced and the serum ALT levels are usually low [308]; whether this is primarily controlled by gMDSC, as proposed by this study, would be interesting to consider.

Finally another possibility to establish the *in vivo* effects of gMDSC or to consider their development and expansion is to utilise novel humanised mice models. In this case, these mice have been reconstituted with both a human liver and a human immune system. This humanised model is currently under development in a number of different groups. The study of gMDSC in these mice compared to the other previously described models, offers one significant advantage: in these humanised mice it should in theory be possible to identify gMDSC using the same panel of markers established during this thesis for use in our patient cohorts.

5.8 Future Outlook: the therapeutic potential for gMDSC

In the context of chronic HBV infection there are two possibilities when it comes to harnessing or exploiting the functionality of gMDSC. On the one hand it could be possible to take advantage of MDSC-mediated suppression to dampen down immune-mediated damage in the liver, specifically in patients undergoing severe hepatic flares that could ultimately lead to decompensation. In these patients expansion and/or the activation of a suppressive MDSC population could prevent or limit overwhelming liver damage mediated driven by the bystander immune response. Therapeutic approaches to achieve this remain to be determined; it is possible that the local induction of candidate cytokines may enable the perturbation of myeloid cell differentiation, allowing MDSC expansion *in vivo*. This approach may also be useful for other diseases where immunosuppression is desirable such as auto-immune hepatitis, or after liver transplantation.

On the other hand however, of more widespread applicability in CHB, is the possibility of depleting MDSC to break immune tolerance. MDSC can suppress HBV-specific immunity, and may also have the capacity to promote further T cell exhaustion. It may be particularly useful in patients with immunotolerant disease, who are not currently considered suitable for treatment, to remove suppressive MDSC to ″break‟ ongoing tolerance. This could make these patients more amenable to treatment, by enhancing the limited and dysregulated anti-viral immunity normally observed in CHB. One major caveat to this approach would be that by removing suppression on the specific antiviral immune responses, a simultaneous enhancement of bystander T cell function would also occur, at the inevitable expense of promoting some liver damage. However this is true of most immunotherapeutic approaches currently under consideration for the treatment of CHB which all carry the risk of disrupting the homoeostatic balance between immunity and immunopathology in the liver.

What we do not currently know is the effect antiviral therapy or peg-IFNα have on MDSC frequencies. No longitudinal studies have been carried out with patients where MDSC are particularly expanded, for example, the inactive patients or those with immunotolerant disease. It is possible that if MDSC are not completely suppressed on therapy, cure rates would improve by depleting MDSC and promoting successful immune responses. It is plausible that use of small molecule inhibitors, or an approach based on recent research in mice, detailing peptide-driven depletion may be the future for MDSC removal. The use of novel therapeutic MDSC-specific peptide-Fc fusion (peptibody) reagents that have been to shown to successfully deplete MDSC by a process of antibody-dependent cell-mediated cytotoxcitiy, from the blood,

spleen and tumour-sites in murine tumour models [276], provides a potential approach that could be translated into patients with CHB (or cancers of various origins) to alleviate MDSC-mediate immune-suppression.

It is also possible that small molecules could be used therapeutically to deplete gMDSC or block their production of metabolic mediators of immunosuppression, which would in turn allow restoration of antiviral immunity. PI3Kδ inhibitors such as the Gilead compound Idelalisib, that is already licensed for the treatment of haematological malignancies, has recently been shown to have efficacy in a murine model of solid tumours. Administration of this PI3Kδ inhibitor enhanced CD8+ T cell function by reducing the frequencies of both Treg and gMDSC, which released antiviral T cells from inhibition [310]. Approaches such as this could potentially be combined with other immunotherapeutic approaches currently being considered for CHB. For example, inhibition of MDSC function has also been recently demonstrated to enhance the therapeutic efficacy of using PD-1 blockade [311].

One therapeutic approach under current investigation in CHB is the use of gene therapy to redirect the specificity of patient T cells in CHB using exogenous TCR transfer. The aim of redirected T cells would be to overcome the dysregulated T cell response observed in patients with CHB [312, 313]. The use of these immunotherapeutics are under development by a number of groups and have recently been demonstrated to be safe for use *in vivo* in one patient with HCC (Antonio Bertoletti - submitted). One problem, however, still remains regarding the use of these cells and that is that although the infused T cells would then have the right specificity they may still succumb to the same mechanisms driving the initial dysfunction. It may be necessary to therefore alter the sensitivity of redirected HBV-specific T cells to conditions of nutrient deprivation. The knowledge of any potential compensatory mechanisms that a T cell may employ to overcome nutrient starvation (specifically in the CHB liver) will be critical for the future design of these cells. One such strategy for protecting against the ongoing milieu in CHB may require the functional over-activation of pathways such as the mTOR pathway.

5.9 Overview of potential gMDSC-mediated immune regulation in the context of CHB

Throughout this thesis, a number of potential gMDSC immune-regulatory functions have been considered. It is clear from data presented in chapters 3 and 4 that gMDSC have the capacity

to modulate immunity by altering amino acid metabolism. What will have become clear from reading this chapter however is that other mechanisms may synergise with this effect in CHB, raising a number of hypotheses for ongoing research. Figure 5.10 summarises all the potential MDSC-mediated functions that have been considered throughout.

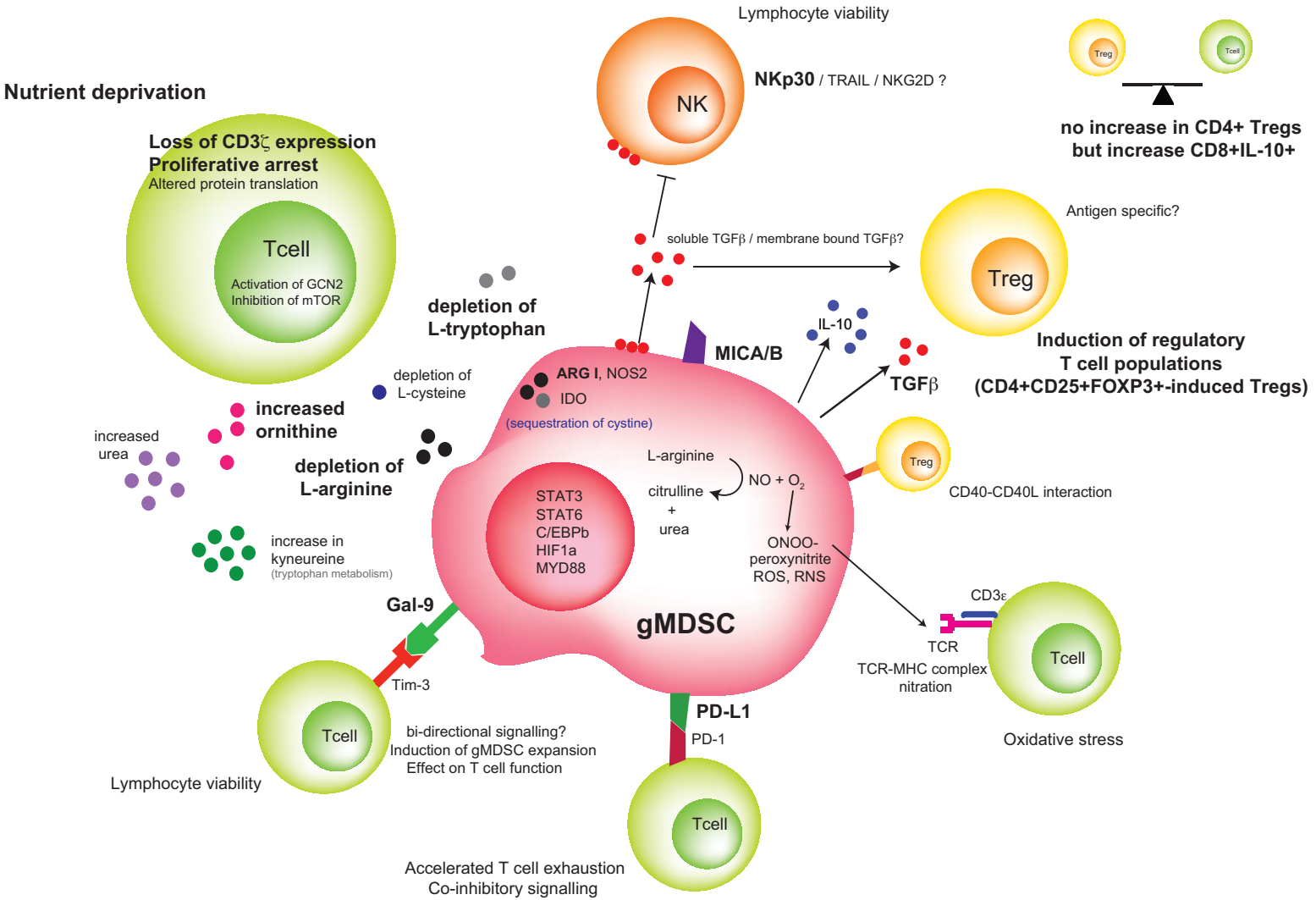

Figure 5.10: Overview of the potential gMDSC-mediated mechanisms of immune regulation
Those considered in the context of CHB in this thesis are shown in bold.

Final Word

Having completed this thesis, I am aware of how proud my family (and friends) are of me.

With that in mind I would like one final word:

Family, if you have got this far and are reading this statement I am equally as proud of you for getting through it!

Bibliography

[1] Blumberg, B.S., Alter, H.J. & Visnich, S. A ″new‟ antigen in leukemia sera. *JAMA: The Journal of the American Medical Association* **191** (1965) 541–546.

[2] Blumberg, B.S. Australia antigen and the biology of hepatitis b. *Science (New York, N.Y.)* **197** (1977) 17–25.

[3] Feinstone, S.M., Kapikian, A.Z. & Purceli, R.H. Hepatitis A: detection by immune electron microscopy of a virus-like antigen associated with acute illness. *Science (New York, N.Y.)* **182** (1973) 1026–1028.

[4] Rizzetto, M., Canese, M.G., Aric, S., Crivelli, O., Trepo, C., Bonino, F. & Verme, G. Immunofluorescence detection of new antigen-antibody system (delta/anti-delta) associated to Hepatitis B virus in liver and in serum of HBsAg carriers. *Gut* **18** (1977) 997–1003.

[5] Balayan, M.S., Andjaparidze, A.G., Savinskaya, S.S., Ketiladze, E.S., Braginsky, D.M., Savinov, A.P. & Poleschuk, V.F. Evidence for a virus in non-A, non-B Hepatitis transmitted via the fecal-oral route. *Intervirology* **20** (1983) 23–31.

[6] Choo, Q.L., Kuo, G., Weiner, A.J., Overby, L.R., Bradley, D.W. & Houghton, M. Isolation of a cDNA clone derived from a blood-borne non-A, non-B viral Hepatitis genome. *Science (New York, N.Y.)* **244** (1989) 359–362.

[7] Park, S.H. & Rehermann, B. Immune responses to HCV and other hepatitis viruses. *Immunity* **40** (2014) 13–24.

[8] Heim, M.H. 25 years of interferon-based treatment of chronic Hepatitis C: an epoch coming to an end. *Nature Reviews. Immunology* **13** (2013) 535–542.

[9] Ott, J.J., Stevens, G.A., Groeger, J. & Wiersma, S.T. Global epidemiology of Hepatitis B virus infection: new estimates of age-specific HBsAg seroprevalence and endemicity. *Vaccine* **30** (2012) 2212–2219.

[10] Lavanchy, D. Hepatitis B virus epidemiology, disease burden, treatment, and current and emerging prevention and control measures. *J Viral Hepat* **11** (2004) 97–107. 2.

[11] Chu, C.M. & Liaw, Y.F. Incidence and risk factors of progression to cirrhosis in inactive carriers of Hepatitis B virus. *Am J Gastroenterol* **104** (2009) 1693–9. 7.

[12] Liaw, Y.F. HBeAg seroconversion as an important end point in the treatment of chronic Hepatitis B. *Hepatol Int* **3** (2009) 425–33. 3.

[13] Liaw, Y.F. Natural history of chronic Hepatitis B virus infection and long-term outcome under treatment. *Liver Int* **29 Suppl 1** (2009) 100–7.

[14] Penna, A., Artini, M., Cavalli, A., Levrero, M., Bertoletti, A., Pilli, M., Chisari, F.V., Rehermann, B., Del Prete, G., Fiaccadori, F. & Ferrari, C. Long-lasting memory T cell responses following self-limited acute Hepatitis B. *J Clin Invest* **98** (1996) 1185–94. 5.

[15] Rehermann, B. Immunopathogenesis of viral hepatitis. *Baillieres Clin Gastroenterol* **10** (1996) 483–500. 3.

[16] Rehermann, B., Ferrari, C., Pasquinelli, C. & Chisari, F.V. The hepatitis B virus persists for decades after patients' recovery from acute viral hepatitis despite active maintenance of a cytotoxic T-lymphocyte response. *Nat Med* **2** (1996) 1104–8. 10.

[17] Rehermann, B. & Nascimbeni, M. Immunology of Hepatitis B virus and Hepatitis C virus infection. *Nature Reviews Immunology* **5** (2005) 215–229.

[18] Liaw, Y.F. & Chu, C.M. Hepatitis B virus infection. *Lancet* **373** (2009) 582–592.

[19] EASL. Clinical practice guidelines: management of chronic Hepatitis B virus infection. *Journal of Hepatology* **57** (2012) 167–185.

[20] Hildt, E., Hofschneider, P.H. & Urban, S. The role of Hepatitis B virus (HBV) in the development of hepatocellular carcinoma. *Seminars in Virology* **7** (1996) 333–347.

[21] Glebe, D. & Urban, S. Viral and cellular determinants involved in hepadnaviral entry. *World J Gastroenterol* **13** (2007) 22–38. 1.

[22] Schulze, A., Gripon, P. & Urban, S. Hepatitis B virus infection initiates with a large surface protein-dependent binding to heparan sulfate proteoglycans. *Hepatology* **46** (2007) 1759–68. 6.

[23] Yan, H., Zhong, G., Xu, G., He, W., Jing, Z., Gao, Z., Huang, Y., Qi, Y., Peng, B., Wang, H., Fu, L., Song, M., Chen, P., Gao, W., Ren, B., Sun, Y., Cai, T., Feng, X., Sui, J. & Li,

W. Sodium taurocholate cotransporting polypeptide is a functional receptor for human Hepatitis B and D virus. *Elife* **1** (2012) e00049.

[24] Urban, S., Schulze, A., Dandri, M. & Petersen, J. The replication cycle of Hepatitis B virus. *J Hepatol* **52** (2010) 282–4. 2.

[25] Locarnini, S. & Zoulim, F. Molecular genetics of HBV infection. *Antiviral therapy* **15 Suppl 3** (2010) 3–14.

[26] Nassal, M. Hepatitis B viruses: reverse transcription a different way. *Virus research* **134** (2008) 235–249.

[27] Lucifora, J., Xia, Y., Reisinger, F., Zhang, K., Stadler, D., Cheng, X., Sprinzl, M.F., Koppensteiner, H., Makowska, Z., Volz, T., Remouchamps, C., Chou, W.M., Thasler, W.E., Hser, N., Durantel, D., Liang, T.J., Mnk, C., Heim, M.H., Browning, J.L., Dejardin, E., Dandri, M., Schindler, M., Heikenwalder, M. & Protzer, U. Specific and nonhepatotoxic degradation of nuclear Hepatitis B virus cccDNA. *Science* **343** (2014) 1221–1228.

[28] Guidotti, L.G. & Chisari, F.V. Immunobiology and pathogenesis of viral hepatitis. *Annu Rev Pathol* **1** (2006) 23–61.

[29] Dandri, M. & Locarnini, S. New insight in the pathobiology of Hepatitis B virus infection. *Gut* **61 Suppl 1** (2012) i6–17.

[30] Beck, J. & Nassal, M. Hepatitis B virus replication. *World journal of gastroenterology: WJG* **13** (2007) 48–64.

[31] Ganem, D. & Prince, A.M. Hepatitis B virus infection - natural history and clinical consequences. *The New England journal of medicine* **350** (2004) 1118–1129.

[32] Bantel, H. & Schulze-Osthoff, K. Apoptosis in Hepatitis C virus infection. *Cell Death & Differentiation* **10** (2003) S48–S58.

[33] Bertoletti, A., Maini, M.K. & Ferrari, C. The host-pathogen interaction during HBV infection: immunological controversies. *Antiviral therapy* **15 Suppl 3** (2010) 15–24.

[34] Guidotti, L.G., Rochford, R., Chung, J., Shapiro, M., Purcell, R. & Chisari, F.V. Viral clearance without destruction of infected cells during acute HBV infection. *Science (New York, N.Y.)* **284** (1999) 825–829.

[35] Thimme, R., Wieland, S., Steiger, C., Ghrayeb, J., Reimann, K.A., Purcell, R.H. & Chisari, F.V. CD8(+) T cells mediate viral clearance and disease pathogenesis during acute Hepatitis B virus infection. *Journal of virology* **77** (2003) 68–76.

[36] Guidotti, L.G., Ishikawa, T., Hobbs, M.V., Matzke, B., Schreiber, R. & Chisari, F.V. Intracellular inactivation of the Hepatitis B virus by cytotoxic T lymphocytes. *Immunity* **4** (1996) 25–36.

[37] Webster, G.J., Reignat, S., Maini, M.K., Whalley, S.A., Ogg, G.S., King, A., Brown, D., Amlot, P.L., Williams, R., Vergani, D., Dusheiko, G.M. & Bertoletti, A. Incubation phase of acute Hepatitis B in man: dynamic of cellular immune mechanisms. *Hepatology (Baltimore, Md.)* **32** (2000) 1117–1124.

[38] Chang, J.J. & Lewin, S.R. Immunopathogenesis of Hepatitis B virus infection. *Immunol Cell Biol* **85** (2007) 16–23. 1.

[39] Dunn, C., Peppa, D., Khanna, P., Nebbia, G., Jones, M., Brendish, N., Lascar, R.M., Brown, D., Gilson, R.J., Tedder, R.J., Dusheiko, G.M., Jacobs, M., Klenerman, P. & Maini, M.K. Temporal analysis of early immune responses in patients with acute Hepatitis B virus infection. *Gastroenterology* **137** (2009) 1289–300. 4.

[40] Bertoletti, A. & Ferrari, C. Innate and adaptive immune responses in chronic Hepatitis B virus infections: towards restoration of immune control of viral infection. *Gut* **61** (2012) 1754–1764.

[41] Wieland, S., Thimme, R., Purcell, R.H. & Chisari, F.V. Genomic analysis of the host response to Hepatitis B virus infection. *Proceedings of the National Academy of Sciences of the United States of America* **101** (2004) 6669–6674.

[42] Stacey, A.R., Norris, P.J., Qin, L., Haygreen, E.A., Taylor, E., Heitman, J., Lebedeva, M., DeCamp, A., Li, D., Grove, D., Self, S.G. & Borrow, P. Induction of a striking systemic cytokine cascade prior to peak viremia in acute human immunodeficiency virus type 1 infection, in contrast to more modest and delayed responses in acute Hepatitis B and C virus infections. *Journal of Virology* **83** (2009) 3719–3733.

[43] Fisicaro, P., Valdatta, C., Boni, C., Massari, M., Mori, C., Zerbini, A., Orlandini, A., Sacchelli, L., Missale, G. & Ferrari, C. Early kinetics of innate and adaptive immune responses during Hepatitis B virus infection. *Gut* **58** (2009) 974–982.

[44] Guidotti, L.G., Ando, K., Hobbs, M.V., Ishikawa, T., Runkel, L., Schreiber, R.D. & Chisari, F.V. Cytotoxic T lymphocytes inhibit hepatitis B virus gene expression by a non-cytolytic mechanism in transgenic mice. *Proceedings of the National Academy of Sciences of the United States of America* **91** (1994) 3764–3768.

[45] Iannacone, M., Sitia, G., Isogawa, M., Marchese, P., Castro, M.G., Lowenstein, P.R.,

Chisari, F.V., Ruggeri, Z.M. & Guidotti, L.G. Platelets mediate cytotoxic T lymphocyte-induced liver damage. *Nature Medicine* **11** (2005) 1167–1169.

[46] McClary, H., Koch, R., Chisari, F.V. & Guidotti, L.G. Relative sensitivity of Hepatitis B virus and other hepatotropic viruses to the antiviral effects of cytokines. *Journal of Virology* **74** (2000) 2255–2264.

[47] Maini, M.K., Boni, C., Lee, C.K., Larrubia, J.R., Reignat, S., Ogg, G.S., King, A.S., Herberg, J., Gilson, R., Alisa, A., Williams, R., Vergani, D., Naoumov, N.V., Ferrari, C. & Bertoletti, A. The role of virus-specific CD8(+) cells in liver damage and viral control during persistent Hepatitis B virus infection. *J Exp Med* **191** (2000) 1269–80. 8.

[48] Boettler, T., Panther, E., Bengsch, B., Nazarova, N., Spangenberg, H.C., Blum, H.E. & Thimme, R. Expression of the interleukin-7 receptor alpha chain (CD127) on virus-specific CD8+ T cells identifies functionally and phenotypically defined memory T cells during acute resolving Hepatitis B virus infection. *Journal of Virology* **80** (2006) 3532–3540.

[49] Boni, C., Fisicaro, P., Valdatta, C., Amadei, B., Di Vincenzo, P., Giuberti, T., Laccabue, D., Zerbini, A., Cavalli, A., Missale, G., Bertoletti, A. & Ferrari, C. Characterization of Hepatitis B virus (HBV)-specific T-cell dysfunction in chronic HBV infection. *J Virol* **81** (2007) 4215–25. 8.

[50] Webster, G.J.M., Reignat, S., Brown, D., Ogg, G.S., Jones, L., Seneviratne, S.L., Williams, R., Dusheiko, G. & Bertoletti, A. Longitudinal analysis of CD8+ T cells specific for structural and nonstructural Hepatitis B virus proteins in patients with chronic Hepatitis B: implications for immunotherapy. *Journal of Virology* **78** (2004) 5707–5719.

[51] Wherry, E.J., Blattman, J.N., Murali-Krishna, K., van der Most, R. & Ahmed, R. Viral persistence alters CD8 T-cell immunodominance and tissue distribution and results in distinct stages of functional impairment. *Journal of virology* **77** (2003) 4911–4927.

[52] Lopes, A.R., Kellam, P., Das, A., Dunn, C., Kwan, A., Turner, J., Peppa, D., Gilson, R.J., Gehring, A., Bertoletti, A. & Maini, M.K. Bim-mediated deletion of antigen-specific CD8 T cells in patients unable to control HBV infection. *The Journal of clinical investigation* **118** (2008) 1835–45. 5.

[53] Wherry, E.J. T cell exhaustion. *Nature Immunology* **12** (2011) 492–499.

[54] Zajac, A.J., Blattman, J.N., Murali-Krishna, K., Sourdive, D.J., Suresh, M., Altman, J.D. & Ahmed, R. Viral immune evasion due to persistence of activated T cells without effector function. *The Journal of Experimental Medicine* **188** (1998) 2205–2213.

[55] Day, C.L., Kaufmann, D.E., Kiepiela, P., Brown, J.A., Moodley, E.S., Reddy, S., Mackey, E.W., Miller, J.D., Leslie, A.J., DePierres, C., Mncube, Z., Duraiswamy, J., Zhu, B., Eichbaum, Q., Altfeld, M., Wherry, E.J., Coovadia, H.M., Goulder, P.J.R., Klenerman, P., Ahmed, R., Freeman, G.J. & Walker, B.D. PD-1 expression on HIV-specific T cells is associated with T-cell exhaustion and disease progression. *Nature* **443** (2006) 350–354.

[56] Bengsch, B., Seigel, B., Ruhl, M., Timm, J., Kuntz, M., Blum, H.E., Pircher, H. & Thimme, R. Coexpression of PD-1, 2B4, CD160 and KLRG1 on exhausted HCV-specific CD8+ T cells is linked to antigen recognition and t cell differentiation. *PLoS Pathog* **6** (2010) e1000947.

[57] Nakamoto, N., Cho, H., Shaked, A., Olthoff, K., Valiga, M.E., Kaminski, M., Gostick, E., Price, D.A., Freeman, G.J., Wherry, E.J. & Chang, K.M. Synergistic reversal of intrahepatic HCV-specific CD8 T cell exhaustion by combined PD-1/CTLA-4 blockade. *PLoS pathogens* **5** (2009) e1000313.

[58] Das, A., Hoare, M., Davies, N., Lopes, A.R., Dunn, C., Kennedy, P.T., Alexander, G., Finney, H., Lawson, A., Plunkett, F.J., Bertoletti, A., Akbar, A.N. & Maini, M.K. Functional skewing of the global CD8 T cell population in chronic Hepatitis B virus infection. *J Exp Med* **205** (2008) 2111–24. 9.

[59] Schurich, A., Khanna, P., Lopes, A.R., Han, K.J., Peppa, D., Micco, L., Nebbia, G., Kennedy, P.T., Geretti, A.M., Dusheiko, G. & Maini, M.K. Role of the coinhibitory receptor cytotoxic t lymphocyte antigen-4 on apoptosis-prone CD8 T cells in persistent Hepatitis B virus infection. *Hepatology* **53** (2011) 1494–503. 5.

[60] Fisicaro, P., Valdatta, C., Massari, M., Loggi, E., Ravanetti, L., Urbani, S., Giuberti, T., Cavalli, A., Vandelli, C., Andreone, P., Missale, G. & Ferrari, C. Combined blockade of programmed death-1 and activation of CD137 increase responses of human liver T cells against HBV, but not HCV. *Gastroenterology* **143** (2012) 1576–1585.e4.

[61] Nebbia, G., Peppa, D., Schurich, A., Khanna, P., Singh, H.D., Cheng, Y., Rosenberg, W., Dusheiko, G., Gilson, R., ChinAleong, J., Kennedy, P. & Maini, M.K. Upregulation of the Tim-3/galectin-9 pathway of t cell exhaustion in chronic Hepatitis B virus infection. *PloS one* **7** (2012) e47648. 10.

[62] Maini, M.K. & Schurich, A. The molecular basis of the failed immune response in chronic HBV: therapeutic implications. *Journal of hepatology* **52** (2010) 616–9. 4.

[63] Peppa, D., Gill, U.S., Reynolds, G., Easom, N.J., Pallett, L.J., Schurich, A., Micco, L., Nebbia, G., Singh, H.D., Adams, D.H., Kennedy, P.T. & Maini, M.K. Up-regulation of

a death receptor renders antiviral T cells susceptible to NK cell-mediated deletion. *The Journal of experimental medicine* **210** (2013) 99–114. 1.

[64] Rodriguez, P.C., Quiceno, D.G. & Ochoa, A.C. L-arginine availability regulates T-lymphocyte cell-cycle progression. *Blood* **109** (2007) 1568–73. 4.

[65] Zea, A.H., Rodriguez, P.C., Culotta, K.S., Hernandez, C.P., DeSalvo, J., Ochoa, J.B., Park, H.J., Zabaleta, J. & Ochoa, A.C. L-arginine modulates CD3zeta expression and T cell function in activated human T lymphocytes. *Cell Immunol* **232** (2004) 21–31. 1-2.

[66] Rodriguez, P.C. & Ochoa, A.C. Arginine regulation by myeloid-derived suppressor cells and tolerance in cancer: mechanisms and therapeutic perspectives. *Immunological reviews* **222** (2008) 180–191.

[67] Bronte, V. & Zanovello, P. Regulation of immune responses by L-arginine metabolism. *Nat Rev Immunol* **5** (2005) 641–54. 8.

[68] Ando, K., Moriyama, T., Guidotti, L.G., Wirth, S., Schreiber, R.D., Schlicht, H.J., Huang, S.N. & Chisari, F.V. Mechanisms of class I restricted immunopathology. a transgenic mouse model of fulminant hepatitis. *The Journal of Experimental Medicine* **178** (1993) 1541–1554.

[69] Sitia, G., Isogawa, M., Kakimi, K., Wieland, S.F., Chisari, F.V. & Guidotti, L.G. Depletion of neutrophils blocks the recruitment of antigen-nonspecific cells into the liver without affecting the antiviral activity of Hepatitis B virus-specific cytotoxic T lymphocytes. *Proceedings of the National Academy of Sciences* **99** (2002) 13717–13722.

[70] Sitia, G., Isogawa, M., Iannacone, M., Campbell, I.L., Chisari, F.V. & Guidotti, L.G. MMPs are required for recruitment of antigen-nonspecific mononuclear cells into the liver by CTLs. *The Journal of Clinical Investigation* **113** (2004) 1158–1167.

[71] Kakimi, K., Lane, T.E., Wieland, S., Asensio, V.C., Campbell, I.L., Chisari, F.V. & Guidotti, L.G. Blocking chemokine responsive to gamma-2/interferon (IFN)-gamma inducible protein and monokine induced by IFN-gamma activity in vivo reduces the pathogenetic but not the antiviral potential of Hepatitis B virus-specific cytotoxic T lymphocytes. *The Journal of Experimental Medicine* **194** (2001) 1755–1766.

[72] Dunn, C., Brunetto, M., Reynolds, G., Christophides, T., Kennedy, P.T., Lampertico, P., Das, A., Lopes, A.R., Borrow, P., Williams, K., Humphreys, E., Afford, S., Adams, D.H., Bertoletti, A. & Maini, M.K. Cytokines induced during chronic Hepatitis B virus infection promote a pathway for NK cell-mediated liver damage. *J Exp Med* **204** (2007) 667–80. 3.

[73] Tan, A.T., Koh, S., Goh, W., Zhe, H.Y., Gehring, A.J., Lim, S.G. & Bertoletti, A. A longitudinal analysis of innate and adaptive immune profile during hepatic flares in chronic Hepatitis B. *Journal of Hepatology* **52** (2010) 330–339.

[74] Campbell, W.A. & Thompson, N.L. Overexpression of LAT1/CD98 light chain is sufficient to increase system l-amino acid transport activity in mouse hepatocytes but not fibroblasts. *The Journal of biological chemistry* **276** (2001) 16877–16884.

[75] Gehring, A.J., Koh, S., Chia, A., Paramasivam, K., Chew, V.S.P., Ho, Z.Z., Lee, K.H., Maini, M.K., Madhavan, K., Lim, S.G. & Bertoletti, A. Licensing virus-specific T cells to secrete the neutrophil attracting chemokine CXCL-8 during Hepatitis B virus infection. *PLoS ONE* **6** (2011) e23330.

[76] Diacovo, T.G., Puri, K.D., Warnock, R.A., Springer, T.A. & Andrian, U.H.v. Platelet-mediated lymphocyte delivery to high endothelial venules. *Science* **273** (1996) 252–255.

[77] Klenerman, P. & Thimme, R. T cell responses in Hepatitis C: the good, the bad and the unconventional. *Gut* **61** (2012) 1226–1234.

[78] McMahon, B.J. The natural history of chronic Hepatitis B virus infection. *Hepatology (Baltimore, Md.)* **49** (2009) S45–55.

[79] You, S.L., Yang, H.I. & Chen, C.J. Seropositivity of Hepatitis B e antigen and hepatocellular carcinoma. *Annals of Medicine* **36** (2004) 215–224.

[80] Kennedy, P.T.F., Sandalova, E., Jo, J., Gill, U., Ushiro-Lumb, I., Tan, A.T., Naik, S., Foster, G.R. & Bertoletti, A. Preserved T-cell function in children and young adults with immune-tolerant chronic Hepatitis B. *Gastroenterology* **143** (2012) 637–645.

[81] Chu, C.M., Yeh, C.T., Sheen, I.S. & Liaw, Y.F. Subcellular localization of Hepatitis B core antigen in relation to hepatocyte regeneration in chronic Hepatitis B. *Gastroenterology* **109** (1995) 1926–1932.

[82] Chen, C.J., Yang, H.I., Iloeje, U.H. & The REVEAL-HBV Study Group. Hepatitis B virus DNA levels and outcomes in chronic Hepatitis B. *Hepatology* **49** (2009) S72–S84.

[83] Villa, E., Fattovich, G., Mauro, A. & Pasino, M. Natural history of chronic HBV infection: special emphasis on the prognostic implications of the inactive carrier state versus chronic hepatitis. *Digestive and Liver Disease: Official Journal of the Italian Society of Gastroenterology and the Italian Association for the Study of the Liver* **43 Suppl 1** (2011) S8–14.

[84] Fattovich, G., Olivari, N., Pasino, M., D'Onofrio, M., Martone, E. & Donato, F. Long-

term outcome of chronic Hepatitis B in caucasian patients: mortality after 25 years. *Gut* **57** (2008) 84–90.

[85] Crispe, I.N. Hepatic T cells and liver tolerance. *Nature Reviews Immunology* **3** (2003) 51–62.

[86] Sheth, K. & Bankey, P. The liver as an immune organ. *Current Opinion in Critical Care* **7** (2001) 99–104.

[87] Jenne, C.N. & Kubes, P. Immune surveillance by the liver. *Nature immunology* **14** (2013) 996–1006.

[88] Bertolino, P., McCaughan, G.W. & Bowen, D.G. Role of primary intrahepatic T-cell activation in the liver tolerance effect. *Immunology and Cell Biology* **80** (2002) 84–92.

[89] Limmer, A., Ohl, J., Kurts, C., Ljunggren, H.G., Reiss, Y., Groettrup, M., Momburg, F., Arnold, B. & Knolle, P.A. Efficient presentation of exogenous antigen by liver endothelial cells to CD8+ T cells results in antigen-specific T-cell tolerance. *Nature Medicine* **6** (2000) 1348–1354.

[90] Crispe, I.N. Immune tolerance in liver disease. *Hepatology (Baltimore, Md.)* (2014).

[91] Racanelli, V. & Rehermann, B. The liver as an immunological organ. *Hepatology* **43** (2006) S54–S62.

[92] Wisse, E., Braet, F., Luo, D., De Zanger, R., Jans, D., Crabb, E. & Vermoesen, A. Structure and function of sinusoidal lining cells in the liver. *Toxicologic Pathology* **24** (1996) 100–111.

[93] Warren, A., Le Couteur, D.G., Fraser, R., Bowen, D.G., McCaughan, G.W. & Bertolino, P. T lymphocytes interact with hepatocytes through fenestrations in murine liver sinusoidal endothelial cells. *Hepatology* **44** (2006) 1182–1190.

[94] Knolle, P.A. & Thimme, R. Hepatic immune regulation and its involvement in viral hepatitis infection. *Gastroenterology* (2014).

[95] Crispe, I.N. The liver as a lymphoid organ. *Annual Review of Immunology* **27** (2009) 147–163.

[96] Diehl, L., Schurich, A., Grochtmann, R., Hegenbarth, S., Chen, L. & Knolle, P.A. Tolerogenic maturation of liver sinusoidal endothelial cells promotes B7-homolog 1-dependent CD8+ T cell tolerance. *Hepatology (Baltimore, Md.)* **47** (2008) 296–305.

[97] Knolle, P.A., Uhrig, A., Hegenbarth, S., Lser, E., Schmitt, E., Gerken, G. & Lohse, A.W.

IL-10 down-regulates T cell activation by antigen-presenting liver sinusoidal endothelial cells through decreased antigen uptake via the mannose receptor and lowered surface expression of accessory molecules. *Clinical and Experimental Immunology* **114** (1998) 427–433.

[98] Schildberg, F.A., Hegenbarth, S.I., Schumak, B., Scholz, K., Limmer, A. & Knolle, P.A. Liver sinusoidal endothelial cells veto CD8 T cell activation by antigen-presenting dendritic cells. *European Journal of Immunology* **38** (2008) 957–967.

[99] Bilzer, M., Roggel, F. & Gerbes, A.L. Role of Kupffer cells in host defense and liver disease. *Liver International: Official Journal of the International Association for the Study of the Liver* **26** (2006) 1175–1186.

[100] Wu, K., Kryczek, I., Chen, L., Zou, W. & Welling, T.H. Kupffer cell suppression of CD8+ T cells in human hepatocellular carcinoma is mediated by B7-H1/programmed death-1 interactions. *Cancer Research* **69** (2009) 8067–8075.

[101] Wu, J., Lu, M., Meng, Z., Trippler, M., Broering, R., Szczeponek, A., Krux, F., Dittmer, U., Roggendorf, M., Gerken, G. & Schlaak, J.F. Toll-like receptor-mediated control of HBV replication by nonparenchymal liver cells in mice. *Hepatology (Baltimore, Md.)* **46** (2007) 1769–1778.

[102] Bowen, D.G., Zen, M., Holz, L., Davis, T., McCaughan, G.W. & Bertolino, P. The site of primary T cell activation is a determinant of the balance between intrahepatic tolerance and immunity. *Journal of Clinical Investigation* **114** (2004) 701–712.

[103] Franco, A., Barnaba, V., Natali, P., Balsano, C., Musca, A. & Balsano, F. Expression of class i and class II major histocompatibility complex antigens on human hepatocytes. *Hepatology (Baltimore, Md.)* **8** (1988) 449–454.

[104] Chen, M., Tabaczewski, P., Truscott, S.M., Van Kaer, L. & Stroynowski, I. Hepatocytes express abundant surface class I MHC and efficiently use transporter associated with antigen processing, tapasin, and low molecular weight polypeptide proteasome subunit components of antigen processing and presentation pathway. *Journal of Immunology (Baltimore, Md.: 1950)* **175** (2005) 1047–1055.

[105] Bode, J.G., Albrecht, U., Hussinger, D., Heinrich, P.C. & Schaper, F. Hepatic acute phase proteins–regulation by IL-6- and IL-1-type cytokines involving STAT3 and its crosstalk with NF-B-dependent signaling. *European Journal of Cell Biology* **91** (2012) 496–505.

[106] Baumann, H. & Gauldie, J. The acute phase response. *Immunology Today* **15** (1994) 74–80.

[107] Benseler, V., Warren, A., Vo, M., Holz, L.E., Tay, S.S., Couteur, D.G.L., Breen, E., Allison, A.C., Rooijen, N.v., McGuffog, C., Schlitt, H.J., Bowen, D.G., McCaughan, G.W. & Bertolino, P. Hepatocyte entry leads to degradation of autoreactive CD8 T cells. *Proceedings of the National Academy of Sciences* **108** (2011) 16735–16740.

[108] Moreira, R.K. Hepatic stellate cells and liver fibrosis. *Archives of Pathology & Laboratory Medicine* **131** (2007) 1728–1734.

[109] Friedman, S.L. Hepatic stellate cells: protean, multifunctional, and enigmatic cells of the liver. *Physiological Reviews* **88** (2008) 125–172.

[110] Vinas, O., Bataller, R., Sancho-Bru, P., Gins, P., Berenguer, C., Enrich, C., Nicols, J.M., Ercilla, G., Gallart, T., Vives, J., Arroyo, V. & Rods, J. Human hepatic stellate cells show features of antigen-presenting cells and stimulate lymphocyte proliferation. *Hepatology (Baltimore, Md.)* **38** (2003) 919–929.

[111] Winau, F., Hegasy, G., Weiskirchen, R., Weber, S., Cassan, C., Sieling, P.A., Modlin, R.L., Liblau, R.S., Gressner, A.M. & Kaufmann, S.H.E. Ito cells are liver-resident antigen-presenting cells for activating T cell responses. *Immunity* **26** (2007) 117–129.

[112] Ichikawa, S., Mucida, D., Tyznik, A.J., Kronenberg, M. & Cheroutre, H. Hepatic stellate cells function as regulatory bystanders. *Journal of Immunology (Baltimore, Md.: 1950)* **186** (2011) 5549–5555.

[113] Schildberg, F.A., Wojtalla, A., Siegmund, S.V., Endl, E., Diehl, L., Abdullah, Z., Kurts, C. & Knolle, P.A. Murine hepatic stellate cells veto CD8 T cell activation by a CD54-dependent mechanism. *Hepatology (Baltimore, Md.)* **54** (2011) 262–272.

[114] Chou, H.S., Hsieh, C.C., Yang, H.R., Wang, L., Arakawa, Y., Brown, K., Wu, Q., Lin, F., Peters, M., Fung, J.J., Lu, L. & Qian, S. Hepatic stellate cells regulate immune response by way of induction of myeloid suppressor cells in mice. *Hepatology* **53** (2011) 1007–19. 3.

[115] Hochst, B., Schildberg, F.A., Sauerborn, P., Gbel, Y.A., Gevensleben, H., Goltz, D., Heukamp, L.C., Trler, A., Ballmaier, M., Gieseke, F., Mller, I., Kalff, J., Kurts, C., Knolle, P.A. & Diehl, L. Activated human hepatic stellate cells induce myeloid derived suppressor cells from peripheral blood monocytes in a CD44-dependent fashion. *Journal of Hepatology* **59** (2013) 528–535.

[116] Zhao, W., Zhang, L., Xu, Y., Zhang, Z., Ren, G., Tang, K., Kuang, P., Zhao, B., Yin, Z.

& Wang, X. Hepatic stellate cells promote tumor progression by enhancement of immunosuppressive cells in an orthotopic liver tumor mouse model. *Laboratory Investigation* **94** (2014) 182–191.

[117] Doherty, D.G., Norris, S., Madrigal-Estebas, L., McEntee, G., Traynor, O., Hegarty, J.E. & O'Farrelly, C. The human liver contains multiple populations of NK cells, T cells, and CD3+CD56+ natural T cells with distinct cytotoxic activities and Th1, Th2, and Th0 cytokine secretion patterns. *Journal of Immunology (Baltimore, Md.: 1950)* **163** (1999) 2314–2321.

[118] Doherty, D.G. & O'Farrelly, C. Innate and adaptive lymphoid cells in the human liver. *Immunological Reviews* **174** (2000) 5–20.

[119] Vivier, E., Tomasello, E., Baratin, M., Walzer, T. & Ugolini, S. Functions of natural killer cells. *Nature Immunology* **9** (2008) 503–510.

[120] Topham, N.J. & Hewitt, E.W. Natural killer cell cytotoxicity: how do they pull the trigger? *Immunology* **128** (2009) 7–15.

[121] Shields, P.L., Morland, C.M., Salmon, M., Qin, S., Hubscher, S.G. & Adams, D.H. Chemokine and chemokine receptor interactions provide a mechanism for selective T cell recruitment to specific liver compartments within Hepatitis C-infected liver. *Journal of Immunology (Baltimore, Md.: 1950)* **163** (1999) 6236–6243.

[122] Oo, Y.H., Shetty, S. & Adams, D.H. The role of chemokines in the recruitment of lymphocytes to the liver. *Digestive Diseases* **28** (2010) 31–44.

[123] Heydtmann, M., Lalor, P.F., Eksteen, J.A., Hbscher, S.G., Briskin, M. & Adams, D.H. CXC chemokine ligand 16 promotes integrin-mediated adhesion of liver-infiltrating lymphocytes to cholangiocytes and hepatocytes within the inflamed human liver. *Journal of Immunology (Baltimore, Md.: 1950)* **174** (2005) 1055–1062.

[124] Heydtmann, M. & Adams, D.H. Chemokines in the immunopathogenesis of Hepatitis C infection. *Hepatology (Baltimore, Md.)* **49** (2009) 676–688.

[125] Northfield, J.W., Kasprowicz, V., Lucas, M., Kersting, N., Bengsch, B., Bengsh, B., Kim, A., Phillips, R.E., Walker, B.D., Thimme, R., Lauer, G. & Klenerman, P. CD161 expression on Hepatitis C virus-specific CD8+ T cells suggests a distinct pathway of T cell differentiation. *Hepatology (Baltimore, Md.)* **47** (2008) 396–406.

[126] Geissmann, F., Cameron, T.O., Sidobre, S., Manlongat, N., Kronenberg, M., Briskin, M.J.,

Dustin, M.L. & Littman, D.R. Intravascular immune surveillance by CXCR6+ NKT cells patrolling liver sinusoids. *PLoS biology* **3** (2005) e113.

[127] Huang, L.R., Wohlleber, D., Reisinger, F., Jenne, C.N., Cheng, R.L., Abdullah, Z., Schildberg, F.A., Odenthal, M., Dienes, H.P., van Rooijen, N., Schmitt, E., Garbi, N., Croft, M., Kurts, C., Kubes, P., Protzer, U., Heikenwalder, M. & Knolle, P.A. Intrahepatic myeloid-cell aggregates enable local proliferation of CD8(+) T cells and successful immunotherapy against chronic viral liver infection. *Nature Immunology* **14** (2013) 574–583.

[128] Mellor, A.L. & Munn, D.H. IDO expression by dendritic cells: tolerance and tryptophan catabolism. *Nature reviews. Immunology* **4** (2004) 762–774.

[129] Larrea, E., Riezu-Boj, J.I., Gil-Guerrero, L., Casares, N., Aldabe, R., Sarobe, P., Civeira, M.P., Heeney, J.L., Rollier, C., Verstrepen, B., Wakita, T., Borrs-Cuesta, F., Lasarte, J.J. & Prieto, J. Upregulation of indoleamine 2,3-dioxygenase in Hepatitis C virus infection. *Journal of Virology* **81** (2007) 3662–3666.

[130] Yan, M.L., Wang, Y.D., Tian, Y.F., Lai, Z.D. & Yan, L.N. Inhibition of allogeneic T-cell response by Kupffer cells expressing indoleamine 2,3-dioxygenase. *World journal of gastroenterology: WJG* **16** (2010) 636–640.

[131] Srivastava, M.K., Sinha, P., Clements, V.K., Rodriguez, P. & Ostrand-Rosenberg, S. Myeloid-derived suppressor cells inhibit T-cell activation by depleting cystine and cysteine. *Cancer research* **70** (2010) 68–77. 1.

[132] Rodriguez, P.C., Ernstoff, M.S., Hernandez, C., Atkins, M., Zabaleta, J., Sierra, R. & Ochoa, A.C. Arginase I-producing myeloid-derived suppressor cells in renal cell carcinoma are a subpopulation of activated granulocytes. *Cancer Res* **69** (2009) 1553–60. 4.

[133] Gabrilovich, D.I., Ostrand-Rosenberg, S. & Bronte, V. Co-ordinated regulation of myeloid cells by tumours. *Nat Rev Immunol* **12** (2012) 253–68. 4.

[134] Laiosa, C.V., Stadtfeld, M. & Graf, T. Determinants of lymphoid-myeloid lineage diversification. *Annual Review of Immunology* **24** (2006) 705–738.

[135] Youn, J.I., Kumar, V., Collazo, M., Nefedova, Y., Condamine, T., Cheng, P., Villagra, A., Antonia, S., McCaffrey, J.C., Fishman, M., Sarnaik, A., Horna, P., Sotomayor, E. & Gabrilovich, D.I. Epigenetic silencing of retinoblastoma gene regulates pathologic differentiation of myeloid cells in cancer. *Nature Immunology* **14** (2013) 211–220.

[136] Wynn, T.A. Myeloid-cell differentiation redefined in cancer. *Nature Immunology* **14** (2013) 197–199.

[137] Bennett, J.A., Rao, V.S. & Mitchell, M.S. Systemic bacillus calmette-gurin (BCG) activates natural suppressor cells. *Proceedings of the National Academy of Sciences of the United States of America* **75** (1978) 5142–5144.

[138] Lee, M.Y. & Rosse, C. Depletion of lymphocyte subpopulations in primary and secondary lymphoid organs of mice by a transplanted granulocytosis-inducing mammary carcinoma. *Cancer research* **42** (1982) 1255–1260.

[139] Bronte, V., Wang, M., Overwijk, W.W., Surman, D.R., Pericle, F., Rosenberg, S.A. & Restifo, N.P. Apoptotic death of CD8+ T lymphocytes after immunization: induction of a suppressive population of Mac-1+/Gr-1+ cells. *The Journal of Immunology* **161** (1998) 5313–5320.

[140] Young, M.R., Wright, M.A., Matthews, J.P., Malik, I. & Prechel, M. Suppression of t cell proliferation by tumor-induced granulocyte-macrophage progenitor cells producing transforming growth factor-beta and nitric oxide. *The Journal of Immunology* **156** (1996) 1916–1922.

[141] Gabrilovich, D.I., Bronte, V., Chen, S.H., Colombo, M.P., Ochoa, A., Ostrand-Rosenberg, S. & Schreiber, H. The terminology issue for myeloid-derived suppressor cells. *Cancer Res* **67** (2007) 425; author reply 426. 1.

[142] Yang, R. & Roden, R.B.S. The terminology issue for myeloid-derived suppressor cells. *Cancer Research* **67** (2007) 426–426.

[143] Maletto, B.A., Ropolo, A.S., Alignani, D.O., Liscovsky, M.V., Ranocchia, R.P., Moron, V.G. & Pistoresi-Palencia, M.C. Presence of neutrophil-bearing antigen in lymphoid organs of immune mice. *Blood* **108** (2006) 3094–3102.

[144] Dancey, J.T., Deubelbeiss, K.A., Harker, L.A. & Finch, C.A. Neutrophil kinetics in man. *The Journal of clinical investigation* **58** (1976) 705–715.

[145] Dresch, C., Najean, Y. & Bauchet, J. Kinetic studies of 51cr and DF32p labelled granulocytes. *British journal of haematology* **29** (1975) 67–80.

[146] Pillay, J., den Braber, I., Vrisekoop, N., Kwast, L.M., de Boer, R.J., Borghans, J.A.M., Tesselaar, K. & Koenderman, L. In vivo labeling with 2h2o reveals a human neutrophil lifespan of 5.4 days. *Blood* **116** (2010) 625–627.

[147] Li, K.W., Turner, S.M., Emson, C.L., Hellerstein, M.K. & Dale, D.C. Deuterium and neutrophil kinetics. *Blood* **117** (2011) 6052–6053; author reply 6053–6054.

[148] Rathmell, J.C. Metabolism and autophagy in the immune system: immunometabolism comes of age. *Immunological Reviews* **249** (2012) 5–13.

[149] Sinclair, L.V., Rolf, J., Emslie, E., Shi, Y.B., Taylor, P.M. & Cantrell, D.A. Control of amino-acid transport by antigen receptors coordinates the metabolic reprogramming essential for T cell differentiation. *Nature immunology* **14** (2013) 500–508.

[150] Verrey, F., Closs, E.I., Wagner, C.A., Palacin, M., Endou, H. & Kanai, Y. CATs and HATs: the SLC7 family of amino acid transporters. *Pflgers Archiv* **447** (2004) 532–542.

[151] Cantor, J.M. & Ginsberg, M.H. CD98 at the crossroads of adaptive immunity and cancer. *Journal of cell science* **125** (2012) 1373–1382.

[152] Cantor, J., Slepak, M., Ege, N., Chang, J.T. & Ginsberg, M.H. Loss of T cell CD98 H-chain specifically ablates T cell clonal expansion and protects from autoimmunity. *The Journal of Immunology* **187** (2011) 851–860.

[153] Cantor, J., Browne, C.D., Ruppert, R., Fral, C.C., Fssler, R., Rickert, R.C. & Ginsberg, M.H. CD98hc facilitates B cell proliferation and adaptive humoral immunity. *Nature Immunology* **10** (2009) 412–419.

[154] Cobbold, S.P., Adams, E., Farquhar, C.A., Nolan, K.F., Howie, D., Lui, K.O., Fairchild, P.J., Mellor, A.L., Ron, D. & Waldmann, H. Infectious tolerance via the consumption of essential amino acids and mTOR signaling. *Proc Natl Acad Sci U S A* **106** (2009) 12055–60. 29.

[155] Ishak, K., Baptista, A., Bianchi, L., Callea, F., De Groote, J., Gudat, F., Denk, H., Desmet, V., Korb, G. & MacSween, R.N. Histological grading and staging of chronic hepatitis. *Journal of Hepatology* **22** (1995) 696–699.

[156] Medzhitov, R., Shevach, E.M., Trinchieri, G., Mellor, A.L., Munn, D.H., Gordon, S., Libby, P., Hansson, G.K., Shortman, K., Dong, C., Gabrilovich, D., Gabryov, L., Howes, A. & O'Garra, A. Highlights of 10 years of immunology. *Nature Reviews Immunology* **11** (2011) 693–702.

[157] Manjili, M.H. Phenotypic plasticity of MDSC in cancers. *Immunological Investigations* **41** (2012) 711–721.

[158] Solito, S., Marigo, I., Pinton, L., Damuzzo, V., Mandruzzato, S. & Bronte, V. Myeloid-derived suppressor cell heterogeneity in human cancers. *Annals of the New York Academy of Sciences* **1319** (2014) 47–65.

[159] Youn, J.I., Nagaraj, S., Collazo, M. & Gabrilovich, D.I. Subsets of myeloid-derived suppressor cells in tumor-bearing mice. *J Immunol* **181** (2008) 5791–802. 8.

[160] Youn, J.I., Collazo, M., Shalova, I.N., Biswas, S.K. & Gabrilovich, D.I. Characterization of the nature of granulocytic myeloid-derived suppressor cells in tumor-bearing mice. *Journal of leukocyte biology* **91** (2012) 167–181.

[161] Fridlender, Z.G., Sun, J., Mishalian, I., Singhal, S., Cheng, G., Kapoor, V., Horng, W., Fridlender, G., Bayuh, R., Worthen, G.S. & Albelda, S.M. Transcriptomic analysis comparing tumor-associated neutrophils with granulocytic myeloid-derived suppressor cells and normal neutrophils. *PloS one* **7** (2012) e31524.

[162] Haile, L.A., Gamrekelashvili, J., Manns, M.P., Korangy, F. & Greten, T.F. CD49d is a new marker for distinct myeloid-derived suppressor cell subpopulations in mice. *Journal of Immunology (Baltimore, Md.: 1950)* **185** (2010) 203–210.

[163] Pak, A.S., Wright, M.A., Matthews, J.P., Collins, S.L., Petruzzelli, G.J. & Young, M.R. Mechanisms of immune suppression in patients with head and neck cancer: presence of CD34(+) cells which suppress immune functions within cancers that secrete granulocyte-macrophage colony-stimulating factor. *Clinical cancer research: an official journal of the American Association for Cancer Research* **1** (1995) 95–103.

[164] Gabrilovich, D.I. & Nagaraj, S. Myeloid-derived suppressor cells as regulators of the immune system. *Nat Rev Immunol* **9** (2009) 162–74. 3.

[165] Brandau, S., Moses, K. & Lang, S. The kinship of neutrophils and granulocytic myeloid-derived suppressor cells in cancer: Cousins, siblings or twins? *Seminars in cancer biology* (2013).

[166] Khaled, Y.S., Ammori, B.J. & Elkord, E. Myeloid-derived suppressor cells in cancer: recent progress and prospects. *Immunology and Cell Biology* **91** (2013) 493–502.

[167] Greten, T.F., Manns, M.P. & Korangy, F. Myeloid derived suppressor cells in human diseases. *International Immunopharmacology* **11** (2011) 802–807.

[168] Poschke, I. & Kiessling, R. On the armament and appearances of human myeloid-derived suppressor cells. *Clinical immunology* **144** (2012) 250–68. 3.

[169] Almand B, Clark JI, N.E.v.B.J.E.N.K.S.C.D.G.D. Increased production of immature myeloid cells in cancer patients: a mechanism of immunosuppression in cancer. *Journal of immunology (Baltimore, Md.: 1950)* **166** (2001) 678–689.

[170] Ochoa, A.C., Zea, A.H., Hernandez, C. & Rodriguez, P.C. Arginase, prostaglandins, and

myeloid-derived suppressor cells in renal cell carcinoma. *Clinical Cancer Research* **13** (2007) 721s–726s.

[171] Ostrand-Rosenberg, S. & Sinha, P. Myeloid-derived suppressor cells: linking inflammation and cancer. *J Immunol* **182** (2009) 4499–506. 8.

[172] Ostrand-Rosenberg, S. Myeloid-derived suppressor cells: more mechanisms for inhibiting antitumor immunity. *Cancer Immunology, Immunotherapy* **59** (2010) 1593–1600.

[173] Talmadge, J.E. & Gabrilovich, D.I. History of myeloid-derived suppressor cells. *Nature reviews. Cancer* **13** (2013) 739–752.

[174] Bronte, V., Chappell, D.B., Apolloni, E., Cabrelle, A., Wang, M., Hwu, P. & Restifo, N.P. Unopposed production of granulocyte-macrophage colony-stimulating factor by tumors inhibits CD8+ T cell responses by dysregulating antigen-presenting cell maturation. *Journal of Immunology (Baltimore, Md.: 1950)* **162** (1999) 5728–5737.

[175] Zhang, Y., Liu, Q., Zhang, M., Yu, Y., Liu, X. & Cao, X. Fas signal promotes lung cancer growth by recruiting myeloid-derived suppressor cells via cancer cell-derived PGE2. *Journal of Immunology (Baltimore, Md.: 1950)* **182** (2009) 3801–3808.

[176] Sinha, P., Clements, V.K., Fulton, A.M. & Ostrand-Rosenberg, S. Prostaglandin E2 promotes tumor progression by inducing myeloid-derived suppressor cells. *Cancer Research* **67** (2007) 4507–4513.

[177] Bunt, S.K., Yang, L., Sinha, P., Clements, V.K., Leips, J. & Ostrand-Rosenberg, S. Reduced inflammation in the tumor microenvironment delays the accumulation of myeloid-derived suppressor cells and limits tumor progression. *Cancer Research* **67** (2007) 10019–10026.

[178] Nefedova, Y., Nagaraj, S., Rosenbauer, A., Muro-Cacho, C., Sebti, S.M. & Gabrilovich, D.I. Regulation of dendritic cell differentiation and antitumor immune response in cancer by pharmacologic-selective inhibition of the janus-activated kinase 2/signal transducers and activators of transcription 3 pathway. *Cancer research* **65** (2005) 9525–9535.

[179] Kortylewski, M., Kujawski, M., Wang, T., Wei, S., Zhang, S., Pilon-Thomas, S., Niu, G., Kay, H., Mul, J., Kerr, W.G., Jove, R., Pardoll, D. & Yu, H. Inhibiting STAT3 signaling in the hematopoietic system elicits multicomponent antitumor immunity. *Nature Medicine* **11** (2005) 1314–1321.

[180] Cheng, P., Corzo, C.A., Luetteke, N., Yu, B., Nagaraj, S., Bui, M.M., Ortiz, M., Nacken, W., Sorg, C., Vogl, T., Roth, J. & Gabrilovich, D.I. Inhibition of dendritic cell differ-

entiation and accumulation of myeloid-derived suppressor cells in cancer is regulated by S100A9 protein. *J Exp Med* **205** (2008) 2235–49. 10.

[181] Vasquez-Dunddel, D., Pan, F., Zeng, Q., Gorbounov, M., Albesiano, E., Fu, J., Blosser, R.L., Tam, A.J., Bruno, T., Zhang, H., Pardoll, D. & Kim, Y. STAT3 regulates arginase-I in myeloid-derived suppressor cells from cancer patients. *The Journal of Clinical Investigation* **123** (2013) 1580–1589.

[182] Sander, L.E., Sackett, S.D., Dierssen, U., Beraza, N., Linke, R.P., Mller, M., Blander, J.M., Tacke, F. & Trautwein, C. Hepatic acute-phase proteins control innate immune responses during infection by promoting myeloid-derived suppressor cell function. *The Journal of experimental medicine* **207** (2010) 1453–1464.

[183] Kusmartsev, S. & Gabrilovich, D.I. STAT1 signaling regulates tumor-associated macrophage-mediated T cell deletion. *Journal of Immunology (Baltimore, Md.: 1950)* **174** (2005) 4880–4891.

[184] Movahedi, K., Guilliams, M., Van den Bossche, J., Van den Bergh, R., Gysemans, C., Beschin, A., De Baetselier, P. & Van Ginderachter, J.A. Identification of discrete tumor-induced myeloid-derived suppressor cell subpopulations with distinct T cell-suppressive activity. *Blood* **111** (2008) 4233–4244.

[185] Kusmartsev, S., Nagaraj, S. & Gabrilovich, D.I. Tumor-associated CD8+ T cell tolerance induced by bone marrow-derived immature myeloid cells. *Journal of Immunology (Baltimore, Md.: 1950)* **175** (2005) 4583–4592.

[186] Bronstein-Sitton, N., Cohen-Daniel, L., Vaknin, I., Ezernitchi, A.V., Leshem, B., Halabi, A., Houri-Hadad, Y., Greenbaum, E., Zakay-Rones, Z., Shapira, L. & Baniyash, M. Sustained exposure to bacterial antigen induces interferon-gamma-dependent T cell receptor zeta down-regulation and impaired T cell function. *Nat Immunol* **4** (2003) 957–64. 10.

[187] Ezernitchi, A.V., Vaknin, I., Cohen-Daniel, L., Levy, O., Manaster, E., Halabi, A., Pikarsky, E., Shapira, L. & Baniyash, M. TCR zeta down-regulation under chronic inflammation is mediated by myeloid suppressor cells differentially distributed between various lymphatic organs. *J Immunol* **177** (2006) 4763–72. 7.

[188] Vaknin, I., Blinder, L., Wang, L., Gazit, R., Shapira, E., Genina, O., Pines, M., Pikarsky, E. & Baniyash, M. A common pathway mediated through toll-like receptors leads to t- and natural killer-cell immunosuppression. *Blood* **111** (2008) 1437–1447.

[189] Sade-Feldman, M., Kanterman, J., Ish-Shalom, E., Elnekave, M., Horwitz, E. & Baniyash,

M. Tumor necrosis factor-alpha blocks differentiation and enhances suppressive activity of immature myeloid cells during chronic inflammation. *Immunity* (2013).

[190] Norris, B.A., Uebelhoer, L.S., Nakaya, H.I., Price, A.A., Grakoui, A. & Pulendran, B. Chronic but not acute virus infection induces sustained expansion of myeloid suppressor cell numbers that inhibit viral-specific T cell immunity. *Immunity* **38** (2013) 309–21. 2.

[191] Jeisy-Scott, V., Davis, W.G., Patel, J.R., Bowzard, J.B., Shieh, W.J., Zaki, S.R., Katz, J.M. & Sambhara, S. Increased MDSC accumulation and Th2 biased response to Influenza A virus infection in the absence of TLR7 in mice. *PLoS ONE* **6** (2011) e25242.

[192] Tacke, R.S., Lee, H.C., Goh, C., Courtney, J., Polyak, S.J., Rosen, H.R. & Hahn, Y.S. Myeloid suppressor cells induced by Hepatitis C virus suppress T-cell responses through the production of reactive oxygen species. *Hepatology (Baltimore, Md.)* **55** (2012) 343–353.

[193] Cai, W., Qin, A., Guo, P., Yan, D., Hu, F., Yang, Q., Xu, M., Fu, Y., Zhou, J. & Tang, X. Clinical significance and functional studies of myeloid-derived suppressor cells in chronic Hepatitis C patients. *Journal of clinical immunology* (2013).

[194] Hoechst, B., Ormandy, L.A., Ballmaier, M., Lehner, F., Krger, C., Manns, M.P., Greten, T.F. & Korangy, F. A new population of myeloid-derived suppressor cells in hepatocellular carcinoma patients induces CD4(+)CD25(+)FOXP3(+) T cells. *Gastroenterology* **135** (2008) 234–243.

[195] Hoechst, B., Voigtlaender, T., Ormandy, L., Gamrekelashvili, J., Zhao, F., Wedemeyer, H., Lehner, F., Manns, M.P., Greten, T.F. & Korangy, F. Myeloid-derived suppressor cells inhibit natural killer cells in patients with hepatocellular carcinoma via the NKp30 receptor. *Hepatology (Baltimore, Md.)* **50** (2009) 799–807.

[196] Qin, A., Cai, W., Pan, T., Wu, K., Yang, Q., Wang, N., Liu, Y., Yan, D., Hu, F., Guo, P., Chen, X., Chen, L., Zhang, H., Tang, X. & Zhou, J. Expansion of monocytic myeloid-derived suppressor cells dampens T cell function in HIV-1-seropositive individuals. *Journal of virology* **87** (2013) 1477–90. 3.

[197] Garg, A. & Spector, S.A. HIV-1 gp120 induced expansion of myeloid-derived suppressor cells is dependent on interleukin-6 and suppresses immunity. *The Journal of infectious diseases* (2013).

[198] Vollbrecht, T., Stirner, R., Tufman, A., Roider, J., Huber, R.M., Bogner, J.R., Lechner, A., Bourquin, C. & Draenert, R. Chronic progressive HIV-1 infection is associated with elevated levels of myeloid-derived suppressor cells. *AIDS* **26** (2012) F31–7. 12.

[199] Kotsakis, A., Harasymczuk, M., Schilling, B., Georgoulias, V., Argiris, A. & Whiteside, T.L. Myeloid-derived suppressor cell measurements in fresh and cryopreserved blood samples. *Journal of immunological methods* **381** (2012) 14–22. 1-2.

[200] Reich, D., Nalls, M.A., Kao, W.H.L., Akylbekova, E.L., Tandon, A., Patterson, N., Mullikin, J., Hsueh, W.C., Cheng, C.Y., Coresh, J., Boerwinkle, E., Li, M., Waliszewska, A., Neubauer, J., Li, R., Leak, T.S., Ekunwe, L., Files, J.C., Hardy, C.L., Zmuda, J.M., Taylor, H.A., Ziv, E., Harris, T.B. & Wilson, J.G. Reduced neutrophil count in people of african descent is due to a regulatory variant in the duffy antigen receptor for chemokines gene. *PLoS Genet* **5** (2009) e1000360.

[201] Verschoor, C.P., Johnstone, J., Millar, J., Dorrington, M.G., Habibagahi, M., Lelic, A., Loeb, M., Bramson, J.L. & Bowdish, D.M. Blood CD33(+)HLA-DR(-) myeloid-derived suppressor cells are increased with age and a history of cancer. *Journal of leukocyte biology* (2013).

[202] Enioutina, E.Y., Bareyan, D. & Daynes, R.A. A role for immature myeloid cells in immune senescence. *Journal of immunology* **186** (2011) 697–707. 2.

[203] Chu, C.M., Sheen, I.S., Lin, S.M. & Liaw, Y.F. Sex difference in chronic Hepatitis B virus infection: studies of serum HBeAg and alanine aminotransferase levels in 10,431 asymptomatic chinese HBsAg carriers. *Clinical infectious diseases: an official publication of the Infectious Diseases Society of America* **16** (1993) 709–713.

[204] Kostlin, N., Kugel, H., Spring, B., Leiber, A., Marm, A., Henes, M., Rieber, N., Hartl, D., Poets, C.F. & Gille, C. Granulocytic myeloid-derived suppressor cells expand in human pregnancy and modulate T-cell responses. *European Journal of Immunology* (2014).

[205] Liu, Y., She, L.H., Wang, X.Y., Zhang, G.L., Yan, Y., Lin, C.S., Zhao, Z.X. & Gao, Z.L. Expansion of myeloid-derived suppressor cells from peripheral blood decreases after 4-week antiviral treatment in patients with chronic Hepatitis C. *International Journal of Clinical and Experimental Medicine* **7** (2014) 998–1004.

[206] Zeng, Q.L., Yang, B., Sun, H.Q., Feng, G.H., Jin, L., Zou, Z.S., Zhang, Z., Zhang, J.Y. & Wang, F.S. Myeloid-derived suppressor cells are associated with viral persistence and downregulation of TCRzeta chain expression on CD8(+) T cells in chronic Hepatitis C patients. *Molecules and cells* **37** (2014) 66–73.

[207] Protzer, U., Maini, M.K. & Knolle, P.A. Living in the liver: hepatic infections. *Nat Rev Immunol* **12** (2012) 201–13. 3.

[208] Daley-Bauer, L.P., Wynn, G.M. & Mocarski, E.S. Cytomegalovirus impairs antiviral CD8+ T cell immunity by recruiting inflammatory monocytes. *Immunity* **37** (2012) 122–133.

[209] Ma, Q., Jones, D. & Springer, T.A. The chemokine receptor CXCR4 is required for the retention of B lineage and granulocytic precursors within the bone marrow microenvironment. *Immunity* **10** (1999) 463–471.

[210] Eash, K.J., Means, J.M., White, D.W. & Link, D.C. CXCR4 is a key regulator of neutrophil release from the bone marrow under basal and stress granulopoiesis conditions. *Blood* **113** (2009) 4711–4719.

[211] Schraufstatter, I.U., Chung, J. & Burger, M. IL-8 activates endothelial cell CXCR1 and CXCR2 through Rho and Rac signalling pathways. *American Journal of Physiology - Lung Cellular and Molecular Physiology* **280** (2001) L1094–L1103.

[212] Lechner, M.G., Megiel, C., Russell, S.M., Bingham, B., Arger, N., Woo, T. & Epstein, A.L. Functional characterization of human CD33+ and CD11b+ myeloid-derived suppressor cell subsets induced from peripheral blood mononuclear cells co-cultured with a diverse set of human tumor cell lines. *J Transl Med* **9** (2011) 90.

[213] Das, A., Ellis, G., Pallant, C., Lopes, A.R., Khanna, P., Peppa, D., Chen, A., Blair, P., Dusheiko, G., Gill, U., Kennedy, P.T., Brunetto, M., Lampertico, P., Mauri, C. & Maini, M.K. IL-10-producing regulatory B cells in the pathogenesis of chronic Hepatitis B virus infection. *J Immunol* **189** (2012) 3925–35. 8.

[214] Chen, S., Akbar, S.M., Abe, M., Hiasa, Y. & Onji, M. Immunosuppressive functions of hepatic myeloid-derived suppressor cells of normal mice and in a murine model of chronic hepatitis B virus. *Clinical and experimental immunology* **166** (2011) 134–42. 1.

[215] Nonnenmann, J., Stirner, R., Roider, J., Jung, M.C., Schrdl, K., Bogner, J.R. & Draenert, R. Lack of significant elevation of myeloid-derived suppressor cells in peripheral blood of chronically HCV infected individuals. *Journal of virology* (2014).

[216] Corzo, C.A., Condamine, T., Lu, L., Cotter, M.J., Youn, J.I., Cheng, P., Cho, H.I., Celis, E., Quiceno, D.G., Padhya, T., McCaffrey, T.V., McCaffrey, J.C. & Gabrilovich, D.I. HIF-1 regulates function and differentiation of myeloid-derived suppressor cells in the tumor microenvironment. *The Journal of experimental medicine* **207** (2010) 2439–2453.

[217] Hosel, M., Quasdorff, M., Wiegmann, K., Webb, D., Zedler, U., Broxtermann, M., Tedjokusumo, R., Esser, K., Arzberger, S., Kirschning, C.J., Langenkamp, A., Falk, C., Bun-

ing, H., Rose-John, S. & Protzer, U. Not interferon, but interleukin-6 controls early gene expression in Hepatitis B virus infection. *Hepatology* **50** (2009) 1773–82. 6.

[218] Klein, C., Wstefeld, T., Assmus, U., Roskams, T., Rose-John, S., Mller, M., Manns, M.P., Ernst, M. & Trautwein, C. The IL-6-gp130-STAT3 pathway in hepatocytes triggers liver protection in T cell-mediated liver injury. *The Journal of Clinical Investigation* **115** (2005) 860–869.

[219] Condamine, T. & Gabrilovich, D.I. Molecular mechanisms regulating myeloid-derived suppressor cell differentiation and function. *Trends in immunology* **32** (2011) 19–25.

[220] Marigo, I., Bosio, E., Solito, S., Mesa, C., Fernandez, A., Dolcetti, L., Ugel, S., Sonda, N., Bicciato, S., Falisi, E., Calabrese, F., Basso, G., Zanovello, P., Cozzi, E., Mandruzzato, S. & Bronte, V. Tumor-induced tolerance and immune suppression depend on the C/EBPbeta transcription factor. *Immunity* **32** (2010) 790–802.

[221] Gabrilovich, D.I., Chen, H.L., Girgis, K.R., Cunningham, H.T., Meny, G.M., Nadaf, S., Kavanaugh, D. & Carbone, D.P. Production of vascular endothelial growth factor by human tumors inhibits the functional maturation of dendritic cells. *Nature Medicine* **2** (1996) 1096–1103.

[222] Kusmartsev, S., Eruslanov, E., Kbler, H., Tseng, T., Sakai, Y., Su, Z., Kaliberov, S., Heiser, A., Rosser, C., Dahm, P., Siemann, D. & Vieweg, J. Oxidative stress regulates expression of VEGFR1 in myeloid cells: link to tumor-induced immune suppression in renal cell carcinoma. *The Journal of Immunology* **181** (2008) 346–353.

[223] Su, I.J., Wu, H.C., Tsai, H.W., Teng, C.F., Hsieh, W.C., Lin, Y.J., Wang, L.H.C. & Yuan, Q. Ground glass hepatocytes coexpressing Hepatitis B virus X protein and surface antigens effect on oncogenic effects and tumorigenesis. *Journal of Clinical Oncology* **32** (2014).

[224] Yang, J.C., Teng, C.F., Wu, H.C., Tsai, H.W., Chuang, H.C., Tsai, T.F., Hsu, Y.H., Huang, W., Wu, L.W. & Su, I.J. Enhanced expression of vascular endothelial growth factor-A in ground glass hepatocytes and its implication in Hepatitis B virus hepatocarcinogenesis. *Hepatology* **49** (2009) 1962–1971.

[225] Ilkovitch, D. & Lopez, D.M. Urokinase-mediated recruitment of myeloid-derived suppressor cells and their suppressive mechanisms are blocked by MUC1/sec. *Blood* **113** (2009) 4729–39. 19.

[226] Grohmann, U. & Bronte, V. Control of immune response by amino acid metabolism. *Immunological Reviews* **236** (2010) 243–264.

[227] Yang, B., Wang, X. & Ren, X. Amino acid metabolism related to immune tolerance by MDSCs. *International Reviews of Immunology* **31** (2012) 177–183.

[228] Barbul, A., Rettura, G., Levenson, S.M. & Seifter, E. Arginine: a thymotropic and wound-healing promoting agent. *Surgical Forum* **28** (1977) 101–103.

[229] Rodriguez, P.C., Hernandez, C.P., Morrow, K., Sierra, R., Zabaleta, J., Wyczechowska, D.D. & Ochoa, A.C. L-arginine deprivation regulates cyclin d3 mRNA stability in human T cells by controlling HuR expression. *Journal of immunology (Baltimore, Md.: 1950)* **185** (2010) 5198–5204.

[230] Munn, D.H., Sharma, M.D., Baban, B., Harding, H.P., Zhang, Y., Ron, D. & Mellor, A.L. GCN2 kinase in T cells mediates proliferative arrest and anergy induction in response to indoleamine 2,3-dioxygenase. *Immunity* **22** (2005) 633–642.

[231] Kimball, S.R. & Jefferson, L.S. Role of amino acids in the translational control of protein synthesis in mammals. *Seminars in Cell & Developmental Biology* **16** (2005) 21–27.

[232] Baniyash, M. TCR zeta-chain downregulation: curtailing an excessive inflammatory immune response. *Nat Rev Immunol* **4** (2004) 675–87. 9.

[233] Kim, D.H., Sarbassov, D.D., Ali, S.M., King, J.E., Latek, R.R., Erdjument-Bromage, H., Tempst, P. & Sabatini, D.M. mTOR interacts with Raptor to form a nutrient-sensitive complex that signals to the cell growth machinery. *Cell* **110** (2002) 163–175.

[234] Hara, K., Yonezawa, K., Weng, Q.P., Kozlowski, M.T., Belham, C. & Avruch, J. Amino acid sufficiency and mTOR regulate p70 S6 kinase and eIF-4E BP1 through a common effector mechanism. *The Journal of biological chemistry* **273** (1998) 14484–14494.

[235] Chappert, P. & Schwartz, R.H. Induction of T cell anergy: integration of environmental cues and infectious tolerance. *Curr Opin Immunol* **22** (2010) 552–9. 5.

[236] Brito, C., Naviliat, M., Tiscornia, A.C., Vuillier, F., Gualco, G., Dighiero, G., Radi, R. & Cayota, A.M. Peroxynitrite inhibits T lymphocyte activation and proliferation by promoting impairment of tyrosine phosphorylation and peroxynitrite-driven apoptotic death. *Journal of Immunology (Baltimore, Md.: 1950)* **162** (1999) 3356–3366.

[237] Nagaraj, S., Gupta, K., Pisarev, V., Kinarsky, L., Sherman, S., Kang, L., Herber, D.L., Schneck, J. & Gabrilovich, D.I. Altered recognition of antigen is a mechanism of CD8+ T cell tolerance in cancer. *Nature medicine* **13** (2007) 828–35. 7.

[238] Godin-Ethier, J., Hanafi, L.A., Piccirillo, C.A. & Lapointe, R. Indoleamine 2,3-dioxygenase expression in human cancers: clinical and immunologic perspectives. *Clinical cancer re-*

search: an official journal of the American Association for Cancer Research **17** (2011) 6985–6991.

[239] Munn, D.H. Indoleamine 2,3-dioxygenase, tumor-induced tolerance and counter-regulation. *Current Opinion in Immunology* **18** (2006) 220–225.

[240] Taylor, M.W. & Feng, G.S. Relationship between interferon-gamma, indoleamine 2,3-dioxygenase, and tryptophan catabolism. *The FASEB Journal* **5** (1991) 2516–2522.

[241] Schmidt, S.K., Mller, A., Heseler, K., Woite, C., Spekker, K., MacKenzie, C.R. & Dubener, W. Antimicrobial and immunoregulatory properties of human tryptophan 2,3-dioxygenase. *European Journal of Immunology* **39** (2009) 2755–2764.

[242] Yu, J., Du, W., Yan, F., Wang, Y., Li, H., Cao, S., Yu, W., Shen, C., Liu, J. & Ren, X. Myeloid-derived suppressor cells suppress antitumor immune responses through IDO expression and correlate with lymph node metastasis in patients with breast cancer. *J Immunol* **190** (2013) 3783–97. 7.

[243] Watkins, S.K., Zhu, Z., Riboldi, E., Shafer-Weaver, K.A., Stagliano, K.E.R., Sklavos, M.M., Ambs, S., Yagita, H. & Hurwitz, A.A. FOXO3 programs tumor-associated DCs to become tolerogenic in human and murine prostate cancer. *The Journal of clinical investigation* **121** (2011) 1361–1372.

[244] Arnr, E.S. & Holmgren, A. Physiological functions of thioredoxin and thioredoxin reductase. *European journal of biochemistry / FEBS* **267** (2000) 6102–6109.

[245] Eagle, H., Washington, C. & Friedman, S.M. The synthesis of homocystine, cystathionine, and cystine by cultured diploid and heteroploid human cells. *Proceedings of the National Academy of Sciences of the United States of America* **56** (1966) 156–163.

[246] Bannai, S. Transport of cystine and cysteine in mammalian cells. *Biochim Biophys Acta* **779** (1984) 289–306. 3.

[247] Angelini, G., Gardella, S., Ardy, M., Ciriolo, M.R., Filomeni, G., Trapani, G.D., Clarke, F., Sitia, R. & Rubartelli, A. Antigen-presenting dendritic cells provide the reducing extracellular microenvironment required for T lymphocyte activation. *Proceedings of the National Academy of Sciences* **99** (2002) 1491–1496.

[248] Gmnder, H., Eck, H.P., Benninghoff, B., Roth, S. & Drge, W. Macrophages regulate intracellular glutathione levels of lymphocytes. evidence for an immunoregulatory role of cysteine. *Cellular Immunology* **129** (1990) 32–46.

[249] Boulland, M.L., Marquet, J., Molinier-Frenkel, V., Mller, P., Guiter, C., Lasoudris, F.,

Copie-Bergman, C., Baia, M., Gaulard, P., Leroy, K. & Castellano, F. Human IL4i1 is a secreted l-phenylalanine oxidase expressed by mature dendritic cells that inhibits T-lymphocyte proliferation. *Blood* **110** (2007) 220–227.

[250] Gallina, G., Dolcetti, L., Serafini, P., De Santo, C., Marigo, I., Colombo, M.P., Basso, G., Brombacher, F., Borrello, I., Zanovello, P., Bicciato, S. & Bronte, V. Tumors induce a subset of inflammatory monocytes with immunosuppressive activity on CD8+ T cells. *The Journal of Clinical Investigation* **116** (2006) 2777–2790.

[251] Shi, O., Morris, Jr, S.M., Zoghbi, H., Porter, C.W. & O'Brien, W.E. Generation of a mouse model for arginase II deficiency by targeted disruption of the arginase II gene. *Molecular and cellular biology* **21** (2001) 811–813.

[252] Munder, M., Mollinedo, F., Calafat, J., Canchado, J., Gil-Lamaignere, C., Fuentes, J.M., Luckner, C., Doschko, G., Soler, G., Eichmann, K., Mller, F.M., Ho, A.D., Goerner, M. & Modolell, M. Arginase I is constitutively expressed in human granulocytes and participates in fungicidal activity. *Blood* **105** (2005) 2549–2556.

[253] Munder, M., Schneider, H., Luckner, C., Giese, T., Langhans, C.D., Fuentes, J.M., Kropf, P., Mueller, I., Kolb, A., Modolell, M. & Ho, A.D. Suppression of T-cell functions by human granulocyte arginase. *Blood* **108** (2006) 1627–1634.

[254] Rodriguez, P.C., Zea, A.H., DeSalvo, J., Culotta, K.S., Zabaleta, J., Quiceno, D.G., Ochoa, J.B. & Ochoa, A.C. L-arginine consumption by macrophages modulates the expression of CD3zeta chain in T lymphocytes. *The Journal of Immunology* **171** (2003) 1232–1239.

[255] Rodriguez, P.C., Quiceno, D.G., Zabaleta, J., Ortiz, B., Zea, A.H., Piazuelo, M.B., Delgado, A., Correa, P., Brayer, J., Sotomayor, E.M., Antonia, S., Ochoa, J.B. & Ochoa, A.C. Arginase I production in the tumor microenvironment by mature myeloid cells inhibits T-cell receptor expression and antigen-specific T-cell responses. *Cancer Res* **64** (2004) 5839–49. 16.

[256] Lindau, D., Gielen, P., Kroesen, M., Wesseling, P. & Adema, G.J. The immunosuppressive tumour network: myeloid-derived suppressor cells, regulatory T cells and natural killer T cells. *Immunology* **138** (2013) 105–115.

[257] Rotondo, R., Bertolotto, M., Barisione, G., Astigiano, S., Mandruzzato, S., Ottonello, L., Dallegri, F., Bronte, V., Ferrini, S. & Barbieri, O. Exocytosis of azurophil and arginase I-containing granules by activated polymorphonuclear neutrophils is required to inhibit T lymphocyte proliferation. *Journal of Leukocyte Biology* **89** (2011) 721–727.

[258] Kuijpers, T.W., Tool, A.T., van der Schoot, C.E., Ginsel, L.A., Onderwater, J.J., Roos, D. & Verhoeven, A.J. Membrane surface antigen expression on neutrophils: a reappraisal of the use of surface markers for neutrophil activation. *Blood* **78** (1991) 1105–1111.

[259] Frumento, G., Rotondo, R., Tonetti, M., Damonte, G., Benatti, U. & Ferrara, G.B. Tryptophan-derived catabolites are responsible for inhibition of T and natural killer cell proliferation induced by indoleamine 2,3-dioxygenase. *The Journal of experimental medicine* **196** (2002) 459–468.

[260] Maini, M.K., Boni, C., Ogg, G.S., King, A.S., Reignat, S., Lee, C.K., Larrubia, J.R., Webster, G.J., McMichael, A.J., Ferrari, C., Williams, R., Vergani, D. & Bertoletti, A. Direct ex vivo analysis of Hepatitis B virus-specific CD8(+) T cells associated with the control of infection. *Gastroenterology* **117** (1999) 1386–1396.

[261] Rodriguez, P.C., Zea, A.H., Culotta, K.S., Zabaleta, J., Ochoa, J.B. & Ochoa, A.C. Regulation of T cell receptor CD3zeta chain expression by L-arginine. *The Journal of biological chemistry* **277** (2002) 21123–21129.

[262] Hayashi, K., Jutabha, P., Endou, H., Sagara, H. & Anzai, N. LAT1 is a critical transporter of essential amino acids for immune reactions in activated human T cells. *Journal of immunology (Baltimore, Md.: 1950)* **191** (2013) 4080–4085.

[263] Campbell, W.A., Sah, D.E., Medina, M.M., Albina, J.E., Coleman, W.B. & Thompson, N.L. TA1/LAT-1/CD98 light chain and system l activity, but not 4F2/CD98 heavy chain, respond to arginine availability in rat hepatic cells. loss of response in tumor cells. *The Journal of biological chemistry* **275** (2000) 5347–5354.

[264] Mieulet, V., Yan, L., Choisy, C., Sully, K., Procter, J., Kouroumalis, A., Krywawych, S., Pende, M., Ley, S.C., Moinard, C. & Lamb, R.F. TPL-2-mediated activation of MAPK downstream of TLR4 signaling is coupled to arginine availability. *Science signaling* **3** (2010) ra61.

[265] Santhanam, L., Lim, H.K., Lim, H.K., Miriel, V., Brown, T., Patel, M., Balanson, S., Ryoo, S., Anderson, M., Irani, K., Khanday, F., Di Costanzo, L., Nyhan, D., Hare, J.M., Christianson, D.W., Rivers, R., Shoukas, A. & Berkowitz, D.E. Inducible NO synthase dependent S-nitrosylation and activation of arginase I contribute to age-related endothelial dysfunction. *Circulation research* **101** (2007) 692–702.

[266] Nath, B. & Szabo, G. Hypoxia and hypoxia inducible factors: diverse roles in liver diseases. *Hepatology (Baltimore, Md.)* **55** (2012) 622–633.

[267] Solito, S., Bronte, V. & Mandruzzato, S. Antigen specificity of immune suppression by myeloid-derived suppressor cells. *Journal of Leukocyte Biology* **90** (2011) 31–36.

[268] Schumacher, K., Maerker-Alzer, G. & Wehmer, U. A lymphocyte-inhibiting factor isolated from normal human liver. *Nature* **251** (1974) 655–656.

[269] Chisari, F.V., Nakamura, M., Milich, D.R., Han, K., Molden, D. & Leroux-Roels, G.G. Production of two distinct and independent hepatic immunoregulatory molecules by the perfused rat liver. *Hepatology (Baltimore, Md.)* **5** (1985) 735–743.

[270] Sandalova, E., Laccabue, D., Boni, C., Watanabe, T., Tan, A., Zong, H.Z., Ferrari, C. & Bertoletti, A. Increased levels of arginase in patients with acute Hepatitis B suppress antiviral T cells. *Gastroenterology* **143** (2012) 78–87.e3.

[271] Ikemoto, M., Tsunekawa, S., Toda, Y. & Totani, M. Liver-type arginase is a highly sensitive marker for hepatocellular damage in rats. *Clinical Chemistry* **47** (2001) 946–948.

[272] Murayama, H., Ikemoto, M., Fukuda, Y. & Nagata, A. Superiority of serum type-I arginase and ornithine carbamyltransferase in the detection of toxicant-induced acute hepatic injury in rats. *Clinica Chimica Acta* **391** (2008) 31–35.

[273] Yan, B.C., Gong, C., Song, J., Krausz, T., Tretiakova, M., Hyjek, E., Al-Ahmadie, H., Alves, V., Xiao, S.Y., Anders, R.A. & Hart, J.A. Arginase-I: a new immunohistochemical marker of hepatocytes and hepatocellular neoplasms. *The American Journal of Surgical Pathology* **34** (2010) 1147–1154.

[274] Mempel, T.R., Henrickson, S.E. & von Andrian, U.H. T-cell priming by dendriticcells in lymph nodes occurs in three distinct phases. *Nature* **427** (2004) 154–159.

[275] Walter, S., Weinschenk, T., Stenzl, A., Zdrojowy, R., Pluzanska, A., Szczylik, C., Staehler, M., Brugger, W., Dietrich, P.Y., Mendrzyk, R., Hilf, N., Schoor, O., Fritsche, J., Mahr, A., Maurer, D., Vass, V., Trautwein, C., Lewandrowski, P., Flohr, C., Pohla, H., Stanczak, J.J., Bronte, V., Mandruzzato, S., Biedermann, T., Pawelec, G., Derhovanessian, E., Yamagishi, H., Miki, T., Hongo, F., Takaha, N., Hirakawa, K., Tanaka, H., Stevanovic, S., Frisch, J., Mayer-Mokler, A., Kirner, A., Rammensee, H.G., Reinhardt, C. & Singh-Jasuja, H. Multipeptide immune response to cancer vaccine IMA901 after single-dose cyclophosphamide associates with longer patient survival. *Nature Medicine* **18** (2012) 1254–1261.

[276] Qin, H., Lerman, B., Sakamaki, I., Wei, G., Cha, S.C., Rao, S.S., Qian, J., Hailemichael, Y., Nurieva, R., Dwyer, K.C., Roth, J., Yi, Q., Overwijk, W.W. & Kwak, L.W. Generation of

a new therapeutic peptide that depletes myeloid-derived suppressor cells in tumor-bearing mice. *Nature Medicine* **20** (2014) 676–681.

[277] Borsellino, G., Kleinewietfeld, M., Di Mitri, D., Sternjak, A., Diamantini, A., Giometto, R., Hpner, S., Centonze, D., Bernardi, G., Dell'Acqua, M.L., Rossini, P.M., Battistini, L., Rtzschke, O. & Falk, K. Expression of ectonucleotidase CD39 by FOXP3+ Treg cells: hydrolysis of extracellular ATP and immune suppression. *Blood* **110** (2007) 1225–1232.

[278] Huang, B., Pan, P.Y., Li, Q., Sato, A.I., Levy, D.E., Bromberg, J., Divino, C.M. & Chen, S.H. Gr-1+CD115+ immature myeloid suppressor cells mediate the development of tumor-induced T regulatory cells and T-cell anergy in tumor-bearing host. *Cancer Research* **66** (2006) 1123–1131.

[279] Pan, P.Y., Ma, G., Weber, K.J., Ozao-Choy, J., Wang, G., Yin, B., Divino, C.M. & Chen, S.H. Immune stimulatory receptor CD40 is required for T-cell suppression and T regulatory cell activation mediated by myeloid-derived suppressor cells in cancer. *Cancer research* **70** (2010) 99–108.

[280] Yang, R., Cai, Z., Zhang, Y., Yutzy, 4th, W.H., Roby, K.F. & Roden, R.B.S. CD80 in immune suppression by mouse ovarian carcinoma-associated Gr-1+CD11b+ myeloid cells. *Cancer research* **66** (2006) 6807–6815.

[281] Stoop, J.N., van der Molen, R.G., Baan, C.C., van der Laan, L.J.W., Kuipers, E.J., Kusters, J.G. & Janssen, H.L.A. Regulatory T cells contribute to the impaired immune response in patients with chronic Hepatitis B virus infection. *Hepatology (Baltimore, Md.)* **41** (2005) 771–778.

[282] Peng, G., Li, S., Wu, W., Sun, Z., Chen, Y. & Chen, Z. Circulating CD4+ CD25+ regulatory T cells correlate with chronic Hepatitis B infection. *Immunology* **123** (2008) 57–65.

[283] Nan, X.P., Zhang, Y., Yu, H.T., Li, Y., Sun, R.L., Wang, J.P. & Bai, X.F. Circulating CD4+CD25high regulatory T cells and expression of PD-1 and BTLA on CD4+ T cells in patients with chronic Hepatitis B virus infection. *Viral Immunology* **23** (2010) 63–70.

[284] Su, Z.J., Yu, X.P., Guo, R.Y., Ming, D.S., Huang, L.Y., Su, M.L., Deng, Y. & Lin, Z.Z. Changes in the balance between Treg and Th17 cells in patients with chronic Hepatitis B. *Diagnostic Microbiology and Infectious Disease* **76** (2013) 437–444.

[285] Franzese, O., Kennedy, P.T.F., Gehring, A.J., Gotto, J., Williams, R., Maini, M.K. &

Bertoletti, A. Modulation of the CD8+ T-cell response by CD4+ CD25+ regulatory T cells in patients with Hepatitis B virus infection. *Journal of Virology* **79** (2005) 3322–3328.

[286] Xu, D., Fu, J., Jin, L., Zhang, H., Zhou, C., Zou, Z., Zhao, J.M., Zhang, B., Shi, M., Ding, X., Tang, Z., Fu, Y.X. & Wang, F.S. Circulating and liver resident CD4+CD25+ regulatory T cells actively influence the antiviral immune response and disease progression in patients with Hepatitis B. *Journal of Immunology (Baltimore, Md.: 1950)* **177** (2006) 739–747.

[287] Fletcher, J.M., Lonergan, R., Costelloe, L., Kinsella, K., Moran, B., O'Farrelly, C., Tubridy, N. & Mills, K.H.G. CD39+FOXP3+ regulatory T cells suppress pathogenic Th17 cells and are impaired in multiple sclerosis. *Journal of Immunology (Baltimore, Md.: 1950)* **183** (2009) 7602–7610.

[288] Serafini, P., Mgebroff, S., Noonan, K. & Borrello, I. Myeloid-derived suppressor cells promote cross-tolerance in B-cell lymphoma by expanding regulatory T cells. *Cancer Research* **68** (2008) 5439–5449.

[289] Peppa, D., Micco, L., Javaid, A., Kennedy, P.T., Schurich, A., Dunn, C., Pallant, C., Ellis, G., Khanna, P., Dusheiko, G., Gilson, R.J. & Maini, M.K. Blockade of immunosuppressive cytokines restores NK cell antiviral function in chronic Hepatitis B virus infection. *PLoS pathogens* **6** (2010) e1001227. 12.

[290] Li, H., Han, Y., Guo, Q., Zhang, M. & Cao, X. Cancer-expanded myeloid-derived suppressor cells induce anergy of NK cells through membrane-bound TGF-beta 1. *Journal of immunology (Baltimore, Md.: 1950)* **182** (2009) 240–249.

[291] Mauti, L.A., Le Bitoux, M.A., Baumer, K., Stehle, J.C., Golshayan, D., Provero, P. & Stamenkovic, I. Myeloid-derived suppressor cells are implicated in regulating permissiveness for tumor metastasis during mouse gestation. *Journal of Clinical Investigation* **121** (2011) 2794–2807.

[292] Nausch, N., Galani, I.E., Schlecker, E. & Cerwenka, A. Mononuclear myeloid-derived "suppressor" cells express RAE-1 and activate natural killer cells. *Blood* **112** (2008) 4080–4089.

[293] Raulet, D.H., Gasser, S., Gowen, B.G., Deng, W. & Jung, H. Regulation of ligands for the NKG2d activating receptor. *Annual Review of Immunology* **31** (2013) 413–441.

[294] Leitner, J., Rieger, A., Pickl, W.F., Zlabinger, G., Grabmeier-Pfistershammer, K. & Stein-

berger, P. TIM-3 does not act as a receptor for galectin-9. *PLoS pathogens* **9** (2013) e1003253.

[295] Li, H., Wu, K., Tao, K., Chen, L., Zheng, Q., Lu, X., Liu, J., Shi, L., Liu, C., Wang, G. & Zou, W. Tim-3/galectin-9 signaling pathway mediates T-cell dysfunction and predicts poor prognosis in patients with Hepatitis B virus-associated hepatocellular carcinoma. *Hepatology (Baltimore, Md.)* **56** (2012) 1342–1351.

[296] Ju, Y., Hou, N., Zhang, X., Zhao, D., Liu, Y., Wang, J., Luan, F., Shi, W., Zhu, F., Sun, W., Zhang, L., Gao, C., Gao, L., Liang, X. & Ma, C. Blockade of Tim-3 pathway ameliorates interferon-γ production from hepatic CD8+ T cells in a mouse model of Hepatitis B virus infection. *Cellular & Molecular Immunology* **6** (2009) 35–43.

[297] Dardalhon, V., Anderson, A.C., Karman, J., Apetoh, L., Chandwaskar, R., Lee, D.H., Cornejo, M., Nishi, N., Yamauchi, A., Quintana, F.J., Sobel, R.A., Hirashima, M. & Kuchroo, V.K. Tim-3/galectin-9 pathway: regulation of Th1 immunity through promotion of CD11b+Ly-6G+ myeloid cells. *Journal of immunology (Baltimore, Md.: 1950)* **185** (2010) 1383–1392.

[298] Jayaraman, P., Parikh, F., Lopez-Rivera, E., Hailemichael, Y., Clark, A., Ma, G., Cannan, D., Ramacher, M., Kato, M., Overwijk, W.W., Chen, S.H., Umansky, V.Y. & Sikora, A.G. Tumor-expressed inducible nitric oxide synthase controls induction of functional myeloid-derived suppressor cells through modulation of vascular endothelial growth factor release. *Journal of immunology (Baltimore, Md.: 1950)* **188** (2012) 5365–5376.

[299] Barber, D.L., Wherry, E.J., Masopust, D., Zhu, B., Allison, J.P., Sharpe, A.H., Freeman, G.J. & Ahmed, R. Restoring function in exhausted CD8 T cells during chronic viral infection. *Nature* **439** (2006) 682–687.

[300] de Kleijn, S., Langereis, J.D., Leentjens, J., Kox, M., Netea, M.G., Koenderman, L., Ferwerda, G., Pickkers, P. & Hermans, P.W.M. IFN--stimulated neutrophils suppress lymphocyte proliferation through expression of PD-L1. *PloS One* **8** (2013) e72249.

[301] Bowers, N.L., Helton, E.S., Huijbregts, R.P.H., Goepfert, P.A., Heath, S.L. & Hel, Z. Immune suppression by neutrophils in HIV-1 infection: role of PD-l1/PD-1 pathway. *PLoS Pathog* **10** (2014) e1003993.

[302] Sinha, P., Chornoguz, O., Clements, V.K., Artemenko, K.A., Zubarev, R.A. & Ostrand-Rosenberg, S. Myeloid-derived suppressor cells express the death receptor Fas and apoptose in response to T cell-expressed FasL. *Blood* **117** (2011) 5381–90. 20.

[303] Mita, E., Hayashi, N., Iio, S., Takehara, T., Hijioka, T., Kasahara, A., Fusamoto, H. & Kamada, T. Role of Fas ligand in apoptosis induced by Hepatitis C virus infection. *Biochemical and Biophysical Research Communications* **204** (1994) 468–474.

[304] Ando K, Hiroishi K, K.T.M.T.M.Y.K.N.Y.H.O.K.I.M. Perforin, Fas/Fas ligand, and TNF-alpha pathways as specific and bystander killing mechanisms of Hepatitis C virus-specific human CTL. *The Journal of Immunology* **158** (1997) 5283–5291.

[305] Condamine, T., Kumar, V., Ramachandran, I.R., Youn, J.I., Celis, E., Finnberg, N., El-Deiry, W.S., Winograd, R., Vonderheide, R.H., English, N.R., Knight, S.C., Yagita, H., McCaffrey, J.C., Antonia, S., Hockstein, N., Witt, R., Masters, G., Bauer, T. & Gabrilovich, D.I. ER stress regulates myeloid-derived suppressor cell fate through TRAIL-Rmediated apoptosis. *Journal of Clinical Investigation* **124** (2014) 2626–2639.

[306] Abeles RD, McPhail MJ, S.D.A.C.V.N.V.G.X.E.K.W.S.D.M.Y.W.J. & D, V. CD14, CD16 and HLA-DR reliably identifies human monocytes and their subsets in the context of pathologically reduced HLA-DR expression by CD14hi/CD16neg monocytes: Expansion of CD14hi/CD16pos and contraction of CD14lo/CD16pos monocytes in acute liver failure. *Cytometry Part A* **81A** (2012) 823–834.

[307] Huang, L.R., Gbel, Y.A., Graf, S., Arzberger, S., Kurts, C., Heikenwalder, M., Knolle, P.A. & Protzer, U. Transfer of HBV genomes using low doses of adenovirus vectors leads to persistent infection in immune competent mice. *Gastroenterology* **142** (2012) 1447–1450.e3.

[308] Dion, S., Bourgine, M., Godon, O., Levillayer, F. & Michel, M.L. Adeno-associated virus-mediated gene transfer leads to persistent Hepatitis B virus replication in mice expressing HLA-a2 and HLA-DR1 molecules. *Journal of Virology* **87** (2013) 5554–5563.

[309] von Freyend, M.J., Untergasser, A., Arzberger, S., Oberwinkler, H., Drebber, U., Schirmacher, P. & Protzer, U. Sequential control of Hepatitis B virus in a mouse model of acute, self-resolving Hepatitis B. *Journal of Viral Hepatitis* **18** (2011) 216–226.

[310] Ali, K., Soond, D.R., Pieiro, R., Hagemann, T., Pearce, W., Lim, E.L., Bouabe, H., Scudamore, C.L., Hancox, T., Maecker, H., Friedman, L., Turner, M., Okkenhaug, K. & Vanhaesebroeck, B. Inactivation of PI(3)k p110delta breaks regulatory T-cell-mediated immune tolerance to cancer. *Nature* **510** (2014) 407–411.

[311] Highfill, S.L., Cui, Y., Giles, A.J., Smith, J.P., Zhang, H., Morse, E., Kaplan, R.N. & Mackall, C.L. Disruption of CXCR2-mediated MDSC tumour trafficking enhances anti-PD1 efficacy. *Science Translational Medicine* **6** (2014) 237ra67–237ra67.

[312] Gehring, A.J., Xue, S.A., Ho, Z.Z., Teoh, D., Ruedl, C., Chia, A., Koh, S., Lim, S.G., Maini, M.K., Stauss, H. & Bertoletti, A. Engineering virus-specific T cells that target HBV infected hepatocytes and hepatocellular carcinoma cell lines. *Journal of Hepatology* **55** (2011) 103–110.

[313] Koh, S., Shimasaki, N., Suwanarusk, R., Ho, Z.Z., Chia, A., Banu, N., Howland, S.W., Ong, A.S.M., Gehring, A.J., Stauss, H., Renia, L., Sllberg, M., Campana, D. & Bertoletti, A. A practical approach to immunotherapy of hepatocellular carcinoma using T cells redirected against hepatitis b virus. *Molecular Therapy. Nucleic Acids* **2** (2013) e114.